Human Liver Organoids Culture as a Personalised Approach in Assessing HBV Infection and Cellular Responses

Chuan Kok LIM MBBS, FRCPA, FRACP

Department of Molecular and Biomedical Sciences

School of Biological Sciences

University of Adelaide

THE UNIVERSITY of ADELAIDE

A dissertation submitted to the University of Adelaide in candidature for the degree of Doctor of Philosophy in the Faculty of Science

August 2021

Table of Contents

Abstract

HBV is a hepatotropic, partially double-stranded DNA virus that has been associated with chronic liver diseases such as liver cirrhosis and hepatocellular carcinoma (HCC). It has eight genotypes and many subtypes, with different risks of disease progression. Risks of HCC development is especially high in certain ethnic groups, suggesting the importance of host genetics in the disease outcome. Despite the development of highly effective nucleoside and nucleotide analogues that can control HBV replication, there is currently no curative treatment. Pegylated IFN-α is able to achieve functional cure in a small proportion of patients, and the exact mechanism of how this phenomenon occurs in some and not the others, is not yet clear.

A major problem with HBV study is the lack of *in vitro* or *in vivo* model system that can recapitulate clinical disease progression. Many *in vitro* model systems utilise hepatoma-derived cell lines that suffer from significant physiological and immunological limitations that restrict understanding of complex viral-host interactions. Primary hepatocytes have been considered the "gold standard" for *in vitro* studies but suffer from major limitations, for instance, they rapidly dedifferentiate in culture, have limited lifespan and are labour intensive to isolate and maintain.

Stem-cell derived hepatocyte-like cells (HLCs) have gain significant research interest in recent years due to their ability to self-replenish in their stem cell stage and following differentiation, are able to achieve mature hepatocyte-like metabolic phenotypes. Studies using induced pluripotent stem cells (iPSC) derived HLCs have shown the ability of this model system to support HBV replication. iPSC, however, is not an ideal model system due to high rates of *de novo* mutations introduced during reprogramming process.

Another stem cell-derived liver model system is the adult stem cell (AdSC) derived liver organoids that was first developed in the Hans Clevers laboratory by Meritxell Huch. This model system recapitulates liver regeneration from ductal stem cells following liver injuries. Following differentiation, the organoids can achieve metabolic phenotypes similar to liver tissue. Importantly, these organoids are genetically stable during culture and carry the genetic signatures of the original host.

In this thesis, we developed and characterise the AdSC derived liver organoids as a novel model system for assessing HBV lifecycle, cellular responses and also demonstrate their utility in assessing antiviral response. We first characterise this culture system and the differentiation processes using mouse liver tissues. We subsequently adapted the culture system to generate human liver organoids from liver biopsy specimens to increase the applicability of this culture system as a personalised drug testing platform. We have shown in this thesis that the differentiated human liver organoids expressed higher levels of metabolic markers such as albumin and CYP3A4 expression. In addition, we demonstrated the importance of assessing functional HBV entry receptor (NTCP) expression during the course of differentiation to determine the optimal timing for HBV infection.

Also arising from this thesis was the observation that the liver organoids can be infected with both cell culture and plasma derived HBV from different genotypes (B, C, D). In contrast to HepG2-NTCP, DMSO has no influence on the differentiation and infectivity of HBV in liver organoids. Importantly, we noticed that HBV infection in different donors resulted in very different viral dynamics, suggesting that individual host factors play an important role in HBV infection and replication. Antiviral response can also be assessed using the liver

organoids culture system as demonstrated by lack of infection following treatment with Myrcludex B.

Another novel discovery is that the interferon-stimulated genes (ISG) response to either RNA mimics or IFN-α stimulation is considerably different in their levels and timing of mRNA induction. These findings confirm our postulation that the liver organoids can demonstrate phenotypic donor variations in innate immunity. Having demonstrated that the liver organoids are immune competent, we assessed ISG induction in liver organoids following HBV infection. We noticed that although there were some donor variations in ISG expressions, the overall level of ISG induction following HBV infection was very poor. This result confirm that HBV is a poor inducer of ISGs and thus resolving some of the previous conflicting findings from studies using less physiological model system.

In summary, we have developed a novel *in vitro* model system to evaluate HBV infection and the innate immune response. We have shown that the organoids demonstrate individualised HBV viral dynamics and ISG response and are responsive to antiviral treatment. We believe we have significantly improved our understanding of the innate immune response to HBV infection and the findings from this thesis will help pave the way for future development of a personalised antiviral platform for novel anti-HBV therapeutics.

Declaration

I certify that this work contains no material which has been accepted for the award of any other degree or diploma in my name, in any university or other tertiary institution and, to the best of my knowledge and belief, contains no material previously published or written by another person, except where due reference has been made in the text. In addition, I certify that no part of this work will, in the future, be used in a submission in my name, for any other degree or diploma in any university or other tertiary institution without the prior approval of the University of Adelaide and where applicable, any partner institution responsible for the joint-award of this degree.

I give permission for the digital version of my thesis to be made available on the web, via the University's digital research repository, the Library Search and also through web search engines, unless permission has been granted by the University to restrict access for a period of time.

I acknowledge the support I have received for my research through the provision of an Australian Government Research Training Program Scholarship.

Chuan Kok LIM

16 August 2021

Acknowledgements

I would like to thank my supervisors Professor Michael Beard and Dr Nick Eyre for providing me with the opportunity to conduct this exciting project. I am sincerely grateful for their support and mentoring throughout my PhD.

I express my utmost gratitude to Professor Stephen Locarnini, Professor Elizabeth Vincan, Dr Bang Manh Tran, Dr Dustin Flanagan and Dr Nadia Warner for the generosity of advice, mentoring and support provided.

I would like to acknowledge all past and present members of the Viral Pathogenesis Research Laboratory, specifically Ornella Romeo, Andrew Chilver, Emily Bennet, Emily Kirby, Rosa Coldbeck-Shackley, Byron Shue, Dr Kylie Van Der Hoek, Thomas Burton, Brandan Tan, Brooke Trowbridge, Stephen Johnson, and Siena Centofanti.

I would like to thank my parents, Chong Hee Lim and Chu Yu Ng for their support. Finally, I would like to thank my husband, Matthew Lynch for his ongoing support and technical advice.

Publications Arising from This Thesis

In preparation

Title: Human Liver Organoids as a Personalised Approach in Assessing HBV Infection and Cellular Responses

Chuan Kok Lim,[1,2,3*] Andrew P Chilver,[1] Ornella Romeo,[1] Bang Manh Tran,[4,5] Emily Kirby,[1] James Breen,[6,7,8] Elizabeth Vincan,[4,5] Nadia Warner, [4,5] Stephen Locarnini, [4,5] Erin McCartney,[9] Mark Van Der Hoek,[6] Andrew Ruszkiewicz,[10] Edmund Tse,[9] Michael Beard[1*]

Presentations Arising from this Thesis

2019 Assessing HBV Infection and Application Using LGR5+ Human Liver Organoids Culture (International HBV Meeting, Melbourne) (Oral Presentation)

2019 Human liver organoids culture as an in vitro model for HBV infection (International Liver Congress, Vienna) (Oral Presentation)

2019 Human liver organoids culture as an in vitro model for HBV infection (ACH2, Canungra) (Oral Presentation)

2018 Human liver organoids culture as an in vitro model for hepatotropic viral infection (ACH2, Yarra Valley) (Oral Presentation)

2018 Human liver organoids culture as an in vitro model for hepatotropic viral infection (Invited Speaker. Organoids Are Us Symposium, The Peter Doherty Institute for Infection and Immunity, Melbourne) (Oral Presentation)

Awards Arising from This Thesis

2021 Australian Centre for HIV and Hepatitis Virology Research Grant. *High throughput liver organoid assay for HBV antiviral discovery* $90,000

2020 Australian Centre for HIV and Hepatitis Virology Research Grant. *Development of Antiviral Targets and Drug Strategies and Tests for Antiviral Drug Resistance and Toxicity* $90,000

2019 Australian Centre for HIV and Hepatitis Virology Research Grant. *Liver Organoid Culture as a Platform for Novel HBV Antiviral Testing* $95,000

2019 Australian Centre for HIV and Hepatitis Virology Travel Award. $1000

2018 Australian Centre for HIV and Hepatitis Virology Travel Award. $1000

2017 The Royal Australasian College of Pathologist (RCPA) Post-graduate Research Foundation Grant Award. *HBV and HCV Infection in Liver Org*anoids $25,000

Material Providers

Abcam	Cambridge, UK
Addgene	Massachusetts, USA
Agilent	California, USA
BD Biosciences	New Jersey, USA
Bethyl Laboratories	Montgomery, USA
Bioline	London, UK
Corning	New York, USA
Macherey-Nagel	Düren, Germany
Millipore Sigma	Massachusetts, USA
Peprotech	New Jersey, USA
Qiagen	Hilden, Germany
R&D Systems	Minneapolis, USA
Santa Cruz	California, USA
Sigma	Missouri, USA
STEMCELL Technologies	Vancouver, Canada
Tecan	Mannedorf, Switzerland
ThermoFisher	Massachusetts, USA
Trevigen	Maryland, USA
Tocris	Bristol, UK

Abbreviations

AdSC	Adult Stem Cell
HBV	Hepatitis B Virus
cccDNA	Covalently Closed Circular DNA
CHB	Chronic Hepatitis B
DM	Differentiation Medium
EM	Expansion Medium
ESC	Embryonic Stem Cell
HCC	Hepatocellular Carcinoma
HCV	Hepatitis C Virus
HLC	Hepatocyte-like Cell
H&E	Haematoxylin and Eosin
IFN	Interferon
IM	Isolation Medium
iPSC	Induced Pluripotent Stem Cell
ISG	Interferon Stimulated Genes
LGR5	Leucine-rich repeat-containing G-protein coupled receptor 5
NA	Nucleoside/Nucleotide Analogue
NTCP	Sodium Taurocholate Co-transporting Polypeptide
PHH	Primary Human Hepatocytes
rcDNA	Relaxed Circular DNA
TEM	Transmission Electron Microscopy

List of Figures

List of Movies

All movies can be accessed at the following link:

https://universityofadelaide.box.com/s/bxtgdj272ig5tjdutbf97q2g3ri1lqi3

List of Tables

1 Introduction

1.1 Epidemiology and Clinical Presentation of Hepatitis B Virus (HBV)

HBV is a hepatotropic virus with partially double-stranded DNA genome consisting of 8 geographically distinct genotypes (A-H), multiple subgenotypes and 9 serotypes. It has a worldwide distribution with the highest prevalence (>8% seroprevalence) in West Africa and East Asia [1]. It affects more than 240 million people worldwide with 887,000 associated deaths in 2015, mainly attributed to cirrhosis and hepatocellular carcinoma [2]. The majority of transmission occurs at birth or early childhood, with 90% of infections progressing to chronic hepatitis B. Acute infections are often subclinical [3] and fulminant hepatitis is uncommon and caused by immune mediated hepatocyte injury. Co-infection of HBV with other hepatotropic viruses such as HCV and Hepatitis Delta virus (HDV) accelerate cirrhosis and risk for HCC (up to 45% lifetime risks). Co-infection of HBV with HIV also significantly increases the risks of HCC and liver-disease associated mortality [4, 5]. Ethnicity (Asian and African) and HBV genotypes (A and C) are major determinants of cirrhosis and HCC development. However, unlike other hepatitis viruses, HBV-associated HCC can occur without liver cirrhosis [6]. In selected patients, HBV replication can be temporarily suppressed with short-term pegylated IFN therapy or long-term nucleoside analogue (NA) therapies. However, there is currently no effective treatment to achieve long term cure, and the NA therapy is often required lifelong. Earlier generation of NA therapy (e.g., Lamivudine) has been associated with development of drug resistance within a short period but this has largely been overcome with newer generation NA (e.g., Tenofovir, Entecavir) [7, 8]. However, interruption to NA can be associated with significant HBV flare and in some cases liver decompensation [9]. The international bodies such as WHO recognise the challenges of achieving HIV cure and the need for better understanding of HBV biology.

Key areas of research identified in the international strategic plan for HBV cure (ICE-HBV) includes viral and host factors attributing to chronic hepatitis B, immunological responses HBV control and co-infection of HBV with other hepatitis viruses and HIV [10].

1.2 HBV Virion Structure and Genome

Human HBV is an enveloped DNA virus from the *Hepadnaviridae* family which consists of mammalian HBV (human HBV, woodchuck WHV, ground squirrel GSHV) and avian HBV (duck DHBV and heron HHBV). Viruses from this family contain (1) a unique genome that consists of a partially double stranded genomic DNA, (2) a RNA-dependent DNA polymerase, (3) pre-genomic RNA as replication template and (4) species and tissue tropism [11]. It has a spherical envelope containing host-derived lipids, glycoproteins and surface antigens (HBsAg). The capsid is a 27nm icosahedral core consisting of core antigen (HBcAg), DNA polymerase and a 3.2kb genome in the form of relaxed circular dsDNA (rcDNA) (Figure 1). The HBV genome contains 4 overlapping reading frames (S, C, P and X) with multiple initiation codons interspersed the S and C domains, hence generating multiple functionally distinctive proteins [12, 13] (Figure 2).

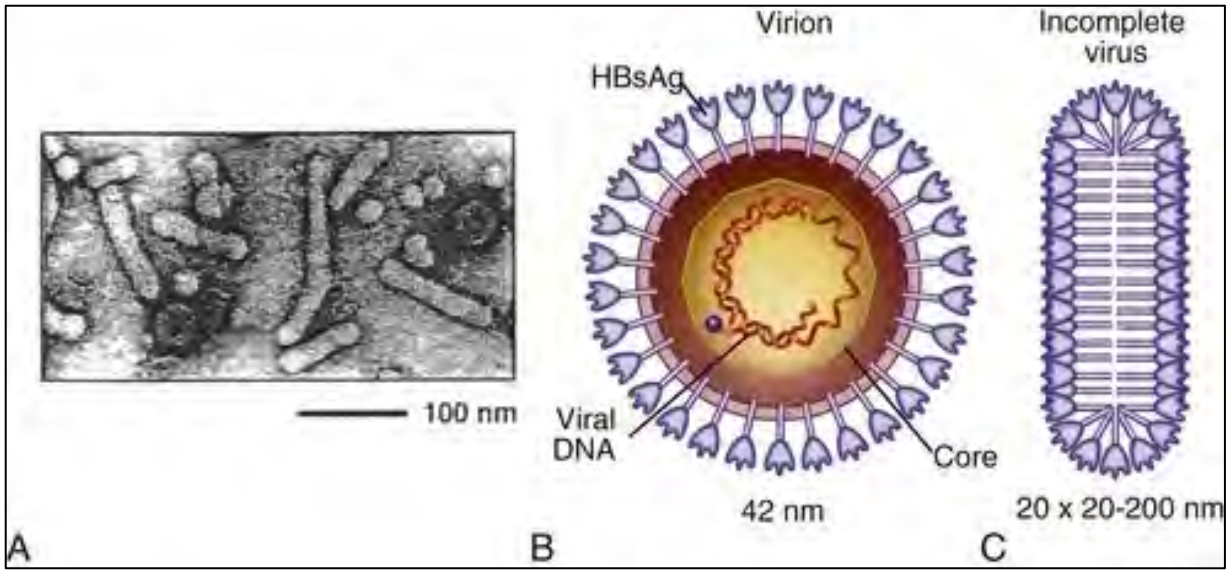

Figure 1: Structure of HBV Virion and Incomplete Virus
From Left to Right. **(A)** An electron microscopy picture showing HBV particles present in serum, representing complete and incomplete viruses (filamentous, spherical, empty virions). **(B)** Complete HBV virus and **(C)** incomplete virus in the form of subviral particles (filamentous form). (Mandell, Douglas, and Bennett's Principles and Practice of Infectious Diseases. Elsevier 2010)

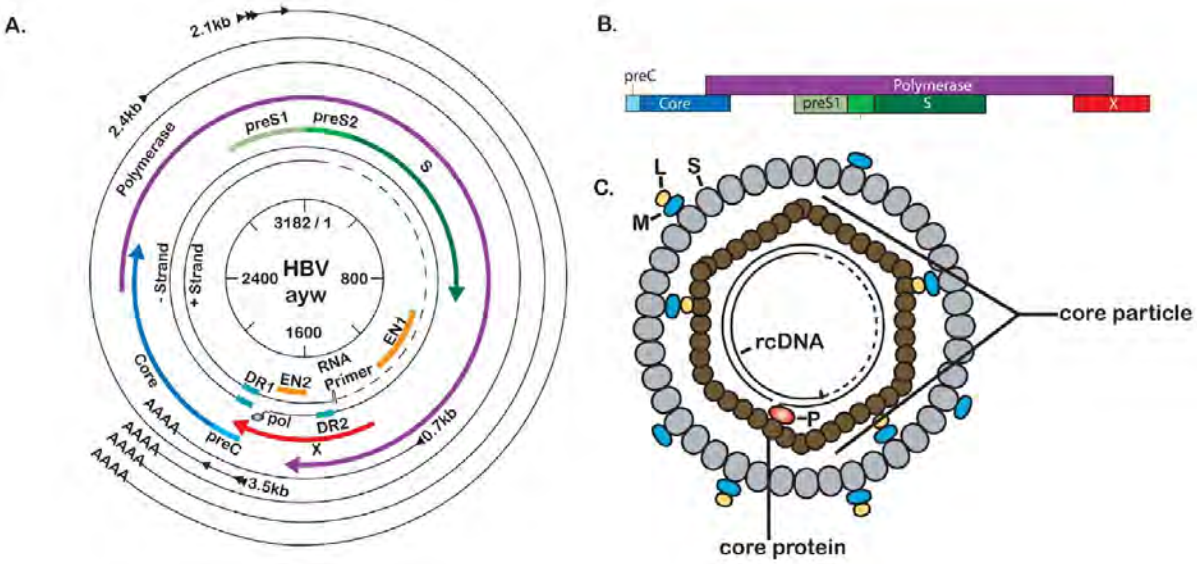

Figure 2: HBV Genome Organisation Map, Viral Transcripts and Proteins (A) Genomic organisation of HBV showing overlapping genes. **(B)** Major transcripts of HBV genome. **(C)** Major proteins expressed by HBV. (Lamontagne. Hepatitis B virus molecular biology and pathogenesis. Hepatoma Research 2016)

1.3 HBV Life Cycle

1.3.1 Viral Entry and NTCP

HBV hepatocyte entry encompasses three sequential events, (1) a low affinity, reversible binding to Heparan Sulfate Proteoglycans (HSPGs), (2) high affinity binding to Sodium Taurocholate Co-transporting Polypeptide (NTCP) [14] and (3) endocytosis mediated internalization. Interestingly, the primary receptor for HBV remained unidentified for many years until recently where NTCP was identified as the primary entry receptor for HBV and HDV through gene silencing experiments on human and Tupaia hepatocytes [15]. This has revolutionised HBV research as cell culture models were developed that paved the way for entry and receptor studies as well as viral inhibition studies. The NTCP receptor is a transmembrane protein expressed at the basolateral membrane of hepatocytes and interacts with the PreS1 region of HBV (Figure 3). In *in vitro* cell culture models, naturally occurring NTCP mutations such as S267F and NTCP inhibitors (e.g., Myrcludex B, Cyclosporin) will abrogate HBV infectivity, suggesting NTCP is essential for HBV entry [14]. NTCP mRNA and HBV infectivity can be enhanced in the HepaRG cell line with the addition of 2.5% DMSO through an unknown mechanism [16]. Myristoylation or cholesterol modification of PreS1 (N-terminus of L protein) is essential for its interaction with NTCP. The post-receptor entry event involves either endocytosis or caveolae-, clathrin- or macropinocytosis-dependent membrane fusion but the process is not fully understood [17].

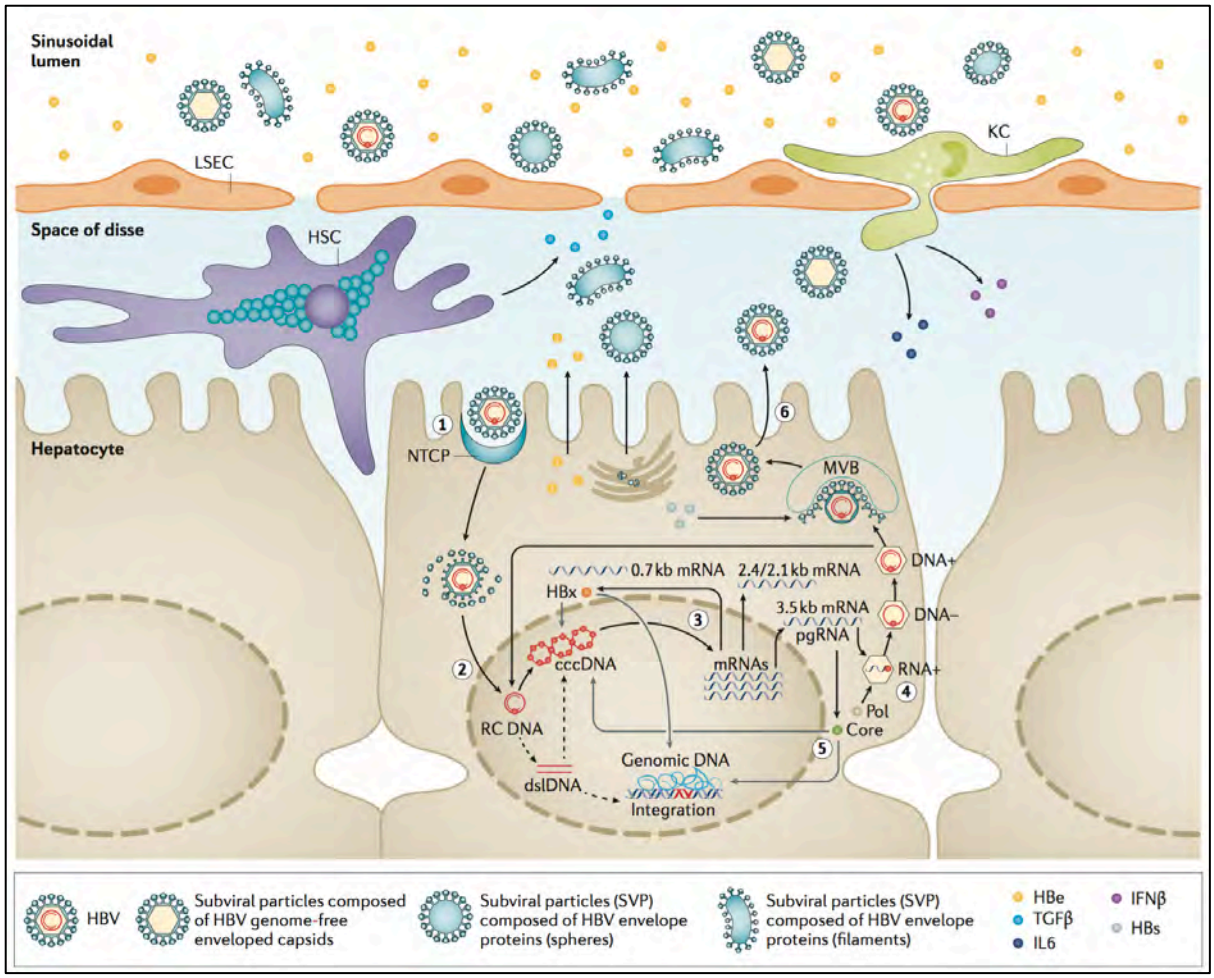

Figure 3: HBV Life Cycle

HBV life cycle as indicated from (1) receptor binding to NTCP, (2) release and transportation of rcDNA into the nucleus, (3) transcription of mRNAs from cccDNA, (4) packaging of RNA into viral nucleocapsid following interactions with Pol and Core, (5) regulatory roles of core protein in cccDNA transcription and (6) excretion of mature virions. (Liang *et al*. Experimental models of hepatitis B and C—new insights and progress. Nature Reviews Gastroenterology & Hepatology. 2016)

1.3.2 Viral Internalisation, cccDNA Formation and Genome Integration

Following viral internalisation, the HBV nucleocapsid and its covalently linked polymerase are transported to the nuclear pore complex through a microtubular-dependent mechanism, facilitated by the importin α and β receptors (Figure 3 step 2). The mature HBV capsid interacts with nucleoporin 153 to release the relaxed circular DNA (rcDNA) genome in the nucleus that is subsequently converted to covalently closed circular DNA (cccDNA) through a multi-step process [18] (Figure 4), including the removal of viral polymerase at the minus strand by tyrosyl-DNA phosphodiesterase 2 (TDP 2) and removal of the RNA primer at the plus strand through unknown host enzymes. This is followed by removal of redundant sequences from the negative strand by flap structure-specific endonuclease 1 (FEN1) and repair of the positive strand by host DNA polymerase κ/δ/δ [19]. The cccDNA is formed by ligation of the both the DNA strands and arranged in a chromatin like structure with histone and non-histone proteins, referred to as minichromosomes. The exact mechanism for formation of cccDNA relies on host-cell factors and is poorly understood. While artificial model systems such as HBV transgenic mice are useful model to study various aspects of HBV lifecycles, they do not produce cccDNA, hence does not fully recapitulate the viral lifecycle. About 10% of rcDNA is linearised for host genome integration (estimated to be 1:10,000 hepatocytes) (Figure 3) [12]. Genome integration is not an essential process for replication of HBV but may play a role in HCC pathogenesis [20].

1.3.3 Genomic Replication

Using cccDNA as a template, HBV exploits the host RNA polymerase II to generate a series of mRNAs. Four major transcripts include the full length 3.5-kb pgRNA, subgenomic RNAs such as 2.4-kb PreS mRNA, 2.1-kb S mRNA and X mRNA. RNA splicing also results in additional transcripts (Figure 5). The major spliced variant SP1 RNA encodes for HBV

splicing-generated protein (HBSP) which has been shown to play a role in cell viability, proliferation and TNF-α signalling [21]. Hepatocyte host factors such as Hepatocyte Nuclear Factor (HNF), RXRalpha plus PPARalpha are major regulators of the pgRNA and play a significant role in determining the hepatotropism of HBV [22]. All four mRNAs utilise the same polyadenylation signal and exportation of mRNAs are assisted by various host factors.

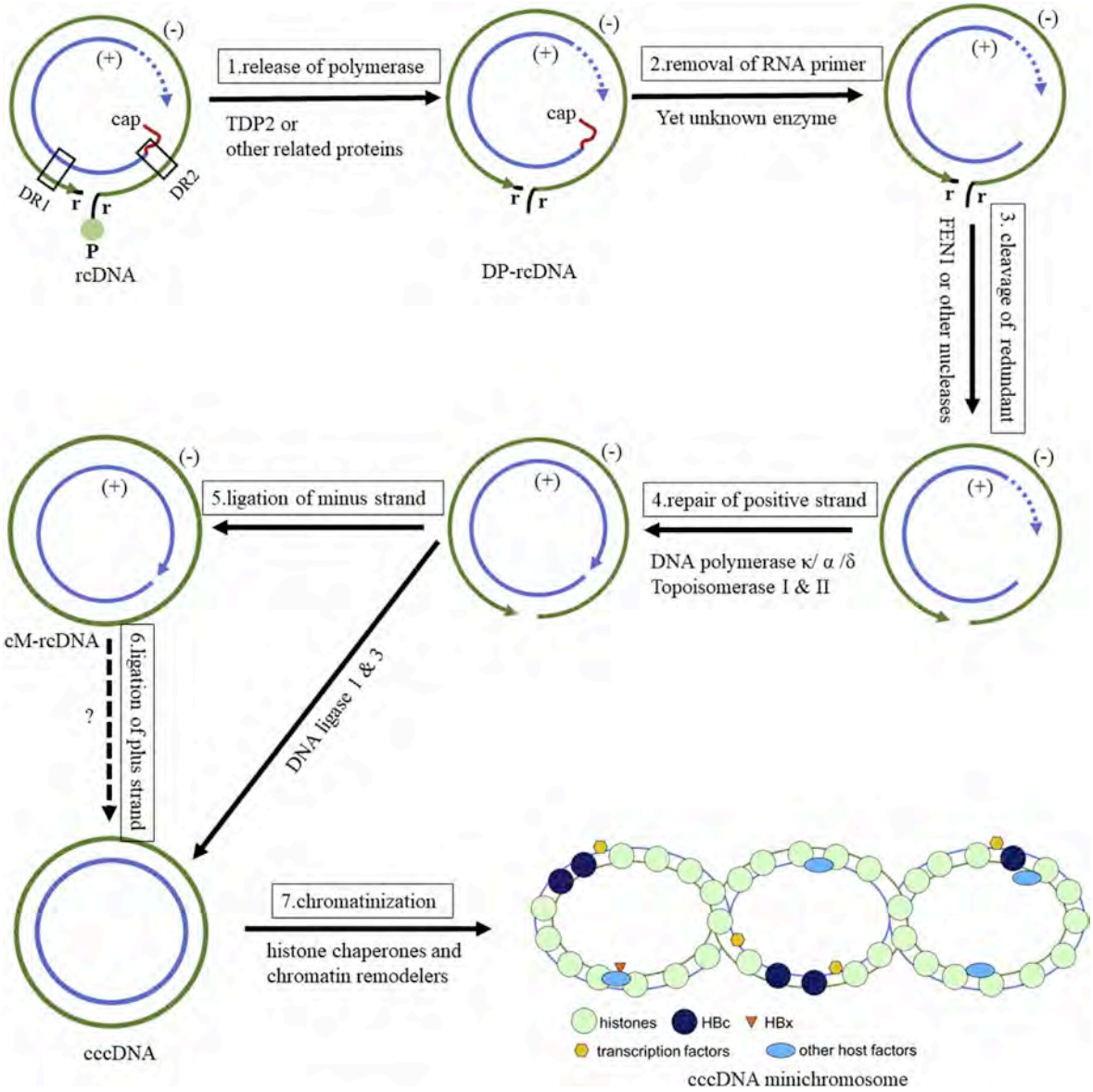

Figure 4: HBV cccDNA Minichromosome Formation
(Yuchen Xia, Haitao Guo. Hepatitis B virus cccDNA: Formation, regulation and therapeutic potential. Antiviral Research. 2020)

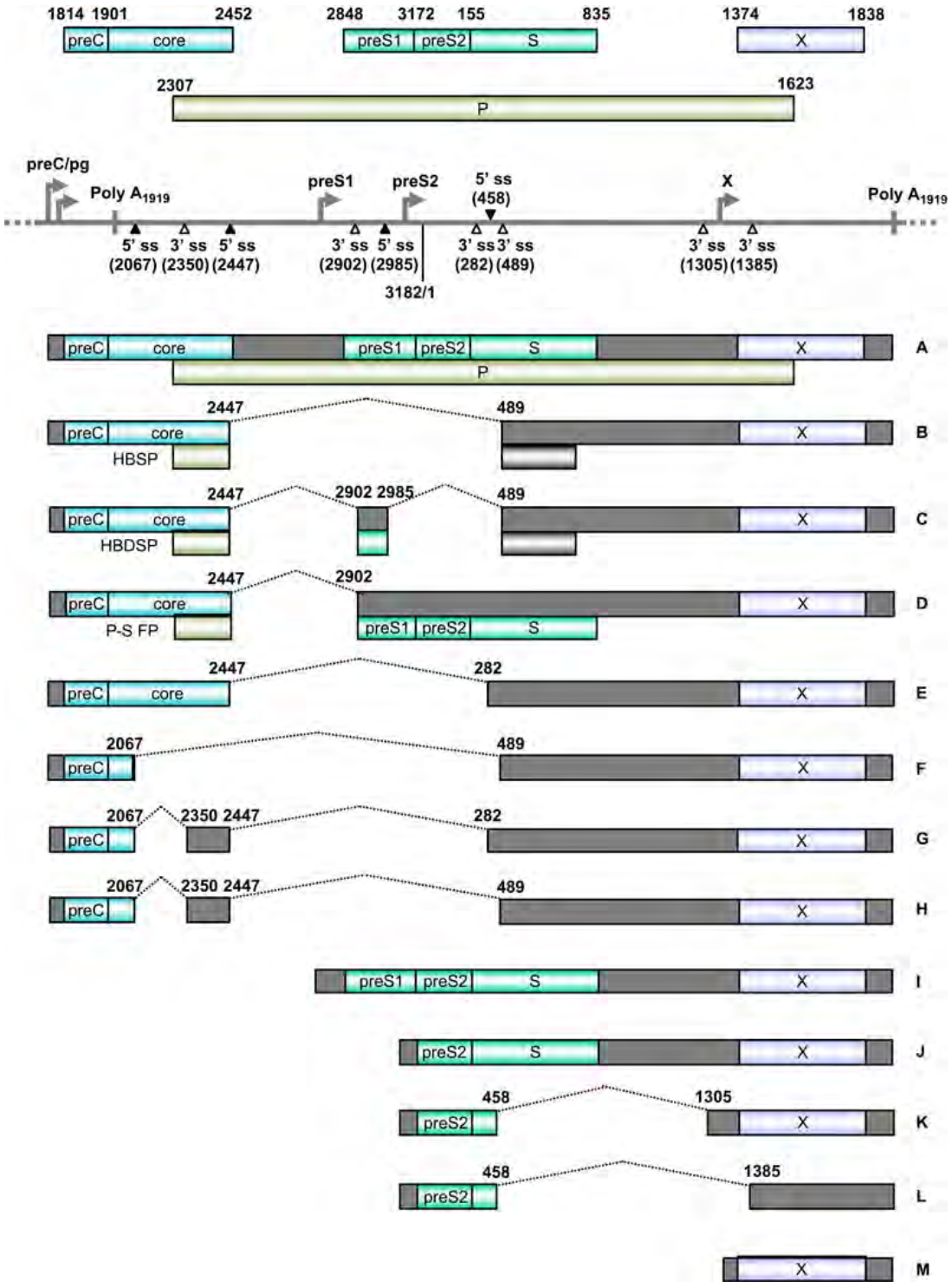

Figure 5: HBV Transcripts
(Ajiro *et al.*. Oncogenes and RNA splicing of human tumour viruses. Emerging Microbes and Infections. 2019)

1.3.4 Genome Packaging and Secretory Pathways

The pgRNA has a bicistronic role as a reverse transcription template for the (-) DNA strand and translation of HBV core proteins. The pgRNA interacts with HBcAg and Pol and the complex undergoes a conformational change to form a mature nucleocapsid. In the post-ER pre-Golgi compartment, mature nucleocapsids interact with envelope proteins (translated from subgenomic mRNAs) to form complete virions which are secreted through the multivesicular body pathway as mature virions (Dane's particles) [23]. Independently, the envelope proteins are also secreted in abundance without the nucleocapsid to form small spherical and filamentous non-infectious subviral particles (Figure 1).

1.4 HBV ORF & Proteins

The relaxed circular DNA organisation of the HBV genome consists of a complete (-) strand with the P protein linked to the 5' end, and an incomplete (+) strand with RNA oligonucleotide that is derived from pre-genomic RNA (pgRNA). The relatively small 3.2kb genome means that the overlapping ORFs must be utilised to maximum coding capacity. The four major ORFs consists of overlapping genes that encode for seven proteins, i.e., HBx, core, polymerase, L-HBsAg, M-HBsAg, S-HBsAg, precore/HBeAg. The precore/core gene encodes for the nucleocapsid and HBeAg. The L-/M-/S- Surface genes encode for envelope for the large, medium and small proteins. The Pol gene encodes for reverse transcriptase, RNase H and terminal protein domains. The X gene encodes regulatory X-protein. Of these proteins, core and HBsAg proteins are structural proteins for the infectious virions whereas HBeAg is independently secreted from the cells. In addition, direct repeat 1 & 2 (DR1, DR2) plays an important role in strand specific DNA synthesis and enhancers 1 & 2 (ER1, ER2) assist with genome transcription.

1.4.1 Polymerase ORF

The HBV Polymerase is a multifunctional protein consists of 4 functional domains, i.e., terminal protein, spacer, Pol/RT and RNaseH [24]. The terminal protein is a unique feature of *Hepadnaviridae,* and a tyrosine residue serves as a primer for the synthesis of minus-DNA strand. The terminal protein also plays an important role in pgRNA binding, RNA binding and protein priming. Only a short segment of the N and C terminal of the spacer are important in polymerase function. The Pol/RT region helps reverse transcribe the (-) strand DNA from pgRNA and subsequent synthesis of the (+) strand DNA. The RT region shares significant homology to the HIV RT, and therapeutic RT inhibitors are active against these two viruses. The fourth domain, RNaseH plays a role in degradation of pgRNA template during the (-) strand DNA synthesis.

1.4.2 Precore/Core ORF, HBcAg, HBeAg

HBcAg is encoded from pre-genomic RNA (pgRNA) as a 21kD protein. It is expressed intracellularly as either soluble dimers or icosahedral capsids. HBV core protein is translated from pgRNA at position 1901 to form the 183 aa protein. (Figure 3) The predominant role of core protein is nucleocapsid assembly. The core protein dimers assemble into viral nucleocapsid which helps package the pgRNA and polymerase. In addition, the core protein plays a role in regulation of nucleosome spacing in cccDNA and the initiation of reverse transcription [25].

HBeAg is expressed by all viruses in the *Hepadnaviridae* family. It is not essential for maintenance of infection but plays a role in viral persistence through immune evasion [26, 27]. The biosynthesis of HBeAg starts with translation of the precore mRNA at position 1814, forming precore protein (p25). The 19aa signal peptide helps traffic the nascent HBeAg to the ER in which intracellular HBeAg (p22) is formed following removal of the signal

peptide by signal peptidase. Further removal of C-terminal domain leads to formation of secreted HBeAg (p17). In cell culture model using the hepatoblastoma cell line HepG2-NTCP, cytosolic HBeAg is proposed to have immunomodulating effect which is not seen with the secreted HBeAg [28]. Cytosolic HBeAg significantly reduces transcription from the IFN-stimulated response element activity by interfering with nuclear translocation of pSTAT1, a key transcription factor involved in the host antiviral IFN response, leading to a dampened ISG response to IFN-α[29]. This finding may have clinical correlation in which HBeAg positive patients are more resistant to IFN-α therapy [30].

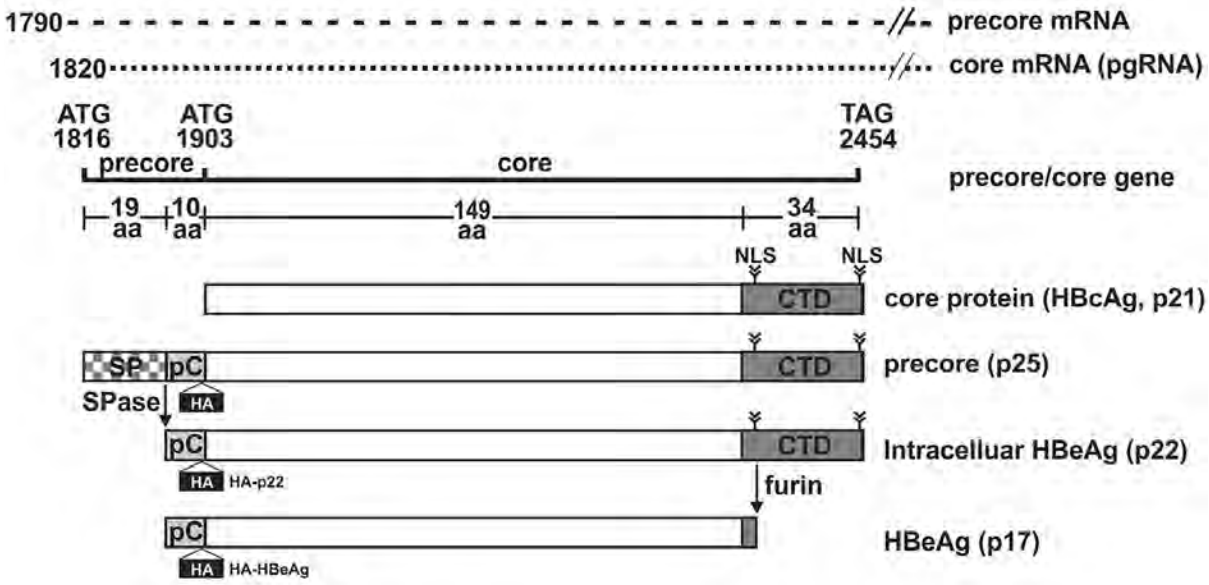

Figure 6: Biosynthesis of HBcAg and HBeAg
(Mitra *et al.*. Hepatitis B Virus Precore Protein p22 Inhibits Alpha IFN Signalling by Blocking STAT Nuclear Translocation. Journal of Virology 2019)

1.4.3 PreS/S ORF, HBsAg

The PreS1/PreS2/S ORF contains three in-frame start codons that encode for three HBV surface proteins (Figure 6): (1) large HBV surface protein (LHBs) which includes the PreS1/PreS2 and S domains (389-400aa), (2) middle HBV surface protein (MHBs) which includes PreS2 and S domains (281aa) and (3) small surface protein (SHBs) which contains only the S domain (226 aa) (Figure 7). These envelope proteins are anchored by the S-domain to the ER membrane at the first transmembrane region (TM1) [31]. Transmembrane region 2 (TM2) is located at aa position 80-98 and helps translocation of the aa across the ER membrane into the ER lumen.

LHBs encompasses two conformations: (1) the PreS1/PreS2 domain is translocated across the ER membrane and is involved in the mature viral particle attachment process, and (2) the PreS1/PreS2 domain is orientated towards the cytoplasm and interacts with nucleocapsid to trigger intracellular signal transduction through protein kinase C.

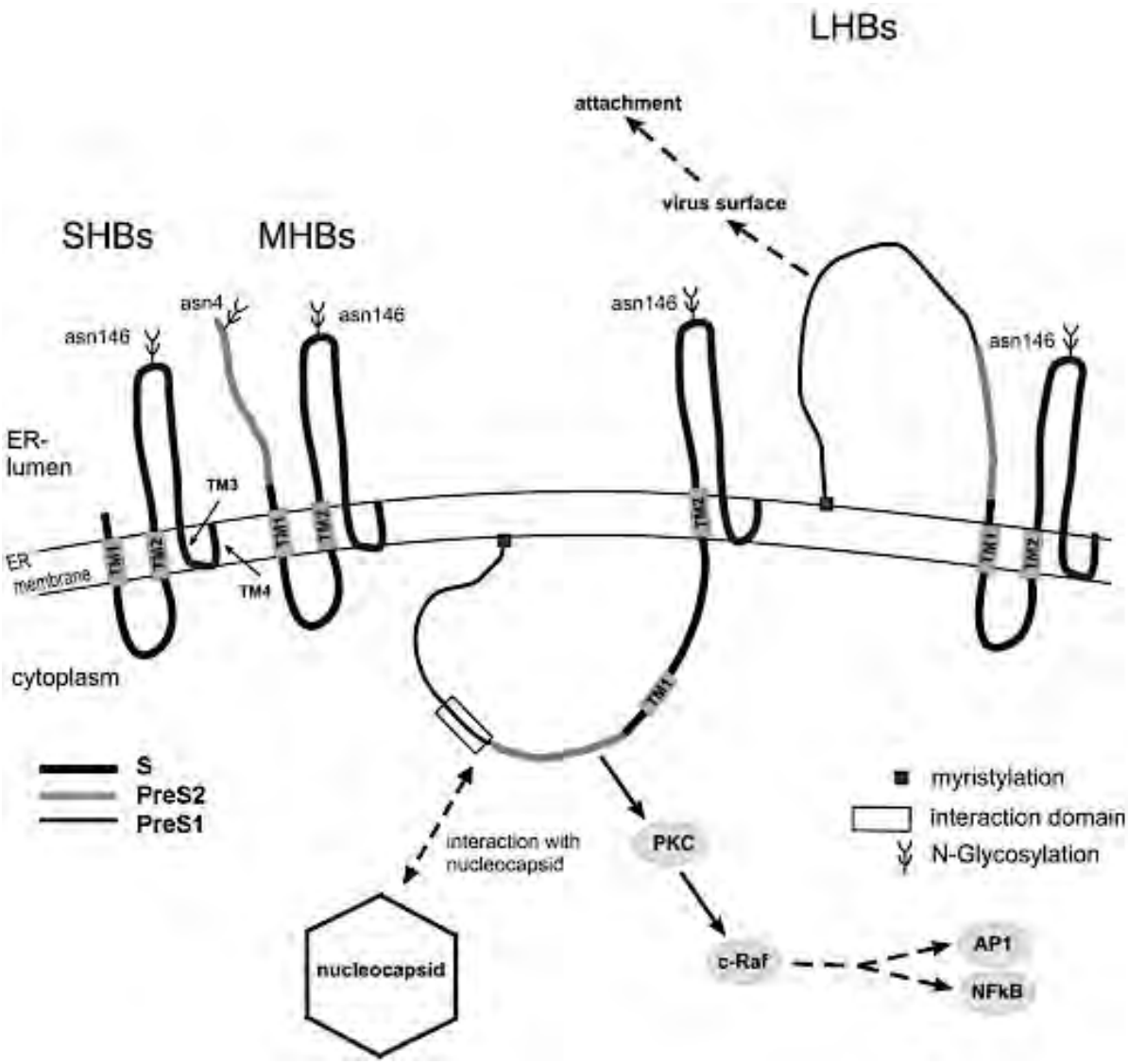

Figure 7: HBV Surface Proteins
(Eble *et al.*. The N-terminal (pre-S2) domain of a hepatitis B virus surface glycoprotein is translocated across membranes by downstream signal sequences. Journal of Virology. 1990)

1.4.4 X ORF, HBxAg

HBx is a regulatory protein encoded by the smallest ORF resulting in a 154aa protein. It plays several important roles, including transcription of cccDNA, enhancement of HBV replication and is associated with oncogenesis [32]. At a cellular level, HBx has extensive effect on the signalling cascades of hepatocytes, including apoptosis pathways [33], transcription factor activation (AP-1, AP-2, NFAT) [34], innate immune pathways (NF-kb) [35-37] and oncogenic pathways (p53, Akt, Wnt/b-catenin) [38-40]. In HCC cells, genome integrated HBx is often active despite absence of HBV replication, suggestive of the role of HBx in maintaining HCC phenotype. At present, the exact roles of HBx on hepatocytes are still unclear due to a lack of single acceptable model system [41].

1.5 Viral Variants and Genotypes

HBV consists of many variants due to lack of a 3' to 5' exonuclease activity to proofread the polymerase gene. These HBV variants are associated with significant geographical variation and clinical phenotypes, e.g., IFN resistance, vaccine escape, immune escape etc. Immune escape variants with precore A1896 mutation and basal core promoter T1762/A1764 mutation for example, are associated with high rates of HCC development [42]. Genetic mutations in these HBV variants are archived in the cccDNA and can re-emerge upon changes in selection pressure. Significant genetic mutations that can result in viral evolution, however, are limited in HBV due to the constraints of overlapping genes, with essential viral proteins often encoded by more than one gene. Thus, the most common genetic variation seen in HBV consists of intra or intergenotypic recombinant virus.

The gold standard for HBV genotyping is phylogenetic analysis of the complete genome, often performed using Sanger sequencing. HBV can be categorised into 10 genotypes (A-J)

and more than 40 subtypes based on nucleotide variations of 8% and 4-8%, respectively [43]. HBV genotypes have been linked to many clinically important features [44]. Genotype B and C are the most common genotypes in Asia (Figure 8) [45]. Genotype B has been associated with more HBeAg loss, lower viral load, less cirrhosis and HCC development than Genotype C (OR 5.11) [46-48]. Genotype A which is widely distributed in Africa is associated with more severe liver inflammation (raised ALT levels) and liver cirrhosis compared to Genotype D [49], whereas South American Genotype F is associated with more death from liver complications when compared with Genotype A & D [50]. In addition, HBV genotypes are also important in determining antiviral response, in particular to IFN-α treatment. Non-comparative studies have independently showed that Genotype A & B have a reasonable IFN response rates between 40-50% [51, 52] whereas Genotype C and D are associated with poor IFN response (13-24%) [53]. Importantly, different route of transmissions in various HBV genotypes with Genotype A predominantly acquired through sexual transmission, Genotype B and C through vertical transmission, and Genotype D a mixture of both [54, 55].

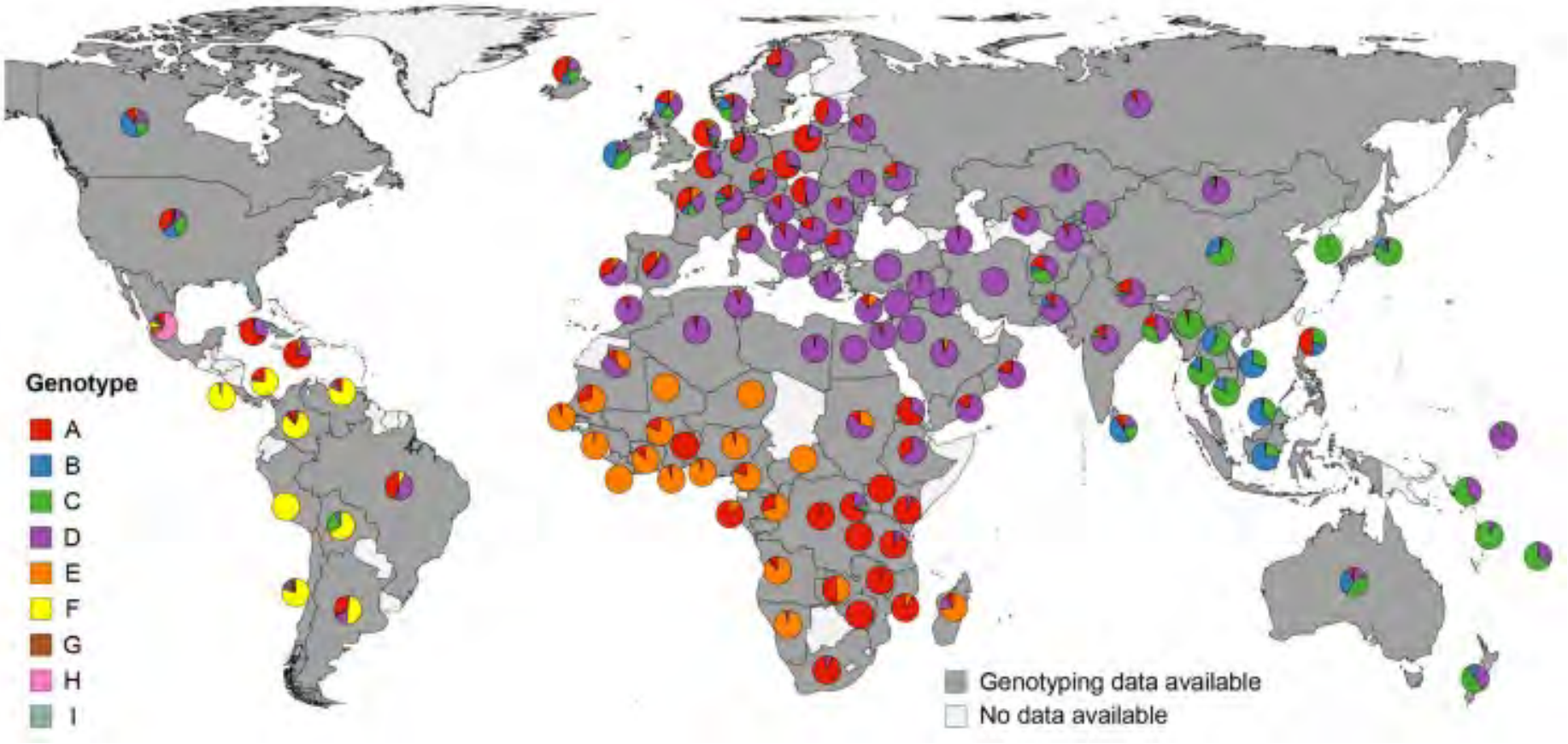

Figure 8: Global Hepatitis B Genotype Distribution
(Velkov. The Global Hepatitis B Virus Genotype Distribution Approximated from Available Genotyping Data. Genes 2018)

1.6 Natural History and Pathogenesis to HBV Infection

1.6.1 HBV Transmission

HBV transmission can occur via three mechanisms, perinatal, sexual and bloodborne. Perinatal infection is the most common form of transmission and in Asian countries and in the pre-vaccination era, 10-30% of babies born from HBsAg positive HBeAg negative mothers developed chronic infection [56], whereas 70-90% of babies born from HBeAg positive mothers developed chronic infection. Sexual and parenteral exposures to HBV result in <5% of chronic infection, presumably due to more mature immune system in the adults.

1.6.2 Phases of Chronic HBV

Clinically, chronic HBV infection can be categorised into four phases: (1) immune tolerant (2) immune active/clearance, (3) inactive carrier (4) immune escape.

1.6.2.1 Immune Tolerant Phase

The immune tolerant phase occurs early in the disease involving infants, children and young adults in which there is high level of viral replication, HBeAg positivity and normal liver functions. The majority of these HBV infected children are asymptomatic. In some cases, newborns to HBV-infected mothers were able to demonstrate HBV-specific T-cell responses, suggesting that there is adaptive immune response in place at the early foetal life. The immune response generated in the foetus or infants, however, are less pro-inflammatory, presumably an evolutionary adaptation to avoid immune reactions *in utero* [57, 58]. Studies of circulating and intrahepatic HBV-specific T cells in CHB patients in the immune tolerant phase have shown that although a T cell response was present, the global T cells ability to produce IFN-δ and TNF-α is impaired. Similarly, IFN-δ release from NK cells is also stunted [59]. ALT elevations have been more strongly associated with intrahepatic recruitment of granulocytes, monocytes and non-antigen specific T cells, which would explain the lack of

significant inflammatory response in these patients [60]. Transcriptomic analyses of peripheral blood samples showed poor expression of type I-III IFNs, proinflammatory cytokines (IL-1RA, IL-6, TNF, IL1β), T and NK cells cytokines (IL-17A, IL-21, IL-13) [61]. Despite a lack of ALT elevation, histologic investigations of children with CHB showed presence of focal necrosis and Kupffer cell hyperplasia [62]. These findings are suggesting that background liver damage is occurring in the immune tolerant phase despite seemingly normal liver enzymes. It remains unclear how this background inflammation translates into the long-term clinical outcome of CHB with unchecked viral replication as few studies examine the natural history of CHB in immune tolerant phase. One study comparing the cumulative risks of HCC and liver-associated events over 10 years in those with immune tolerant phase did not find any difference in the clinical outcome untreated patients and those treated with NA [63].

1.6.2.2 Immune Active

The immune active phase is characterised by high level of HBV DNA, liver inflammation with elevated liver transaminases, and sometimes evidence of liver fibrosis. The HBeAg to HBeAb seroconversion may occur during this period and is a marker for an active targeted immune response to HBV. Serum IL-10 and IL-12 are elevated during the immune active phase, possibly as a result of liver inflammation [64]. IL10-1082 G/G genotype is associated with higher serum IL-10 levels whereas IL-12β-10993 C/G genotype is associated with higher IL-12 secretion in PBMC [65]. Similarly, IL-10, IL-12β and IFN-γ mRNA expressions were upregulated in liver tissues from patients with immune active phase [66, 67]. In the liver tissue, there is lower furin and higher PD-1/PD-L1 expression, presumably induced by IFN-γ to avoid excessive hepatocyte damage [68, 69]. Furin suppression may

contribute to reduction in HBeAg and HBsAg biosynthesis, thus accelerating HBeAg seroconversion.

The annual spontaneous HBeAg to HBeAb seroconversion rate is very low (1.70%) in the first decade of life [70]. The majority of the children with chronic HBV infection as in the immune tolerant phase enter the immune active phase after puberty onset. The exact trigger that leads to immune active phase is not currently known. However, a number of studies have drawn possible associations. For example, in one study, an increased in 5-alpha reductase type II (SRD5A2), an enzyme responsible for converting testosterone to more potent dihydrotestosterone, is associated with early HBeAg seroconversion in males [71]. Dehydroepiandrosterone sulphate (DHEAS) has been considered a potential candidate for inducing HBeAg seroconversion due to its potent immune-modulating activity and that it increases 2-3 years before the onset of puberty [72]. Early menarche is also associated with early HBeAg seroconversion in females. However, it remains unclear whether the changes in HBV-directed immune response is a direct result of hormonal changes or a bystander effect. Studies examining the timing of HBeAg seroconversion suggests ethnicity and genotype may have some impact. The average age of HBeAg seroconversion is in the third decades for most Asians and Italians, whilst most Greeks seroconvert in second decades of life [48, 73, 74]. Studies on Asians with CHB suggests a decade earlier HBeAg seroconversion in genotype B in comparison with genotype C [48].

1.6.2.3 Immune Control

Following seroconversion from HBeAg to HBeAb, patients with CHB enter the immune control phase. This is accompanied by a non-replicative phase characterised with low serum HBV DNA, normalization of ALT and histologic activity. However, the highest number of

basal core promoter (BCP) and pre core (PC) mutants are seen in this phase. The clinical consequence of the emergence of BCP & PC mutants is unclear due to conflicting results on their associations with HCC and liver cirrhosis [42, 75, 76]. The overall prognosis of the inactive carrier is generally good. Spontaneous HBsAg clearance may occur at <0.5% annually [77]. Peripheral blood analyses showed higher level of T cell and lower level of IFN transcription activities during the immune control phase [61].

1.6.2.4 Immune Escape

Due to selection pressure from HBeAg/HBeAb seroconversion, replication competent HBV variants with precore or core-promoter region may be selected. The most common variant (G1896A) is HBeAg deficient due to presence of a stop codon in the precore region. Other variants contain mutations in the start codon of the precore region (A1762T) or in the core promoter region (G1764A), resulting in reduced HBeAg production. Dual BCP mutations A1762T/G1768A have been associated with HCC development due to upregulation of SKP2 and downregulation of p21. BCP mutations but not PC have been associated with liver inflammation and cirrhosis [78]. Gene signature analyses from serum in immune escape phase suggest restoration of NK cell activities with associated ALT elevation, consistent with the findings of liver inflammation in clinical studies [78].

1.6.3 Immune Response in Acute Infection

The innate immune response represents the first line of defence against viral infection and is key for establishing an antiviral state and the generation of a robust adaptive response [79]. Conserved regions of viral nucleic acids or proteins, often referred to as pathogen associated molecular patterns (PAMPs) are first recognized by the pattern recognition receptors (PRRs), inducing downstream cytokines and ISG expressions, eventually leading to an antiviral state.

Traditionally HBV has been regarded as a stealth virus due to lack of downstream ISGs stimulation. However, it is now recognized that HBV can be detected by a number of PRRs. HBV core antigen can trigger signalling through TLR-2 receptor recognition on Kupffer cells, leading to suppression of HBV-specific T cell immunity [80] while HBV pgRNA can bind to RIG-I in hepatocytes and trigger a weak type I but strong type III interferon responses [81]. HBV DNA can also be detected by the cyclic GMP-AMP Synthase (cGAS) when exposed in the cytoplasm [82].

In adult infection, the majority of individuals undergo an acute infection and subsequent viral clearance. The dynamics of acute HBV infection suggest that there is an early non-cytopathic mechanism in restricting HBV replication which precedes elevation of ALT and T-cell infiltration [83-86]. In human and chimpanzee models, acute HBV infection has not resulted in type-I interferon upregulation except immunosuppressive cytokine IL-10 [87] . It is highly probable that this early control of HBV replication is achieved by NK and NKT cells due to their early peak in peripheral blood during acute infection. In the HBV transgenic mice model, NK and NKT cells have been shown to restrict HBV replication while in the chimpanzee model, IFN-γ release by NK and NKT cells is associated with reduction in HBV DNA [87]. Ex-vivo experiments also suggest that IFN-γ can destabilise cccDNA. Importantly, T cell mediated responses are essential in eliminating HBV from infected hepatocytes. It is achieved by a strong polyclonal T-cell response towards HBV core and e antigen and various cytokines released from CD8+ T cells [84, 85].

1.6.4 Immune Response in Chronic Infection

In chronic HBV infection, NK cells demonstrate a restricted functional response and are able to induce CD8 T-cell depletion occurs through caspase-8-mediated apoptosis [88]. *In vitro* studies using HepaRG cells and primary human hepatocytes (PHH) have shown a lack of

IFN-mediated immune response [89]. Other studies have shown direct interactions between HBV viral proteins with innate immune signalling molecules, resulting in active suppression of ISG expression (Table 1). Collectively, HBV is a poor inducer and active suppressor of innate immune responses, although the cellular response and ability of HBV to dampen the innate responses is not well characterised.

Table 1: Immunomodulating Effect of HBV

	Mechanisms	**Reference**
LUBAC	HBV induces parkin and linear ubiquitin assembly complex to attenuate MAVS activation	[90]
HBsAg	Inhibits TLR2 and JNK, preventing IL-12 production	[91]
HBV polymerase	Inhibits α5 and protein kinase C-δ, preventing activation of STAT1/2 heterodimers	[92]
HBsAg/HBeAg	Inhibits interaction of major vault protein (MVP) and MyD88, thus suppressing type I IFN	[93]
HBsAg/HBeAg	Inhibits ISG tetherin which plays a role in preventing viral budding	[94]
HBV polymerase	Interacts with DDX3 and subsequently inhibits TBK1	[95]
HBV polymerase	Interacts with HSP90β to prevent activation of IKKs	[96]
HBx	Inhibits IRF3 & IRF7 translocation	[97]

1.7 Hepatocellular Carcinoma in HBV

While the mechanisms that contribute to HCC development remain unclear, it is obviously a result of multifactorial insults to the liver over an extended period of active HBV replication. This is clearly shown in many clinical studies in which HBV viral load is independently associated with HCC risks across many HBV genotypes, ethnicity, age and geographical locations [98]. One of the hallmarks of chronic HBV infection is its ability to induce oncogenesis through four major mechanisms: (1) chronic inflammation and regeneration, (2) direct impact of HBV proteins on oncogenes and tumour suppressor genes, (3) epigenetic changes and (4) tumour favourable microenvironment. The HBx plays a central role in many of these mechanisms, through its interactions in a myriad of cellular signalling, such as Ras/Raf/MAPK/ERK, JAK/STAT, PI3K/AKT, Wnt/β-catenin and apoptosis (external and intrinsic) pathways [37, 99-107].

In chronic infection, HBV is able to minimise the activation of innate immune response in order to persist in hepatocytes. Persistent viral replication and ineffective viral clearance from NK, NKT and PMN cells help mediate hepatocyte injury. This creates an environment of chronic inflammation, oxidative stress, hepatocyte destruction, fibrosis and tissue regeneration which encourages genetic instability. Numerous signalling pathways, such as Ras/Raf/MAPK/ERK, JAK/STAT, PI3K/AKT, Wnt/β-catenin and apoptosis (external and intrinsic) pathways, have been implicated for the pathogenesis of HBV-induced HCC through pro-proliferative, anti-apoptotic and increasing the malignant transformation potential of cells [106, 108-113]. However, the extent of individual pathway in oncogenesis is less defined. HBx has been shown to directly activate the MAPK-ERK pathway through interaction with Ras, leading to hepatocytes entering into a proliferative S phase, which is vulnerable to malignant transformation [114]. In addition, activation of JAK-STAT signalling activation has been shown to be strongly associated with the development of HCC, and HBx is capable

of constitutively enhancing the expression of STAT3 and STAT5 within this pathway [115]. Another pathway activated by HBx is the PI3K/AKT pathway which leads to dysregulation of cell growth and transformation [116]. The Wnt/β-catenin pathway has been increasingly recognised in its association with many cancers, including HCC. This pathway plays an important role in regulation of stem cell activation and proliferation and studies using hepatoma cell lines suggests that HBx, in addition to Wnt-1 is critical in the activation of Wnt/β-catenin signalling cascade [112].

In addition to chronic inflammation, HBV viral proteins also have direct impact on carcinogenesis through interactions with oncogenes. HBx upregulates miRNA miR-181 which in turn downregulates PTEN, resulting in uncontrolled cellular proliferation [117]. Upregulation of miR-148a and miR-602 by HBx results in inhibition of tumour suppressor proteins. HBx also directly binds to the C-terminus of p53, the tumour suppressor gene, leading to interference in p53-mediated apoptosis, which may have a role in early stages of HCC development [118].

In chronic HBV infection, HBV integration into the host genome is often a random event, although integration at chromosomal fragile sites, scaffold attachment regions and repeat sequence-rich regions have been described [119, 120]. Host genome integration events often result in integration of HBx and truncated PreS/S sequences into many sites of host DNA, inducing oncogenesis through trans-acting mechanisms. Upregulation of EpCAM and β-catenin by HBx in adult hepatocytes suggest induction of stem cell phenotypes in HBV infection [121]. In HCC xenograft models, invasive tumours can only be generated from EpCAM+ cells, suggesting the association of stem cell phenotypes with HCC oncogenesis [122].

In animal models, HBx and HBs induce calcium accumulation in the mitochondria with resultant activation of PYK2, SRC kinases and increased reactive oxygen species which are involved in early HCC oncogenesis [123]. In addition, CD8 T cell exhaustion induced by HBx-stimulated upregulation of TGFβ1 promotes a tolerogenic environment in the liver [101]. Furthermore, HBx also upregulates ANG2, promoting angiogenic environment for HCC.

1.8 Antiviral Therapy and Drug Development

Interferon-α was the most widely used drug for HBV treatment in the 1990s. Since then, various nucleoside/nucleotide analogues (NA) have been developed with great success in controlling HBV replication.

NA are prodrugs that require cellular uptake and conversion by cellular kinases into active triphosphate metabolites. The active form of NA serves as a competitive inhibitor of natural nucleotide for DNA synthesis, resulting in chain termination. NAs also have an additional mechanism of action by interfering with protein priming. Guanosine analogues (e.g., Entecavir) can interfere with HBV protein priming whereas adenosine analogues (e.g., Adefovir, Tenofovir) can impair synthesis of dGAA trinucleotide. Both HBV and HIV share many structural and functional similarities in their reverse transcriptase, and therefore could be inhibited by similar NA. Tenofovir (Tenofovir disoproxil fumarate TDF or Tenofovir alafenamide TAF) and Entecavir are the two most biologically active and most widely used direct-acting antivirals for HBV. TDF is the initial formulation used in the treatment of HBV and HIV. TAF is a later formulation in the form of a prodrug in which the phosphorylated moiety tenofovir diphosphate accumulates in the intracellular compartment at much higher concentration. The differences in pharmacokinetics allow TAF to be used at a lower

treatment dose, minimising potential renal and bone complications. Both Tenofovir and Entecavir (ETV) treatment have been associated with reduced viral reactivation, hepatitis and mortality compared with other NAs [124].

NA are often prescribed for long-term suppression of HBV, thus preventing NA resistance is crucial in the management of CHB. This is particularly relevant to HBV due to its high estimated mutation rate of 1.4-3.2 $x10^{-5}$ nucleotide substitution per site and high level of viral replication in the liver [125]. Most common resistance mutations occur during NA therapy are L180M (spacer region) and M204I/V (YMDD motif, Pol/RT region) [126]. Clinically, cumulative resistance associated with Lamivudine (LMV), Adefovir and Telbivudine use is significantly higher than Tenofovir and Entecavir [127]. Virological breakthrough in TDF or ETV often requires accumulation of several mutations in the RT regions. Interestingly, due to the structural similarities between the RT between HIV and HBV, use of ETV in HIV can select for M184I/V mutation, promoting resistance of other anti-HIV drugs such as LMV and emtricitabine [128].

The effect of NA on the development of HCC is not entirely clear-cut. Meta-analysis of Nucleos(t)ide analogues suggest that ETV-treated patients have a lower incidence for HCC compared with LMV. Despite this, NA-treated patients with pre-existing liver cirrhosis have a 5.49x higher incidence of HCC than those without cirrhosis [129].

Pegylated interferon-α (2a/2b) is the only drug that can achieve functional cure at a modest rate (3-7%) in selected HBV genotypes. Functional cure is an important treatment endpoint for CHB, which is defined by sustained HBV surface antigen clearance. Sustained HBV surface antigen loss is associated with lower liver cirrhosis and liver associated mortality

[130]. HBV genotype A and B appear to have a higher rate of HBeAg and HBsAg loss than genotype C and D, although these are not direct comparative studies [131]. Higher pre-treatment level of liver inflammation (ALT levels) is a strong predictor of favourable response [132]. The mechanism of interferon-α in restricting HBV is not fully elucidated due to the complexity of HBV interactions with the innate immune system. In cell culture and murine models, interferon-α induces degradation of HBV cccDNA by induction of APOBEC3s (a cytidine deaminase) and cell-mediated innate immune response [133].

Current treatment strategies have two major shortfalls: (1) treatment of HBV patients is often life-long and (2) HCC risk under NA treatment is reduced but not eliminated [134]. As such novel therapeutic strategies (Table 2) are in constant development and employ the use of (1) direct acting antivirals that target various parts of the HBV life cycles and (2) immune modulators that induce HBV clearance from infected cells with various host-targeting strategies. Drug development has been challenging due to a lack of physiologic *in vitro* model system in the discovery of novel antiviral host targets and prediction of drug toxicity.

Table 2: Novel HBV Treatment

Mechanism of Action	Drug	Clinical Trial Stage	NIH Clinical Trial Identifier	Reference
Direct Acting Antivirals				
Entry receptor inhibitor	Myrcludex B	Phase 2	NCT02881008	[135]
RNA silencers	ARC-520/-521	Terminated	NCT02452528	[136]
	ARB-1467	Terminated	NCT02631096	
	ARB-1740	Preclinical		[137, 138]
	ALN-HBV02	Phase 1/2	NCT02826018	
	GSK 3228836	Phase 1	NCT04676724	
Core protein inhibitors	AL-3778	Phase 1/2	NCT03125213	
	ABI-H0731	Phase 1	NCT03109730	
	BAY 41-4109	Phase 1		[139]
	GLS4	Phase 1		[140]
	JNJ-56136379	Phase 1	NCT03361956	
	AB-423	Preclinical	N/A	
HBsAg release inhibitors	REP 2139	Phase 2	NCT02565719	
	REP 2165	Phase 2	NCT02565719	
Immune Modulators				
RIG-1 NOD2 activator	SB 9200	Phase 2	NCT02751996	[141-143]
SMAC inhibitor	Birinapant	Terminated	NCT02288208	
Checkpoint inhibitors	PD-1/PDL-2 mAb	Phase 1B	ACTRN12615001133527	[144]
	CTLA-4 mAb	Phase 1	NCT01445379	
IL-7	CYT107	Phase 1/2a	N/A	
Interferon-λ		Phase 2	NCT01204762	[145]
TLR-7 agonist	GS-9620	Phase 2	NCT01590654	
Therapeutic vaccines	GS-4774	Phase 2	NCT01943799	
	ABX 203	Phase 2/3	NCT02249988	
	AIC649	Phase 1	N/A	
	FB-02.2	Phase 1	NCT02496897	
	INO-1800	Phase 1	NCT02431312	
	TG1050	Phase 1/1B	NCT02428400	[146]

1.9 HBV *in vitro* Model Systems

The evolution of cell culture techniques and our understanding of stem cell biology have allowed significant development of HBV *in vitro* model systems over the past decade. Technologies such as 3D culture, co-culture systems and tissue engineering techniques are gradually closing the gaps between *in vitro* and *in vivo* culture systems. Earlier culture systems using hepatoma derived cell lines such as HuH-7 or HepG2 predominately suffer from poor susceptibility to HBV infection, thus requiring the use of transfected plasmids to study the HBV life-cycle. With the recent discovery of NTCP as the HBV entry receptor, the short-coming of transformed cell lines has been predominately overcome with the creation of NTCP-expressing cell lines [147]. The major focus of HBV culture system development is now drawn to the applicability of such model systems. Qualities such as physiologic and anatomical resemblance to the liver organ, their ability to model for disease pathogenesis (E.g., HCC, liver cirrhosis, viral resistance) and application such as drug responsiveness to various therapeutic targets have become very important, if we are to develop novel treatment strategies with the ultimate aim of HBV cure.

Here we describe some of the currently used *in vitro* model systems for HBV modelling, focusing on human tissue derived culture systems. These models can be broadly categorised into: (1) immortalised cell lines, (2) primary hepatocytes and (3) stem cell-derived hepatocyte-like cells (HLCs) and are summarised in Table 1 outlining the advantages and disadvantages of each model system.

Table 3: Classification of *In vitro* Model Systems for HBV

	In vitro Model	Advantages	Limitations	Reference
Immortalised Cell Lines	HepaRG	Long-term culture Metabolic activities and immune response comparable to primary hepatocytes	Low level infection Requires differentiation Difficult to work with	[148]
	HLCZ	Low viral inoculum. Supports long-term HBV infection	Defective immune responses	[149]
	HuS-E/2	Immortalised hepatocytes, susceptible to HBV and HCV	Transformed cells Tumour transformation with prolonged culture	[150]
	PH5CH	Immortalised hepatocyte-like cells, susceptible to HBV and HCV	Transformed cells, limited characterisation	[151]
	Huh7-NTCP	Long-term culture	Defective immune responses	[14]
	HepG2-NTCP	Long-term culture	Defective immune responses	[14]
	HepaRG-NTCP	Long-term culture	Requires differentiation	[14]
Primary Hepatocytes	PHH	Gold standard for metabolic activities	Limited life-span	[152, 153]
	Microfluidic Culture + Kupffer Cells	Low viral inoculum. Good viral spread Maintains PHH differentiation	Highly complex system.	[154-157]
	5C-Cultured PHH	Low viral inoculum Support HBV infection for a reasonably long period	Similar complexity with PHH isolation	[158]
Stem Cell Derived Hepatocyte Like Cells	Human Liver Organoids (adult stem cells)	Genetic and phenotypic resemblance with host hepatocytes Long-term culture possible	Lack of other immunologically important cell types	[159]
	iPSC-HLC	Sustain full HBV lifecycle Can be co-cultured with non-parenchymal cells	Genome instability Limited lifespan Optimisation of differentiation required Incomplete reprogramming	[160-165]
	ESC-HLC	Long-term culture of well characterised ES cell line. Sustain full HBV lifecycle and viral spread.	Limited availability due to cellular origin Complex differentiation process	[164]
Others	PHH-Progenitor Reversion	Expandable PHH	Limited life-span	[166]

Table 4: Culture Characteristics of *in vitro* Models

Model	Chromosomal Abnormalities	Cellular Origin	NTCP Expression	Susceptibility to HBV Infection	Level of HBV Replication	Co-culture	3D Culture	Culture Complexity	Innate Immune Response	Donor Variation	Genetic Manipulation	Other infection
HepaRG	Present	Bipotent progenitors from hepatoma	Yes. Following differentiation	Inoculum of ≥ 200 GE/cell ccHBV	Low. pgRNA peaks between day 5-8	Cannot tolerate T cell co-culture	Improved metabolic activities Effect on HBV unknown	Moderate	Good	No	Yes	HCV
HLCZ	Unknown	Hepatocytes	Yes	Inoculum of 20 GE/cell ccHBV or pHBV	High. Similar to PHH	Unknown	Unknown	Low	Unknown	No	Yes	HCV
HuS-E/2	Unknown	Hepatocytes	Yes. Following differentiation	Inoculum of ≥ 200 GE/cell ccHBV or pHBV from transgenic mice	Unknown. No comparison.	Unknown	Yes	Low	Unknown	No	Yes	HCV
PH5CH	Unknown	Liver epithelial cells	Unknown	Yes. Inoculum unknown	Unknown	Unknown	Unknown	Low	Unknown	No	Yes	HCV
Huh7-NTCP	Present	Hepatoma	Yes	Poor	Poor	Unknown	Yes	Low	Poor	No	Yes	Unknown
HepG2-NTCP	Present	Hepatoma	Yes	10-100 GE/cell ccHBV	Good	Unknown	Yes	Low	Poor	No	Yes	No
HepaRG-NTCP	Present	Hepatoma	Yes	Yes	Good	Unknown	Yes	Moderate	Good	No	Yes	Unknown
PHH	No	Hepatocyte	Yes	Yes	High	Yes	Yes	High	Good	Yes	Poor	HCV HAV
Microfluidic Culture + Kupffer Cells	Unknown	Hepatocyte	Yes	Yes. Low inoculum 0.05 GE/cell	High	Yes	Yes	High	Good	Yes	Unknown	Unknown
5-C PHH	Unknown	Hepatocyte	Yes	Yes. 10 GE/cell	High	Unknown	Unknown	High	Good	Yes	Unknown. Probably low	HCV
Human Liver Organoids (adult stem cells)	No	Bipotent stem cell	Yes. Following differentiation	Inoculum of ≥ 200 GE/cell ccHBV or less for sHBV	pgRNA peaks day 8-10	Yes	Yes	High	Good	Yes	Yes	HCV
iPSC-HLC	Unknown	Somatic cells	Yes. Following differentiation	Inoculum 500-5000 GE/cell	High	Yes	Yes	High	Good	Yes	Poor	HCV
ESC-HLC	Unknown	Embryonic cell mass (germ layers) within blastocyst	Yes. Following differentiation	Inoculum of 50-300 GE/cell	pgRNA and cccDNA peak at day 12	Unknown	Yes	High	Unknown	Yes	Poor	HCV

Table 5: HBV Disease Modeling

Model	Acute Infection	Chronic Infection	Drug Resistance Development	Viral Spread	Innate Immunity	Liver Injury & Regeneration	Modeling for HCC Development	Assessment of Host Factors
HepaRG	Yes	No	No	Limited	Yes	No	Unknown	Yes
HLCZ	Yes	Yes	No	Yes	Unknown	No	No	Limited
HuS-E/2	Yes	No	No	Limited	Unknown	No	No	Limited
PH5CH	Yes	No	No	Unknown	Unknown	Unknown	No	Unknown
HepG2-NTCP	Yes	No	No	No	No	No	No	Limited
Primary Hepatocytes	Yes	No	No	Yes	Yes	No	No	Yes
Microfluidic 3D culture	Yes	No	No	Yes	Yes	No	No	Yes
5-C PHH	Yes	Yes. Up to 35 days	No	Yes	Yes	No	No	Yes
ESC HLCs	Yes	Yes. Up to 28 days	No	Yes	Unknown	No	No	Yes
iPSC HLCs	Yes	Yes	No	Yes		No		
AdSC Organoids	Yes	Unknown	Unknown	Yes	Yes	Potentially with T cell co-culture	Unknown	Yes

Table 6: Potential Clinical Applications of HBV Model Systems

Model	Drug Screen	Personalised Drug Response	Personalised Drug Toxicity	Viral Reactivation	Co-infection with other Viruses
HepaRG	Yes	No	No		
HLCZ	Yes	No	No	Unknown	Yes
HuS-E/2	Yes	No	No	Unknown	Yes
PH5CH	Unknown	No	No		
HepG2-NTCP	Yes	No	No. Lack drug metabolism		No
Primary Hepatocytes	Yes	Yes	Yes	Unknown	Yes
Microfluidic 3D Culture	Yes	Yes	Yes	Unknown	Unknown
5-C PHH	Yes	Yes	Yes	Unknown	Yes
ESC HLCs	Yes	Yes	Yes	Unknown	Yes
iPSC HLCs	Yes	Yes	Yes		Yes
AdSC Organoids	Yes	Yes	Yes	Unknown	Yes

1.9.1 Immortalised Hepatocyte/Hepatoma Cell Lines (Table 3)

1.9.1.1 HepaRG

HepaRG cells are a bipotent human progenitor cell line that originates from a resected liver tumour of a HCV infected patient [167]. HepaRG cell carry some karyotypic abnormalities with translocations between chromosome 12 and 22, albeit much lower genetic aberrations than the immortalised hepatoblastoma cell line, HepG2 [167]. HepaRGs are genetically stable in culture and are not tumourigenic despite their origin. Proteome and secretome analyses suggest that HepaRG closely resembles primary hepatocytes [167]. They can be differentiated into a mix of hepatocyte- and cholangiocyte-like cells and assume hepatocyte polarity when exposed to either DMSO or Forskolin [168]. HepaRGs are serum-dependent, and when cultured with 2% DMSO during the process of differentiation, can demonstrate high levels of hepatocyte metabolic activities, including drug detoxifying enzymes and drug sensing receptors. In addition, HepaRG cells have an intact Wnt-β-catenin pathway with significant upregulation of progenitor cell marker, LGR5 upon Wnt stimulation [169, 170].

Phenotypically, HepaRG cells retain some features of the biliary oval cells with high expression of CK19 and M2-PK. Progenitor markers are suppressed during the differentiation process. When transdifferentiated under low density *in vitro* culture conditions, they change from a proliferative phase to static phase and finally assume a differentiated phase consisting of a mixture of hepatocyte and biliary-like cells. Transplantation in mice with differentiated or undifferentiated HepaRG, however, results in a predominant hepatocyte phenotype capable of repopulating the liver [171].

Despite significant similarity between HepaRG and PHH, susceptibility of HepaRG to HBV infection is low and requires well-defined culture conditions. This includes the use of PEG to

precipitate the virus, prolonged differentiation of more than two weeks with 2% DMSO and glucocorticoids. Proliferative HepaRG cells do not express functional NTCP receptor, and thus are unlikely to be permissive to HBV [172]. Defined differentiation medium consisting of DMSO and 4SM results in highly differentiated HepaRG cells, however, the level of HBV replication is still lower than PHH [173]. Culture of HepaRG cells in a 3d spheroids format can improve expression of metabolic markers but the effect on HBV infection is unclear [174]. Typically, HBV replication in HepaRG cells peaks between day 5-8 with gradual decline over 4-6 weeks, hence limiting its capacity to model for chronic infection [148]. In order to compensate for this short-coming, HepaRG-FRG chimeric mice have been developed and are able to sustain HBV infection for more than 40 weeks [173]. Another limitation of HepaRG cells is its intolerability of other culture media, hence restricting T-cell co-culture system development to assess complex innate immune interactions [175].

1.9.1.2 HLCZ

The HLCZ cell line is a clonal line derived from a hepatoma resected from a HCV patient, with subsequent isolation following inoculation into immunodeficient mice [149]. This cell line is permissive to HBV infection with very low inoculum and efficiently replicates HBV to similar levels of PHH. The HBV pgRNA gradually increases overtime supporting cellular spread and HBV replication for at least 90 days and therefore serves as a potential candidate for chronic HBV infection modelling in long-term studies. In addition, this cell line also supports the full life cycle of HCV and allows co-infection of HBV/HCV[149]. HLCZ is yet to be fully characterised, and current understanding of its genetics, metabolic activities and innate immune response in comparison with PHH is limited. It is unclear if this cell line would permit modelling for development of drug-resistance HBV and assessment for viral reactivation following antiviral cessation.

1.9.1.3 HuS-E/2

HuS-E/2 is a primary hepatocyte cell line derived from a 9-year-old patient with primary hyperoxaluria [176]. Isolated hepatocytes were transduced with CSII-EF-hTERT and LT or HPV18/E6E7 to induce proliferation and immortalization. The HPV18/E6E7 immortalised clones were named HuS-E. The genetic background and stability in culture is yet to be characterised.

HuS-E/2 expresses comparable levels of albumin, apoliporotein-A1, transferrin and CYP450 to PHH at earlier stage of isolation. The CYP450 expression appears to decrease over time, suggesting gradual dedifferentiation in culture. Albumin and HNF4 expression can be further enhanced with 3D culture. Due to the transformed nature of HuS-E/2, increase in MMP2, MMP9 and AFP activities were seen with prolonged culture, consistent with development of tumour phenotypes.

HuS-E/2 is poorly susceptible to HBV infection unless it is cultured in 2% DMSO. DMSO treatment significantly increases NTCP expression and infected cells from 1% to 30% [177]. However, despite DMSO treatment, as the culture start to develop more tumour-like phenotype, the susceptibility to HBV also decreases.

1.9.1.4 PH5CH

PH5CH is an epithelial cell line originated from a liver resection for a patient with HCC. The normal liver tissue was isolated and subjected to SV40 large T antigen transduction to create an immortalised cell line [178]. The PH5CH expresses both cytokeratin and albumin, consistent with an epithelial/ductal cell origin. Earlier characterisation showed no p53 oncogene abnormalities, but karyotypic and genetic characteristics are largely unknown. This

cell line while difficult to maintain in culture, is susceptible to both HBV and HCV infection, although the susceptibility and level of HBV replication is unclear [179].

1.9.2 NTCP-expressing Cell Lines

Human hepatoma derived cell lines such as Huh7 and HepG2 are not permissive to HBV infection and vector delivery systems are required to introduce the HBV genome, such as a 1.3x mer-HBV [180]. Hence it is not possible to study the HBV entry mechanism using these cell lines. However, the recent discovery of NTCP as a HBV entry receptor has allowed engineering of NTCP transduced hepatoma cell lines with high permissiveness to HBV infection [147].

HepG2-NTCP is now widely used to study HBV infection in culture and allows infection with as low as 10 genome copies/cell when infected under spinoculation and cultured in the presence of DMSO and PEG [181]. This culture system allows short-term assessment of viral spread evident with co-culturing with HepDE19-GFP cells that produce HBV. It is unclear whether this cell line would sustain HBV replication beyond 2-3 weeks. It has also been used in drug efficacy screening for HBV antivirals. Other NTCP-expressing cell lines, including Huh7-NTCP and AML-NTCP (murine liver) are considerably less permissive to HBV infection [147, 182]. Some murine/rodent cell lines reconstituted with human NTCP (Hep56.1D-NTCP, Hepa1-6-NTCP and TC5123-NTCP) are non-permissive to HBV infection but are susceptible to HDV infection [14, 183]. As HDV utilises NTCP as an entry receptor, additional host-factors that permit HBV infection may account for these differences. The infection rates in HepaRG-NTCP are slightly less than HepG2-NTCP but appears to have similar levels of replication and HBeAg/HBsAg secretion. Most recently, a derivative of Huh7 cell line, Huh7D-NTCP has been shown to produce higher levels of HBV replication compared to HepG2-NTCP [184].

The major limitation of hepatoma-derived cell lines is the non-physiological nature of the culture system. Hepatoma cell lines in general, suffer from altered cellular metabolism, and hence is not a suitable model for assessing antiviral metabolism and toxicity. In addition, altered innate immunity significantly limits the assessment of cellular responses to various hepatotropic viral infections [185].

1.9.3 Primary Human Hepatocytes

While primary hepatocytes isolated from liver donors can be infected with HBV, and once often considered the gold standard, they are difficult to isolate, refractory to passage, rapidly dedifferentiate in culture and there is significant donor variability [186]. In general, close association with a liver transplant unit is essential to receive normal liver "cut down" samples. By culturing multiple islets of primary hepatocytes among the fibroblast cells, micropattern co-culture system (MPCC) is able to maintain hepatocyte differentiation for up to 3 weeks [160], although this culture system is technically challenging.

3D microfluidic PHH culture is another liver-on-a-chip culture system developed to mimic the liver physiology and architecture in an attempt to reduce hepatocyte dedifferentiation in culture [155, 156]. In this system, the PHH are seeded in collagen-coated scaffolds, and allowed to form islands of 3D microtissue. It is continuously perfused with growth medium to provide nutrients. This system can be cultured with non-parenchymal cells such as Kupffer cells, stellate cells and liver sinusoidal endothelial cells. The PHH developed typical hepatocyte polarity and sustained metabolic activities and NTCP expression at the level of freshly isolated PHH were observed for up to 40 days. Despite having similar levels of metabolic marker expression with PHH spheroids, the 3D microfluidic has a distinctive advantage in which it can be infected with very low inoculum of HBV. Inoculum as low 0.05

GE/cell can lead to sustained infection of at least 25 days, at a level much higher than self-assembling PHH. This culture system also allows assessment of innate immune response, cell-cell interactions and antiviral response.

Xiang *et al.* subsequently developed a five chemical (5-C) culture system for PHH to maintain the phenotypes of terminally differentiated hepatocytes [158]. They established a defined culture medium consisting of FSK, SB43, DAPT, IWP2 and LDN193189 in order to block TGF-β signalling and epithelial-mesenchymal transition (EMT) expression. This leads to maintenance of mature hepatocyte surrogate markers such as albumin, urea and CYP450 enzymes expression for up to four weeks. The 5-C PHH can be infected with HBV as low as 10 GE/cell, with HBV replication up to at least 35 days. Drug and innate immune response can be assessed using this culture system and the 5-C PHH can also be infected with HCV. However, the use of PHH is not feasible for most laboratories due to the technical demanding nature of their isolation and culture.

Another novel model system developed by Hu *et al.* involves reprogramming mature hepatocytes into proliferative hepatocyte organoids, with transcriptomic profiles of these organoids very similar to PHH [187]. Proof-of-concept transplantation experiment was carried out successfully by repopulating damaged mouse liver with human hepatocyte organoids. This model system shows great similarity to PHH and could serve as an alternative model system to study HBV.

1.9.4 Stem-cell derived Hepatocyte-like Cells (HLCs)

1.9.4.1 Embryonic Stem Cells Model

Embryonic stem cells are pluripotent stem cells derived from the inner layers of blastocyst stage pre-implantation embryos [188]. Various embryonic cell lines have now been developed and characterised for their karyotypic features, gene expression for "stemness" and genetic stability in culture conditions. Bhattacharya *et al.* noted a significant variation of gene expression between different embryonic cell lines during the early stages of cell line differentiation into embryoid bodies [189]. These differences may reflect the inherent potential of each cell line to differentiate towards specific lineages. One such example is the H1, H7 and H9 cell lines which have been used to generate HLCs [190].

Generation of immature hepatocyte-like cells from ESC requires a three-stage process: (1) development of definitive endoderm from H1 line (Activin A, Wnt3A), (2) Differentiation into early hepatocytes (KSR, KODMEM) and (3) differentiation into immature hepatocytes (OSM, HGF). This process can take at least 17 days and further development into HLCs with high level of hepatocyte markers may require even more advanced and prolonged differentiation process with addition of dexamethasone and insulin [191, 192].

Xia *et al.* assessed the differentiation and susceptibility of H9-derived HLCs to HBV infection [164]. H9 cell line consists of normal 46, XX karyotype with all three germ layers with typical expressing stem cell markers (SSEA-3/4, TRA-I-60, TRA-1-81, alkaline phosphatase). The ESC-derived HLCs achieved highest levels of NTCP mRNA at day 12 of differentiation and is susceptible to HBV infection from low inoculum of 50 GE/cell. With inoculum of 300 GE/cell, infection rates between 50-70% can be achieved. HBV replication as indicated by cccDNA and HBV RNA expression peak at day 14 post-infection, coincides

with extracellular secretion of HBeAg/sAg. This culture system could support HBV infection for at least 28 days. Drug responsiveness to infected HLCs to Myrcludex or Entecavir appear to be more apparent than PHH or hepatoma cell lines.

While embryonic stem cells have their place, the main drawback of using ESC-derived HLCs in HBV modelling is its ethical concerns of using embryonic tissue in research. This model system is now predominately superseded by iPSC derived HLCs which can support similar levels of HBV replication without the ethical concerns of cellular origin.

1.9.4.2 Induced Pluripotent Stem Cells Model (iPSC)

iPSC are pluripotent stem cells derived from reprogramming of well-differentiated somatic cells such as skin fibroblasts, keratinocytes, melanocytes, adipose cells, blood cells etc. Using ectopic expression of Yamanaka factors (Oct3/4, Sox2, Klf4 and c-Myc) through either genetic and non-genetic approaches, somatic cells can be reprogrammed to achieve pluripotency [193]. In the process of reprogramming, c-Myc is the most important factor. This process is relatively conserved among all primates and the resultant iPSC shares many similarities with ESC such as pluripotent gene expression, DNA methylation and embryoid body formation. Ang *et al.* detailed a roadmap to differentiation of hepatocytes from pluripotent stem cells [194]. Following reprogramming of somatic cells to iPSC, a multi-step sequential differentiation is required to achieve hepatocyte phenotypes. iPSC is initially differentiated to definitive endoderm phenotype, followed by formation of liver bud, and further differentiation into hepatocyte and cholangiocyte lineages. The hepatocyte-like cells derived from iPSC have been shown to demonstrate similar levels of metabolic markers and NTCP as PHH. The iPSC-HLCs are permissive with HBV, although requires very high inoculum to achieve infection and to assess HBV spread through the culture [162].

Further improvement of HBV replication can be achieved by culturing the iPSC-HLC in 3D extracellular matrix to allow self-organisation into liver organoids [165]. Ten days post-infection, these iPSC-HLC liver organoids demonstrate HBV pgRNA, cccDNA and extracellular DNA at the levels of PHH and are able to sustain infection for at least 20 days. It can also be used to study ISG kinetics post HBV infection for up to 3 weeks, albeit the ISG induction is more restricted compared to primary hepatocytes [160, 195, 196].

The main limitation of iPSC-derived culture system is the high rates of *de novo* mutations. Chromosomal abnormalities can occur following reprogramming and during passages, resulting in large clonal differences [197, 198]. The use of lentiviral vectors to deliver reprogramming transcription factors raise concerns of insertional mutagenesis and carcinogenesis potentials. Incomplete reprogramming can also occur resulting in cells that are vastly different from parental cells. These cells may demonstrate tendency for teratoma formation, poor growth, poor differentiation and abnormal transcription [199, 200]. The use of iPSC in translational medicine would require application of stringent criteria to link both biological and molecular phenotypes of iPSC with parental cells [201].

1.9.4.3 LGR5+ Stem Cell Model

LGR5+ intrahepatic ductal cells represent the bipotent adult stem cells that would regenerate the liver in the event of significant liver injuries. These stem cells, sometimes addressed as adult stem cells, originate from a subpopulation of hepatoblasts (~2%) during early embryonic development and persists into adulthood in non-proliferative state [202, 203]. During liver tissue damage, TET1-mediated hydroxymethylation and Kupffer cell mediated activation of Wnt/β–catenin pathway initiates these liver progenitor cells to undergo

regenerative pathways [204-207]. These stem cells have the potential to develop into either hepatocyte or cholangiocyte lineages.

Upon stimulation with the exogenous factors Wnt3a, R-spondin and Noggin, these liver bipotent stem cells proliferate in culture and develop into self-organising liver organoids [208]. These organoids are genetically stable with 10-fold fewer base substitutions compared with iPSC during cell reprogramming. Following differentiation, liver organoids developed both hepatocyte and ductal phenotypes with upregulation of metabolic markers and detoxifying reactions. All these features suggest that the LGR5+ liver organoids have the potential to be used to predict individual cellular physiology due to the integrity of their genetic signatures. Similarly, liver organoids could potentially be used to assess hepatotropic viral infections in each individual and predict personalised drug response. To date, the utility of LGR5+ liver stem cells as a model of hepatotropic viral infection has not been extensively explored and as such, is the major focus of this thesis.

1.10 Challenges and Gaps in Current Modeling

Despite significant development in HBV modelling systems in recent years, there is still lack of a "one size fits all" system. Earlier model systems that utilise immortalised hepatocytes suffer from poor infectivity and lack of genomic, transcriptomic and proteomic characterisations and it is unclear if these models truly resemble the human hepatocytes. Subsequent development of NTCP expressing hepatoma cell lines allow better HBV infection and replication but suffers from significant genetic and immunological aberrations. PHH which are often considered the "Gold Standard" also experiences transcriptomic alterations in culture and lose their mature hepatocyte phenotypes soon after plating.

The most fundamental goal of a HBV model system is to achieve the ability to predict clinical response and replicate disease pathogenesis. This encompasses characteristics such as physiologic resemblance to hepatocytes, maintenance of differentiation, ability to support chronic infection, intact innate immune response, ability to assess drug response and viral dynamics and predict individual responses to therapy. Advances in tissue engineering techniques allow maintenance of PHH phenotypes and HBV replication for longer, thus achieving some of these goals. However, reproducibility of these model systems cannot be assessed due to lack of regenerative potentials. In addition, most of the PHH culture systems do not utilise physiologic oxygen tension in the liver, thus potentially altering the hepatocyte metabolism. Furthermore, these PHH models are highly dependent on being able to obtain fresh normal liver for isolation of hepatocytes.

In contrast, stem cell derived culture systems in general have the advantage over PHH in regard to long-term expansion capability in the undifferentiated state. However, *in vitro* differentiation processes in these stem cells still could not achieve a complete transcriptomic resemblance to PHH. As such, high HBV inoculum is often required to achieve infection and replication. This finding could be due to the lack of liver non-parenchymal cells which are important in the development and maintenance of mature hepatocyte functions. Similar to PHH, the reproducibility of stem cell culture system in HBV infection is difficult to assess due to the heterogeneity within the stem cell population and variation following passages.

In order to advance the clinical utility of HBV model systems, a standardised quality control for homogenous differentiation and genetic stability is required. Comparison with a standard culture system such as PHH would allow estimation of the level of HBV infection and replication. The laborious nature of PHH maintenance and costs, however, are often

prohibitory to such comparison. In addition, assessments of NTCP expression and HBV cccDNA quantification are not standardised, thus limiting inter-studies comparison.

Integration of non-parenchymal cells, T cells and plasma cells in the culture would likely improve the hepatocyte differentiation and clinical utility in assessing the global immune response, potentially replacing *in vivo* culture systems. Future development in HBV model system should evaluate the epigenetics of HBV infection and early HCC oncogenesis.

1.11 Hypothesis and Aims

The main goal to this thesis is to develop and assess human liver organoids as an *in vitro* model for hepatotropic viral infection, using HBV as an example. In addition, we will assess the interindividual differences in HBV infection and the innate immune response to viral infection. The long-term goal is to develop a personalised platform for assessing viral infection dynamics and drug response.

Hypothesis - human liver organoids are a suitable *in vitro* model system to assess HBV infection and the cellular response to infection.

Aims:

1. To establish and characterise mouse and human liver organoids for downstream hepatotropic viral infections
2. To assess HBV infection and the antiviral response in human liver organoids
3. To investigate the innate immune response in human liver organoids following HBV infection

2 Methods

2.1 General Molecular Methods

2.1.1 Oligonucleotides

All DNA oligonucleotides (primers) that were used for PCR, qRT-PCR and sequencing were synthesised by Sigma-Aldrich in lyophilized form at the HPLC purification standard. Stock was diluted in nuclease-free TE buffer to 20µM and stored at -20°C long-term. The volume required for dilution was determined using the GraphPad molarity calculator [209].

2.1.2 RNA Extraction

Confluent cells or organoids from one well (24-well plate) is required as starting material. Organoids were pooled and washed in 15-mL centrifuge tube with cold PBS followed by centrifugation at 300 x g at 4°C for 10 minutes. This process was repeated twice to achieve a defined cellular pellet and separation from extracellular matrix (BME2). Following removal of extracellular matrix, 500µL of TRIsure (Bioline) was added. Total RNA and viral RNA were extracted using phase separation as per manufacturer's instructions. Quality of RNA was examined with either spectrometry or Nanodrop 2000 using 260/280 absorbance ratio before proceeding to downstream analysis.

2.1.3 qRT-PCR

All RNA samples were diluted to the same concentration with nuclease-free water before proceeding to qRT-PCR. cDNA first strand synthesis and amplification were performed using a one-step preparation Luna Universal qPCR mastermix (NEB). For each sample, 10µL reaction mix was prepared consisting of 0.2µL forward and reverse primers (20µM), 5µL of 2X SYBR Green Mix (NEB), 0.5µL of reverse transcriptase, 1.6µL of nuclease-free water and 2.5µL of RNA. qPCR was performed on StepOnePlus Real-time PCR System (Applied Biosystems) under the following cycling conditions: initial denaturation 95°C for 60s,

denaturation 95°C for 15s, extension 60°C for 30s for 40 cycles and melt curve analysis 60-95°C (ramp rate 5°C /s) continuous. Primer sequences used are provided in the supplementary material. For assessment if relative gene transcription, expression of a stable liver house-keeping genes mRNA (e.g., RPLP0, GAPDH) in each sample is used as control.

2.1.4 Statistical Analyses

All experiments were performed in triplicates for each culture condition and tested in duplicates for qPCR or antigen quantification with chemiluminescent assays. For qRT-PCR analysis, expression of genes is first normalised to house-keeping gene for each sample. Differential expression of genes between 2 or more groups were compared using 2-way ANOVA analysis in Prism 8. Charts were presented as mean +/- SEM with level of significance according to standard GraphPad format for p values.

2.1.5 Immunoblotting

Confluent organoids from 12-well trays were harvested by washing the tray with ice-cold PBS and centrifuged at 300 x g for 10 minutes at 4°C to pellet the cells. This process was repeated twice to ensure a good separation between cell pellet and extracellular matrix. Following removal of extracellular matrix, organoids were resuspended in 100µL cell lysis buffer (Abcam) with the addition of protease inhibitor (Sigma Aldrich). Cell lysate was incubated on ice for 20 minutes followed by centrifugation at 12,000 xg for 10 minutes at 4°C. Protein fraction was collected for downstream immunoblotting.

For protein transfer, 15µL of protein sample was first mixed with 4x loading buffer and boiled at 95°C for 5 minutes. Sample was loaded in polyacrylamide gel with 7µL of Precision Plus Protein Kaleidoscope marker (BioRad) added as protein standard. Gel electrophoresis was carried out in running buffer (900mL dH2O, 100mL 10x Tris Glycine SDS) at 100V for 60 minutes. Protein transfer was carried out using the Trans-Blot Turbo Transfer System

using the mixed MW protocol (BioRad) onto nitrocellulose membrane. Membrane was subsequently blocked with 5% skim milk in 0.1% TBS-T for 1 hour in gentle agitation. Following rinsing with 0.1% TBS-T twice, membrane was incubated with primary antibody diluted in 1% skim milk at 4°C overnight in gentle agitation. Membrane was washed five times at 5 minutes interval before addition of horseradish peroxidase-conjugated secondary antibody diluted in 1% skim milk and further incubated for 1 hour at ambient temperature. Membrane was washed five times at 10 minutes interval. Chemiluminescent detection was carried out using the SuperSignal West Femto Maximum Sensitivity Substrate kit (Thermo Scientific) and imaged with Chemi DocTM MP Imaging System (BioRad).

2.2 Immunofluorescence Microscopy

Immunofluorescence staining of a three-dimensional structure such as liver organoids can be carried out using wholemount technique or μ-slide Chamberslide and examined with confocal or 3D-microscope.

2.2.1 Wholemount

Wholemount staining was used if large quantity of organoids was required or if organoids were cultured in different experimental conditions. Confluent wells of organoids in 6-well tray were placed on ice for 30 minutes and washed with ice cold 0.1% BSA repeatedly until no visible extracellular matrix left before proceeding to fixation with 4% PFA for 30 minutes at room temperature. After fixation, organoids were incubated with 50mM NH_4Cl for 30 minutes to remove autofluorescence. This was replaced with blocking solution (1xPBS, 0.1% Triton X-100 vol/vol, 1% DMSO vol/vol, 1% BSA) and the organoids were incubated at room temperature for two hours. Additional blocking was performed by incubating with 5% BSA for a further 30 minutes. Organoids were subsequently incubated with appropriate dilution of primary antibodies (in 0.1% BSA) at 4°C on gentle agitation for 16-48 hours. Four

times of interval washes with 0.1%BSA/PBS was performed, followed by a 2-hour incubation with secondary antibodies and 10 minutes incubation with DAPI at 1:1000 dilution. Following gentle centrifugation, organoids were resuspended in Vectashield antifade mounting medium (Vector Laboratories) and transferred to a glass slide. After mounting the coverslip, the slide was sealed with nail polish and placed at 4°C overnight to dry the seal.

2.2.2 μ-slide Chamberslide

Chamberslide staining of organoids provide a faster and more cost-effective option for immunofluorescence due to the smaller volume of reagents required. Organoids stained using this method are more likely to retain an intact 3D structure due to lack of compression from a coverslip. Organoids were first cultured in μ-Slide 8 well chamberslide (Ibidi) until 80-90% confluent before performing the staining procedures as above. Vectashield was added to each chamber before imaging with confocal microscope.

2.2.3 Confocal Microscope

Immunofluorescence labelled organoids were visualised using the Olympus FV3000 confocal laser scanning microscope. Laser intensity and exposure were adjusted based on positive control sample and percentage of signal offset was determined using the negative control sample to minimise artefact detection. Multi-dimensional imaging of organoids was performed using the Z-series. For organoids with diameters between 150-200μm, 30-50 slices acquisition is sufficient to generate a 3D reconstruction. Image deconvolution, volume and Z-plane views were generated using CellSens software (Olympus). 3D reconstruction and animation were performed using Imaris software (Bitplane).

2.2.4 3D-Microscope

Immunofluorescence-labelled organoids were placed in a micro-centrifuge tube and loaded with 1.5% low melting agar (Sigma) that was pre-heated to 35°C. Using a 1mL Tuberculin syringe, the gel embedded organoids were pumped into a size 4 glass capillary (GmbH). The

capillary was immersed in PBS with light protection and allowed to set at room temperature. Visualisation of the organoids were done using Zeiss Lightsheet Z.1 with a 20x lens.

2.3 Electron Microscopy

Organoids were washed with cold medium to remove BME2 and fixed with 4%PFA/1.25% glutaraldehyde/4% sucrose for 1 hour. After fixation, organoids were treated with 2% OsO4 for 1 hour, washed with 4% sucrose, followed by gradual dehydration with 70, 90 and 100% ETOH and gradual infiltration from 100% propylene oxide to 100% resin before polymerization at 70°C for 24-48 hours. Blocks were sectioned at 40nm slices and imaged using the FEI Tecnai G2 Spirit TEM.

2.4 Histopathology

Organoids were washed twice with cold PBS to remove the extracellular matrix before fixation with 4% PFA for 30 minutes at room temperature. Organoids were pelleted with gentle centrifugation at 70xg for 5 minutes and subsequently embedded in pre-heated HistoGel (Thermo Scientific) in a cryomould. HistoGel was allowed to set on ice for 10 minutes and placed in 10% formalin overnight before transferring into 70% ETOH for histology processing and paraffin embedding. Organoids were sectioned at 5µm and fixed to glass slide by heating to 60 for 20 minutes. Haematoxylin and Eosin staining was performed as previously described [210].

2.5 Tissue Culture

2.5.1 General Cell Lines

Cell lines used in this thesis includes HepG2, HepG2-NTCP, HepAD38 and Huh 7.5. HepG2 (ATCC HB-8065) is an immortalised hepatocellular carcinoma cell line derived from a 15

years old Caucasian male. It is used as a negative control for NTCP expression. HepG2-NTCP is a HepG2 cell line that is stably transfected with human NTCP and is permissive to HBV infection[211]. Huh-7.5 (CVCL_7927) derives from parental clone Huh-7 cells, which are hepatocellular carcinoma cell line originated from a 57 years old Japanese male. Following selection for their high permissiveness to HCV infection and replication, Huh-7.5 cells were cured of HCV through prolonged treatment with IFN-α[212]. This cell line was kindly provided by Professor Charles Rice.

2.5.2 Organoids Culture

2.5.2.1 Generation of Wnt-3a, Rspo1 and Noggin Conditioned Media

2.5.2.1.1 Wnt-3a

Wnt3a cell line was provided by Professor Hans Clevers from the Hubrecht Institute[159]. Wnt3a cells are cultured in DMEM (Gibco cat 12430054), 10%FBS, 1% penicillin/streptomycin and 300g/mL Zeocin and passaged using TrypLE Express (ThermoFisher). For conditioned medium production, 1.5-2 x10^6 cells were seeded in T175 flask and cultured until 75% confluence. Growth medium was replaced with 40mL of harvest medium (without Zeocin) and cultured for a further 7 days. Harvest the conditioned medium by filtering through a 0.45μm filter cup. Conditioned medium was stored at 4°C for up to 6 months or -20°C for up to 12 months. L Wnt-3A (ATCC CRL-2647) is a mouse fibroblast cell line which can also be used as an alternative for conditioned medium production given high amino acid sequence homology between human and mouse Wnt-3a.

2.5.2.1.2 Rspo1

The 293T-HA-Rspo1-Fc cell line was provided by Professor Nick Barker. The Rspo1 growth medium consists of DMEM, 10% FBS, 1% penicillin/streptomycin and 150g/mL Zeocin. Similar to Wnt-3a conditioned medium production, after reaching 75% confluency, the growth medium was replaced with harvest medium which consists of Advanced DMEM/F-

12, 1% penicillin/streptomycin, 1x Glutamax and 10mM Hepes. Conditioned medium was stored at 4°C for up to 6 months or -20°C for up to 12 months.

2.5.2.1.3 Noggin

The Noggin cell line was provided by Professor Hans Clevers from the Hubrecht Institute. It was cultured in DMEM, 10% FBS, 1% penicillin/streptomycin and 500µg/mL G-418. Noggin conditioned medium production and harvest medium are similar to Rspo1.

2.5.2.2 Quantification of Conditioned Media Activity with TCF/LEF Assay

TCF/LEF assay is a beta-catenin reporter assay and is routinely used for testing of Wnt-3a and Rspo1 activities before the conditioned media are used for organoids culture. Conditioned media produced from L cells (ATCC CRL-2648) and L-Wnt3a (ATCC CRL-2647) were used as negative and positive controls respectively.

HEK293T cells were transfected with either M50 Super 8x TOPFlash (#12456 Addgene) or M51 Super 8x FOP Flash (TOPFlash mutant, #12457 Addgene) plasmid using Lipofectamine 2000 along with a Renilla luciferase vector (pRL-TK) as a transfection control. 24 hours post-transfection, culture medium was replaced with respective conditioned media (Wnt3a, Wnt3+Rspo1 1:1 vol/vol, L2 and L-Wnt3a) and cultured for a further 48 hours. Cells were harvested and tested for luciferase expression using the Dual-Luciferase Reporter Assay (Promega). TOP/FOP_{Wnt} ratio of >25 indicates adequate Wnt activity and $TOP/FOP_{Wnt/RSPO}$:TOP/FOP_{Wnt} >5 indicates adequate Rspo1 activity.

2.5.2.3 Patient Selection and Organoids Isolation

Patients who underwent liver resections for metastatic carcinoma or core biopsies were recruited through the Gastroenterology and Liver Tissue Repository at the Royal Adelaide Hospital with ethics approval from the hospital research committee. Tissue distant from resected tumour (>10cm away) or fragments of core biopsied tissues (weight 20-50mg) were used for organoids isolation. Tissues were minced and digested with collagenase to single

cells before embedded in reduced growth factor extracellular matrix (Cultrex BME2, R&D Systems). Selective isolation of ductal stem cells was achieved using Isolation Medium (IM) consisting of Expansion Medium (EM) supplemented with 5%v/v Noggin conditioned medium (homemade), 30% v/v Wnt3a conditioned medium (homemade) and 10μM of Y-27632 (Sigma), cultured under standard incubator conditions (80% N_2, 15% O_2 and 5% CO_2) until organoids were visible. Organoids were subsequently cultured and passaged in EM which consists of Advanced DMEM/F12 (ThermoFisher) supplemented with 1x B27 (ThermoFisher), 1x N2 (ThermoFisher) 1.25mM N-acetylcysteine (Sigma), 10mM nicotinamide (Sigma), 10% v/v R-spondin conditioned medium (homemade), 10nM recombinant human gastrin (Sigma), 50ng/mL EGF (Peprotech), 100ng/mL FGF-10 (Peprotech), 25ng/mL HGF (Peprotech), 10μM forskolin (Tocris), and 5μM A83-01 (Tocris).

2.5.2.4 Organoids Differentiation

Following digestion with TrypLE (ThermoFisher), organoids were seeded as single cells and cultured with EM supplemented with 10μM Y-27632 for 4-5 days to avoid anoikis. Once organoids reformed (20-30μm diameter), medium was changed to EM supplemented with BMP-7 (Peprotech) for 5 days, followed by 10 days in Differentiation Medium (DM) to induce hepatocyte differentiation. DM consists of Advanced DMEM/F12, 1x B27 (ThermoFisher), 1x N2 (ThermoFisher), 1mM N-acetylcysteine (Sigma), 10nM recombinant human gastrin (Sigma), 50ng/mL EGF (Peprotech), 25ng/mL HGF (Peprotech), 100ng/mL FGF-10, 0.5uM A83-01 (Tocris), 10uM DAPT (Sigma), 3uM Dexamethasone (Sigma), 25ng/mL BMP-7 (Peprotech), and 100ng/mL (FGF-19 (Peprotech).

2.5.2.5 Organoids Transfection and PolyI:C Stimulation

Organoids were cultured in 6-well tray until confluent. Following removal of extracellular matrix, organoids were placed in 3mL of TrypLE Express (Thermo Fisher) and incubated at 37°C for 15 minutes. Interval aggressive agitation by pipetting was performed every 5

minutes and a small aliquot was examined under the light microscope to ensure complete dissociation of organoids into single cells. Cells were washed with Advanced DMEM/F12 (Gibco) and centrifuged at 300 x g for 5 minutes. Supernatant was removed and cells were resuspended in growth medium supplemented with 10μM Y-27632. Transfection reagents were prepared according to the Lipofectamine 3000 protocol. For PolyI:C stimulation, 1μg/mL concentration was used. Following mixing with transfection reagents, organoids were placed in a non-adherent tray for spinoculation at 600xg at room temperature for 1 hour. Media change was performed after 24 hours.

2.6 HBV Infection System

2.6.1 Generation of Cell Culture-derived HBV Viral Stock

Cell culture derived HBV (genotype D) were prepared from supernatant of HepAD38 cells cultured in Advanced DMEM/F12 (ThermoFisher) supplemented with 10% FCS and 400μg/mL G-418 for ten days. Culture supernatant was collected through a 0.4 μm filter and precipitated using PEG8000 (final concentration 8%) overnight before centrifuged at 15,000xg at 4°C for one hour. Viral pellet was reconstituted in Advanced DMEM/F12 at 1/50-1/100 of the original volume. Genotyping was performed using S gene sequencing described by Li et al..[213]

2.6.2 Generation of Plasma-derived HBV Viral Stock

Untreated HBV-infected patients with high viral load were recruited from the Royal Adelaide Hospital via GLiTR. 80-100mL of blood in EDTA-free gel tube was acquired from each patient. Following centrifugation at 2000xg at 4°C for 15 minutes, plasma was stored unprecipitated in in -80°C as viral stock.

2.6.3 Genotyping of Plasma HBV

HBV DNA was extracted from stored plasma using NuceloSpin Blood (Macherey-Nagel) and eluted to 50µL. PCR for S gene was performed using Q5 High Fidelity 2x Master Mix (NEB) for the following conditions: initial denaturation 98°C 30s, cycling 95°C 10s, 60°C 30s, 72°C 40s for 35 cycles and final extension 72°C 2 minutes. 10µL of DNA was run on 1% agarose gel to check for 1.2kb PCR product before proceeding to PCR clean-up with Isolate II PCR and Gel Kit (Bioline) following manufacturer instructions. DNA was quantified and checked for purity with Nanodrop 2000 before performing Sanger sequencing with S gene primers. Sequencing reads were checked for Q20 values and signal intensity before alignment with reference sequences using NCBI Nucleotide [214]and HBVdb[215].

2.6.4 Quantification of HBV Viral Load

HBV viral load was determined with qPCR using a standard curve generated from a dilution of linearised 1-mer HBV plasmid. The HBV standard was prepared by HindII-HF and xhoI digestion of 1.3-mer pBB45HBV plasmid. Following DNA gel electrophoresis, linearised 6769 kb band was cut out and gel extracted using Isolate II PCR clean up kit. Concentration of the DNA was determined using Nanodrop2000. The mass of a single plasmid molecule was calculated using the following formula and was determined to be 7.418e-18g.

$$m = [\,n\,]\left[\,1.096\text{e-}21\ \frac{g}{bp}\,\right]$$

where: n = plasmid size (bp)
m = mass
e-21 = $\times 10^{-21}$

Plasmid mass at different copy numbers were determined next.

Copy#		Mass of plasmid DNA (g)
300,000		2.23e-12
30,000	X7.418e-18g	2.23e-13
3,000		2.23e-14
300		2.23e-15
3		2.23e-16

First dilution of plasmid standard was prepared using the formula C1V1=C2V2 followed by 10-fold dilutions.

Following qPCR, Ct values of samples were compared with the Ct values of the standards using linear regression analysis performed on Prism 8 (GraphPad). The log_2DNA copies determined for each sample can be converted to normal DNA copies using the EndMemo log2 conversion tool[216].

2.6.5 Viral Infection Protocol

Before infection with virus, BME2 was first removed by repeat washing with ice cold DMEM. Organoids were resuspended in culture medium and a 50µL aliquot is taken for cell counting. The aliquot of organoids was pelleted with benchtop centrifuge and the medium replaced with 50µL of TrypLE Express and incubated for 15 minutes at 37°C. Aggressive pipetting was performed to ensure dissociation of organoids into single cells before cell counting with a haemocytometer. Total number of cells were calculated as follow:

$$\text{Total Cell Number} = \frac{\text{Cell Count from Aliquot} \quad X \quad \text{Total Volume}}{\text{Aliquot Volume}}$$

Known inoculum of virus was added to the cells to achieve the desired MOI or genome copies/cell. PEG8000 was added to achieve a final concentration of 8% before plate spinoculation at 600xg for one hour at 35°C in a non-adherent plate. Equal volume of culture medium + 10% Rspo1 conditioned medium (vol/vol) + 10µM Y-27632 were added and the organoids were cultured for a further 20-24 hours. Virus inoculum was removed by repeated washing with DMEM to avoid subsequent detection of input virus. When large viral inoculum was used, organoids were washed at least 8-10x and the step repeated after 48hours. Organoids were subsequently seeded into new non-adherent plate and cultured with appropriate culture medium.

2.6.6 Quantification of HBV infection from Infected Organoids

2.6.6.1 Supernatant HBV DNA

Following infection with HBV, 200 µL of supernatant from culture was subjected to two DNaseI treatment (2U/µL) in the presence of 1µL of 1M $MgCl_2$/sample to remove non-encapsidated HBV DNA. Samples were incubated at 37°C for 2 hours followed by addition of 25µL of 5x STOP buffer (2.5% w/v SDS; 100mM Tris pH7.5; 125mM EDTA). HBV DNA was isolated using the NuceloSpin Blood (MaCherey-Nagel) and quantified using qPCR using a standard curve generated from dilutions of 1-mer HBV.

2.6.6.2 cccDNA

Intracellular DNA was extracted using NucleoSpin Tissue Kit (Macherey-Nagel) and eluted to 50µL. 10µL of DNA was subjected to T5 exonuclease digestion to remove rcDNA, dsl

DNA, PF-rcDNA. For each 10µL reaction, 10U/µL of T5 exonuclease (NEB) and 10x NEB buffer 4 were added and incubated at 37°C for 30 minutes followed by inactivation at 99°C for 5 minutes. qPCR was performed using the following cycling conditions: denaturation 95°C 10 minutes, amplification 95 15s, 60°C 5s, 72°C 45s, 88°C 2s for 40 cycles, melt curve analysis 951s, 65°C 15s, 95°C 2 acquisitions per °C continuous. The cccDNA primers were validated against previously described primers by Singh et al..[217]

2.6.6.3 HBV RNA

Extracted cellular RNA was checked for purity and quantified using Nanodrop 2000 and diluted to 20ng/µL. 50ng of RNA was used in each qRT-PCR reaction to assess for HBV pgRNA and total RNA. Quantification was performed by comparing the CT values to a standard curve generated from linear regression analysis of 10-fold dilutions of a linearised 1-mer HBV plasmid. Parallel samples without reverse transcription was used to rule out DNA contamination. In the setting of DNA contamination due to large viral inoculum, RNA was treated with DNase followed by inactivation using the TURBO DNA-free Kit (Invitrogen) according to manufacturer instructions.

2.6.6.4 Secreted HBeAg and HBsAg

Supernatant (200µL) was collected from infected organoids for HBeAg and HBsAg quantification using the Elecsys HBeAg and HBsAg II kit chemiluminescent microparticle immunoassay (CMIA) on the Cobas e602 instrument (Roche). Results were reported as S/CO ratio.

2.7 RNA Sequencing & Analyses

Total RNA was extracted using TriSURE as above followed by RNA clean-up using the RNeasy PowerClean pro CleanUp Kit (Qiagen). Quantification was performed using Qubit RNA HS Assay Kit (Invitrogen) and diluted to 200ng/μL for each sample. Total RNA was converted to strand specific Illumina compatible sequencing libraries using the Nugen Universal Plus mRNA mRNA-Seq library kit from Tecan (Mannedorf, Switzerland) as per the manufacturer instructions (MO1442 v2). Briefly, 500ng of total RNA was polyA selected and the mRNA fragmented prior to reverse transcription and second strand cDNA synthesis using dUTP. The resultant cDNA is end repaired before the ligation of Illumina-compatible barcoded sequencing adapters. The cDNA libraries were strand selected and PCR amplified for 12 cycles prior to assessment by Agilent Tapestation for quality and Qubit fluorescence assay for amount. Sequencing pools were generated by mixing equimolar amounts of compatible sample libraries based on the Qubit measurements. Sequencing of the library pool was done with an Illumina Nextseq 500 using single read 75bp (v2.5) sequencing chemistry. Illumina high-throughput sequencing data was processed using a standard RNA-seq analysis workflow. Raw single-end FASTQ reads were assessed for quality using *FastQC[218]* and *ngsReports*[219] (https://bioconductor.org/packages/release/bioc/html/ngsReports.html), and then aligned to the GRCh37.p13 version of the human genome (https://www.ncbi.nlm.nih.gov/genome/annotation_euk/Homo_sapiens/105/) using the transcriptome algorithm STAR[220]. After alignment, mapped sequence reads were summarised to GRCh37 gene annotation using *featureCounts*, available through the package *RSubread* (https://bioconductor.org/packages/release/bioc/html/Rsubread.html).

Differential gene expression was carried out using R/Bioconductor packages *limma[221]* and *edgeR[222]*, using mean-variance relationship estimates of the log-counts from the limma *voom* method[223] and contrasts defined between each sample group. KEGG pathway and

Gene Ontology enrichment were also carried out using R/Bioconductor packages, and heatmaps and upset produced using *pheatmap* (https://cran.r-project.org/web/packages/pheatmap/index.html) and *upSetR* (https://cran.r-project.org/web/packages/UpSetR/index.html). All code carried out in the study is available in the RMarkdown document (Supplementary Materials).

3 Chapter 3: Generation and Characterisation of Mouse and Human Liver Organoids

3.1 Development of Mouse Liver Organoids

Prior to the development of human liver organoids, mouse liver organoids were generated and characterised as a proof of concept. As human liver tissues are hard to come by, mouse livers are readily available. Mouse liver organoids were generated with a 100% success rate from four C57bl/6 male and female mice each. Ductal structures isolated from collagenase digested livers were first handpicked using transfer pipettes and seeded into extracellular matrix (Cultrex BME2 or Matrigel). Organoids were cultured in Isolation Medium (IM) consisting of Expansion Medium (EM) supplemented with 5%v/v Noggin conditioned medium (inhouse), 30% v/v Wnt3a conditioned medium (inhouse) and 10µM of Y-27632 (Sigma) for three days. These conditioned medium cell lines were provided by Professor Nick Barker and Professor Hans Clevers. Subsequently, organoids were incubated in EM (refer to methods), and after seven days, we observed the organoid emergence from the ductal structures (Figure 9A). Four weeks after isolation and expansion, a confluent collection of cystic organoids appeared and were visible with the naked eye. (Figure 9B). At this point in the isolation process, the undifferentiated organoids were frozen to establish a biobank for later use. Organoids were harvested and frozen down with 10% DMSO/Advanced DMEM/F12 and thawed successfully, similar to routine cell culture freezing and thawing (Figure 9C). No foetal calf serum was required in the freezing and thawing process which is a major advantage of this culture system.

The gross morphology of organoids appeared as round cystic structures and next, we investigated the cellular morphology of the liver organoids. Undifferentiated liver organoids

were fixed with 4% PFA and incubated with a specific antibody against cell membrane adhesion molecule, E-Cadherin, which will outline the shape of the cells and provide a clear cellular organisation of the organoids. Stained organoids were embedded in low-melting agar and examined using a Lightsheet Z.1 3D microscope (Figure 9D, Movie 1). At 20x magnification, the organoids with diameter from 50-200μm can be visualised in entirety (Figure 9D). Reconstruction of images captured at four different angles showed the internal structure of the organoids, with mostly thin one to two layered epithelial linings and multiple cavities (Figure 9D, right).

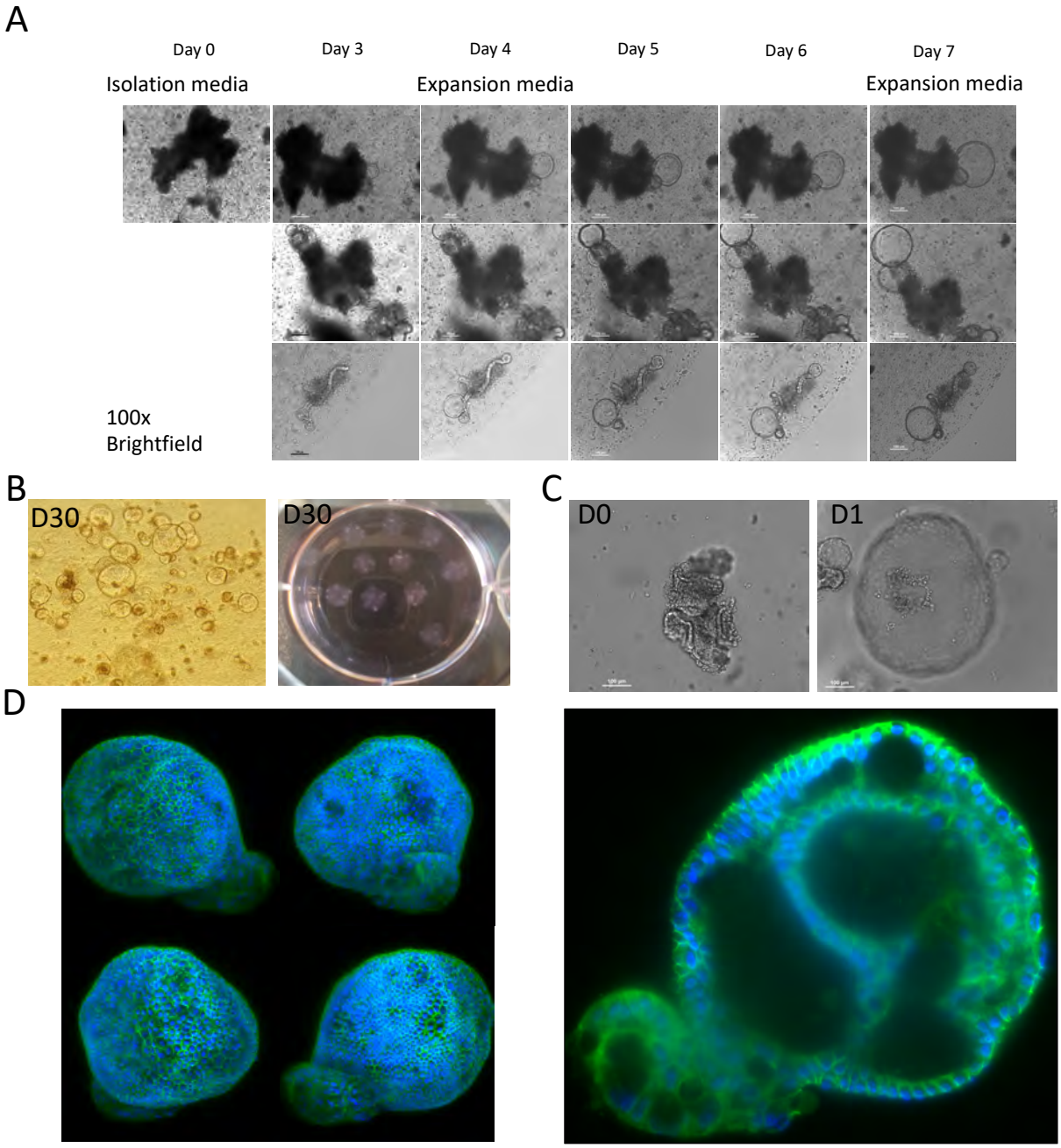

Figure 9: Mouse Liver Organoids Isolation from Ductal Structures
Brightfield microscopy of C57bl/6 mice livers (n=4). **(A)** Representative pictures of three ductal structures isolated following collagenase and dispase digestion. Temporal progression showed emergence of stem cell collections (organoids) through the ductal structures. Scale bar = 100µm **(B)** confluent organoids as cystic structure at day 30 from isolation (left) and visible to the naked eyes (right). **(C)** organoids thawed from -80°C at day 0 (left) and regeneration at 24 hours after cultured in EM supplemented with ROCKi (right). **(D)** Four angle views (left) of mouse liver organoids captured under 20x lens on 3D microscope, Zeiss Lightsheet Z.1. Immunostaining with E-cadherin (green) and DAPI (blue). Cross section of mouse liver organoids (right).

Movie 1: 3D Microscopy of Mouse Liver Organoids
Gross morphology of mouse liver organoids captured under 20x lens on 3D microscope, Zeiss Lightsheet Z.1. Immunostaining with E-cadherin (green).

The undifferentiated organoids comprise predominantly of immature stem cells with the potential to be differentiated into mature hepatocytes. To initiate this process, the undifferentiated organoids were cultured for at least 12 days in Differentiation Medium (DM), with the last three days supplemented with dexamethasone (refer to methods). Throughout the differentiation process, the organoids showed morphological alterations from clear cystic structures to darkened, more distorted shapes (Figure 10A). The cellular structure also changed from more oval shaped cells to polygonal shaped, similar to mature hepatocytes (Figure 10B-C). Next, we assessed the expression at the mRNA level of metabolic markers (albumin, CYP3A4) as surrogates for mature hepatocyte function. Albumin and CYP3A4 expression were upregulated following differentiation, albeit lower than the corresponding liver tissue from which the organoids originated from (Figure 11A-B). We then assessed the expression of LGR5, a cellular marker of intrahepatic ductal stem cells. We would expect LGR5 to be highly expressed in undifferentiated organoids due to the high proportion of stem cells, compared to differentiated ones. Indeed, this was the case with LGR5 mRNA expression significantly higher in the undifferentiated organoids (Figure 11B). We further assessed the mRNA expression of hepatocyte nuclear factor-4 (HNF4a), which is an essential element that promotes the transition of endodermal cells to hepatocyte progenitor cells [224]. In addition to its role as a marker for early hepatocyte cell fate differentiation, post-translational modification of HNF4a also leads to suppression of cellular proliferation, through epigenetic repression of pro-mitotic genes [225]. Following differentiation, the mouse liver organoids expectedly express HNF4 mRNA expression, with concomitant reduction in cellular proliferation as indicated by lack of organoids growth. The expression of HNF4a mRNA was lower than liver tissue, suggesting a lower proportion of organoid cells committing to the hepatocyte cell fate as compared with the liver. Immunofluorescence

staining of organoids with anti-albumin antibody showed significantly more albumin expression following differentiation (Figure 11C).

Overall, the differentiation process changes the expression of cellular markers (CYP450, LGR5 and HNF4a) at the mRNA level towards a mature hepatocyte phenotype. At the protein level, increased cellular albumin staining was demonstrated, an indication of mature hepatocyte synthetic function.

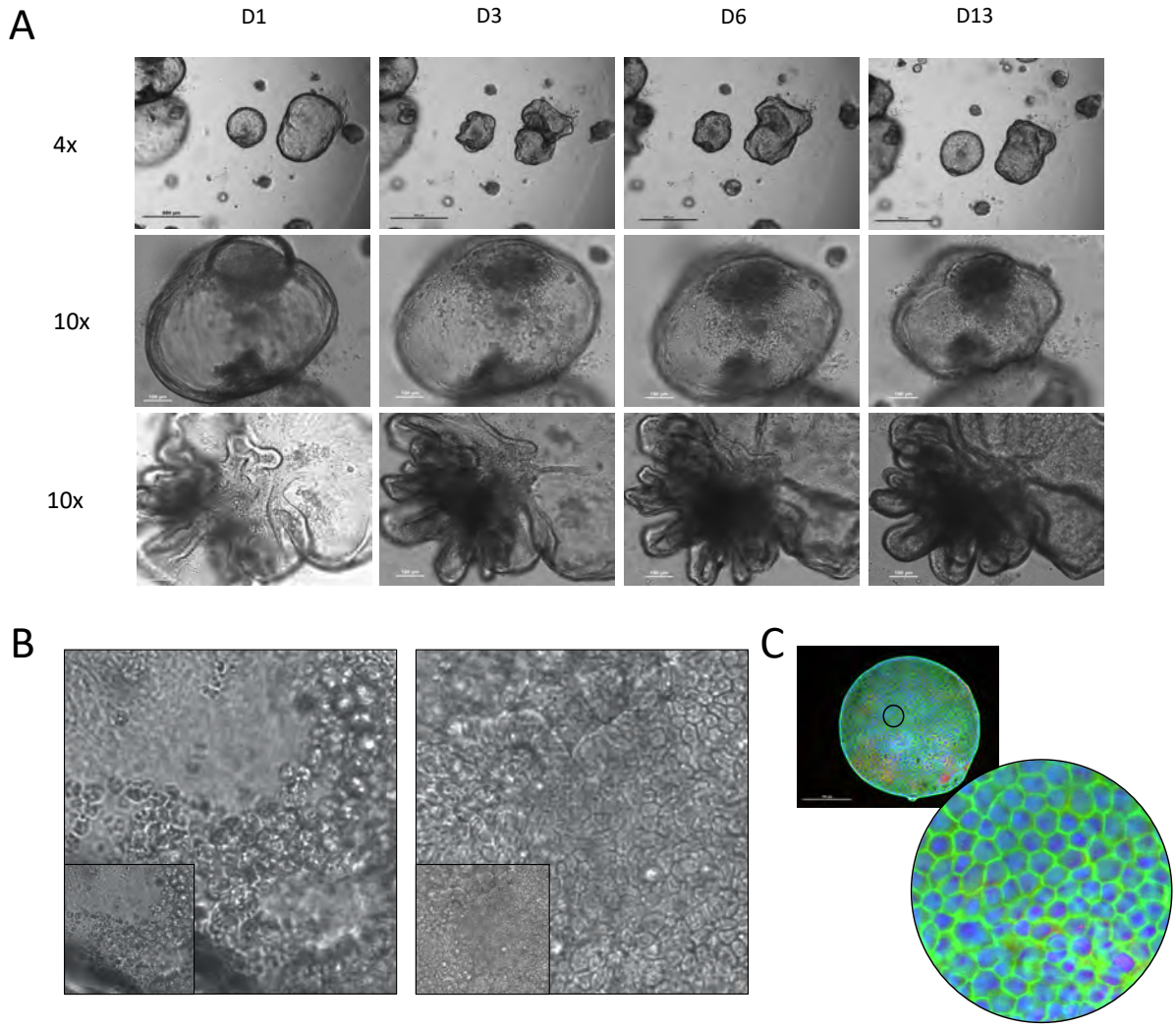

Figure 10: Morphological Changes of Mouse Liver Organoids Following Differentiation Brightfield microscopy and immunofluorescence of mouse liver organoids during the process of differentiation (n=4). Black scale bar = 500mm, white scale bar = 100mm **(A)** Temporal morphological changes of mouse liver organoids at different stages of differentiation (day 1, 3, 6 and 13). Undifferentiated organoids were cultured in EM until day 1 of differentiation in which medium was changed to DM from day 1-9, and DM supplemented with dexamethasone from day 10-12. **(B)** Microscopy showed cellular morphological changes from early differentiation (day 3, top) and late differentiation (day 13, bottom). 20x magnification. **(C)** Immunofluorescence staining of differentiated organoids with E-Cadherin (Green) and DAPI (Blue). 20x magnification.

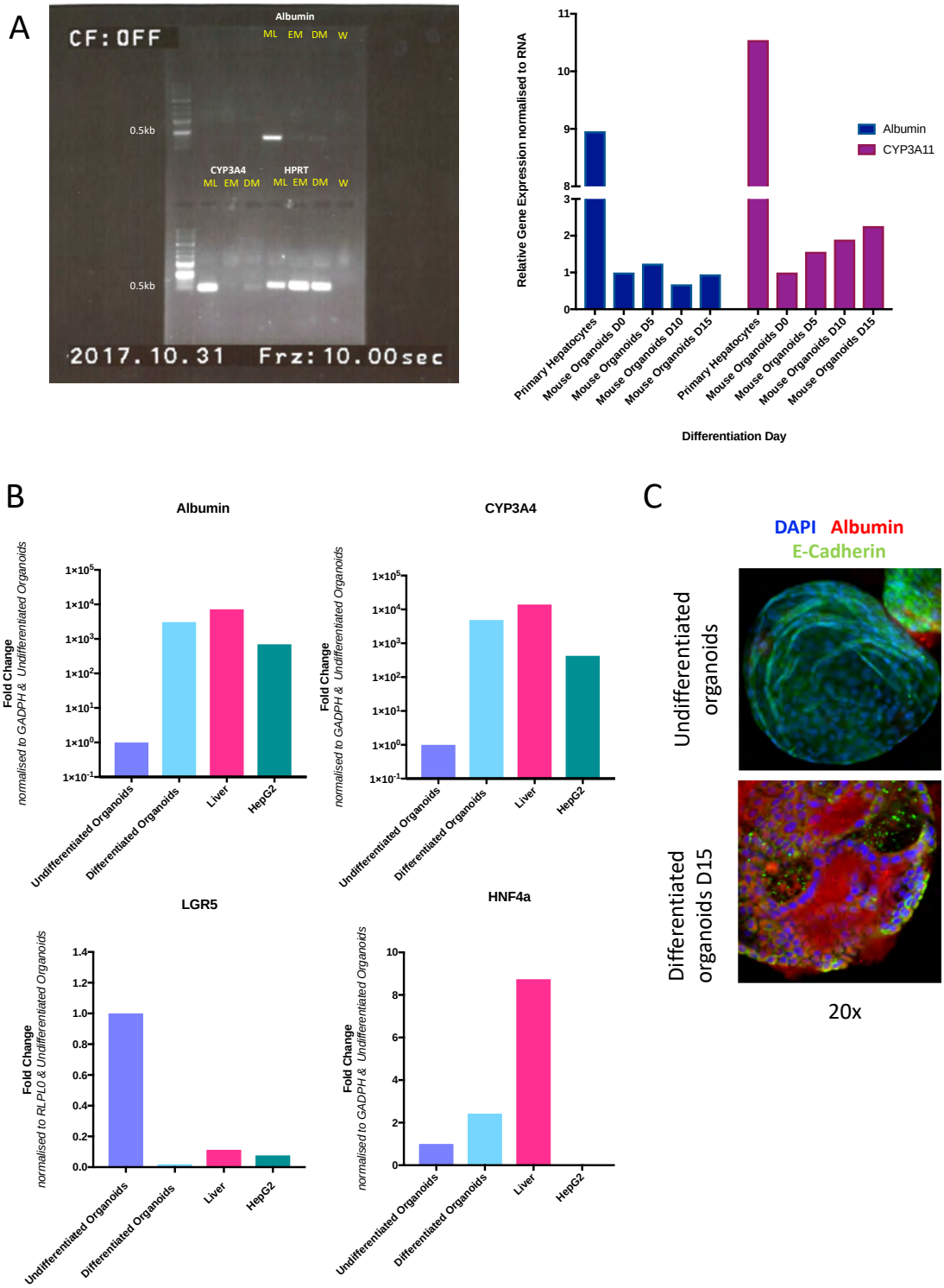

Figure 11: Metabolic Activities of Mouse Liver Organoids

Hepatocyte metabolic marker comparison between corresponding mouse liver and isolated organoids (n=2). **(A)** Metabolic markers (albumin, CYP3A4) of mouse liver (ML), undifferentiated organoids in expansion medium (EM), and differentiated organoids (D12) in differentiation medium (DM). Water (W) as contamination control and HPRT as gene expression control. **(B)** qRT-PCR of metabolic markers (albumin, CYP3A4) and cellular markers (LGR5 as stem cell marker, HNF4a as hepatocyte marker) relative to GAPDH, normalised to undifferentiated organoids. **(C)** Representative figures of two experiments.

Following characterisation of structural and metabolic features of mouse liver organoids, we performed a proof-of-concept experiment to assess the susceptibility of mouse liver organoids to viral infection as this is a major focus of this thesis. Zika virus (ZIKV) was selected due to its broad tissue tropism and its ability to infect hepatoma cell lines. Using a ZIKV strain PRVABC59, derived from an infected patient in Puerto Rico, we designed an experiment to assess susceptibility of infection throughout the organoid differentiation process (Figure 12A) [226]. This lineage of ZIKV was selected due to its high replicative capabilities *in vitro* and *in vivo* [226]. The use of extracellular matrix (Cultrex BME2 or Matrigel) to culture organoids may preclude viral access to the organoids. To ensure accessibility of virus, organoids were resuspended and washed in cold medium to remove the extracellular matrix before introduction of ZIKV at MOI of 5. The organoids were incubated with the virus for two hours at 37°C followed by multiple washes to remove the inoculum. A schematic representation of ZIKV infection protocol is shown in Figure 12B. No significant cell death was observed using light microscopy at the time of harvest. At 24hpi, organoids were fixed with 4% PFA and stained with a hybridoma-derived anti-Flavivirus envelope antibody (D1-4G2-4-15, ATCC HB-112) and anti-Zona Occludens-1 antibody [227]. Envelope positive cells were seen in both differentiated and undifferentiated organoids with different patterns of infection that range from scattered staining of individual cells to more distinctive foci (Figure 12C, right top, bottom). Loss of tight junction marker, ZO-1 was seen at the viral foci (Figure 12C, right middle). We also quantify ZIKV RNA following extraction of total RNA from infected organoids throughout differentiation using qRT-PCR. This revealed that indeed organoids could support ZIKV infection with undifferentiated organoids harbouring the most infection (Figure 12D). To determine if ZIKV infected organoids produce infectious viruses, supernatant was collected at 24hpi for quantification of extracellular infectious virus using plaque assay (Figure 12E). However, results were

inconsistent and difficult to correlate to qRT-PCR or immunofluorescence due to low level of infection in this early timepoint of harvest. It may be that if the organoids were harvested at a later timepoint, more infectious viruses may be recovered. In summary, mouse liver organoids can support ZIKV infection and replication and provide proof-of-concept for further studies.

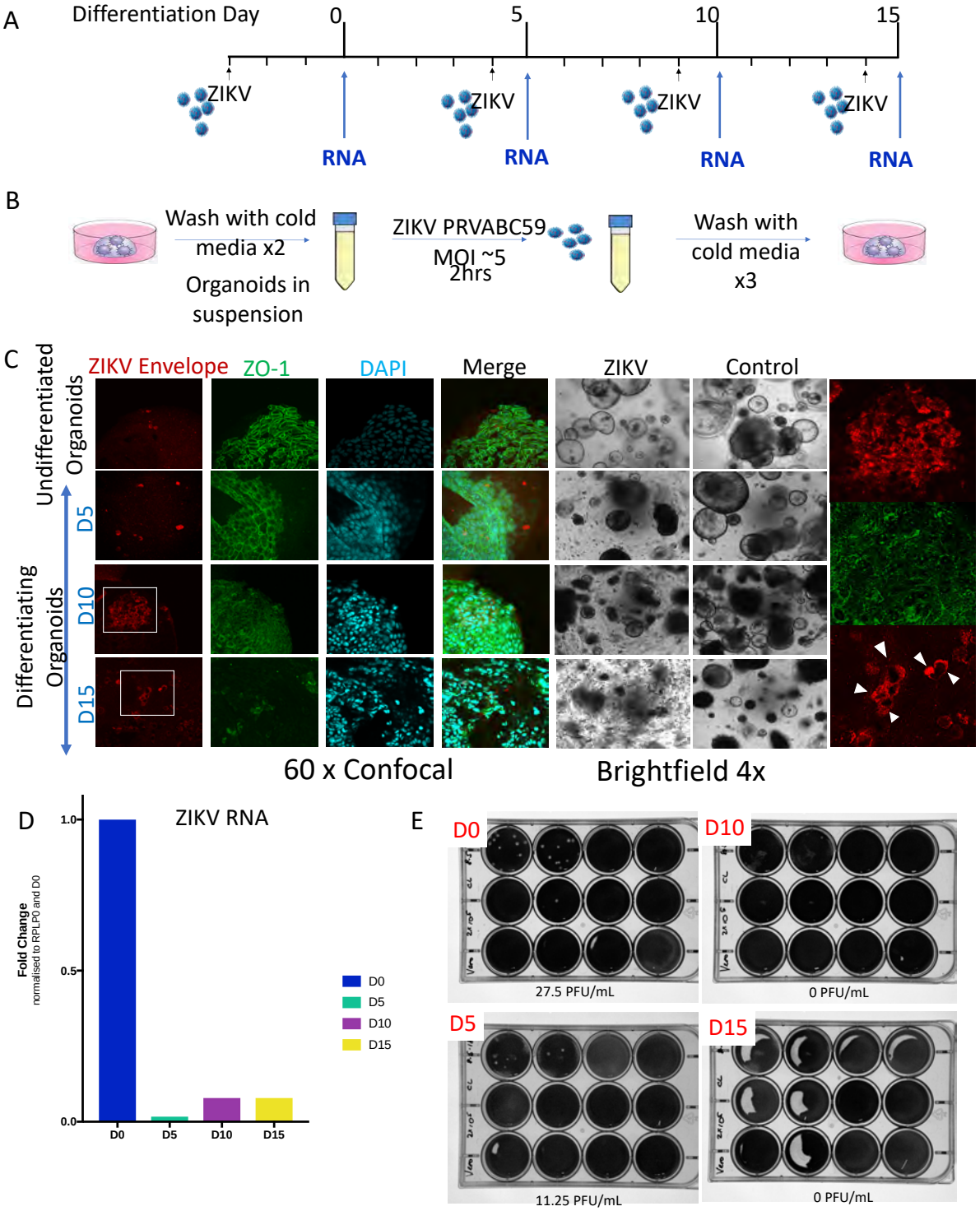

Figure 12: ZIKV Infection in Mouse Liver Organoids

(A) Schematic representation of the timeframe and experimental design of ZIKV infection in mouse liver organoids at different stages of mouse liver organoids. **(B)** Process of ZIKV infection in mouse liver organoids. **(C)** Immunofluorescence staining of mouse liver organoids at 24hpi at with ZIKV at MOI 5. Enlarged pictures on the right indicate infectious focus (top), loss of tight junctions (middle) and scattered distribution of infected cells (bottom). **(D)** qRT-PCR quantification of intracellular ZIKV RNA relative to RPLP0. **(E)** Plaque assay quantification of extracellular ZIKV infectious particles using Vero cells.

3.2 Innate Immune Competency of Mouse Liver Organoids

One of the issues in using transformed cell lines to study host responses is that these cell types often have defect or deficiencies in their innate sensing ability to detect pathogens. In many cases, the use of primary cells can overcome this and thus we investigated the innate immune response of mouse liver organoids. We anticipated that the primary nature of these cells would allow a robust response, however, it was unclear of the innate immune competency of cells as they differentiate. In previous studies assessing infectivity of human embryonic stem cells (hESC), hESCs at the pluripotent stage are highly resistant to infection by RNA viruses whereas partially differentiated multipotent stem cells are partially permissive [228]. Transcriptomic analysis of hESC and iPSC using RNA-seq and protein expression studies suggest selective expression of a subset of ISGs (EIF3L, IFITM1, IFITM3 and BST2). These ISGs were expressed at high basal level in pluripotent stem cells, but the cells are refractory to IFN stimulation. In contrast, well differentiated cells are highly responsive to IFN stimulation [229, 230]. The ISG expression in liver organoids have not been previously characterised. It is possible that the liver organoids may have slightly different ISG expression and susceptibility to viral infection as compared with pluripotent stem cells, as the liver organoids cells are bipotent and more differentiated towards the biliary/hepatic cell fate.

Before assessing the intricacies of human liver organoid differentiation and the corresponding changes in innate immune response, we first explored the ability of mouse liver organoids to mount an ISG response to either IFN stimulation or viral infection. As proof-of-concept studies, mouse liver organoids were separately stimulated with either mouse IFN-α at 1000U/mL or infected with ZIKV at MOI of 5 at various timepoint of differentiation. Unstimulated and uninfected organoids at similar differentiation timepoints were used as normalization controls. The high IFN-α dose of 1000U/mL is expected to stimulate a

significant ISG response in any innate immune competent cells. IFIT-1 and Viperin were used as surrogate markers for IFN response as significant upregulation of mRNA of these two ISGs have been observed in various cell lines (Huh7, Hela) following viral infection or stimulation with either PolyI:C or IFN [231-233]. As predicted mouse liver organoids respond to mIFN-α across differentiation time points with peak expression of IFIT1 mRNA and Viperin mRNA at 5- and 10-days post-differentiation, respectively (Figure 13). Interestingly, IFIT mRNA was induced to the same degree following IFN- α stimulation at day 5, however it significantly decreased thereafter. However, Viperin mRNA was not induced to the same extent at any time. Collectively, this most likely reflects the low level of infection of the cultures with possible limited spread of ZIKV over the 15-day time course. Alternatively, the ISG response may be dampened, similar to previous reports in hepatoma cells as infection progresses [231]. Another potential explanation for this finding could be attributed to the differences in mechanism of ISG induction by IFN- α and ZIKV infection. In contrast to IFN- α stimulation, ISG induction by ZIKV relies on TLRs/PAMPs. Functional expression of TLRs in organoids can be further explored using PolyI:C stimulation experiments.

In any case, these proof-of-concept experiments indicate that liver organoids have an intact JAK/STAT IFN signalling pathway and can respond to viral infection. Further studies using the viral RNA genome mimic PolyI:C would also determine the competency of cytosolic pattern recognition receptors such as RIG-I/MDA5 and the TLRs.

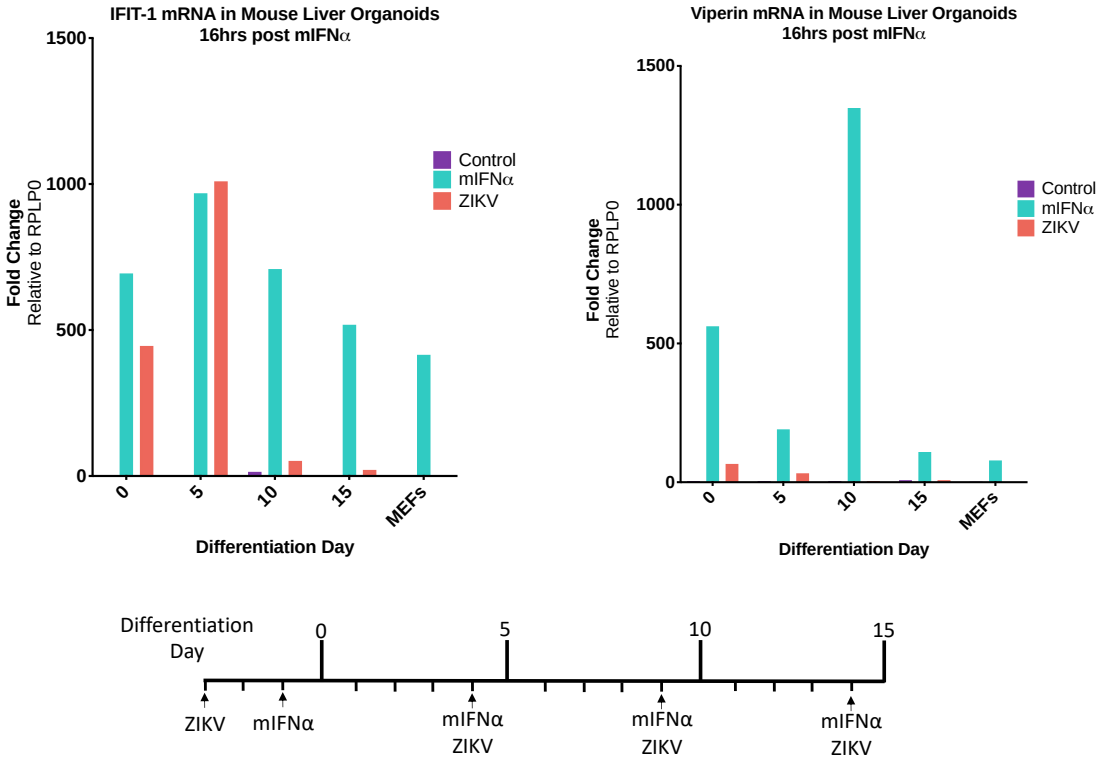

Figure 13: ISG Response in Mouse Liver Organoids to Interferon Stimulation and ZIKV Infection

qRT-PCR for IFIT-1 and Viperin mRNA in mouse liver organoids following stimulation with mIFN-α at 1000U/mL or infected with ZIKV at MOI of 5, normalised to RPLP0. RNA was harvested at 16hpi/hps.

3.3 Development of Human of Liver Organoids

Following the successful production and differentiation of mouse liver organoids and their ability to be infected with a non-hepatotropic virus, we proceed with the development and characterisation of human liver organoids. The recruitment of patients was through a collaboration with the Department of Gastroenterology and Hepatology at the Royal Adelaide Hospital with existing human research ethics committee approval via the Gastroenterology and Liver Tissue Repository (GLiTR). The study cohort consisted of patients undergoing hepatectomy for liver tumour resection and patients who underwent elective liver biopsy for diagnosis of underlying liver disease. The exclusion criteria for enrolment are, (1) history of chemotherapy over the last six months, (2) known history of blood borne viral infection (e.g., HIV, HBV, HCV), (3) prior history of cirrhosis and, (4) those who were unable to provide a consent. The inclusion criteria were left deliberately broad to allow recruitment of a range of patients with relatively normal liver. The large majority of tissues were derived from patients undergoing liver resection for metastatic liver cancer. For this reason, most of the donors recruited for this study are males with a median age of 63 (range 43-72). This creates a gender and age bias in our study. However, future studies will need to increase the recruitment of female donors, possibly through liver biopsy. Two patients with prior history of chemotherapy (>6 months) were included in this study.

For liver resection, resected livers and tumours were placed on ice and transported to the histopathology laboratory as soon as possible. Livers were examined by a consultant tissue pathologist at SA Pathology and excess healthy liver tissue distant from the tumour (i.e.,, >10cm from tumour margin) was resected and placed in ice cold basal medium. For liver biopsies, excess core biopsy sample (e.g., sample too small for histopathology examination) was obtained and placed directly in ice cold basal medium.

The process of human liver organoid generation starts with a simple collagenase digestion of liver tissue that is a slight departure from the complex two-step digestion in PHH isolation [234]. Instead of harvesting ductal structures as was the case in the mouse liver, the human liver was digested to single cells and inoculated into extracellular basement matrix and cultured in isolation medium. Isolation medium consists of expansion medium, Wnt-3a and Noggin (supplied as culture supernatant) and supplemented with Rho-kinase inhibitor which is crucial in preventing anoikis (cell dissociation apoptosis) (see methods). Liver organoids were generated from 9 liver resections and 3 core biopsies. Patient and sample characteristics summarised in Table 7. Resected liver tissue from one patient failed to culture liver organoids on two separate occasions, possibly related to prior chemotherapy. Despite the small amount of starting material from liver core biopsies, we observed that organoids grew to confluency within 2-3 weeks from isolation with 100% success rate. Subsequent differentiation requires a two-step process with initial culture with EM supplemented with BMP7 for three days followed by differentiation medium (includes gastrin, EGF, HGF, FGF-10, A83-01, DAPT, dexamethasone, BMP-7 and FGF-19) for 12 days. This process is outlined in Figure 14A.

3.4 Storage and Regeneration of Liver Organoids

Following successful isolation and expansion of undifferentiated liver organoids, we established a pool of organoids for freezing in liquid nitrogen for long-term storage. Undifferentiated organoids consist of predominantly stem cell population which have the capacity to regenerate from fragments or single cells. However, this feature diminishes following differentiation. The storage process begins with culturing the undifferentiated organoids until confluent in extracellular matrix before undergoing multiple washes with cold DMEM to remove the extracellular matrix. Organoids of different sizes were then digested

with 1mL of TrypLE Express for 10 minutes, followed by mechanical disruption into either single cells or fragments by pipetting. Organoids were then resuspended in freezing media consisting of Advanced DMEM/F12, 10% DMSO supplemented with Y-27632 to avoid cell dissociation induced apoptosis, and temporarily stored in -80ºC using standard freezing chamber for 24 hours in 500µL aliquot (see methods). Organoids were transferred to liquid nitrogen for long-term storage.

As part of the culture optimisation, we assessed if frozen organoids can be revived easily after storage. To revive the organoids, frozen aliquots of organoids were thawed quickly in a 37°C waterbath and washed gently with cold Advanced DMEM/F12 to remove the DMSO. Organoids were resuspended in cold extracellular matrix and cultured in droplets of matrix (previously described) in either isolation media or expansion media with Y-27632 for the first 5 days. Expansion of organoids by day 5-7 is a good indication of successful revival. Time-lapse microscopy showed cellular expansion within the organoids that can be observed within 24 hours (Movie 2).

Movie 2: 24-hour Time-lapse of Undifferentiated Human Liver Organoids

Time-lapse of undifferentiated human liver organoids in expansion medium over 24 hours, examined with confocal microscopy at 10x magnification.

Table 7: Human Liver Organoids Isolation - Patient Demographics

Age	Gender	Disease	Recent Chemotherapy	Cirrhosis	Procedure	Weight (g)
43	M	Metastases	Y	N	Resection	0.55
53	M	Gall bladder CA	N	N	Resection	0.97
67	M	Metastases	N	N	Resection	3.9
69	M	Metastases CRC	N	N	Resection	2.0
71	M	Gall bladder CA	N	N	Resection	2.7
72	M	Metastases	N	N	Resection	1.14
62	M	HCC	N	Y	Resection	2.04
57	F	Abnormal Liver Function	N	N	Biopsy	0.02
64	M	NAFLD	N	N	Biopsy	0.05
26	M	HCC	N	N	Biopsy	0.03
62	M	Metastases	N	N	Resection	NA
67	M	Metastases	Y	N	Resection	2.03

3.5 Structural Characteristics of Liver Organoids

To characterise differentiation of human liver organoids and to determine if organoids develop a specific liver organ phenotype, we assessed the sequential morphological changes of organoids throughout differentiation. In an undifferentiated state, the liver organoids were cystic and clear and readily expanded. However, following initiation of the differentiation process, they assumed a branched and budding appearance that extended from the cystic spheroid structure (Figure 14B). A differentiation phenotype can be seen as early as 5 days after culture in differentiation media (+BMP7) while more consistent differentiation phenotypes are seen across all the organoids thereafter up to 15 days. We also attempted to culture organoids in the absence of extracellular matrix in non-adherent wells, under expansion conditions. In this case, organoids assumed a dark appearance without branching, and were slow to expand, suggestive of partial differentiation when cultured in suspension. This highlights the dependency of a 3D matrix to maintain undifferentiated phenotype and for ongoing expansion of organoids. Histological examination (H&E) suggests a change from a ductal-like phenotype with single-layered epithelium to a multilayered hepatocyte-like phenotype following differentiation (Figure 14C). Given the lack of endothelial cells and other non-parenchymal cells, ontogenic development of liver zonation and sinusoids are not seen [235]. Clearly there is significant change in the morphology of human liver organoids as they differentiate to a more hepatocyte-like phenotype.

Next, we explored the expression of Zona occludens-1 (ZO-1) in liver organoids, a scaffolding protein localised specifically to the tight junctions. ZO-1 interacts directly with F-actin and other cytoskeletal proteins and play an important role in regulating the organisation of the apical cytoskeleton [236]. ZO-1 localisation is often used to indicate apical polarity of hepatocytes. In liver organoids, the differentiation process is accompanied by partial

hepatocyte polarisation as evident by immunostaining of Zona Occludens-1 (tight junction marker) redistribution as assessed by confocal microscopy and 3D reconstruction using Imaris software (Figure 13). In an undifferentiated state, ZO-1 distribution appears to outline the complete surface of the cells, forming a lattice-like structure. However, following differentiation, ZO-1 distribution relocalised to the interior of differentiated organoids, showing interconnecting network with appearance similar to the distribution of bile canaliculi in liver tissue. This is in contrast with columnar polarisation seen in MDCK cell sandwich culture (Figure 15) [237]. Similarly, HLCs from other stem cells such as hESC or iPSC can also be cultured under Transwell conditions to develop columnar polarisation. Columnar polarisation is useful in the functional assessment of albumin, urea, lipoproteins and bile acids secretions and secretion of HAV and HEV [238]. However, the effect of columnar polarisation on hepatocyte differentiation and hepatotropic viral replication are largely unknown. HLCs that developed hepatic polarisation under 3D culture conditions (spheroids, suspensions or in extracellular matrix) or in micropatterned co-cultures can recapitulate hepatocyte functions to a greater degree and had been shown to support HBV replication [239-241]. In summary, the location of ZO-1 expression following liver organoid differentiation suggest the HLCs developed a hepatocyte-like polarised phenotype.

We next examined the liver organoids at the ultrastructural level using transmission electron microscopy that revealed evidence of hepatocyte phenotypes and liver microarchitectures (Figure 16). The undifferentiated organoids showed evidence of glycogen granules, microvilli and tight junctions (Figure 16A). Before the process of differentiation, these organoids are columnar in appearance and consist of single layered epithelium. They are unpolarised with microvilli on one surface, similar to a biliary ductal structure. Tight junctions were consistently spaced in between the cells. Following differentiation for 15

days, there were significant changes in the cellular structures and arrangements (Figure 16B). The cells appeared to be more dysmorphic in size and morphology, with some cells expressing increased lipid vacuoles, glycogen, tight junctions, bile cannaliculi, mitochondria and rough endoplasmic reticulum. In some areas, cells assumed a hexagonal shape and arranged in a “honeycomb” like structure. Microvilli appeared to be expressed on all surfaces of the cells and appears sparser and more elongated. Similarly, tight junctions are also less frequently seen, located on certain surfaces, bordering the bile canaliculi. This appearance is consistent with the confocal microscopy findings, with redistribution of tight junctions from consistent spacing across the cell surfaces to limited distribution of tight junctions, suggestive of cellular and structural polarisation of the hepatic phenotype. The differentiated organoid cells also contain glycogen granules with typical floret arrangement, consistent with a hepatocyte phenotype. Collectively, these results confirmed changes in cellular ultrastructure and architecture of liver organoids following the process of differentiation, with demonstration of liver organ phenotypes.

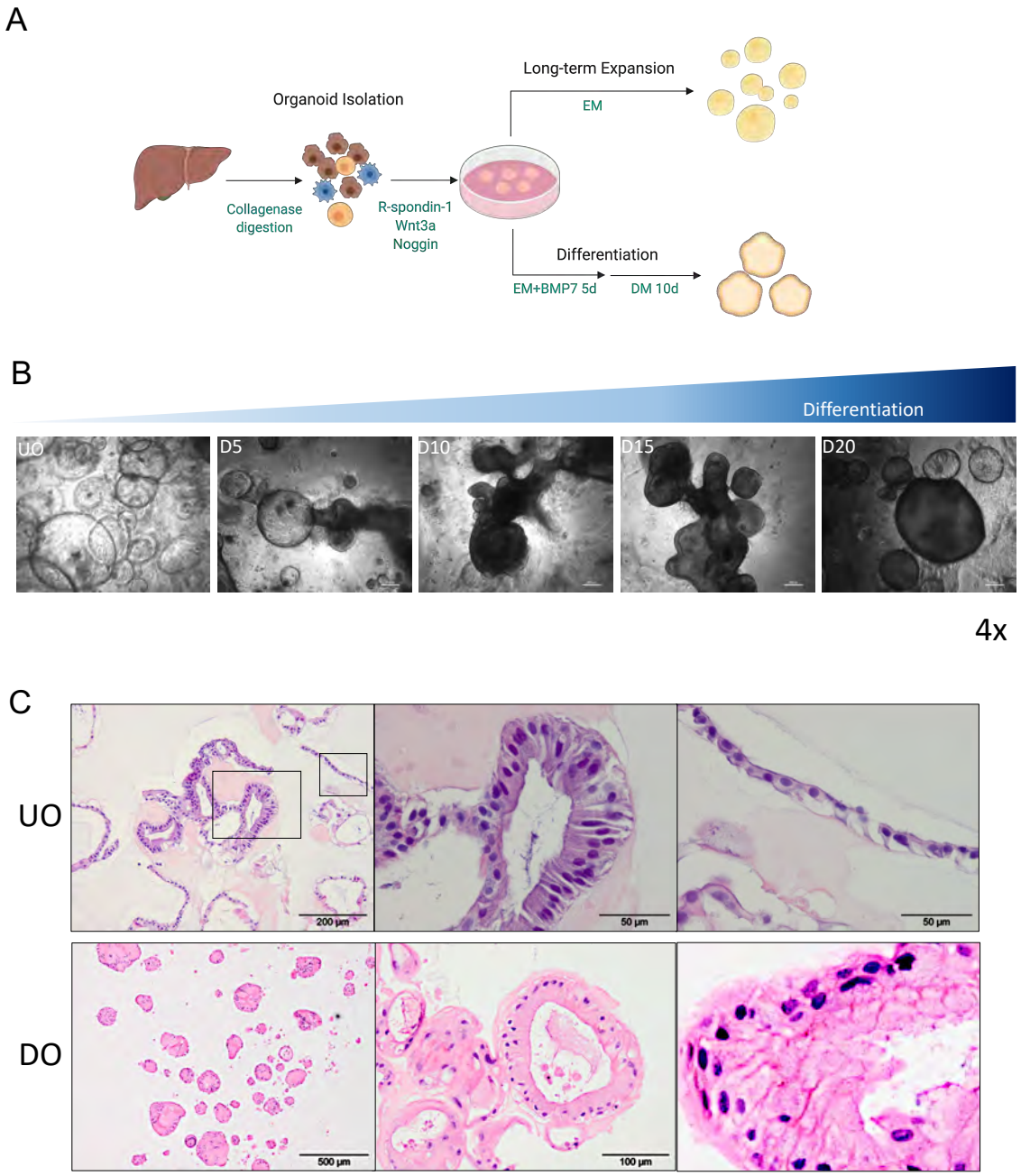

Figure 14: Morphological Characteristics of Human Liver Organoids
(A) Schematic illustration of human liver organoid isolation, expansion and differentiation. **(B)** Morphological changes of human liver organoids during differentiation, examined with brightfield microscopy, 4x magnification. **(C)** Haematoxylin and eosin staining of undifferentiated organoids (UO) and differentiated organoids (DO).

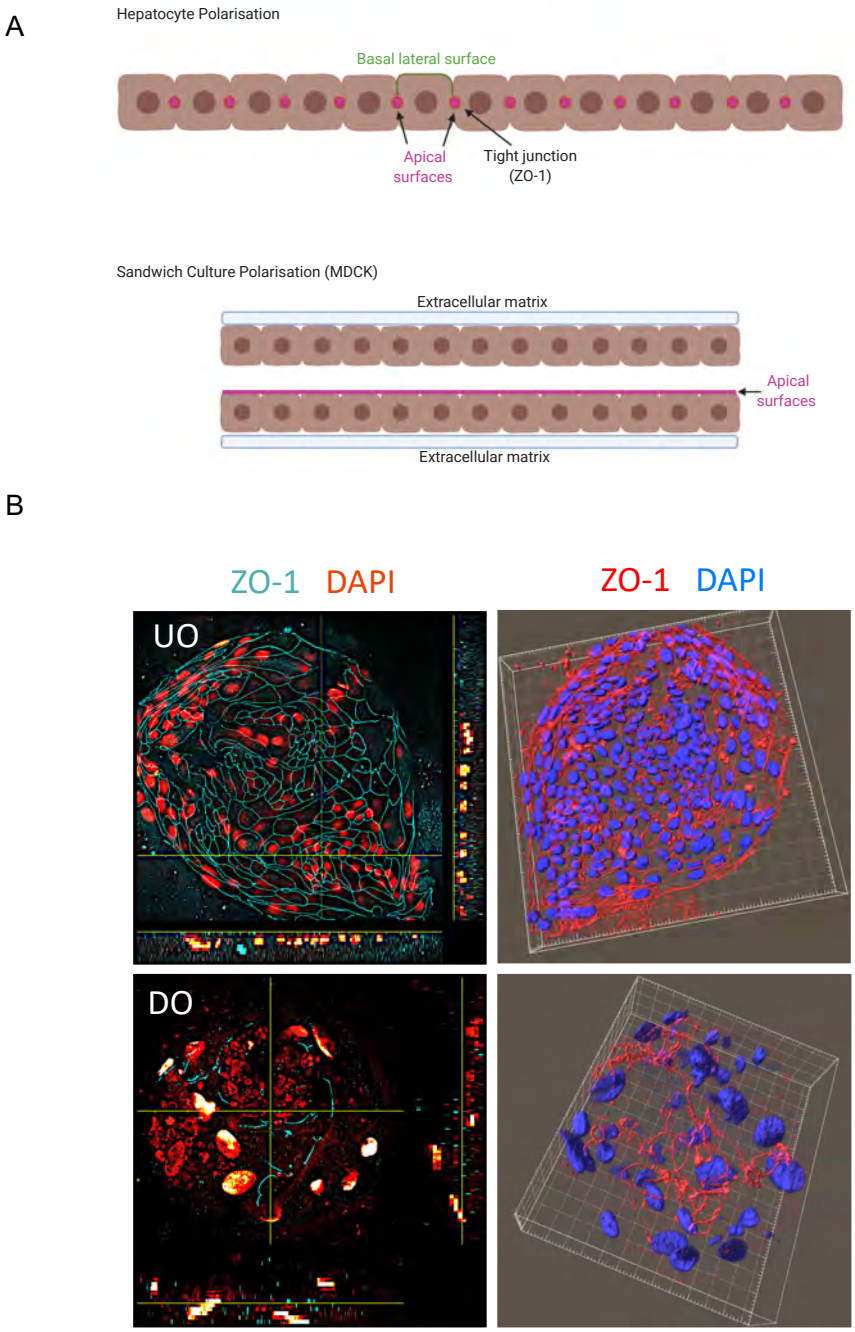

Figure 15: Hepatic Polarisation of Human Liver Organoids
(A) Differences between true hepatocyte polarity and cellular polarity in sandwich culture. **(B)** Left: Confocal microscopy images of undifferentiated organoids (UO) and differentiated organoids (DO) stained with Zona-occludens-1 (ZO-1, tight junction marker) and DAPI. 20x magnification. Right: 3D reconstruction of confocal images with Imaris software to illustrate the surface lattice-like distribution of ZO-1 and redistribution following differentiation. Note the change in ZO-1 localisation between UO and DO liver organoids suggesting a polarised phenotype.

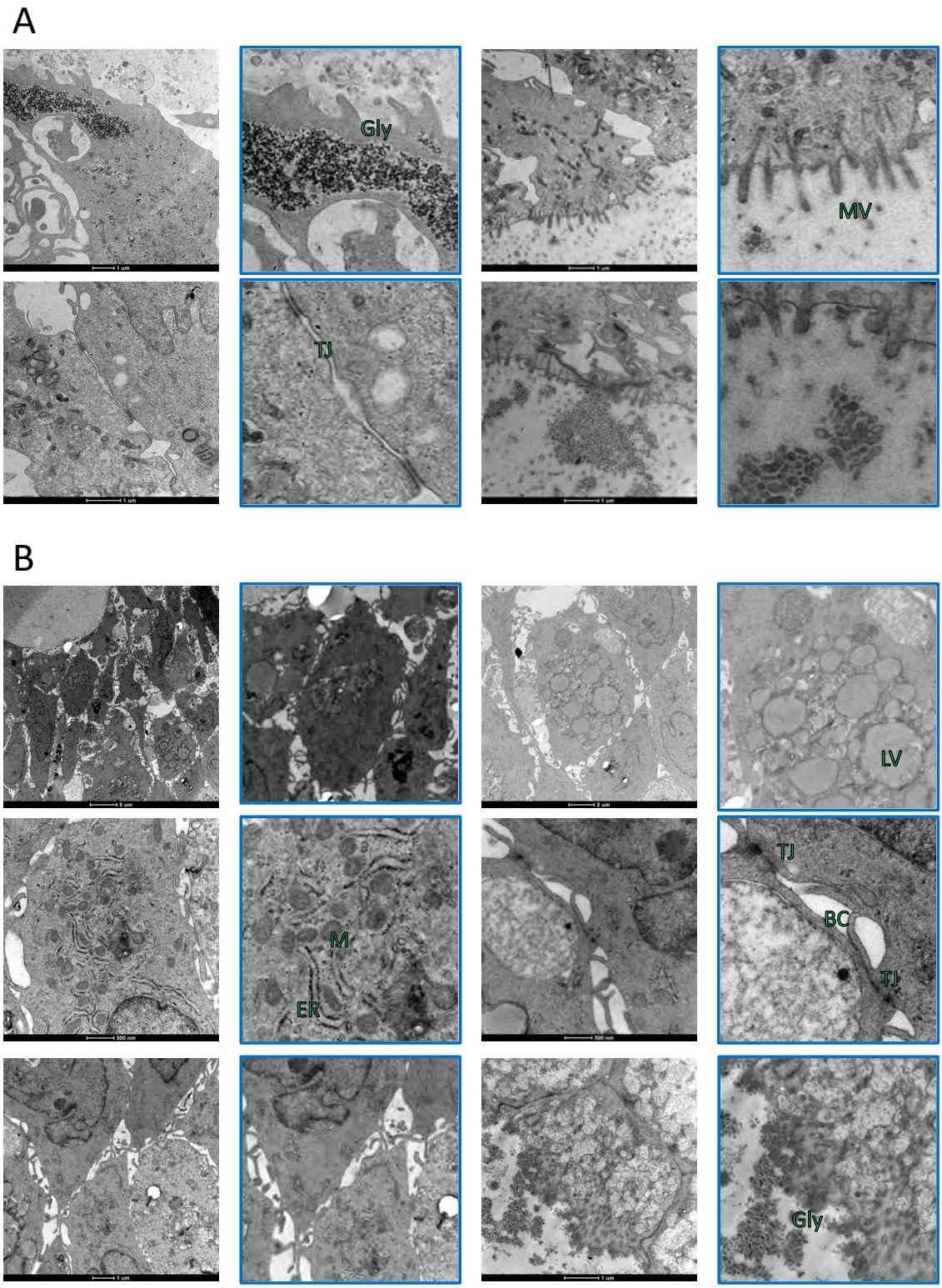

Figure 16: Electron Microscopy of Liver Organoids
TEM of human liver organoids. Images with blue borders were digitally enlarged from the corresponding images on the left **(A)** undifferentiated human liver organoids. **(B)** differentiated organoids. Tight junction (TJ), microvilli (MV), glycogen (Gly), lipid vacuoles (LV), mitochondria (M), endoplasmic reticulum (ER) and bile cannaliculi (BC).

3.6 Metabolic Characteristics of Liver Organoids

Next, we examined whether differentiation associated structural and morphological development is accompanied by physiological changes in liver organoids. Mature hepatocytes carry out many different functions, including production of albumin, urea, bile acids, drug metabolism through CYP450 enzymes, and detoxifying reactions to name a few. Albumin production can occur in early hepatic progenitor cells although at very low levels [242]. Significant upregulation of albumin production is often used as an indicator for hepatocyte maturation and comparison with PHH is often used as an indicator for the degree of differentiation [243, 244]. The CYP450 family of enzymes on the other hand, represents the most important drug metabolising enzymes in the liver. CYP450 enzymes undergo sequential upregulation of different isotypes during the process of liver maturation. CYP1A1 represents the predominant subtype during organogenesis, followed by CYP2E1 during the second trimester foetal stage. In infants, CYP2D6 is the predominant subtype and CYP3A4 becomes the predominant subtype in adult liver [245]. Although each isotype has been responsible for the metabolism of different drugs and compounds, the reason for such transition from CYP1A1 predominant to CYP3A4 predominant has not been entirely elucidated. CYP1A1, CYP2D6 and CYP2E1 are mostly responsible for xenobiotics metabolism and play a small role in drug metabolism. CYP2E1 and CYP3A4 are important for alcohol metabolism and are inducible by alcohol consumption in adults [246]. CYP3A, CYP2C9 and CYP2C19 account for the bulk majority of drug metabolism in adults [247]. Thus, in many studies investigating liver stem cell or organoid maturation, assessment of CYP450 enzyme expression is used to determine liver differentiation.

Using qRT-PCR, we assessed the albumin, CYP3A4 and CYP2D6 mRNA expression as markers of liver organoid differentiation, in undifferentiated, differentiated and in

corresponding liver tissue from which the organoids were derived. Three organoids (from different patients) were differentiated using the standard protocol for 15 days, after which total mRNA was extracted for qRT-PCR analysis. As seen in Figure 17, there was significant upregulation of albumin mRNA following differentiation. When compared with the undifferentiated state, interestingly, we noted variation in the expression between individual donors. The level of albumin expression in differentiated organoids as expected was not as high as the liver tissue. CYP3A4 mRNA expression was also upregulated following differentiation, with equal variability between donors. There was no correlation between the level of albumin expression and CYP3A4 expression (Figure 17A). There is also no clear correlation between higher albumin expression in liver tissue with corresponding albumin expression in liver organoids before or after differentiation. CYP2D6 expression was upregulated but at a slightly lesser degree than CYP3A4, consistent with a partial maturation of hepatocytes. Collectively, the differentiation process of liver organoids resulted in increased mRNA expression of metabolic markers, consistent with liver maturation.

Leucine-rich repeat-containing G-protein coupled receptor 5 (LGR5) is a marker for liver regenerating stem cells in both adults and children and is often used as a marker for hepatocyte stem cell isolation and undifferentiation [248, 249]. In the liver, LGR5 expression is extremely low, however, following liver injury, immunohistochemistry staining identified weak positive cells within the bile ducts in normal liver [203]. In chronic liver injury, such as hypoxia, LGR5+ cells rapidly expanded and make up of >50% of regenerated liver in children. Lineage tracing shows that these regenerative LGR5+ stem cells originate within the pericentral hepatocytes rather than the ductal cells [250]. The LGR5+ stem cells are Wnt-responsive and the subsequent β-catenin pathway activation results in cellular proliferation and hepatocyte zonation [251, 252]. In our undifferentiated organoids, we noticed very high

levels of LGR5 mRNA expression as expected as we selectively stimulate the proliferation of these LGR5+ stem cells using Wnt-3a conditioned medium and co-receptor sensitiser R-spondin-1, resulting in activation of canonical and non-canonical β-catenin pathways [253-256]. Also, as expected, there is significant downregulation of stem cell marker (LGR5) following the differentiation process, consistent with the withdrawal of Wnt3a/R-spondin-1, indicating a phenotypic shift from a stem-cell lineage to more differentiated hepatocytes (Figure 18). This process corresponds with cell cycle arrest in which the organoids no longer expand. Interestingly, we noticed some of the liver tissues also expressed low levels of LGR5 mRNA, suggestive of potential liver injuries, possibly initiated by immune response to the liver tumours in these patients.

Hepatocyte nuclear factors (HNFs) are hormone receptors expressed in hepatocytes and among the different subtypes, HNF4a is the most abundant [257]. HNF4a helps recruit RNA polymerase II to genes that are important in inducing the transdifferentiation of endoderm into hepatic progenitors [224]. Hence, HNF4a is not exclusively expressed in mature hepatocytes. Cytokeratin-19 (KRT19) and Sry-related high mobility group-box gene 9 (SOX9) are expressed in biliary cells and are often used as markers for cholangiocyte differentiation [258, 259]. In human liver organoids, HNF4a and KRT19 have comparable level of expressions, before and after differentiation, suggesting equal proportions of cells with hepatocyte and ductal phenotypes. Immunofluorescence staining for hepatocyte marker HNF4a and ductal marker SOX9 confirmed these findings (Figure 17B).

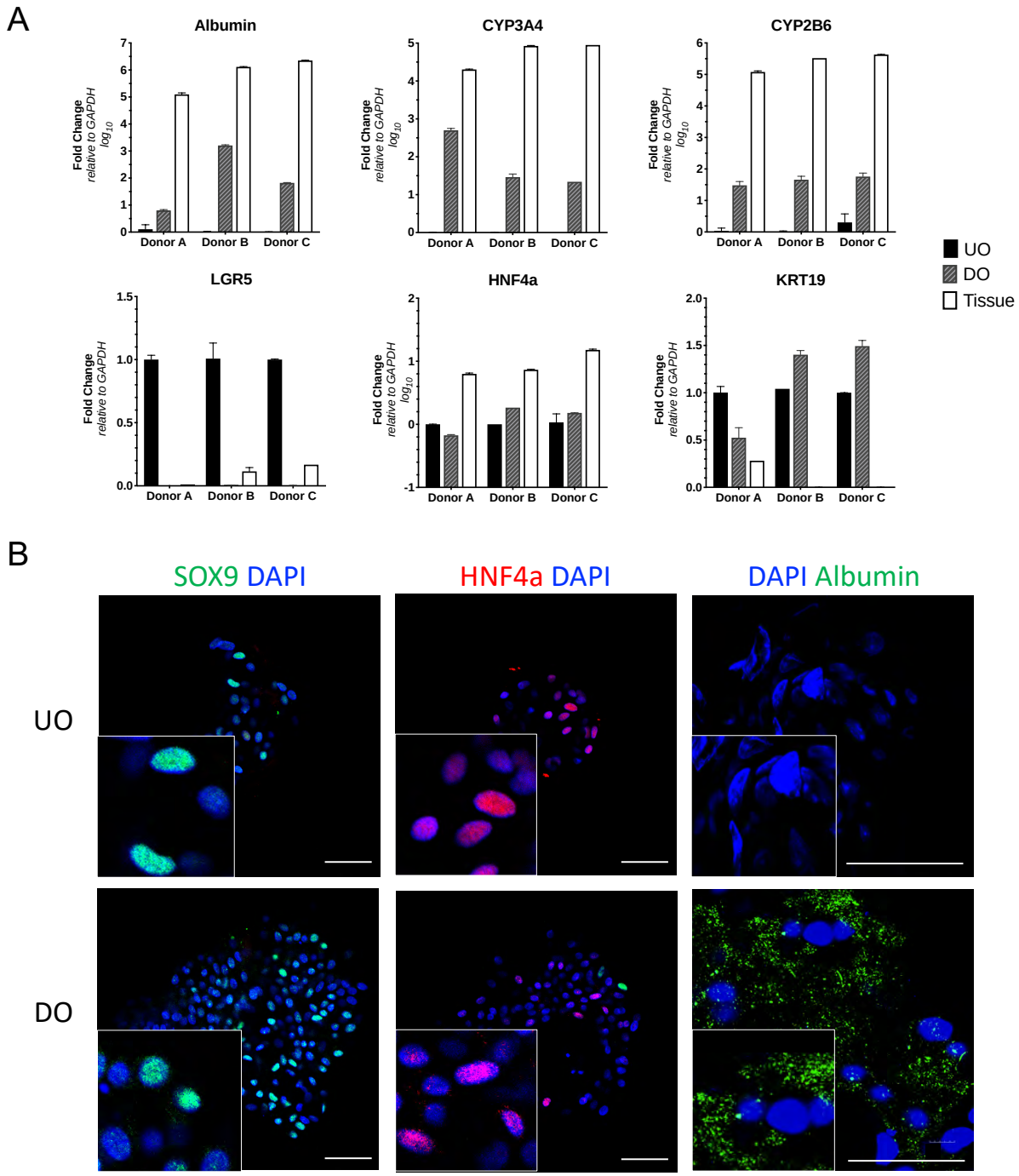

Figure 17: Metabolic and Cellular Markers of Human Liver Organoids
(A) qRT-PCR from three different organoids following differentiation, in comparison with tissue of origin. Expressed as fold change, relative to GAPDH. Mean+/-SEM. **(B)** Immunofluorescence staining of UO and DO with SOX9, HNF4a and albumin. 20x magnification.

Our qRT-PCR analysis revealed gene expression to suggest a hepatocyte phenotype in differentiated organoids. To further explore this at the whole transcriptome level, we generated 4 organoids from 4 different donors and differentiated them for 15 days using the standard differentiation protocol. Total RNA was extracted from the liver tissue and corresponding undifferentiated and differentiated organoids using TriSURE. RNA clean-up was performed using the RNeasy PowerClean pro CleanUp Kit (Qiagen) followed by quantification using the Qubit RNA HS assay. All RNA extracts were normalised to 200ng/μL and sent for RNASeq at SAHMRI. Total RNA was converted to strand specific Illumina compatible sequencing libraries using the Nugen Universal Plus mRNA mRNA-Seq library kit (Tecan) as described earlier. Equimolar of cDNA library was prepared and sequenced using Illumina NextSeq. Bioinformatic analysis was performed by Dr J. Breen from SAGC. A heat map of selected liver specific metabolic markers and cellular markers to visualise the differences between primary liver tissue and corresponding organoids revealed three distinct clusters between liver tissue, undifferentiated and differentiated organoids (Figure 18A), suggesting that indeed the differentiation process generated cell populations with different phenotypes. Upset Plot analysis (Figure 18B) was performed to provide visualisation of the proportion and cross-section between the transcriptomics of liver tissue, undifferentiated and differentiated organoids. The horizontal bars on the lower left of the Upset Plot indicates the proportion of all mRNA transcripts in each category. Together, differentiated organoids and liver tissue made up the bulk majority of the transcripts. Similarly, undifferentiated organoids and liver tissue also made up a large portion of the transcripts. In comparison, differentiated and undifferentiated organoids consist of only a small proportion of transcripts. The vertical bars at the top right indicate the cross sections between these groups. The largest portion of mRNA intersections occur between the undifferentiated organoids-liver and differentiated organoids-liver, suggesting that large

proportions of these transcripts (n=1673) are expressed in the liver tissue and not in the organoids. Consistent with what has been observed in the heatmap, Upset Plot analysis confirms that despite improved metabolic marker expression in differentiated organoids, the overall transcriptome of differentiated liver organoids is more similar to undifferentiated organoids.

Assessment of liver metabolic markers (albumin, CYP3A4, CYP2C9, CYP2C19, etc) revealed increased expression of these mRNA in comparison to undifferentiated organoids, that is consistent to our qRT-PCR data for at least CYP3A4. There was similar expression between differentiated and undifferentiated organoids with higher expression of ductal markers such as KRT7, KRT19 and SOX9, suggesting that as previously stated, that the differentiated organoids contain ductal cells in addition to hepatocytes. As predicted from our qRT-PCR analysis, the stem cell marker LGR5 was significantly suppressed in expression in differentiated organoids as compared with undifferentiated organoids, whereas hepatocyte marker HNF4a was similar between all three groups. Distinct donor variations were seen among the differentiated organoids despite similar culture and differentiation conditions. Interestingly one donor revealed high expression of albumin, CYP3A4, CYP2C9, suggesting greater differentiation to a more hepatocyte like phenotype. As previously described, differentiated organoids exhibit more ductal markers overall compared to liver tissue, consistent with a smaller hepatocyte to ductal cell ratio in the differentiated organoids.

Transcriptomic analysis of HBV pathways in hepatocyte (KEGG) was performed to assess the basal expression levels of cellular factors that are involved in HBV infection pathways. Figure S1 (Supplementary) shows that the mRNA expression profiles associated with this pathway clustered according to differentiation phenotype. Interestingly, expression levels

were remarkably similar between undifferentiated and differentiated organoids. The overall cellular factor expression is largely similar between the organoids and liver tissues within this pathway, with the exception of NTCP (SLC10A1), Matrix Metallopeptidase-9 (MMP-9) and Transforming Growth Factor-β (Figure 18). NTCP mRNA appears to be expressed at very low levels in undifferentiated organoids with slight increase following differentiation. It is unclear if this finding would translate into protein expression. This will be explored further in chapter 4. MMP-9 is an enzyme that catalyses proteolysis in extracellular matrix [260]. it is released by hepatocytes or macrophages in response to HBV infection and has been shown to play an important role in HBV replication through its binding to IFN receptor, resulting in suppression of JAK-STAT signalling pathway [261]. MMP-9 also plays a role in tissue remodelling in cirrhotic liver [262]. TGF-β has pleiotropic functions in hepatocytes and is secreted by macrophages in response to liver injury. It can promote liver differentiation and liver regeneration during liver development [263]. In chronic liver injury, TGF-β promotes liver fibrosis and cell death [264]. The lack of TGF-β signalling in liver organoids was consistent with the lack of inflammatory cell types.

We also assessed for the potential of liver organoids to support other hepatotropic viruses, and examined the transcriptomic expression of HCV-associated host factors (Figure S2). The analysis showed equal expression of HCV entry receptors Occludin (OCLN), Scavenger receptor class B, type I (SCARBI), Claudin-1 (CLDN-1) and CD81 [265-270] among undifferentiated and differentiated organoids. The mRNA expression of CLDN-1 and CD81 appeared to be slightly lesser than the liver tissue. Again, the susceptibility of organoids to HCV infection would require further evaluation of the receptor expression at the protein levels, not to mention expression of appropriate host factors for HCV replication.

In the innate immune arm of analysis, strong mitogen-activated protein kinases expression was noted among the liver organoids (Figure S3). The MAPK ERK1/2 pathway has been previously shown to be important in supporting hepatocyte proliferation in response to EGF [271]. mRNA profiling of RIG-I pathway among the liver organoids and liver tissue was largely similar (Figure S4).

In addition, due to the low oxygen tension in the liver organ, we assessed the transcriptomic profiles of HIF-1 pathway (Figure S5). The HIF-1 associated genes such as lactate dehydrogenase (LDHB), Vascular Endothelial Growth Factor (VEGF) and Epidermal Growth Factor (EGF) were all expressed at similar levels between the organoids and liver tissue, with the exception of aldolase B and transferrin (TF) (Figure S5).

Next, we assessed the necroptosis and apoptosis pathways in view of their relevance to the HBV pathogenesis and potential therapeutic targets (Figure S6 & S7). Necroptosis is a programmed cell death mechanism induced by inflammation. This could be initiated by cellular injury or pathogen invasion. Some of the important therapeutic target genes such as Fas-Associated protein with Death Domain (FADD) and CASP8 were both expressed at similar levels in the organoids as the liver tissue [272, 273]. Targeted therapy on these genes have been previously used in the treatment of cancer. Drugs that antagonise the inhibitors of apoptosis (IAP) proteins have been shown to induce cell death in HBV-infected cells [274, 275].

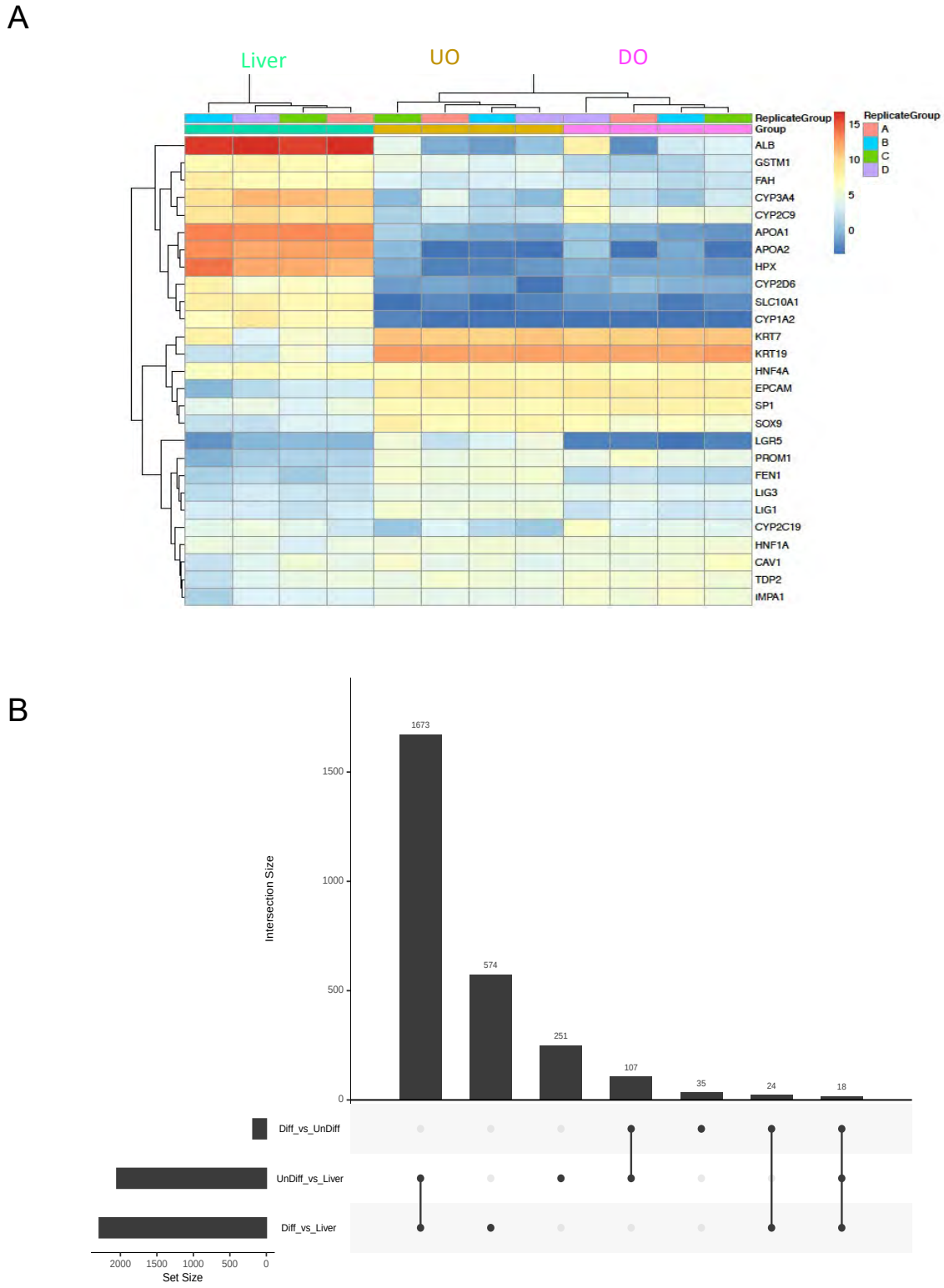

Figure 18: RNA Sequencing of Liver Organoids and Corresponding Parental Liver Tissue

RNA Seq for four undifferentiated and differentiated human liver organoids, with corresponding liver tissue of origin. **(A)** Heatmap for selected hepatic metabolic markers **(B)** Upset plot for overall transcriptome of human liver organoids in comparison with liver tissue.

3.7 Optimisation of Human Liver Organoids Culture

Once we had established that the human liver organoids could be successfully isolated and differentiated into hepatocyte-like cells, we assessed various aspects of culture techniques that could increase efficiency of differentiation and potentially influence the success of downstream infection experiments.

In order to develop an infection method that is applicable to multiple different hepatotropic viruses, we explored the possibility of using a single cell suspension method that would ultimately increase viral infection efficiency. This is based on the hypothesis that cellular viral entry receptors could be expressed on different surfaces (i.e., basal vs apical) of hepatocytes, thus limiting access of virus to entry receptors. Using HCV as an example, the entry receptors SR-BI, CD81 and CLDN1 are all expressed on the basal lateral surfaces whereas OCLN is expressed solely on the apical surfaces and HCV infection occurs in a stepwise process [269, 270, 276, 277]. While not physiologically correct, by dissociating the organoids into single cell suspension, it is possible that the virus has access to all receptors resulting in efficient internalisation. One of the challenges of single cell dissociation of organoid cultures is the loss of cellular anchorage that can lead to activation of anoikis. Anoikis is a programmed cell death upon cell-cell detachment, and physiologically serves as a protective mechanism to prevent detached epithelial cells from colonizing elsewhere in the body [278]. Hepatocytes and stem cells are very susceptible to anoikis [279, 280]. To protect against anoikis we reasoned that the use of the Rho-kinase inhibitor Y-27632 in culture could prevent this detachment induced apoptosis [281, 282] and render the differentiated organoids susceptible to infection in single cell suspension as the differentiation process renders the organoids non-proliferative.

To determine if single cell suspension was a viable option for generation of differentiated organoids, we differentiated liver organoids from two different donors using the previously described protocol for 15 days. In brief, the organoids were washed with cold basal medium to remove the extracellular matrix and digested with 1mL of TrypLE Express supplemented with Y-27632 for 10 minutes and mechanically dissociated into single cells. It is at this point that organoid would be infected with hepatotropic viruses. The organoids were then reseeded into extracellular matrix and cultured under three different conditions, (1) EM (2) DM + 30% Wnt3a + 10% RSPO-1 (vol/vol) and (3) DM + 10% RSPO-1 (vol/vol). Both Wnt3a and RSPO-1 helped induce LGR5+ stem cell expansion through the β-catenin pathway. All media were supplemented with Y-27632 for 48 hours to ensure optimal cell survival. Serial light microscopy pictures and measurements showed median diameter of regenerated liver organoids to be largely similar between all three media (Figure 19). Organoids from one donor show large variability in sizes when cultured with DM supplemented with Wnt3a and RSPO-1 but the median size was similar to the other culture conditions. Overall, this experiment shows that regeneration of organoids following dissociation into single cells can occur with either EM or DM supplemented with RSPO-1 and/or Wnt3a. If required, downstream infection experiment can be performed on differentiated organoids dissociated into single cells and allowed to reform into multi-cellular organoids.

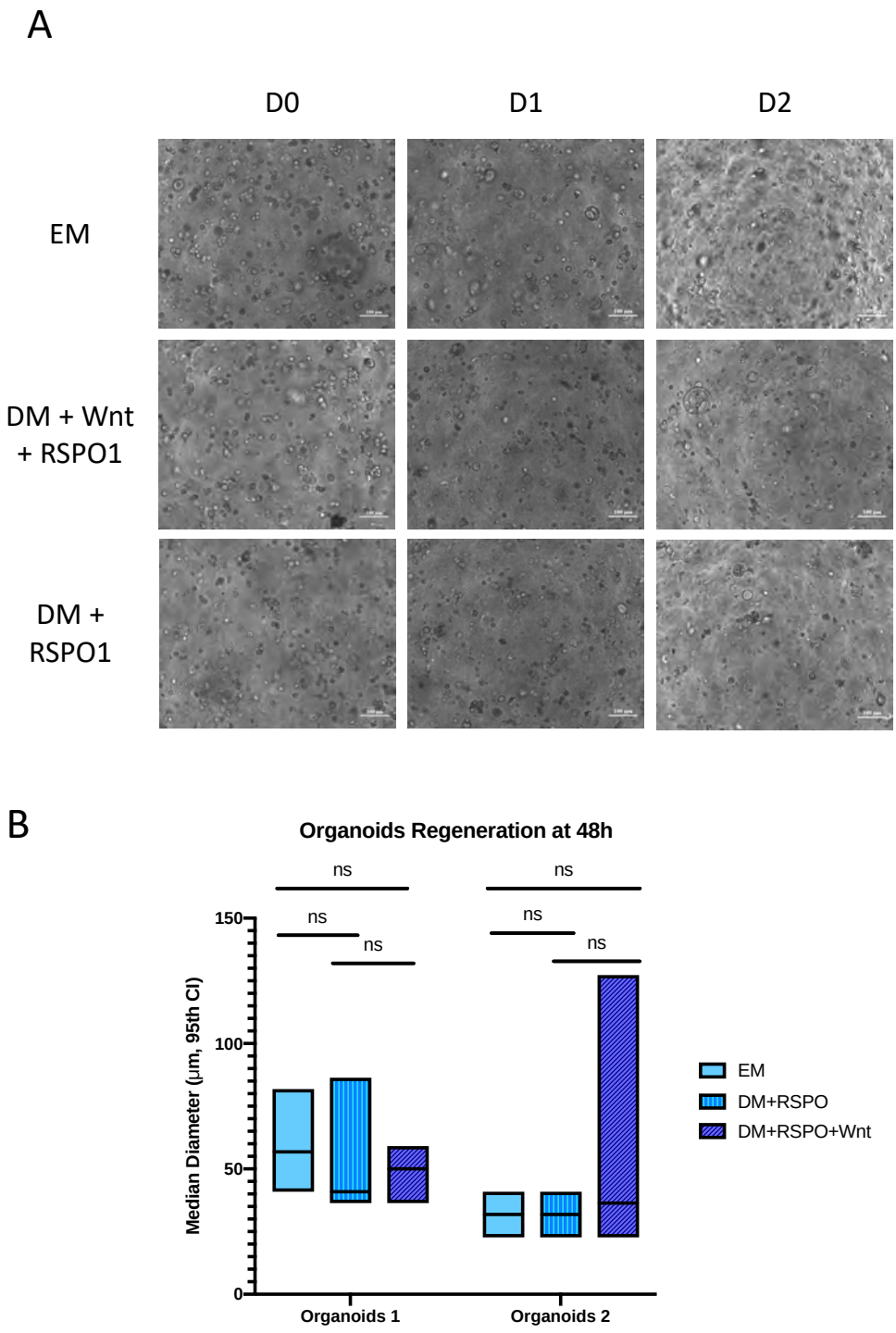

Figure 19: Human Liver Organoids Regeneration from Single Cells
(A) Liver organoids regeneration under different culture conditions, examined using light microscopy, 10x magnification, representative images from two organoids. **(B)** organoids sizes under different culture conditions at 48 hours post-dissociation into single cells. Average diameters of 10 organoids from each field.

3.8 Optimisation of Human Liver Organoids Differentiation

Our collective findings from earlier differentiation experiments show that similar to other stem cell derived HLCs, the adult stem cell derived liver organoids undergo differentiation. However, this seems to be limited in comparison to the metabolic markers expressed in PHHs. Non-parenchymal cells (e.g., liver fibroblasts, Kupffer cells, stellate cells etc.) play an important role in liver physiology mainly through expression of cytokines, such as FGF from stellate cells, OSM, TFG-β, IL-6, TNF from Kupffer cells, HGF from sinusoidal cells, that all help regulate liver regeneration and function [283-289]. To compensate for the lack of non-parenchymal cells, the organoids culture media consists of an array of cytokines such as HGF, FGF, TGF-β, BMP7 and dexamethasone. Among all these cytokines, HGF and OSM are considered the most important in mature hepatocyte function [290].

Next, we designed an experiment with different growth factor and supplement combinations to assess their effects on albumin and NTCP mRNA expression, as markers for liver maturation and possible susceptibility to HBV infection (Figure 20). Addition of Ascorbic Acid 2-Phosphate (AAP) with or without insulin to differentiation media resulted in increased albumin mRNA expression in comparison with undifferentiated organoids and differentiated organoids. However, the increased in NTCP was not significant when compared with differentiated organoids. Addition of Oncostatin M (OSM) resulted in suppression of differentiation markers, in contrast with previous reports in iPSC-HLC and hepatocyte-derived organoids. This finding suggests that OSM plays an important role in liver maturation only at an early stage, consistent with previous reports that the more differentiated liver progenitor cells have suppressed hepatocyte maturation with OSM [291, 292]. In conclusion, the adult stem cell derived organoids follow a different path of liver maturation from iPSC. AAP and insulin slightly improve the expression of metabolic

markers, but assessment of other growth factors and culture conditions is required for further improvement of liver organoid differentiation.

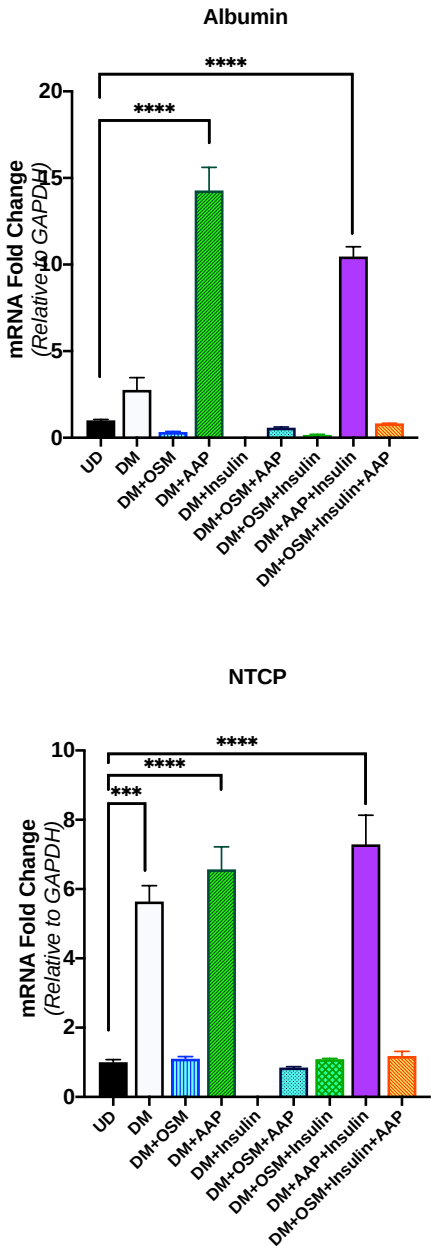

Figure 20: Optimisation of Human Liver Organoids Differentiation
Albumin and NTCP mRNA expression in liver organoids following differentiation for 15 days in different culture media, normalised to GAPDH and undifferentiated organoids (UD), expressed as Mean±SEM. Representative figure from one donor.

3.9 Discussion

In vitro cell culture model systems are critical for the study of virus replication, pathogenesis, and testing and development of antiviral strategies. However, while some viruses propagate well in culture this is not the case for HBV and over the years there have been significant impediments to HBV research due to the lack of relevant model systems. While the discovery of the HBV receptor, NTCP and its ectopic expression on HepG2 cells has been a significant advance in HBV biology it does have limitations primarily with the fact that HepG2 are tumour derived and have a number of limitations when compared to primary hepatocytes. With this in mind we embarked to develop primary liver organoid cultures, initially murine liver organoids as a proof of concept and ultimately primary human liver organoids as an *in vitro* model for HBV infection studies.

Generation of organoid culture is a complex process and therefore prior to our human studies we sought to optimize our skills in the generation of mouse liver organoids. We adopted a protocol described by Huch *et al.* and colleagues in which we isolated ductal structures from the livers of C57b/6 mice following collagenase digestion. In contrast to human liver organoids, it is the ductal structures in the mouse liver that contain the stem cells essential for organoids development. Culture of these isolated ductal structures in isolation medium and in extracellular matrix provides a 3D substrate and the necessary growth factors for stem cell expansion and early in the process it was evident that these ball-like structures were budding off from ductal structures (Figure 9 & 10) until the extracellular matrix was completely full of these undifferentiated liver organoids. Immunostaining of these undifferentiated organoids using a specific antibody to E-cadherin to visualise the cell membrane and coupled with Lighsheet 3D microscopy revealed that indeed the structures were multi-cystic in nature in which organoid wall was 1-2 cells thick.

In human liver organoids generation, we successfully characterised the structural changes and metabolic changes before and after differentiation. The organoids underwent morphogenic changes in cell structure, arrangement and polarity. Hepatic polarisation, a hallmark of differentiation was seen in histopathology, immunofluorescence and TEM. The differentiated organoids assume partial hepatic polarity due to the lack of sinusoidal structure. The differentiated liver organoids expressed increased levels of albumin and CYP3A4, which are key markers of hepatocyte differentiation. The level of expression was not as high as the liver tissue, most probably due to incomplete differentiation in the current organoid culture conditions, evident with residual ductal marker, SOX9 expression in differentiated organoids as assessed with immunofluorescence staining (Figure 17). Transcriptomic analysis revealed the similarities and differences of liver organoids and corresponding liver tissue in hepatotropic viral pathways, innate immune response and necroptosis. Some of the differences could be explained by the lack of other non-parenchymal and liver inflammatory cell types in the organoids. Individual pathway assessment and correlation with the organoids proteomics are required to confirm these findings.

In liver regeneration, proliferating hepatic progenitors arranged in an unstructured manner. Polarity of hepatocytes only occur following interaction with bile duct and sinusoidal cells, unless the hepatic mass assumes a large enough parenchymal density [293]. Cell-cell contact is essential for this process to occur, and is mediated by adhesion molecules such as E-cadherin [294]. Establishment of tight junctions and spatially restricted events lead to reorganistion of intracellular cytoskeleton [295, 296]. Interaction with the sinusoidal proteins and bile canaliculi help with the establishment of apical and basolateral surfaces [297] although the mechanism of apical polarity induced by contact with bile canaliculi is less well understood [298]. Hepatic polarisation is associated with changes in trafficking machinery

and allows maturation of cellular transportation function of hepatocytes. Similarly, in undifferentiated human liver organoids, cellular proliferation is not associated with polarisation, given the lack of sinusoidal cells. Following expansion and differentiation, partial polarity is seen in organoids, possibly due to the interaction between maturing hepatocyte-like cells and differentiated cholangiocytes.

When using *in vitro* culture such as either rat hepatocytes or iPSC, increase blood flow and oxygenation has led to improve albumin secretion and other metabolic functions [299]. However, this is in contrast with the liver microenvironment which is predominantly perfused with poorly oxygenated blood. The portal venous system is the main blood supply of liver and is poorly oxygenated. The well oxygenated hepatic arteries only contribute to 25% of blood flow, creating an oxygen gradient across the liver tissues. It is unclear if changes in oxygen tension would alter the metabolism and maturation of liver organoids. However, it would be possible in future experiments to culture organoids in different concentration of oxygen and to access hepatocyte differentiation.

In conclusion, human liver organoids can be generated from Wnt-driven selective culture of hepatic progenitor cells from digested liver tissues. Following differentiation, these organoids can express some mature hepatocyte functions including albumin secretion and CYP450 metabolism. In comparison with corresponding liver tissues, liver organoids express less mature hepatocyte markers, possibly due to a combination of factors: (1) equal proportion of cells undergoing hepatocyte and cholangiocytes differentiation, whereas large proportion of hepatic regeneration *in vivo* assume hepatocyte differentiation, (2) lack of sinusoidal endothelial cells to assist with maturation of cellular protein trafficking mechanisms, (3) lack of growth factors from non-parenchymal cells and (4) non-physiological oxygen tension in

culture. Future optimisation of organoids culture should explore the co-culture system with non-parenchymal cells and culture in different oxygen tension, as previously discussed. Our ability to generation human liver organoids with a differentiated hepatocyte phenotype now presents us with a model system to explore this as a model for HBV infection.

4 Chapter 4: Human Liver Organoids Express The Functional HBV Entry Receptor, Sodium Taurocholate Co-transporting Polypeptide (NTCP) and Support HBV Replication

4.1 Introduction

Prior to the discovery of Sodium Taurocholate Co-transporting Polypeptide (NTCP) as a HBV entry receptor, studies on HBV infection and life cycle had been challenging [300]. Many potential cellular molecules were identified to bind to the HBV envelope, but none were found to be essential for HBV infection [301, 302]. HBV infection also demonstrates species and organ specificity, with only a limited number of cell types being susceptible to infection [14]. In a breakthrough study from the Urban lab, it is now identified that the NTCP protein is an essential entry receptor that could render non-susceptible cell lines infectable to HBV and HDV [16].

4.2 Characterisation of NTCP in Liver Organoids

HBV entry requires two main factors: (1) a conserved 75aa sequence of the HBV preS1 region [303] with myristylation to the N-terminal[304-306] and (2) expression of functional NTCP that could interact with the PreS1 region. To assist in downstream HBV infection studies, we first examined (1) if organoid culture expressed NTCP and (2) the temporal and spatial relationship of NTCP expression in organoids throughout differentiation to determine the optimal timing for infection experiments. To investigate this, we differentiated human liver organoids as described previously over a period of 20 days and examined albumin and NTCP expression. In the undifferentiated state, NTCP mRNA was expressed at very low levels in liver organoids, however, NTCP mRNA expression increases following differentiation especially from day 15 onwards (Figure 21). To determine whether NTCP expression can be further improved through advanced differentiation, we tested a number of reagents used in terminal differentiation of iPSC-derived liver buds to form mature

hepatocyte-like cells (Figure 20). Ascorbic acid-2 phosphate (AAP) has been shown to upregulate HGF and maintaining hepatocyte differentiation [194, 307, 308] whereas insulin has been shown to enhance hepatocyte differentiation via the PI3K/AKT pathway [309-311]. AAP and insulin significantly upregulate albumin expression but the effect on NTCP expression is only modest. In contrast to iPSC and hepatocyte-derived organoids, oncostatin M significantly downregulates NTCP expression in LGR5+ liver organoids (Figure 20). Following 15 days of differentiation, we observed significant donor variations in the level of NTCP expression (Figure 21).

Next, we assessed if NTCP mRNA expression translates into functional protein expression. In addition to changing hepatocyte polarity in liver organoids during differentiation, an inverted polarisation phenotype has been described in other types of organoids, posing potential challenges to HBV infection as NTCP may not be accessible [312]. Using confocal immunofluorescence microscopy, we observed significant NTCP expression as detected on the cell surface towards the external part of the organoids and in between adjoining cells, removed from ZO-1 (localized to apical surface) (Figure 22). However, the expression of NTCP on the cell surface alone may not necessarily indicate susceptibility to HBV infection. One reason is that NTCP is a transmembrane protein with two N-linked glycosylation sites on the external part of the receptor (Figure 23), and it has been shown that glycosylation deficient NTCP failed to support HBV infection [313]. Another reason is that in our study, the NTCP antibody used to detect NTCP (Figure 23) are polyclonal in nature and detects intracellular C-terminal region of the NTCP. Thus, the detection of NTCP by immunofluorescence is not necessarily a true indication of functional receptor expression and may not inform susceptibility to HBV infection. For this reason, we therefore visualised the NTCP expression using a functional binding assay with fluorescent labelled myristoylated

HBV PreS1 peptide (Myrcludex B) [15, 314-316]. As schematic of Myrcludex B and its interaction with NTCP is provided in Figure 21A. We first incubated the HBV PreS1 peptide with live organoids, followed by fixation and permeabilisation with Triton-X for NTCP antibody staining. This procedure ensures binding of HBV PreS1 peptide to NTCP is exclusively on the external portion of the receptor and non-specific binding is not being visualised. As seen in figure 23, the Myrcludex peptide bound to the liver organoids indicating cell surface functional NTCP expression. Interestingly, using NTCP antibody staining revealed low level and inconsistent positivity in undifferentiated organoids that in time, changed from a cytoplasmic localisation to assuming a cell surface localisation from day 10 post-differentiation (Figure 23B). This was confirmed using Myrcludex B in which we observed that PreS1 peptide staining was only seen following day 10 post differentiation. This suggests that while undifferentiated organoids can express NTCP at a low level, its expression is limited to the cytoplasm, and as differentiation proceeds functional NTCP is expressed on the cell surface.

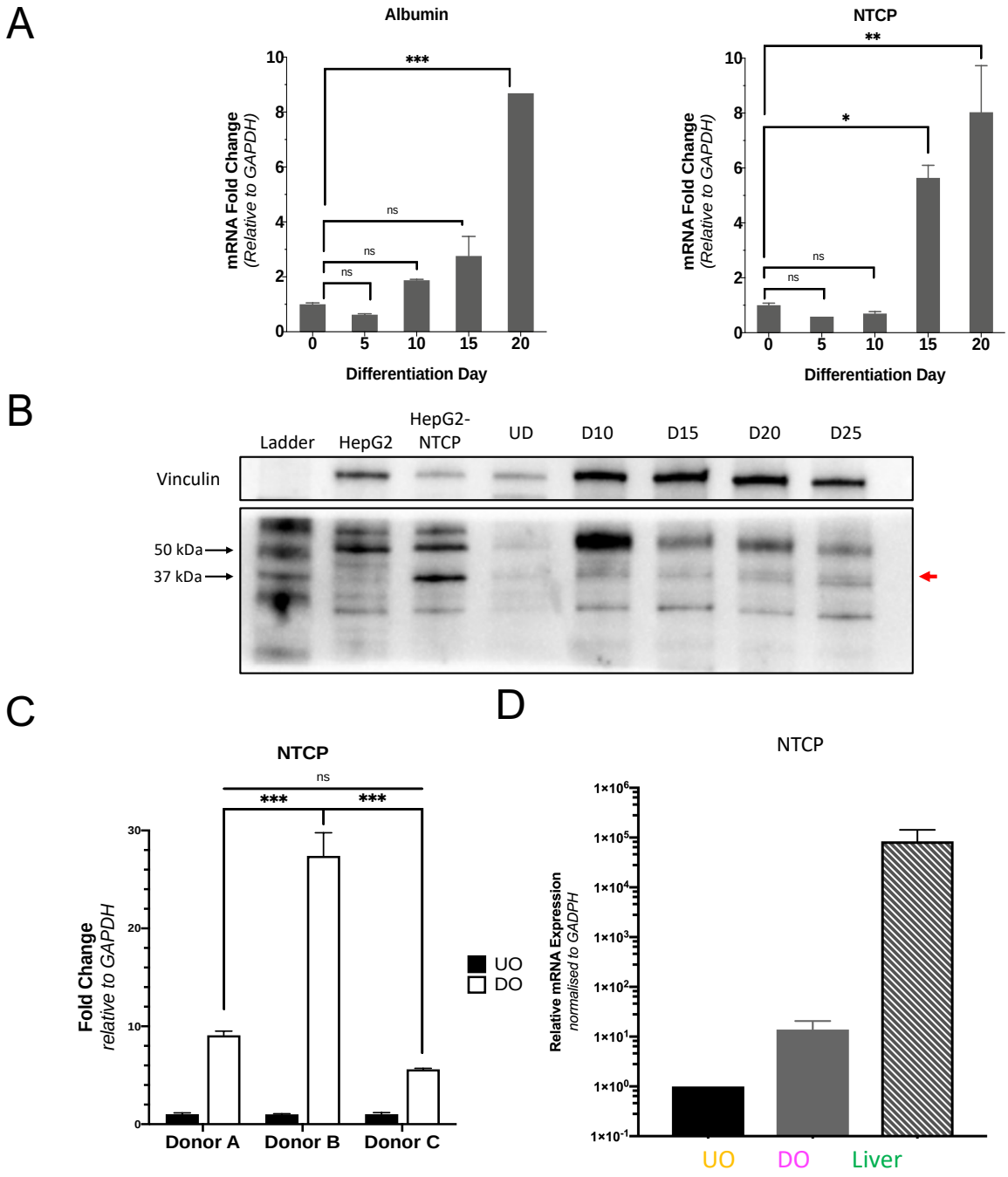

Figure 21: NTCP Expression in Liver Organoids
qRT-PCR of organoids showing **(A)** NTCP and albumin mRNA expression during the course of differentiation, normalised to GAPDH and day 0, expressed as Mean±SEM. **(B)** NTCP western blot across differentiation timeline, in comparison with HepG2 and HepG2-NTCP, vinculin as expression control. Red arrow indicates the NTCP bands **(C)** NTCP mRNA expression between three different organoids donors. **(D)** NTCP expression in UO, DO and corresponding liver tissue.

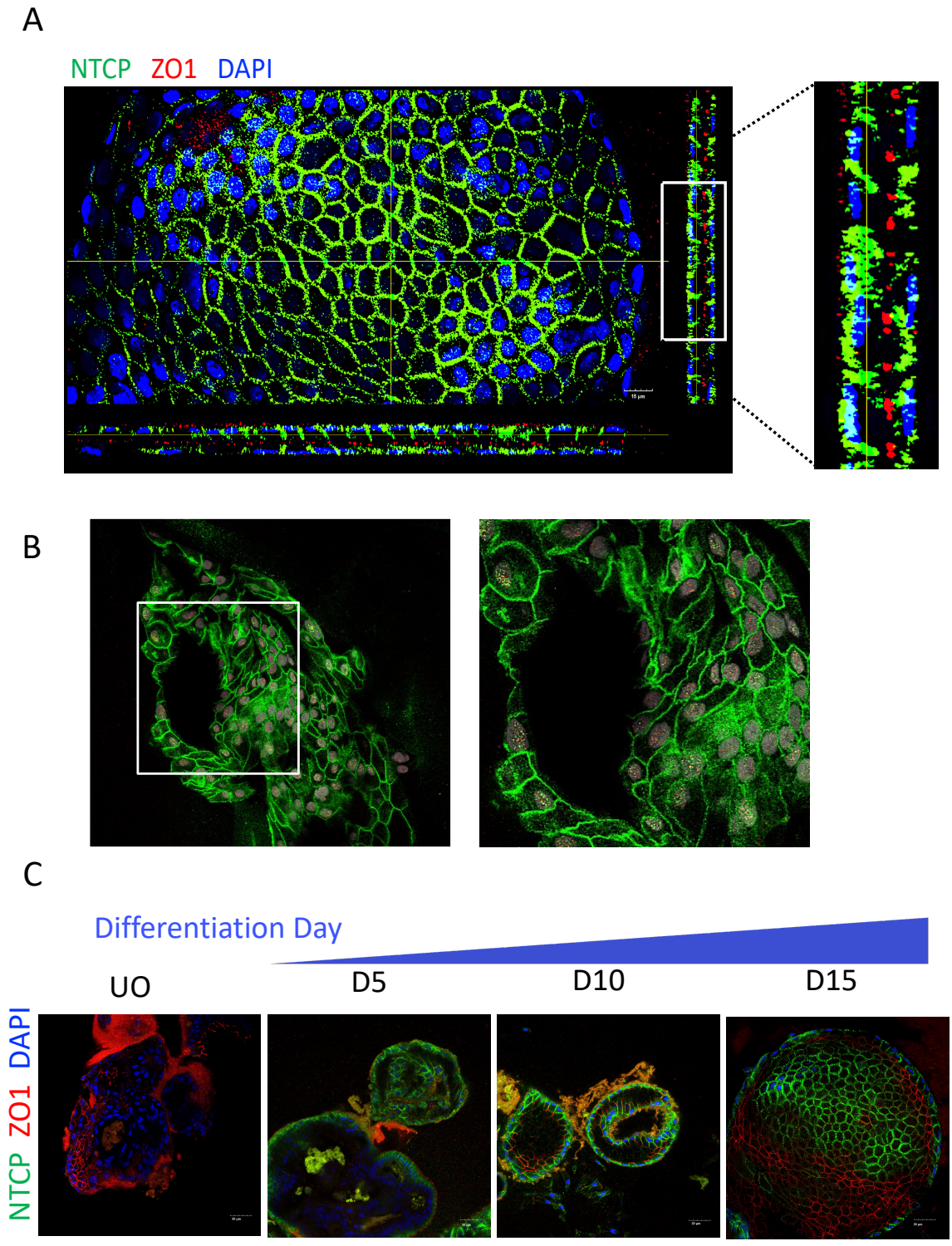

Figure 22: NTCP Expression in Liver Organoids
Comparison between immunofluorescence staining of organoids with NTCP and PreS1 functional assay. **(A)** Three slide views of confocal image of a differentiated organoid, staining with antibodies against C-terminal of NTCP. **(B)** NTCP staining of differentiated organoids and **(C)** across differentiation timeline.

Movie 3: NTCP Expression in Liver Organoids
Confocal microscopy of differentiated human liver organoids at 20X, Green – NTCP, Blue – DAPI, Red – ZO-1

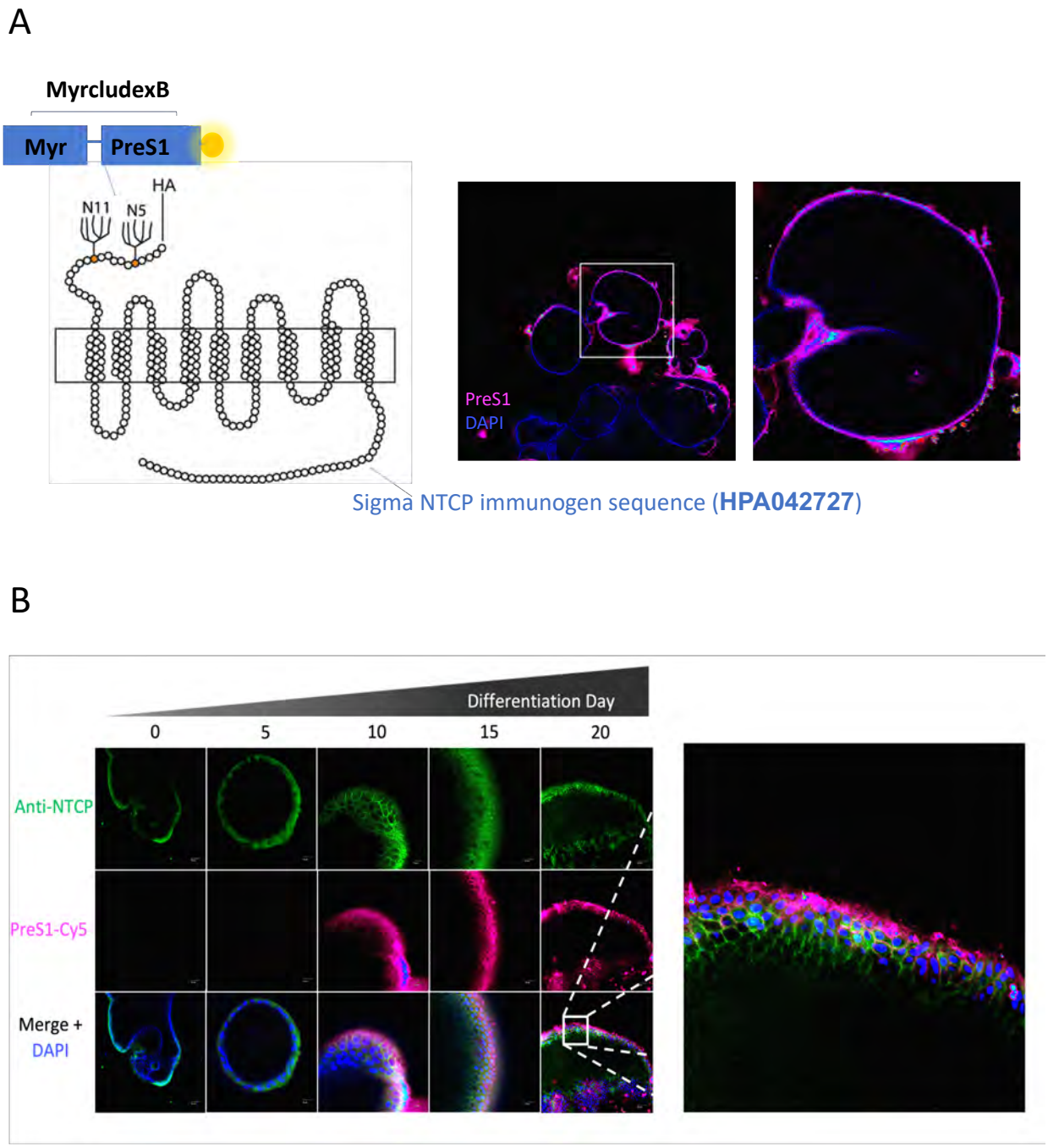

Figure 23: Expression of Functional NTCP during Organoid Differentiation
Confocal microscopy of HBV PreS1 peptide staining, images at 10x magnification. **(A)** Schematics of PreS1 peptide and NTCP antibodies binding sites, with corresponding live cell images of PreS1 binding assay. **(B)** Combined NTCP antibodies and PreS1staining across differentiation timeline. Note the lack of functional NTCP expression during the early stages of differentiation.

Movie 4: Functional Receptor Expression in Differentiated Organoids
PreS1 binding assay in human liver organoids following 20-day differentiation, examined with confocal microscopy. Pink – PreS1, Blue – DAPI.

4.3 Optimisation of HBV Infection in Human Liver Organoids

Having established the expression of functional NTCP, on organoids and its optimal expression window, we next decided to perform infection experiments with HepAD38-derived or plasma-derived HBV using organoids that have been differentiated for at least 15 days.

During the process of optimisation, we infected the organoids with 1000 genome equivalents of plasma HBV (genotype B) by incubating the differentiated organoids with the inoculum with and without 4% PEG 8000. PEG has been previously shown to improve HBV infection and reproducibility in cell culture models using PHH and hepatoma cell lines [182, 317, 318]. The organoids were washed with cold media to remove the extracellular matrix and incubated with the inoculum and 4% PEG 8000 for 3 hours before multiple washing steps to remove the inoculum and unbound HBV. The infected organoids were incubated with differentiation medium supplemented with 4% PEG throughout the experiment. A control without PEG during the process of infection and post-infection period was used as comparison. Brightfield microscopy showed minimal cellular death at 15 days post-infection. Immunofluorescence staining with antibodies directed against HBcAg and HBsAg at day 8 confirmed the presence of intracellular HBsAg expression although the number of infected cells were low (Figure 24). qRT-PCR using RNA harvested at day 12 post-infection to quantitate HBV pgRNA, toral HBV RNA, revealed higher levels of HBV total RNA and full-length 3.5kb RNA in the PEG-incubated organoids in comparison to no PEG. Quantification of HBV DNA in supernatant through the time course of infection showed a reduction in HBV DNA over the period of 12 days, suggesting that the infection level was insufficient to sustain ongoing HBV replication and spread. Despite the washing steps to remove the HBV inoculum, it is likely that the detection of HBV DNA at the early time point reflects the input HBV due to the high

viral inoculum used. Low level HBV viral replication may not be readily visible due to the large quantity of residual viral DNA detected with qPCR. This experiment was repeated with two different organoids, showing variability in supernatant HBV DNA between the two organoids. This work indicates that differentiated organoids can be infected with HBV, although further improvement is required to overcome the issue of low infectivity and inconsistency of infection.

Spinoculation has been shown to enhance HBV infection in PHH, therefore we performed an infection experiment using tube spinoculation to increase the chance of cell and virus contact [319] (Figure 25). DMSO has also been shown to enhance NTCP expression in hepatoma cell lines and increased HBV infection in PHH, presumably by arresting cell cycle and inducing hepatocyte differentiation[213, 320-323]. After washing off the extracellular matrix with cold medium, the differentiated organoids were incubated with either plasma or AD38-derived HBV at 1000 genome copies/cell. The organoids were then incubated with 4% PEG, supplemented with Rho-kinase inhibitor to prevent apoptosis and subjected to tube spinoculation at 300 x g for one hour at room temperature before resuspension and re-inoculation into extracellular matrix. The infected organoids were incubated in DM and Rho-kinase inhibitor for the rest of the experimental time frame to prevent cell death. At day 10 post-infection total RNA was harvested and qRT-PCR for detection of total HBV RNA and pgRNA was performed (Figure 25, 26). Clearly organoids were infected with both pHBV and AD38 HBV, although DMSO did not enhance infection with pHBV. qPCR showed increased HBV total RNA and pgRNA at day 10 but intracellular and supernatant HBV DNA were inconsistent. Unlike immortalised cell lines (HepG2-NTCP, HepaRG), DMSO did not improve infection in liver organoids.

One of the major challenges in HBV infection model system is the requirement of high inoculum to achieve infection and difficulties in achieving consistencies [318, 324]. To further improve our organoid infection model to achieving greater surface areas exposed to HBV, we incubated undifferentiated organoids that had been treated with TrypLE express until they dissociate into single cells prior to infection. TrypLE dissociates the organoids into single cells without removing key surface molecules that would normally occur using Trypsin. These organoids were allowed to regenerate in EM for 5 days to form small organoids of 20-50μm in diameter, before differentiation process. During the 15-day differentiation process, the organoids did not proliferate and retain original sizes. In order to allow larger contact area between the organoids and HBV, plate spinoculation method was used instead (Figure 27). Using organoids regenerated from single cells in combination with spinoculation, we managed to achieve consistent infections with AD38-derived HBV. The success of infection at different inoculum was also assessed using immunofluorescence staining. HBcAg staining 4 days post-infection showed that inoculum of at least 200 genome copies/cell of cell culture derived HBV is essential for establishment of infection. Infected cells showed mainly cytoplasmic HBcAg staining, consistent with viral replication (Figure 28, 29, Movie 4) [325, 326]. Infection in liver organoids occurred as clusters similar to infection foci observed in primary hepatocytes [327].

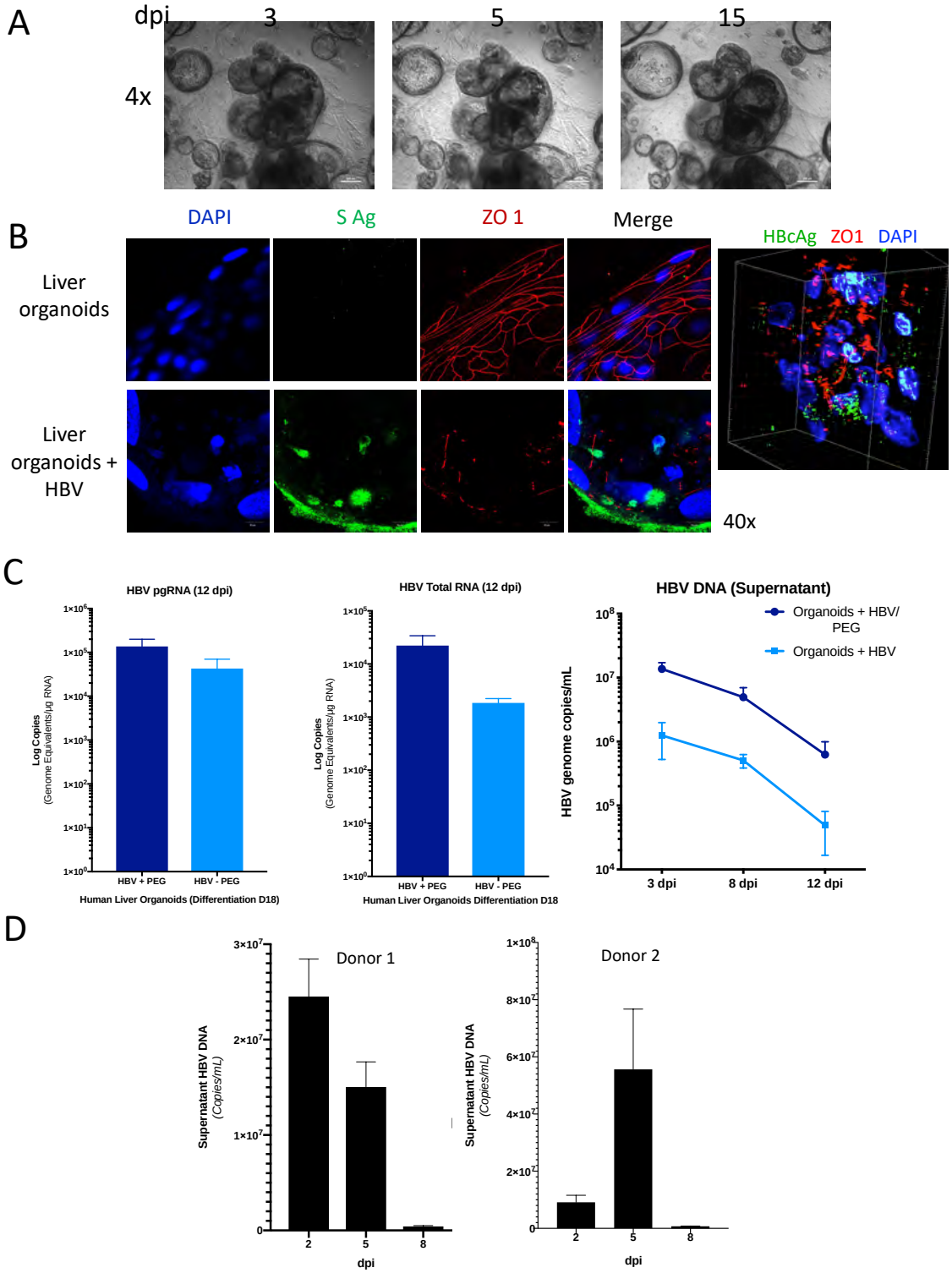

Figure 24: Optimisation of HBV Infection in Organoids

Optimisation of HBV infection (plasma HBV genotype B) under different culture conditions. **(A)** brightfield microscopy. **(B)** Corresponding immunofluorescence staining of organoids with antibodies against cAg and sAg. **(C)** qPCR for HBV pgRNA, total RNA and supernatant DNA with or without 8% PEG during infection and culture, normalised to total RNA, expressed as Mean±SEM. **(D)** qPCR for supernatant DNA in a separate infection experiment with two different organoids.

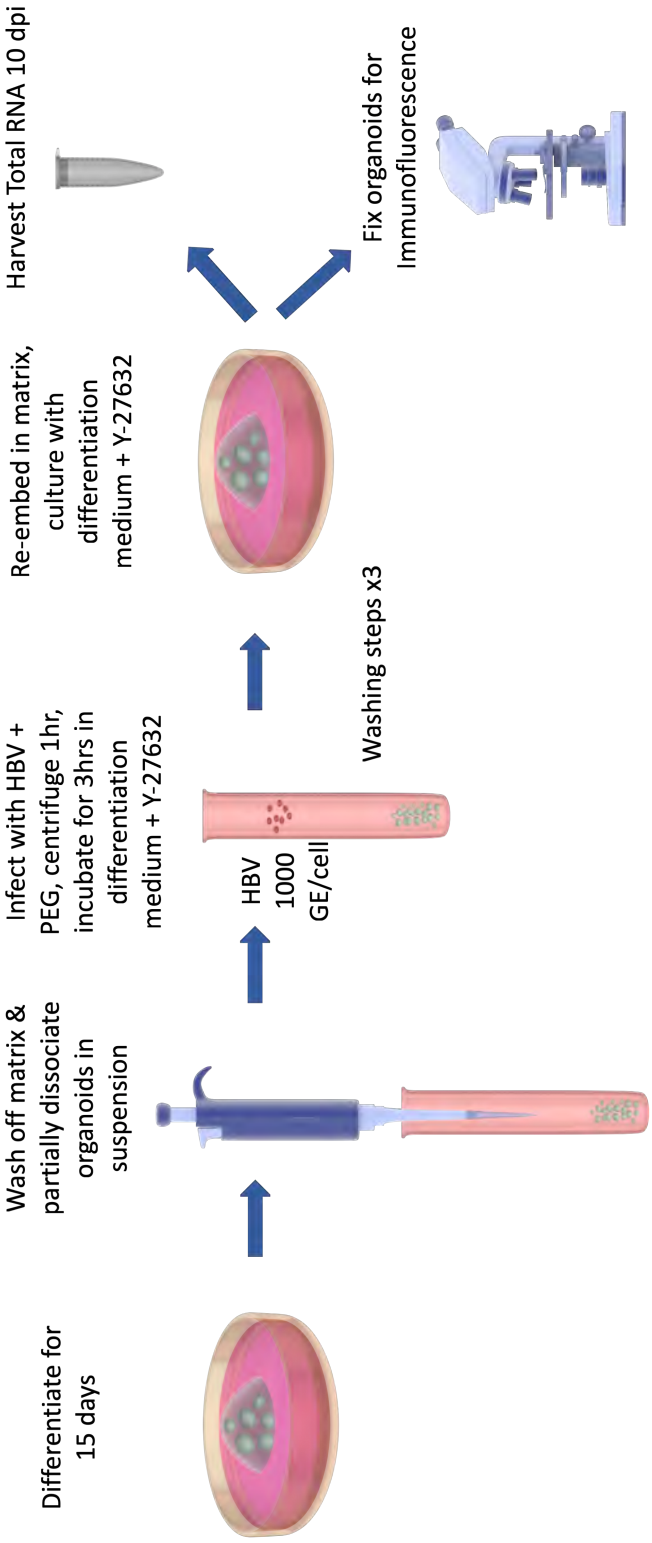

Figure 25: HBV Tube Spinoculation Schematics

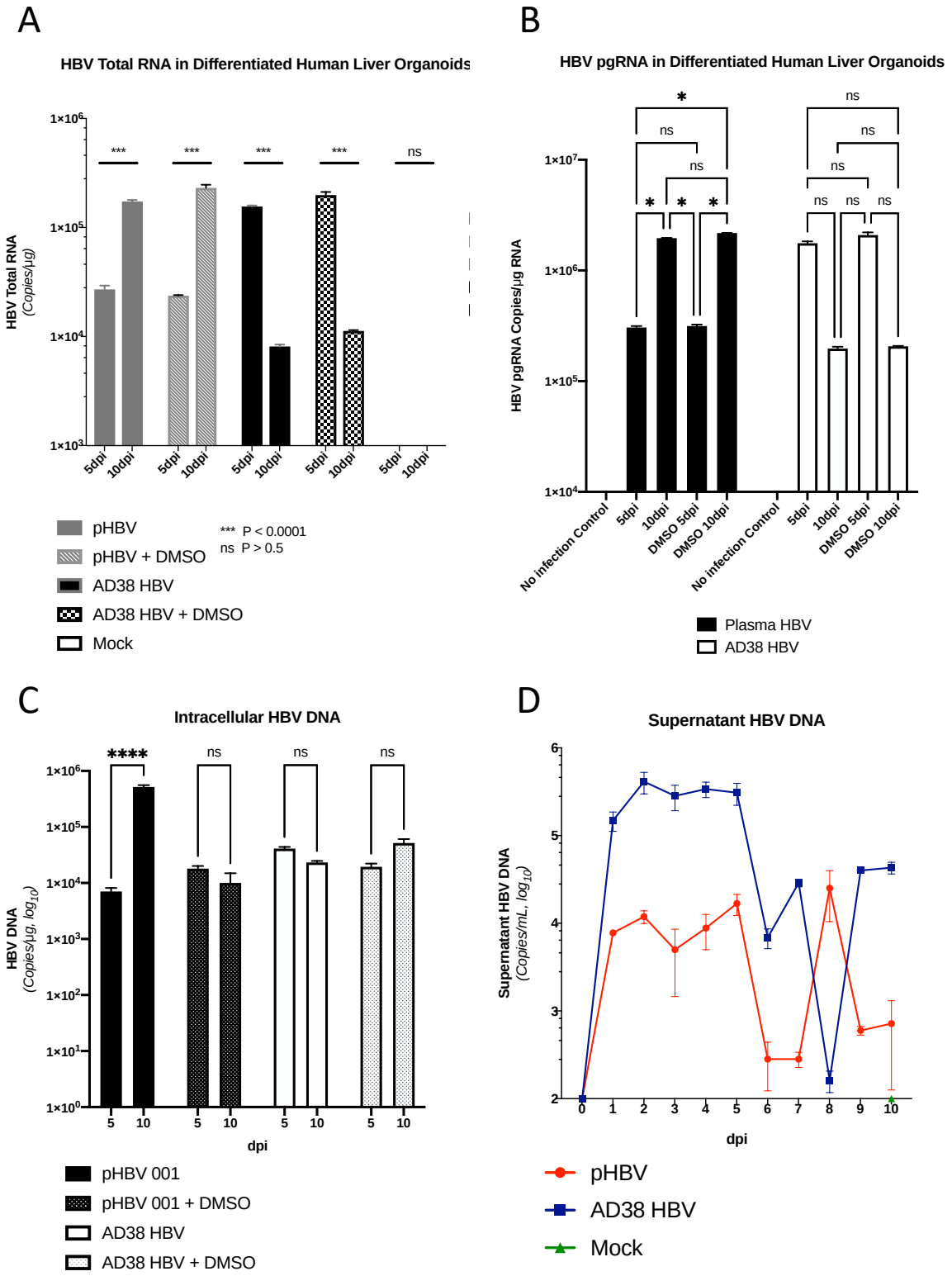

Figure 26: HBV Infection in the Presence of DMSO (Tube Spinoculation)
HBV infection experiment schematics (organoids n =2, replicates = 3) (A) with or without 4% DMSO. (B) qRT-PCR for HBV total RNA and pgRNA for two organoids, normalised to total RNA, expressed as Mean±SEM. **(C)** qPCR for intracellular DNA and **(D)** supernatant DNA.

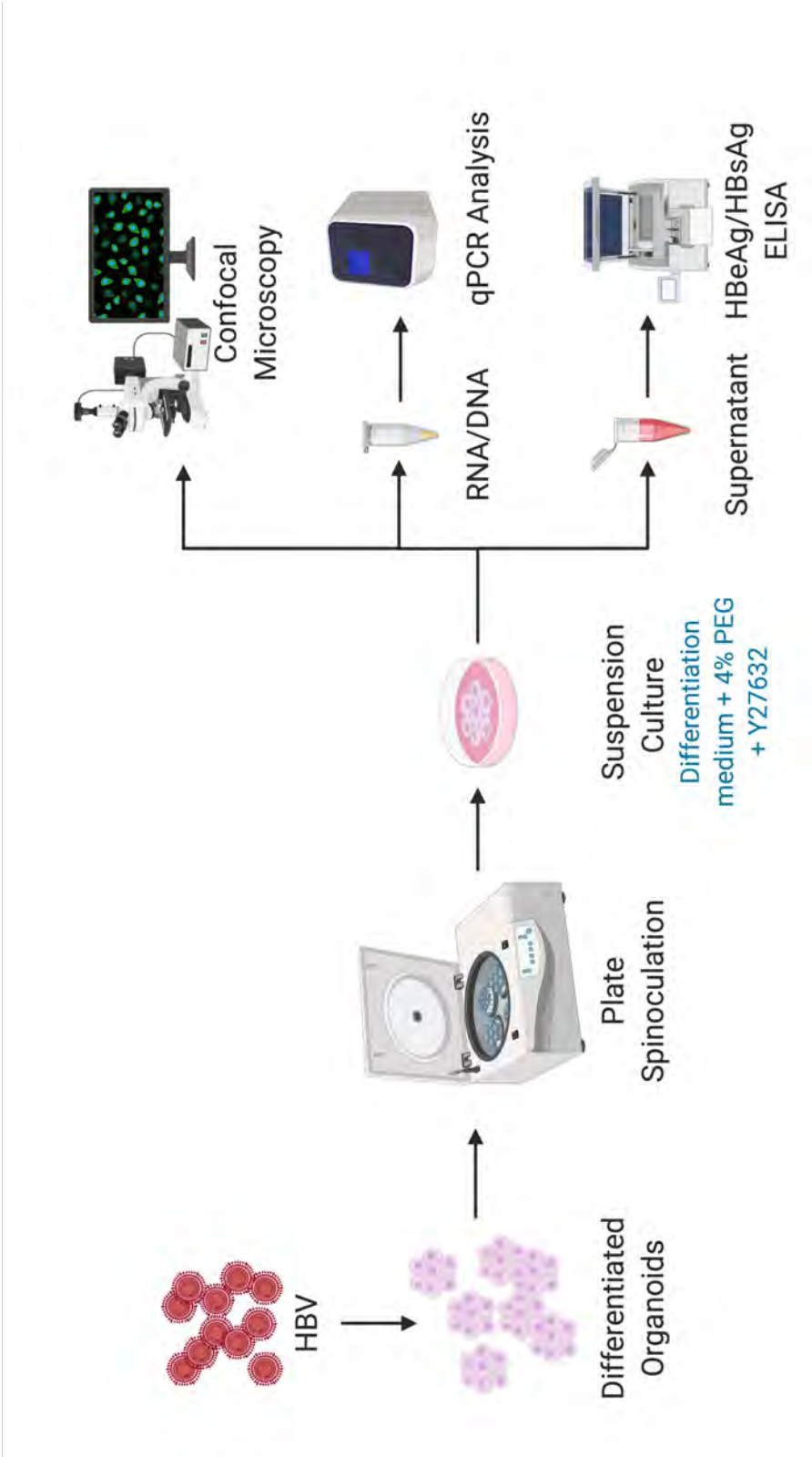

Figure 27: HBV Plate Spinoculation Schematics

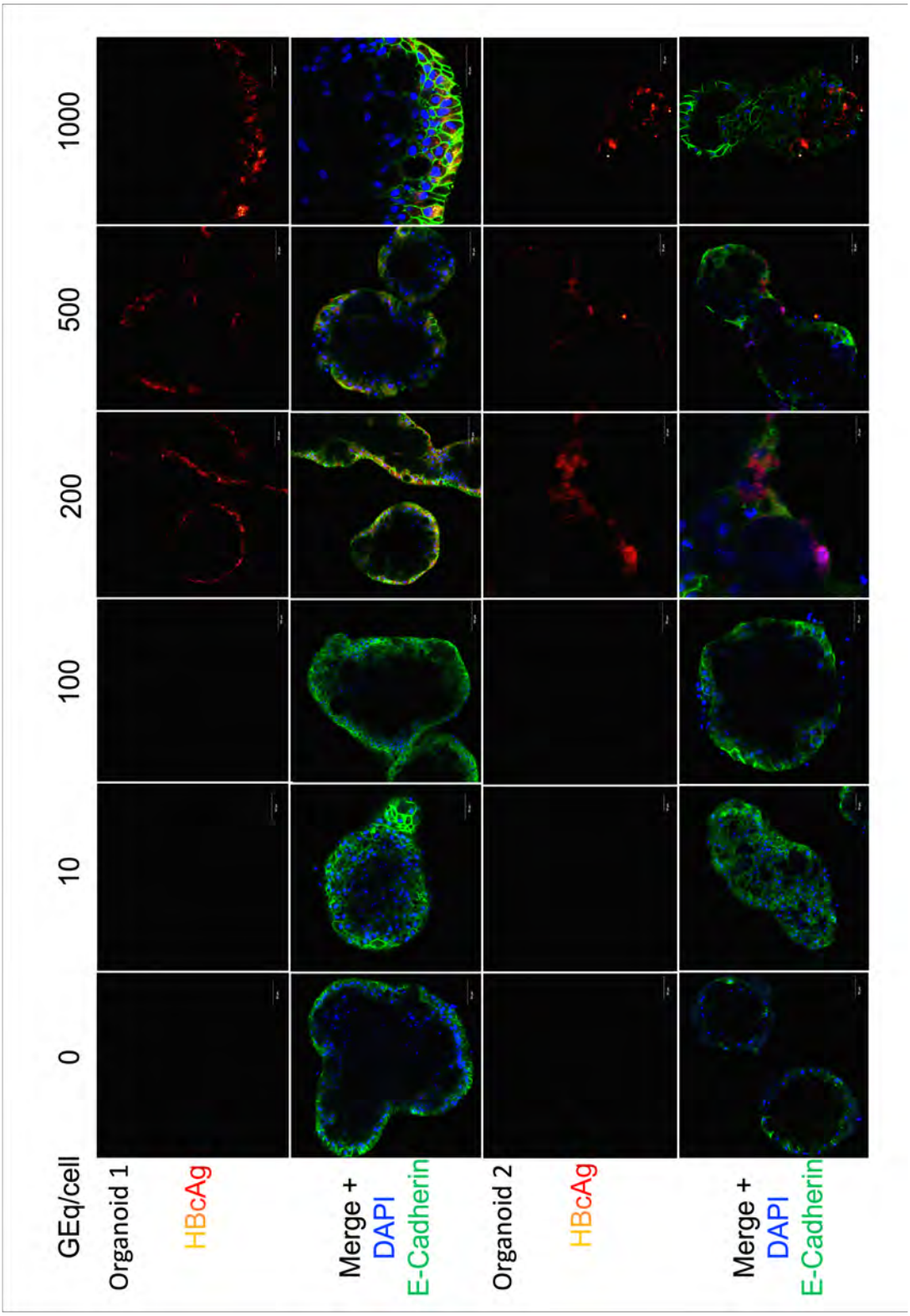

Figure 28: Organoids Infection Titre Using Plate Spinoculation
Confocal microscopy of organoids infected with different inoculum of cell-culture derived HBV, representative images at 20x magnification, staining performed with antibodies against HBcAg (red), E-Cadherin (green) and DAPI (blue).

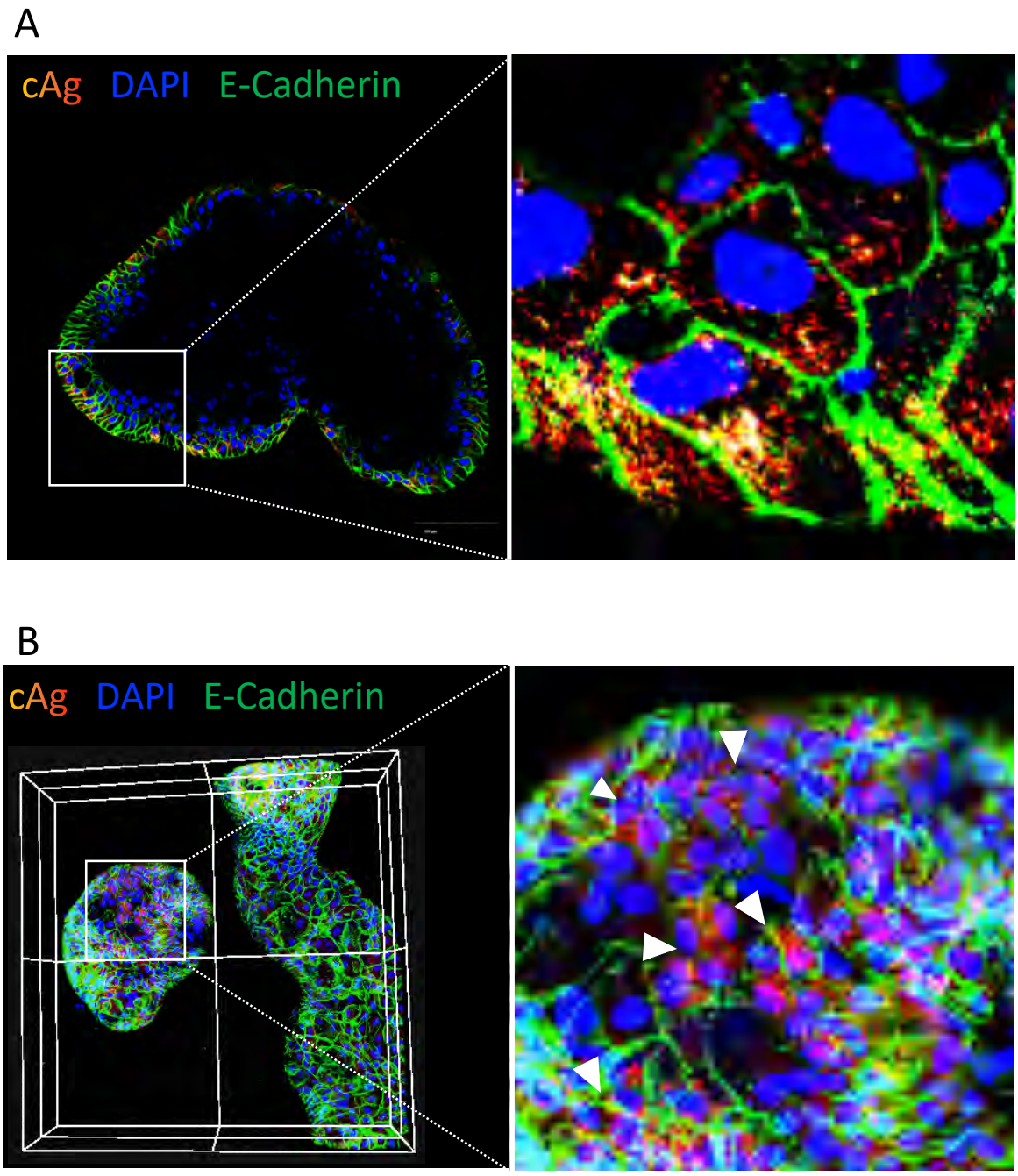

Figure 29: Organoids Infection with Plate Spinoculation
Confocal microscopy of organoids infected with different inoculum of cell-culture derived HBV **(A)** Enlarged image of infected organoids showing intracellular HBcAg staining and **(B)** white arrows indicate infected cells.

Movie 5: HBV Infection in Human Liver Organoids
Differentiated human liver organoids infected with HBV, examined with confocal microscopy under 20X magnification. Reconstruction of Z-stack images using Imaris.
Green – E-Cadherin, Blue – DAPI, Red – HBV Core Antigen

4.4 Assessing HBV Replication and Spread in Human Liver Organoids

Having established that our liver organoids were permissive for HBV infection, we next investigated various stages of HBV life cycle, including genome replication (3.5kb pgRNA transcription), viral replication (cytoplasmic core antigen immunostaining) and production of viral particles into the supernatant (HBeAg, HBsAg, extracellular HBV DNA) over the period of 2 weeks. Using identical AD38 derived HBV inoculum of 1000 GE/cell, the infection was performed in parallel for three individual donor organoids using plate spinoculation as described previously (Figure 30A). Organoids were incubated with the virus for a further 24 hours at 37°C with 4% PEG and Rho-kinase inhibitor. To avoid the confounding effect of input virus, organoids were extensively washed with 10mL of cold basal medium (10x) on day 2 and repeated on day 3. Supernatant and RNA were harvested at three separate time points, day 4, 8 and 12. As a replication defective control and to assess input DNA, similar inoculum of heat-inactivated HBV (100°C boiling for 30 minutes) was used as comparison for all three organoids. For all donor organoids, there was an increase in HBV Total RNA, pgRNA and cccDNA across the 12-day time course, consistent with viral replication, although with significant variations between donors (Figure 30, 31). In contrast, we noted no increase in HBV parameters in organoids infected with heat-treated AD38 HBV. Low level of HBeAg and HBsAg was detected in the supernatant of donor 3 treated with heat-treated HBV. Without a corresponding increase in HBeAg and HBsAg over time, this finding is most consistent with detection of residual heat-inactivated virus. Extracellular HBV DNA increases over time and corresponds to HBsAg and HBeAg secretion. The HBV DNA in supernatant for donor 3 appears to decline slightly at 12 dpi and similarly, HBsAg S/CO also decline correspondingly (Figure 31). Overall, this experiment suggests more consistent infection of organoids using the plate spinoculation method and HBV-infected

organoids can support HBV cccDNA replication, genomic transcript replication and production of viral particles.

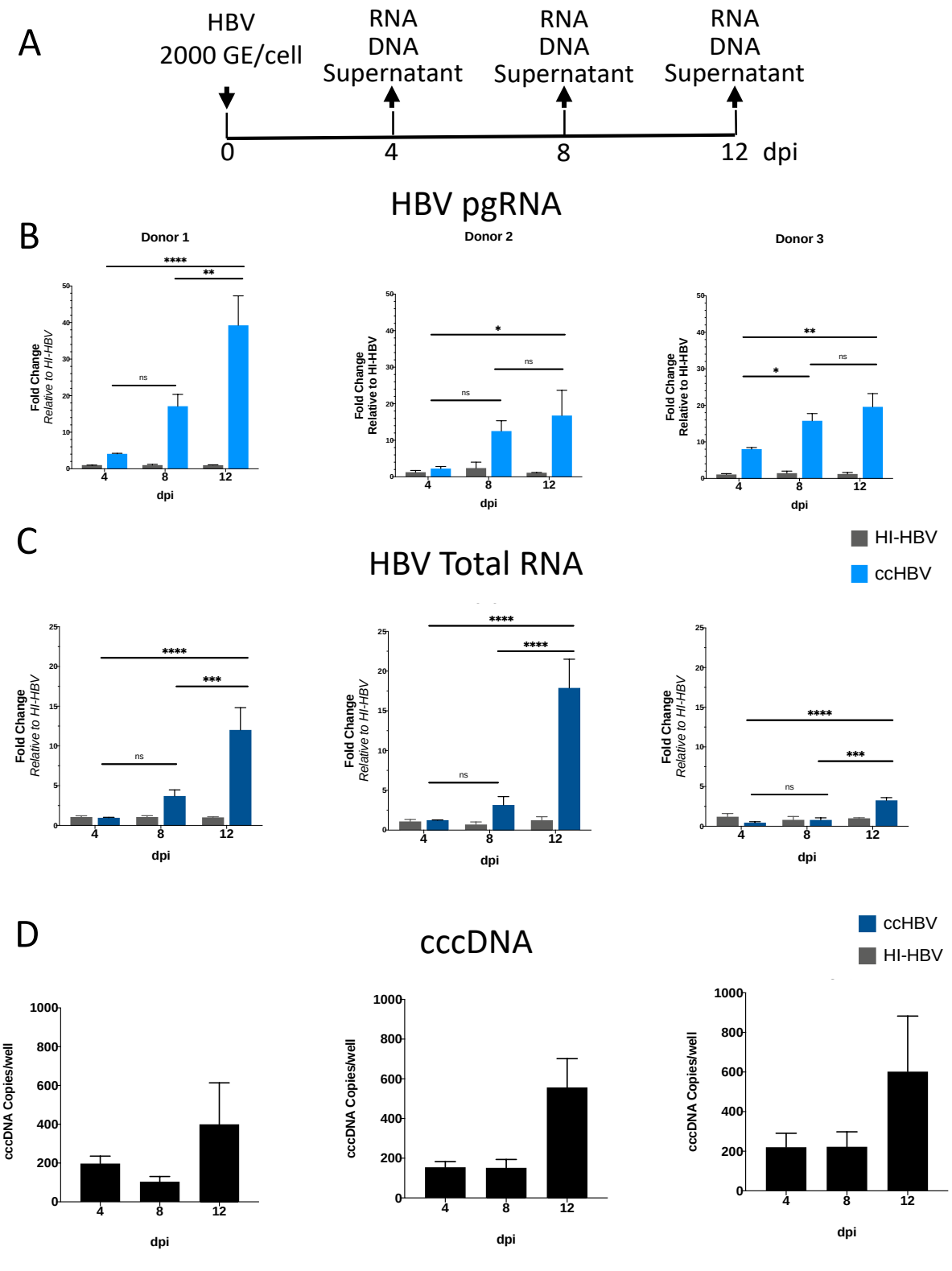

Figure 30: HBV Replication Dynamics in Human Liver Organoids
(A) Infection experiment timeline with cell-culture derived HBV (ccHBV) for organoids derived from three different donors, in replicates of three. Assessment of HBV infection dynamics at three different time points with qPCR for (B) HBV pgRNA, (C) total RNA and (D) cccDNA, according to corresponding donors, expressed as fold change, normalised to heat-inactivated HBV (HI-HBV), Mean±SEM.

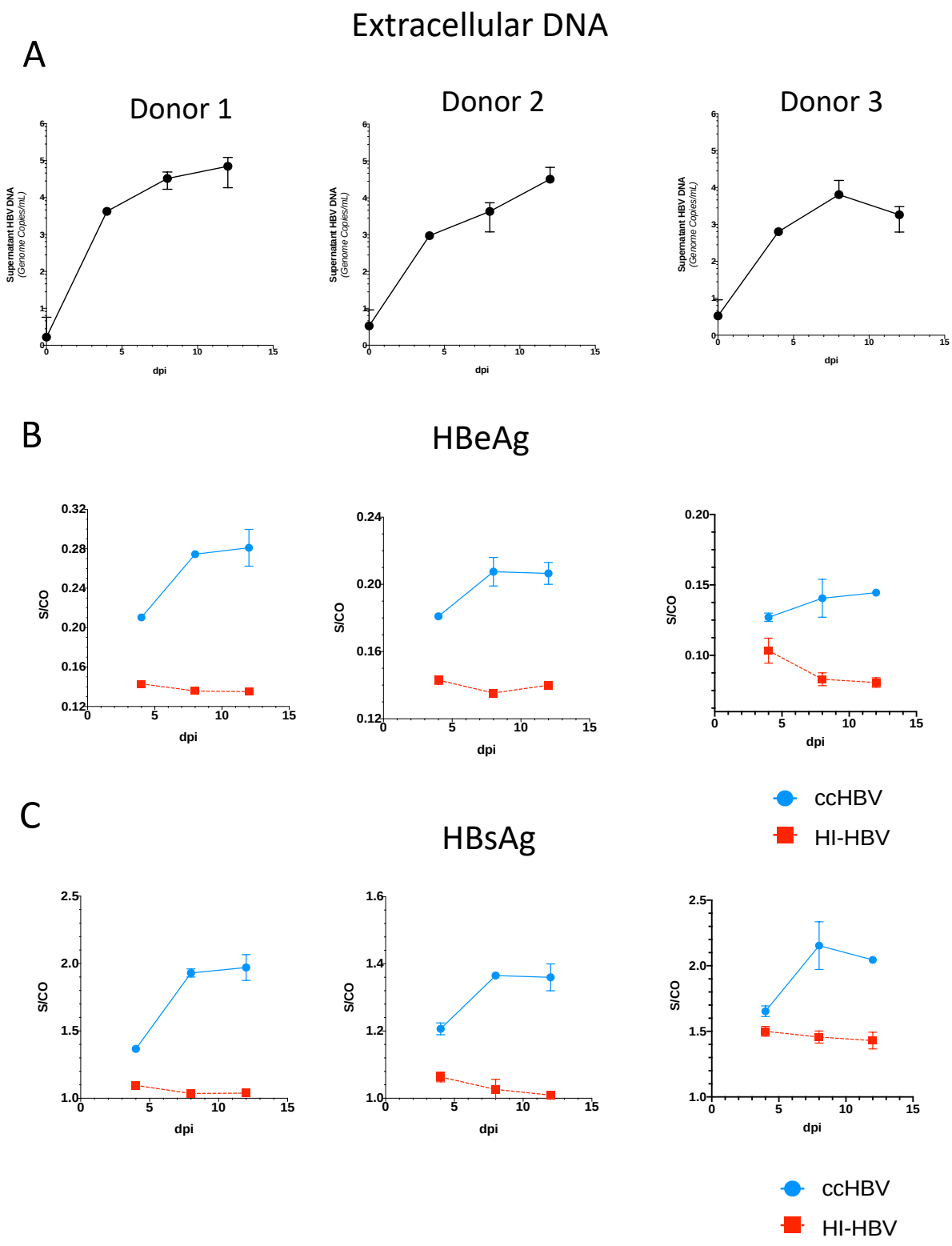

Figure 31: Extracellular HBV DNA and Protein Dynamics in Human Liver Organoids
(A) HBV DNA in supernatant over three time points, fold change, Mean±SEM. **(B)** & **(C)** eAg and sAg secretion in supernatant, measured with CLIA, normalised to heat-inactivated HBV, expressed as Mean±SEM.

4.5 Patient-derived HBV Infection and Drug Responsiveness

Having established that the differentiated liver organoids can support AD38 derived HBV infection and replication, we further evaluated the potential of this model system in assessing HBV infection using patient-derived HBV. If feasible this would have significant benefit to study different HBV genotypes and variants. Plasma from one patient (HBV genotype C) was used to determine the inoculum required to achieve infection. Immunofluorescence confocal microscopy revealed the presence of HBV cytoplasmic HBcAg staining consistently with inoculum of at least 50 GE/cell (Figure 32, 33). This was significantly lower than inoculum derived from AD38 cells.

Next, we assessed whether our HBV organoid infection model could be used to evaluate antiviral strategies and viral reactivation. Organoids were treated with drug either pre (24hrs) or post (48hrs) infection with plasma HBV (genotype B). Organoids were further incubated for 21 days, after which HBV replication was evaluated through detection of HBV RNA by qRT-PCR. Pre-treatment with Myrcludex resulted in a significant decreased in HBV RNA, whereas post-infection treatment had no clearance of HBV RNA compared with the control group (Figure 34). This finding is consistent with the mechanism of Myrcludex in which it prevents HBV entry. On the contrary, treatment pre-infection with a JAK inhibitor did not change the HBV RNA. After infection has established, treatment with JAK inhibitor results in an increase in HBV RNA, suggesting that JAKi may have an effect on HBV replication post-entry. To further confirm these findings, repeat experiment with Myrcludex and JAKi was performed with similar findings. Concurrent immunofluorescence staining for HBcAg also confirm the lack of infection in Myrcludex treated organoids. Similar treatment of two different organoids have shown variation in the degree of HBV RNA changes with drugs.

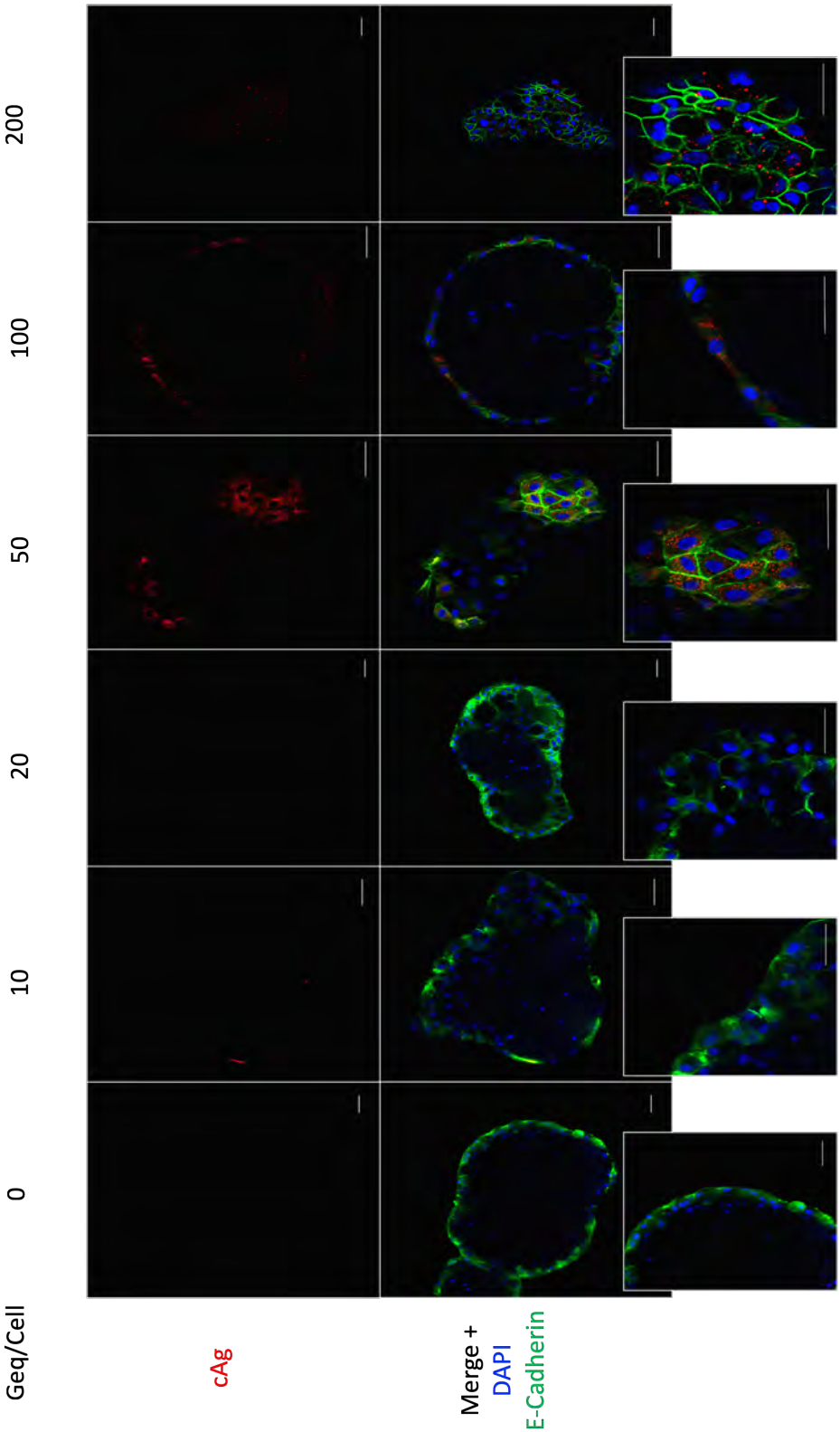

Figure 32: Organoids Infection Titre with Patient-derived HBV
Confocal microscopy images of organoids infected with plasma derived HBV (genotype C) at different inoculum, inset indicates enlarged images of infected areas.

A

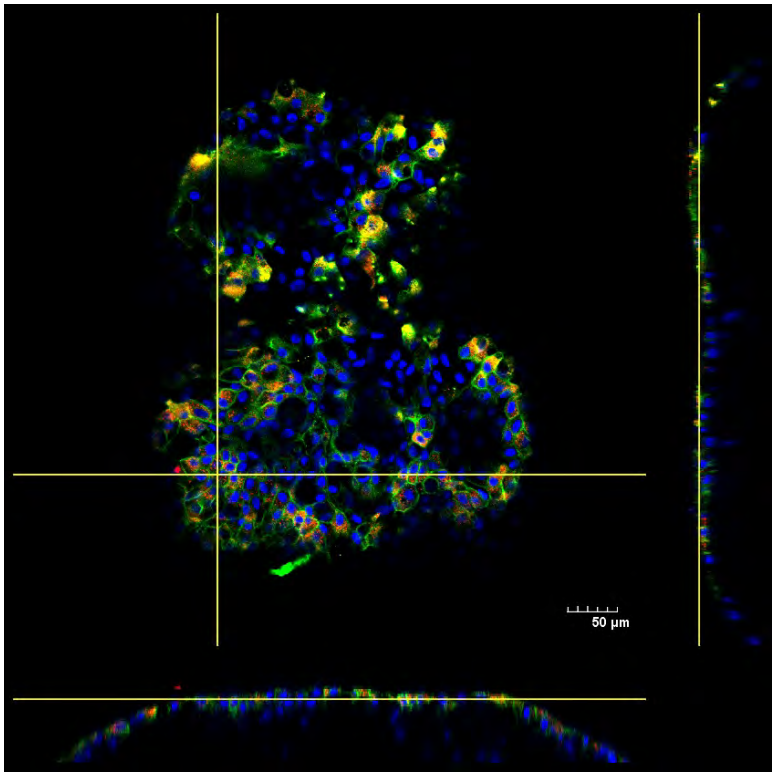

B

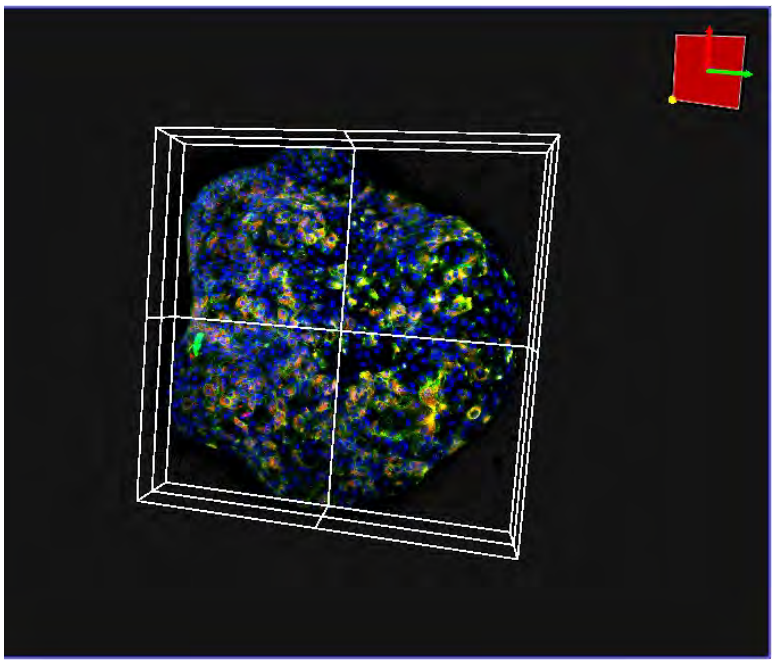

Figure 33: Organoids Infection with Patient-derived HBV
(A) Three slide view of reconstructed Z-stack image and **(B)** 3D view of organoids infected with plasma HBV (genotype C)

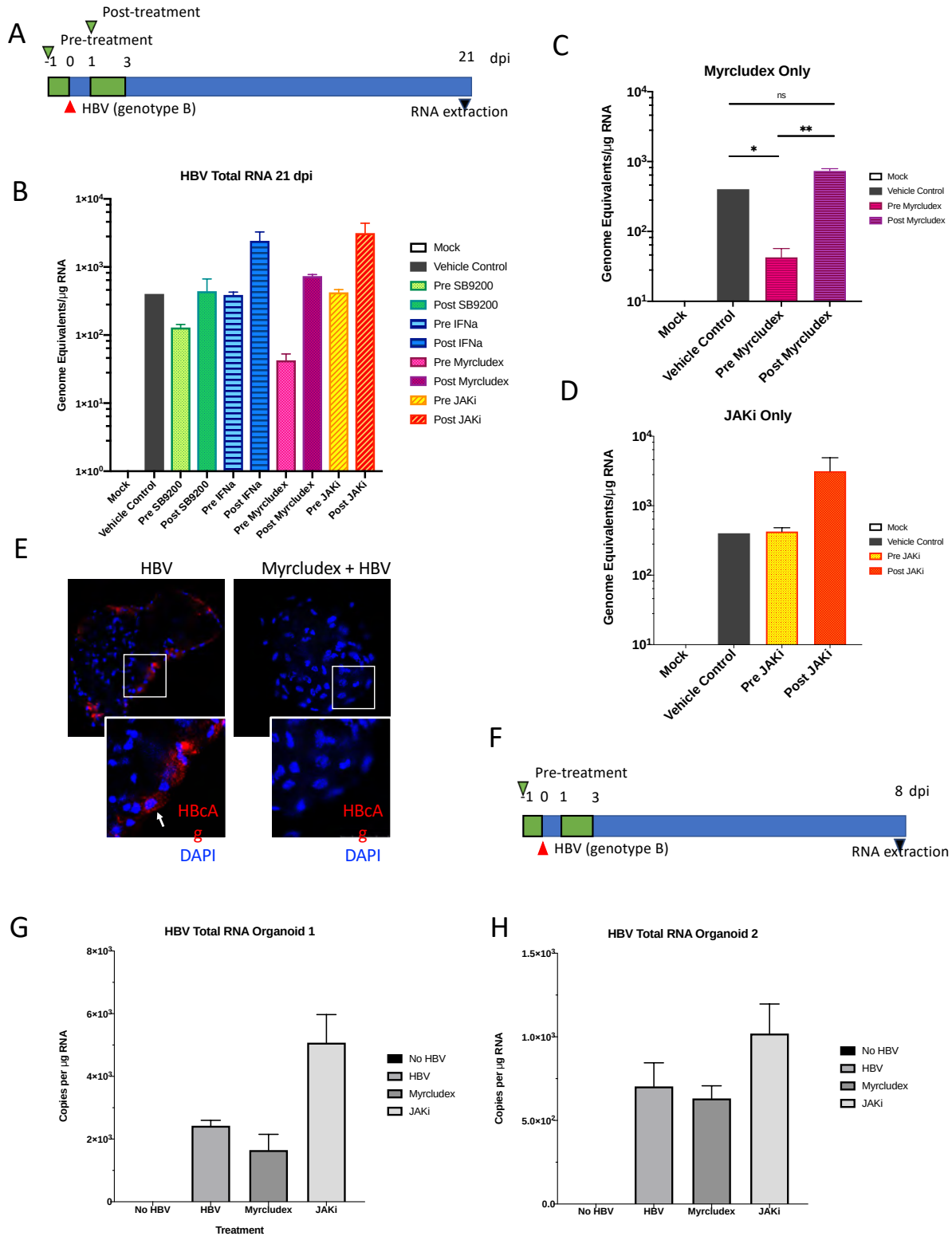

Figure 34: Drug Response in Liver Organoids

Drug treatment of liver organoids infected with plasma HBV (genotype B) for 21 days. **(A)** Schematic timeline of experiment and **(B)** qRT-PCR of infected organoids, normalised to total RNA, expressed as Mean±SEM. **(C)** qRT-PCR or Myrcludex-treated and **(D)** JAKi-treated (Baricitinib) organoids. **(E)** Corresponding immunofluorescence for HBcAg in the same experiment. **(F)** Schematics of treatment timeline for organoids in a shorter time frame. **(G) (H)** qRT-PCR of infected organoids, normalised to total RNA, expressed as Mean±SEM.

4.6 Organoids Infection with Other Hepatotropic Viruses

4.6.1 HCV

Having established that our organoids can support HBV replication, the next logical step was to evaluate other hepatotropic viruses. HCV is a member of the Flaviviridae family with sole tropism for hepatocytes. HCV entry into hepatocytes a sequential process that is tightly linked to the lipid metabolism of the hepatocytes. It first involves binding to the LDL-R, GAG and SR-B1 on the basal lateral surfaces of polarised hepatocytes, with subsequent binding to CD81, CLDN-1, EGFR and finally Occludin in the apical surfaces before internalisation through membrane fusion process (Figure 35A) [270].

We evaluated the presence of HCV entry receptors in both undifferentiated and differentiated organoids using qRT-PCR for mRNA expression and immunofluorescence staining for in situ receptor expression. qRT-PCR results showed that the 4 major HCV entry receptors, Occludin, claudin-1, SR-B1 and CD81 were expressed at the mRNA level in both undifferentiated and differentiated organoids (Figure 35). Similarly, immunofluorescence staining showed presence of all four receptors at both differentiated and undifferentiated stages. Co-staining with ZO-1 antibody showed that most but not all the Occludin staining co-localise with ZO-1, predominantly in the internal surface of the organoids (Figure 36A).

An initial attempt to infect the undifferentiated and differentiated organoids with cell culture derived HCV (Jc1/JFH1, MOI 0.004 Figure 36B) for 72 hours was unsuccessful. Further attempt to infect the differentiated organoids with Jc1-GFP was not successful (Data not shown).

4.6.2 ZIKV & Semliki Forest Virus

As a proof of concept, we assessed the susceptibility of human liver organoids to a positive strand RNA virus that has been associated with various human pathology due to its broad tissue tropism [328]. It has been previously shown that ZIKV can infect and impart a cytopathic effect on hepatocytes and hepatoma-derived cell lines [329, 330]. Most recently, human stem cell derived HLCs have been shown to not only support ZIKV replication, but also can be used to assess efficacy of potential antivirals [331].

Semliki Forest Virus (SFV) is a positive strand, single stranded RNA virus from the Togaviridae family. It can be transmitted to human through mosquitoes vector and is occasionally associated with significant encephalitis [332]. Studies of SFV lifecycle and cellular responses predominantly derived from experiments on rodent-derived cell lines and the true human tissue tropism is unclear [333-337].

Infection experiment with ZIKV and SFV was performed on undifferentiated human liver organoids at MOI of 5 and 0.1, respectively, using plate spinoculation method. The organoids were incubated for a further 24 hours before fixation for immunofluorescence staining. The ZIKV infected organoids were stained with anti-flavivirus E-antigen whereas the SFV infected organoids were stained with anti-dsRNA. Immunofluorescence microscopy showed typical cellular staining patterns of infected cells within the organoids (Figure 37). Concurrently brightfield microscopy did not show significant cytopathic effect at 24 hpi for both viruses.

A

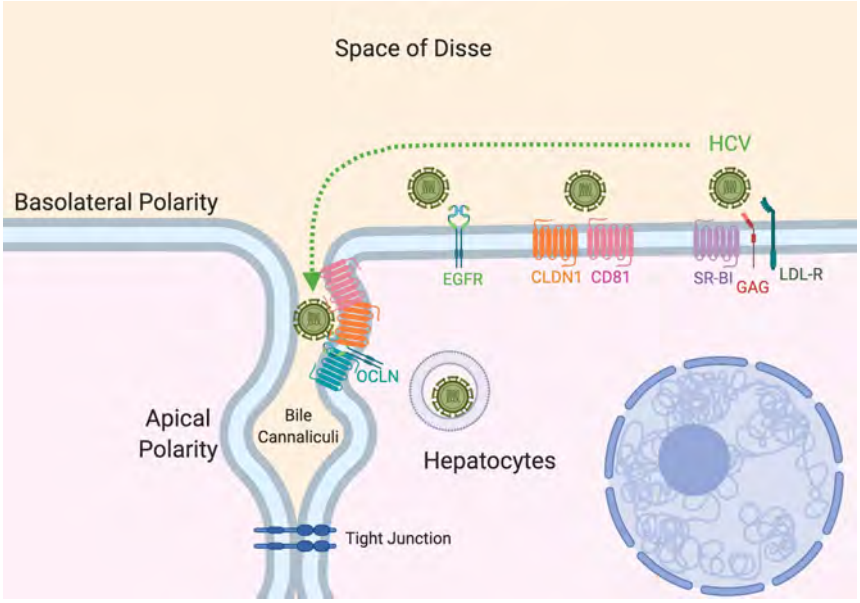

B

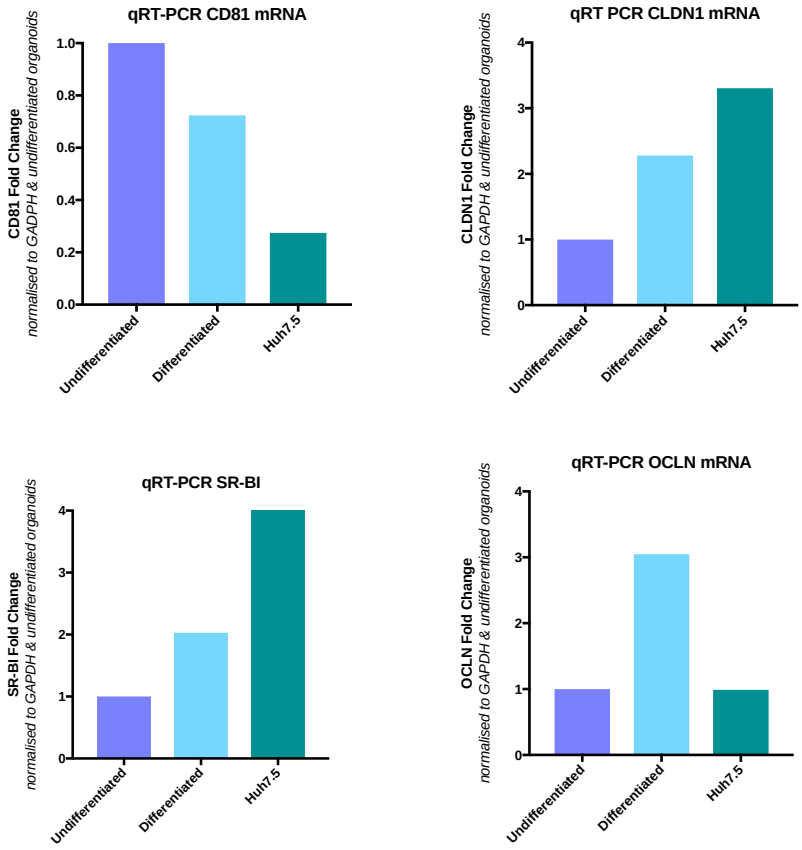

Figure 35: HCV Entry Receptors in Liver Organoids
(A) Schematic diagram depicting the location of HCV entry receptors. **(B)** HCV entry receptors mRNA, relative to GAPDH. Experiment performed using pooled organoids for each condition.

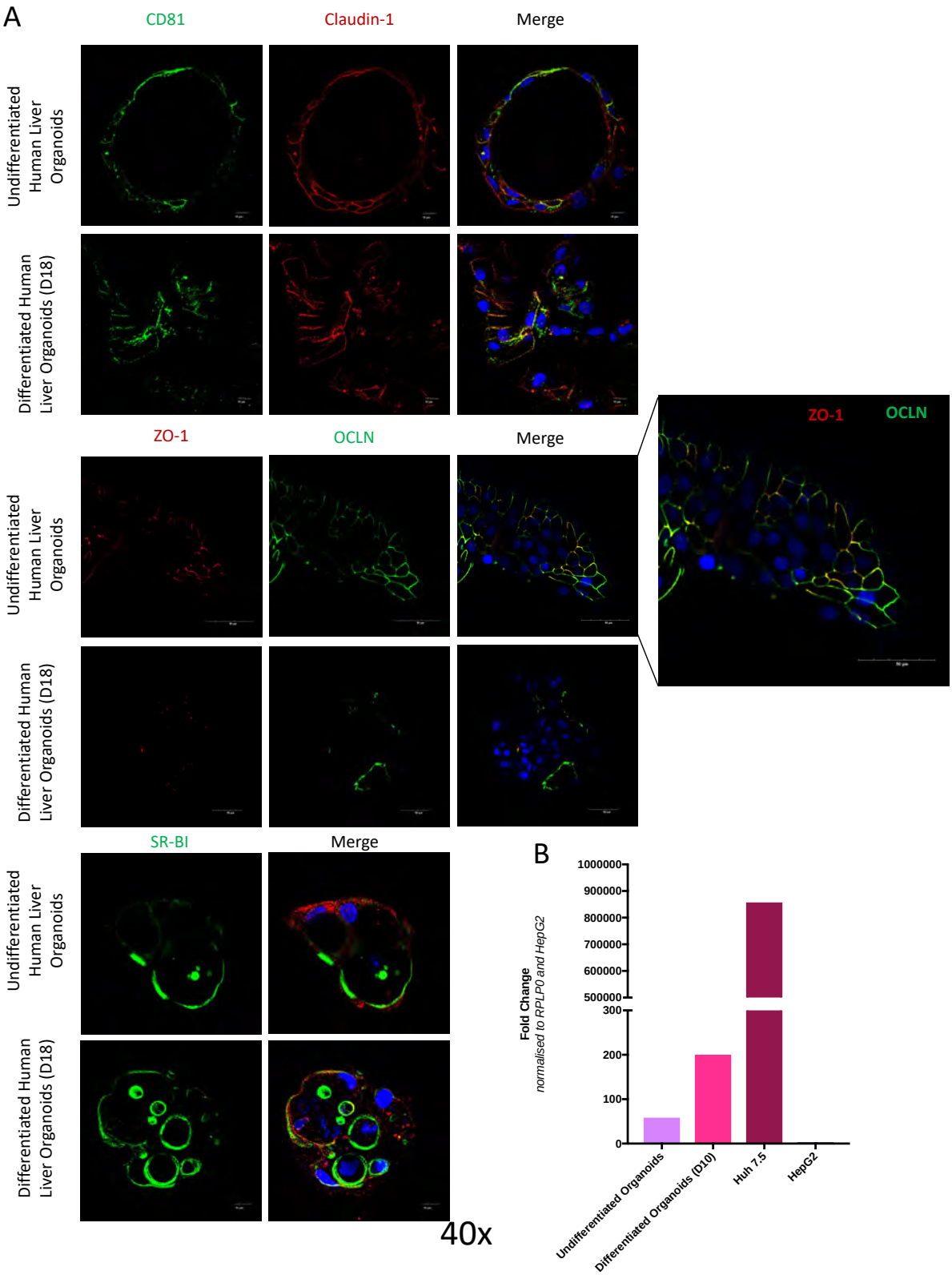

Figure 36: HCV Entry Receptors in Liver Organoids
(A) Immunofluorescence staining of HCV entry receptors in UO and DO, 40x magnification.
(B) HCV RNA fold change in UO, DO, Huh7.5 and HepG2, relative to RPLP0 and HepG2.

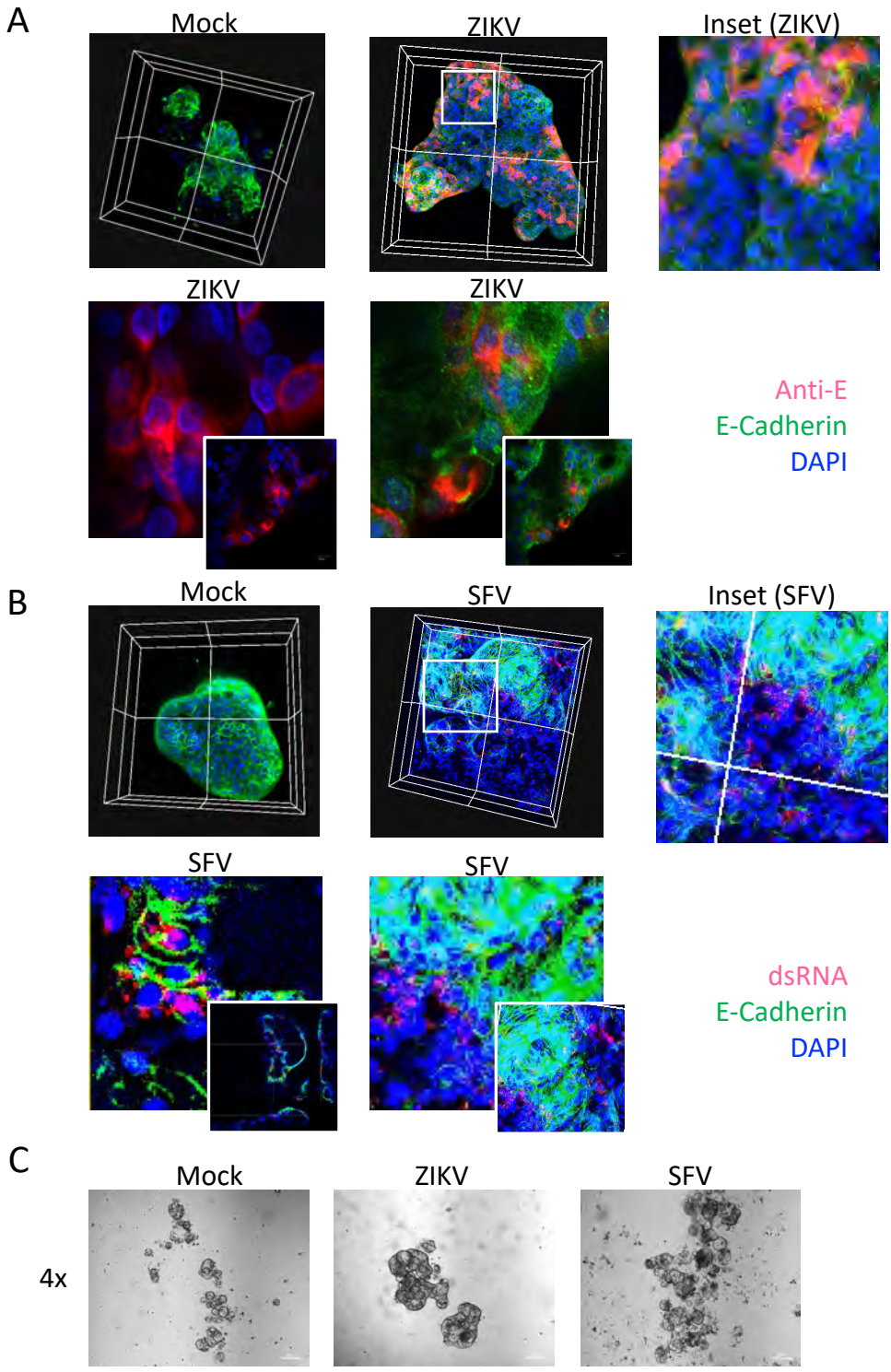

Figure 37: ZIKV and SFV Infection in Liver Organoids
(A) Confocal microscopy of ZIKV infection (MOI 5) and **(B)** SFV infection (MOI 0.1) of undifferentiated liver organoids. ZIKV infected organoids were stained with anti-E whereas SFV infected organoids were stained with anti-dsRNA, using ZIKV (MOI 10) as a positive control (not shown). **(C)** Brightfield microscopy at 24hpi.

Movie 6: ZIKV Infection in Human Liver Organoids
Undifferentiated human liver organoids infected with ZIKV. Z-stack images from confocal microscopy at 20X. Green – E-Cadherin, Blue – DAPI, Red – Flavivirus E Antigen

Movie 7: SFV Infection in Human Liver Organoids
Undifferentiated human liver organoids infected with SFV. Z-stack images from confocal microscopy at 20X. Green – E-Cadherin, Blue – DAPI, Red – dsRNA

4.7 Discussion

As we have outlined previously, the *in vitro* models for HBV infection are somewhat lacking and thus there is a clear need for an *in vitro* model that would allow for pathogenesis studies and evaluation of new drugs and targets. The main focus of this chapter was to assess human liver organoids as an *in vitro* model for HBV infection. We show that adult stem cell derived human liver organoids express functional HBV entry receptor NTCP and can support the full life cycle of HBV. Interestingly we show that NTCP is expressed during differentiation, demonstrating the importance of assessing the functional receptor expression rather than NTCP mRNA or antibody staining which correlate poorly with infectivity for HBV.

NTCP plays a significant physiologic role in hepatic bile acid transport. In the adult liver, NTCP is expressed on the basal lateral surface of hepatocytes in contact with the sinusoids, and is responsible for transporting conjugated bile acids from the blood into hepatocytes. NTCP deficiency in children as a result of homozygous mutations in the SLC10A1 gene (NTCP), results in cholestatic jaundice and bileacidaemia [338-341]. In early infancy, NTCP mRNA is poorly expressed, with its localisation predominantly to a perinuclear location. In children older than 1 year of age, NTCP mRNA is significantly upregulated, suggesting some form of age related regulation [342]. NTCP also undergoes post-translational glycosylation in an age-dependent manner with immunodetection in mature hepatocytes, demonstrating a predominantly apical expression of the glycosylated NTCP protein. Similarly, NTCP localisation of the differentiated human liver organoids was consistent with a membranous staining pattern, suggesting maturation of NTCP. Interestingly, the N-glycosylation of NTCP and movement to the cell surface has been linked to susceptibility to HBV infection [313, 343]. These post-translational modifications of NTCP especially at the N-terminal to which HBV binds, is clearly demonstrated in the human liver organoids. The inability of Myrcludex

to bind to NTCP in the undifferentiated stage, despite the presence of mRNA and protein expression (intracellular) suggest that during differentiation, NTCP is post-translationally modified to access cell surface expression and ultimately HBV binding and internalisation. The dependence on post-translational modification may partially explain the lack of incremental susceptibility of some hepatoma cell lines to HBV infection when using a NTCP overexpression construct [344]. While not a major focus of this thesis, our observation in regards to NTCP expression is our organoid system proves a useful system to study NTCP gene regulation and localisation future studies.

Due to differences in culture conditions and lack of standardisation of methods in evaluating HBV infection, comparison of HBV infection in liver organoids with *in vitro* models such as NTCP expressing HepG2 cell or PHH is difficult. Despite this, we achieved HBV infection in differentiated human liver organoids as evaluated by HBV core antigen staining, HBV pgRNA, HBV DNA and HBsAg excretion. In comparison with HBV patient liver samples in which a high percentage of hepatocytes are positive for HBcAg, this was not the case in our cultures. We noticed that the expression of mature hepatocyte markers is not complete in differentiated organoids when immunodetection of stem cell and ductal markers showed that a significant proportion of cells within the organoids retain the ductal or immature phenotypes despite differentiation and therefore would not support HBV replication. This finding is consistent with other stem-cell derived HLC models in which the differentiation process is not complete *in vitro*. Further optimisation with other culture conditions (e.g., higher and lower oxygen, high nutrients, microfluidic model) and co-culture with other liver non-parenchymal cells may potentially be useful in achieving a more hepatocyte-like phenotype. During our optimisation experiments, the addition of AAP with or without insulin did result in increased albumin and NTCP mRNA expression. As achieving complete

hepatocyte differentiation is beyond the scope of this thesis, we have yet to ascertain if the increase in albumin and NTCP expression is due to improved maturation of HLCs or an increase in the proportion of cells undergoing the hepatocyte differentiation. Furthermore, whether improvement in differentiation in the hepatocyte lineage would result in increased HBV infection is yet unknown and will require further evaluation.

One major challenge for all stem-cell derived HLCs especially in 3D culture format is the ability to achieve consistency. This could be due to a number of reasons: (1) the unpredictable size of organoids and thus access to nutrients are not consistent, (2) differentiation between and within organoids are not consistent due to different cell types, (3) the growth rates of organoids are not consistent between passages due to polyclonal nature and some cells will undergo senescence at later passages, (4) despite genetic stability, the composition of stem cells may change and proliferating cells are selected out during passages, and (5) prolonged period of differentiation and infection experiment introduces variation in culture conditions. In order to utilise human liver organoids as a translational tool to predict clinical response, intra- and inter-experimental consistencies are compulsory to achieve clinical diagnostic standards. Having established that we could indeed infect our organoids with HBV, our next aim was to modify infection model to a more consistent platform. By digesting the organoids into single cells and regenerate for 5 days before differentiation, we managed to achieve more consistent sizes of organoids for experiments. HBV infection performed in these smaller organoids using plate spinoculation method has resulted in consistent infection. Due to the large viral inoculum required, significant amount of washing steps are required to ensure all the input virus are completely removed before assessing for viral replication using HBsAg and HBV DNA quantification from the supernatant. These steps introduce further risks to experimental consistencies. In order to

assess for inter-experimental variation, establishing an HBV-producing organoid cell line is crucial. Nishitsuji et al. has established a number of hepatoma cell lines transduced with HBV plasmid constructs that express nanolucifease or Gaussia luciferase in cell culture supernatant [345-347]. These cell lines can be used to assess HBV host-factor expressions and antiviral response. A material transfer agreement has been established for acquiring these constructs. However, the transport process has been significantly interrupted due to the COVID-19 pandemic and the establishment of NanoLuc/gLuc HBV-producing organoids cannot be achieved during the period of the PhD.

Similar with other HLCs and hepatoma cell lines, the liver organoids required a high inoculum of cell-culture derived HBV to achieve infection[160, 181, 318, 348, 349]. For example, using spinoculation, we did not achieve infection until we had added 200GE/cell of HBV, that represents a significant amount of viral genomes. Apart from a less complete hepatocyte phenotype and lower levels of NTCP expression compared to PHH, the requirement for a high inoculum cannot be entirely attributed to the cell culture model alone. Consistent with other stem-cell derived HLCs, in our study, the differentiated organoids were more susceptible to plasma-derived HBV than cell-culture derived HBV. However, for reasons that are not entirely clear, previous studies have demonstrated that human plasma contains a high number of infectious virions (Dane particles) compared with cell-culture produced HBV which consists of a large proportion of non-enveloped viral particles with or without HBV DNA[350-352]. Furthermore, cell culture-derived HBV can be generated from a number of different cell lines, for instance, HepAD38, HepDE19, HepG 2.2.15 and its derivatives[353-358]. It is unclear what proportion of infectious virions is produced from these cell lines. In comparison to other viruses in which infectious viruses can be quantified by plaque TCID50 assay, routine quantification of inoculum using qPCR for HBV DNA is

unable to accurately identify the true infective viral inoculum. In addition, there are multiple different viral concentration techniques, introducing more complexity to the evaluation of viral integrity and true infective inoculum [359-364].

While we have demonstrated HBV infection of human liver organoids, the question remains, can they be used as a model for other hepatotropic infection either alone or in co-infection experiments. To assess the potential of human liver organoids as a model for HCV infection, we characterised the expression of HCV entry receptors before and after differentiation. The initial infection experiment with Jc1/JFH1 and Jc1/GFP was not successful, probably due to the low viral inoculum used in the infection experiment. Attempts to produce high titre virus from cell culture was not successful when using PEG8000 for viral precipitation. Future experiment could include ultracentrifugation of HCV or using plasma derived HCV. As Occludin co-localises with ZO-1 which is internalised during the differentiation process, infection of differentiated organoids may require cellular disruption to expose the receptor.

Overall, we have established the optimal timing of organoids differentiation in which functional entry receptor, NTCP is expressed. This information, together with the assessment of infection inoculum, assist us in establishing consistent HBV infection in organoids to evaluate HBV replication and downstream assessment of innate immune response to HBV infection.

5 Chapter 5: Human Liver Organoids Demonstrate Robust Innate Immune Response

The innate response to viral infection is the first line of defense against invading pathogens and is crucial for the outcome of viral infection and shaping a robust adaptive response. Furthermore, most viruses have evolved mechanisms to evade this response and for many viruses this is well documented [79, 231]. However, in contrast, studies on the innate immune response and antiviral effector ISGs in HBV infection are conflicting due to the different model systems used. Interestingly, it is thought that HBV is a stealth virus, in which it does not activate an appreciable innate response and thus can evade early antiviral responses [95]. Assessment of individual HBV proteins demonstrated their ability to suppress ISG expression, however, the overall effect of sensing HBV PRR and subsequent activation of the innate immune signalling pathway have not been completely resolved [91, 95, 365].

A number of ISGs such as RIG-I, PKR, IFITM1, IRF1, MX1, MYD88, NOS2, PLSCR1 and RNASEL have been implicated to inhibit HBV replication through different mechanisms, however, their exact role is unclear [366-370]. Thus, a physiologically intact HBV model system that mimics hepatocyte infection would help improve our understanding of the natural history of HBV infection, in particular innate immune responses and knowledge as to individuals who are able to achieve functional cure after a prolonged period of infection.

The aim of this chapter is to characterise the innate immune response or competency of our liver organoid model and to further characterise HBV initiated innate responses.

5.1 ISGs expression in response to Interferon-α Stimulation

Prior to investigation of the innate response of liver organoids to HBV infection, we first determined if the organoids are indeed responsive to IFN stimulation initially at the stem cell state and following differentiation towards a hepatocyte phenotype.

IFN is a key innate immune cytokine and responsible for induction of hundreds of ISG mRNAs [371]. To dissect the response of liver organoids to IFN-α, timepoint experiments were performed using both undifferentiated and differentiated human liver organoids stimulated with 1000U/mL of IFN-α (Figure 38). A relatively high concentration of IFN-α was used in this initial proof of concept experiment to evaluate the extent of ISG induction when the cells were saturated with IFN-α. In hepatoma cell-based model systems such as Huh7 or HepG2, IFN-α of at least 500U/mL upwards are often required to achieve a meaningful fold induction in ISGs [372-374]. Total RNA was harvested at 6-, 16- and 24-hours post-stimulation followed by qRT-PCR to detect a select panel of ISGs. Significant upregulation of mRNA for IFITM1, ISG15 and Viperin of at least 100-fold were seen as early as 6 hours for both differentiated and undifferentiated organoids. Although there were slight differences in ISG temporal dynamics, overall, it appears that IFITM1, ISG15 and Viperin reached sustained induction up to 24 hours. We expected a difference in response between undifferentiated and differentiated organoids. Interestingly, IFITM1 was significantly increased in differentiated organoids at 16 and 24 hour-post stimulation. However, despite a trend for increased Viperin and ISG15 expression in differentiated organoids, the differences did not reach statistical significance across all time points.

Having established that our liver organoids were responsive to Type I IFN, we next evaluated ISG induction using a more physiologic concentration of IFN-α (10U/mL and 100U/mL). In

primary human hepatocytes and in hepatoma cell lines, IFN-α concentration of less than 250U/mL are routinely used to assess activation of the JAK-STAT signalling pathway and downstream ISG induction [375]. Using IFN-α at concentration of 10 and 100 IU/mL, we observed significant upregulation of ISGs and the proinflammatory cytokine, CXCL10 in the human liver organoids.

Overall, the trend suggests a dose response to IFN-α. Having determined that the organoids have a highly responsive JAK-STAT signalling pathway, we evaluated the role of donor variation on three organoids in response to IFN-α (Figure 39). Variation between ISG induction can be seen at 10U/mL concentration of IFN-α but was more robust at 100U/mL. Interestingly, donor 3 had a significant upregulation of CXCL10 in comparison with other donors. Such variation in ISG response between individuals could have a significant downstream implication, with opportunity to further understand the individual differences in disease pathogenesis and individual immune response to various hepatotropic viral infections.

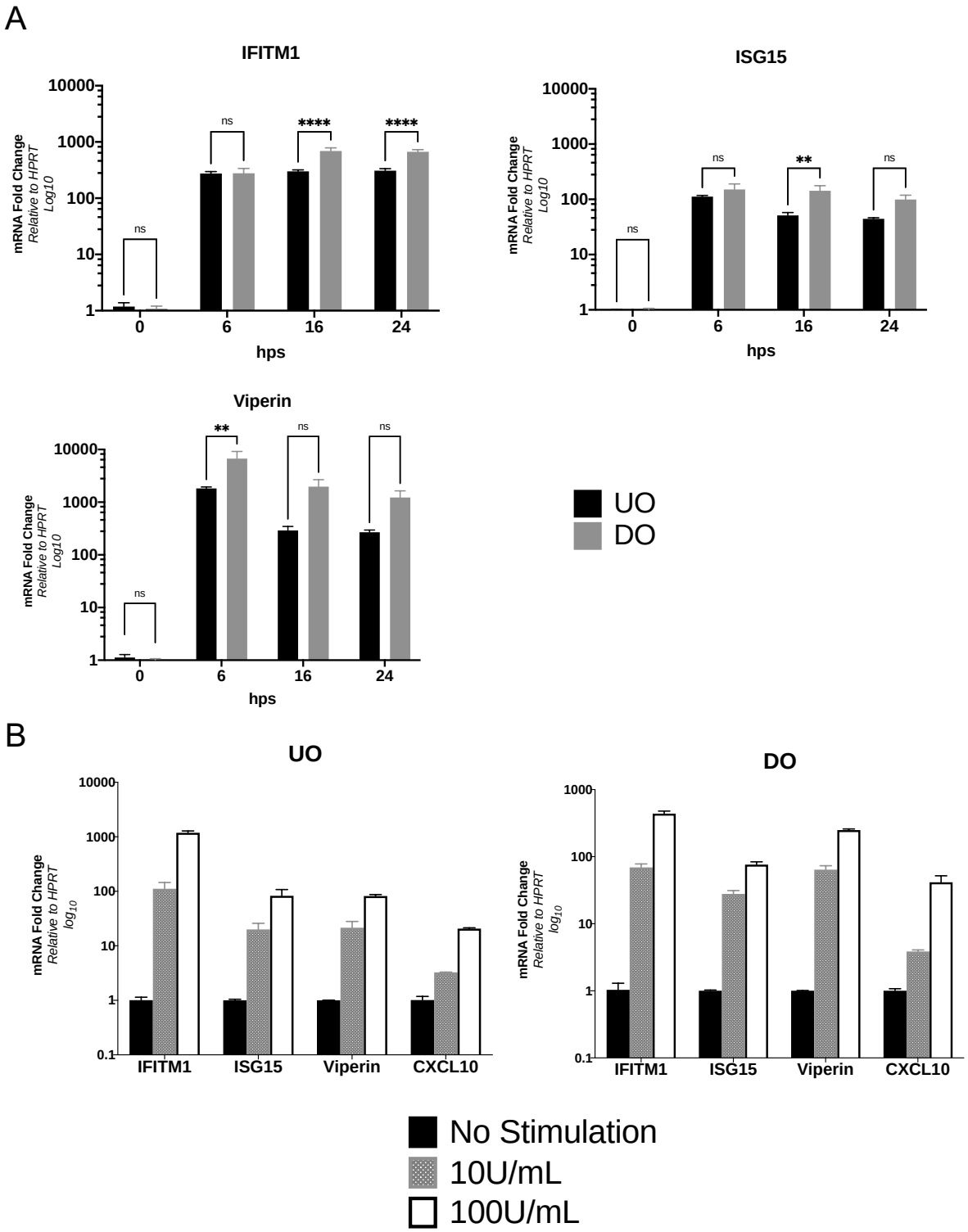

Figure 38: ISG Response to IFN-α Stimulation
(A) Temporal fold induction of ISG mRNAs in UO and DO (replicates of 4) at 6, 16 and 24h post-stimulation with IFN-α at 1000U/mL (Mean±SEM, n=2). UO = undifferentiated organoids, DO = differentiated organoids **(B)** Fold induction of ISG mRNAs at 24h post-stimulation with two concentrations of IFN-a (Mean±SEM).

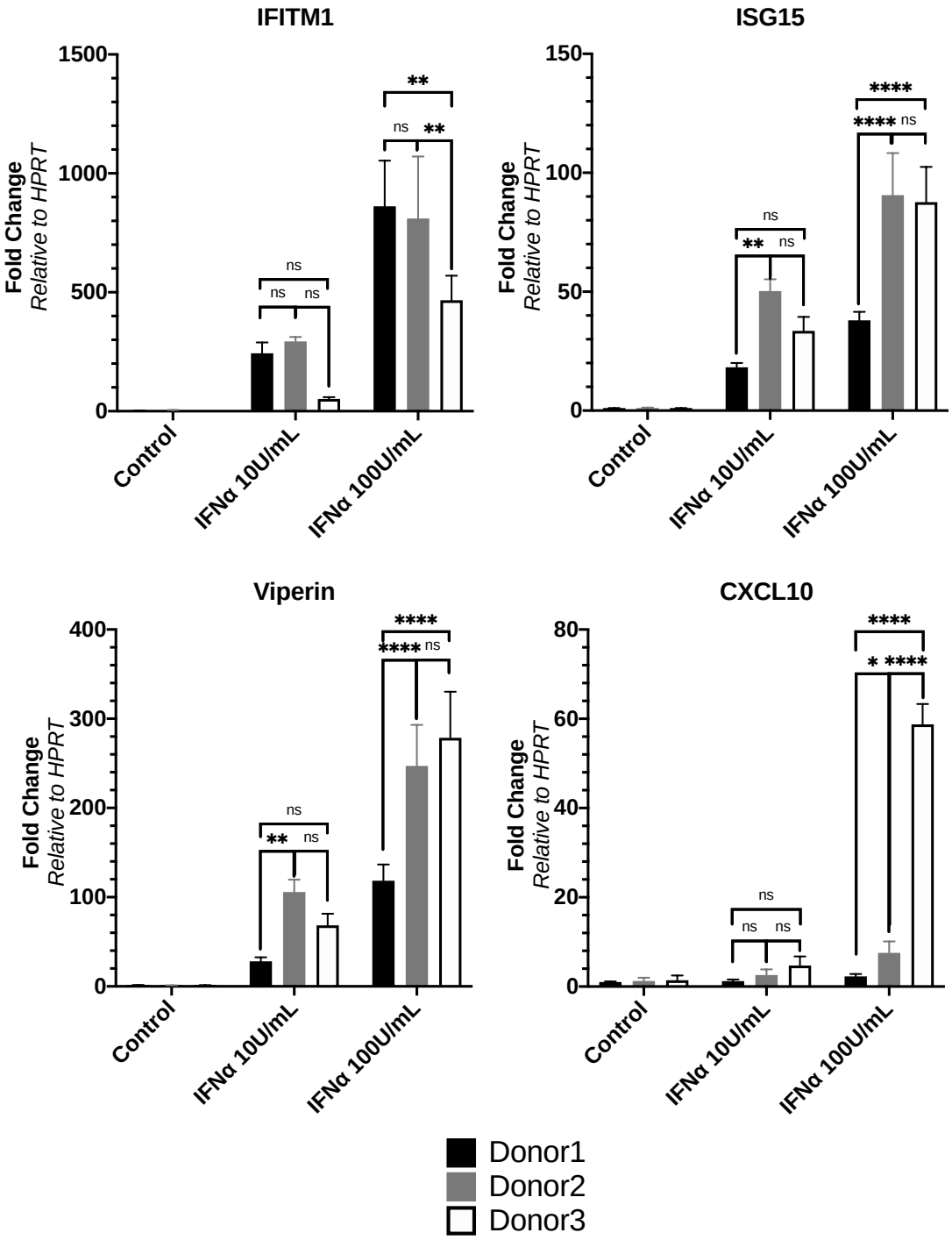

Figure 39: Donor Variation of ISG Response in Human Liver Organoids
Fold induction of ISG mRNAs in DO derived from three separate donors (replicates = 4) at 24h post-stimulation with IFN-α (Mean±SD).

5.2 ISGs expression in response to PolyI:C Stimulation and HBV infection

Recognition of HBV PAMPS by PRR and subsequent induction of ISGs has been controversial. Dansako *et al*. previously reported HBV dsDNA recognition by the PRR cGAS with subsequent induction of cGAS-STING pathway and expression of the antiviral effector IFIT1 [376]. However, the study was performed using human hepatoma Li23 cells and induction of ISG was not assessed. In another study, Sato *el al.* subsequently described RIG-I mediated sensing of the 5'-ε of the HBV pgRNA as the primary mechanism of HBV sensing in PHH, resulting in a predominant type III IFN activation [81]. However, collectively our understanding of the hepatocyte recognition of HBV PAMPS is still in its infancy.

Having established that liver organoids can respond to IFN-α stimulation, we next assessed if organoids could respond to the viral dsRNA genome mimic PolyI:C (Figure 40). In order to stimulate the cytosolic RIG-I pathway, we stimulated the organoids with PolyI:C through transfection to stimulate intracellular PRRs. To improve transfection efficacy, the liver organoids were dissociated into single cells through TrypLE digestion before incubation with the PolyI:C at 2mg/mL and Lipofectamine 3000 transfection reagents. In comparison to transfection reagent only as a vehicle control, significant induction of mRNA for RIG-I, MDA5, IFITM1, ISG15, Viperin, CXCL10 and IFN-β was seen at 24 hour post-stimulation with PolyI:C. Although HBV RNA sensing through the RIG-I pathway has been described previously in PHH and hepatoma cell lines [81], HBV infection in liver organoids was not associated with upregulation of RIG-I or MDA5 mRNA at 4-, 8- and 12-days post-infection despite a corresponding increase in HBV RNA (Figure 41). Interestingly, while HBV replication was established in all these donors, we noted no significant difference in ISG expression across three timepoints from 4-12 days post-infection.

In conclusion, we demonstrated that the liver organoids were responsive to PolyI:C stimulation with a robust innate immune response. Despite HBV replication in liver organoids, no significant induction of ISG was observed, suggesting HBV has either an immune evasive or immune suppressive property. This finding supports our current understanding of innate immune response in HBV infection and that the human liver organoids could be used to explore the innate immune antiviral strategies.

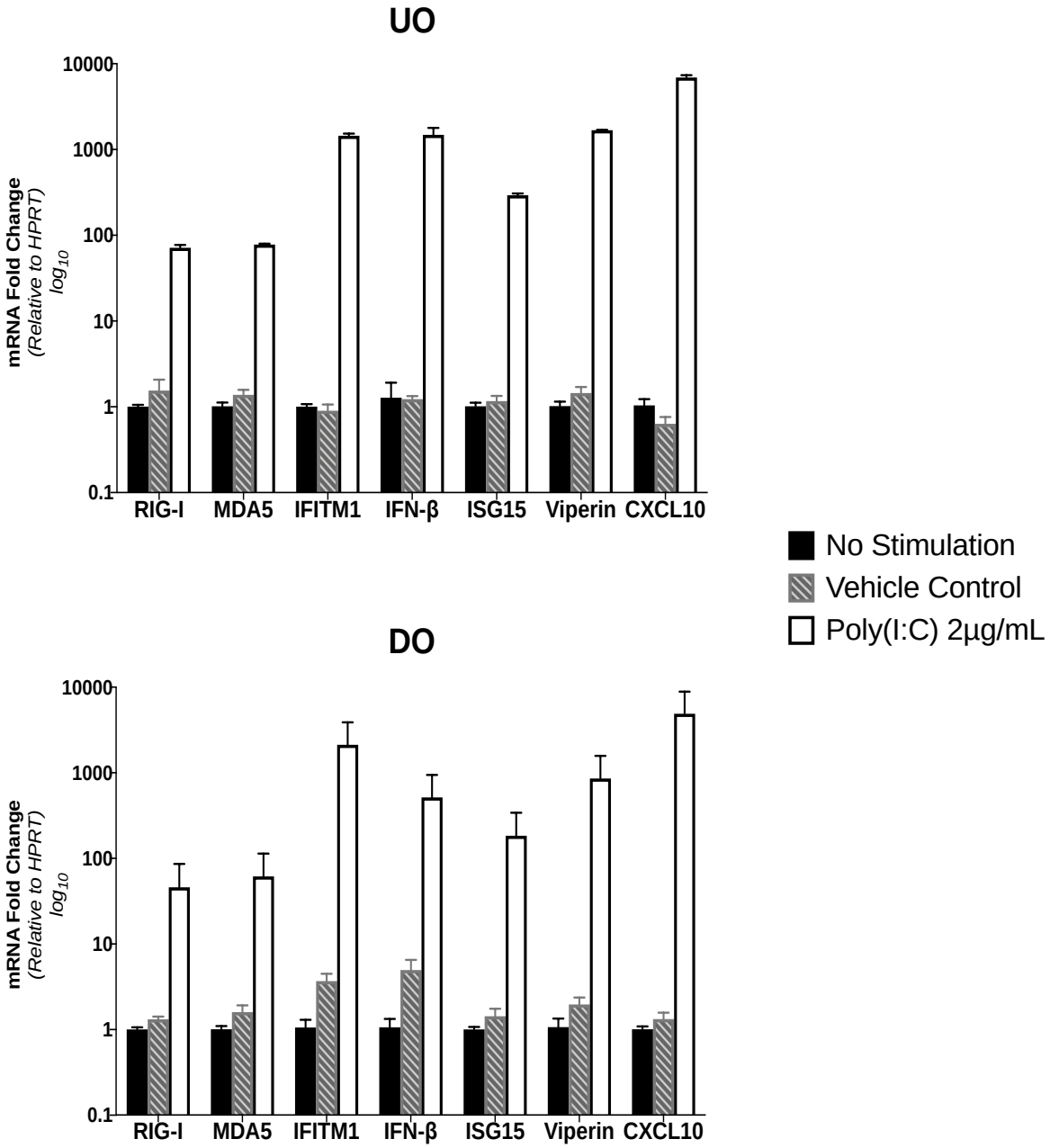

Figure 40: ISG Response to PolyI:C in Liver Organoids
Fold induction of viral sensing and anti-viral effector ISGs in UO an DO 24h post-stimulation with PolyI:C at 2mg/mL

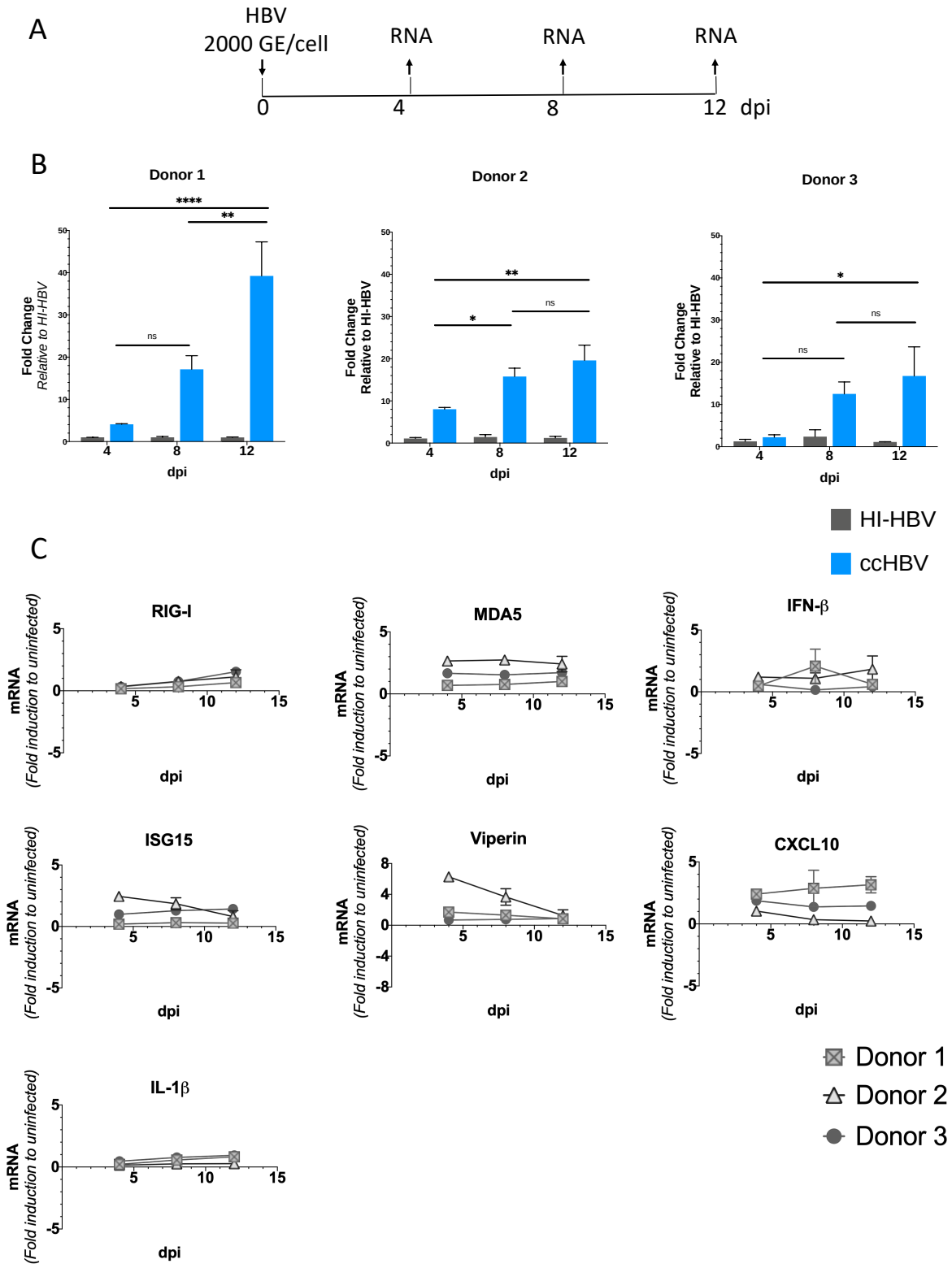

Figure 41: ISG Response to HBV Infection in Liver Organoids
(A) Schematics of HBV infection experiment **(B)** HBV pgRNA fold change, and **(C)** Fold induction of viral sensing and anti-viral effector ISGs in UO an DO following HBV infection among three donors at 1000 GEq/cell using cell-culture derived HBV (ccHBV) and heat-inactivated HBV (HI-HBV) as control. mRNA expression relative to HPRT and normalised to uninfected controls at each specific time points (Mean±SEM).

5.3 Discussion

Defining the innate response to viral infection is key to our understanding of pathogenesis and informing therapeutic and vaccine strategies. Characterisation of the innate response to HBV has been problematic, primarily due to the use of cell-based models, many of which are tumour derived that may contain defects in innate signalling pathways. We therefore in this chapter investigated the use of human liver organoids to study innate responses. In this series of experiments, we have demonstrated that the human liver organoids are highly responsive to IFN and dsRNA mimic stimulations, in both undifferentiated and differentiated states. Donor variation in ISG induction was seen, as expected of a physiologic model system. Importantly, despite a high inoculum, HBV infection and replication are associated with poor ISG induction. Among the panel of ISGs, IFITM1 was selected as it is strongly regulated by type I and II IFNs. It has selective antiviral activities against a range of Flaviviruses through prevention of viral entry through the lipid bilayer [377]. Although IFITM1 has been shown to be antiviral against HCV, the role of IFITM1 on HBV is less clear[378]. In the HepaRG model, HBcAg has been shown to interrupt the stability of polybromo-associated BRM-associated factors (PBAF) complex, thus interfering with downstream IFITM1 transcription [379]. The rationale for this is that our initial experiments focused on firstly if our organoid model could respond to IFN and secondly if there were differences between activation in undifferentiated and differentiated organoids. Stem cell models such as iPSC and ESC have higher levels of basal ISG expression but are poorly responsive to IFN stimulation [228]. It has been theorised that this phenotype serves as a protective mechanism of stem cells to maintain their pluripotency during viral infection, as IFN induction drives the stem cells towards differentiation phenotypes [380]. Following differentiation, stem cells progressively lose their basal ISG expression but become more “inducible” upon stimulation or infection [228, 381], especially in the EIF3L, IFITM and BST groups of ISGs [382]. The

characteristics of canonical type I IFN signalling in LGR5+ liver stem cells have not been previously described. Transcriptomic analyses showed a slightly higher basal mRNA expression of RIG-I and Toll-like pathway cytokines compared with liver tissues (Figure S3 & S4), although these findings were yet to be confirmed with protein analysis. Our findings of the high inducibility of the organoids to Type I IFN stimulation, in both differentiated and undifferentiated forms, is consistent with the findings of other stem cells as LGR5+ stem cells are much further down the differentiation pathway and have lost that ability for pluripotency [248]. Collectively, we have shown that the human liver organoids have a competent IFN and RIG-I pathway, and therefore serve as a good model system to study innate responses.

In these experiments, we also assessed for ISG15 expression as it is often highly expressed in the liver tissue following viral infections. In hepatoma model using HepG2.2.15 cells, overexpression of ISG15 is associated with upregulation of HBV DNA in culture [383]. High ISG15 expression has also been found in HCC tissue and other hepatoma cell lines, suggestive the link between ISG15 and oncogenesis [384]. The levels of ISG15 induction in liver organoids following IFN and PolyI:C stimulation were substantial but the level of induction following HBV infection was very low, similar to the findings of iPSC-HLC model [160].

One limitation of our study to determine innate immune activation in response to HBV infection was the duration of experiment was only up to 12 days, thus restricting our understanding of ISG induction to acute infection model. Future optimisation of this model system to sustain HBV infection for a prolonged period of time would expand our understanding of the innate immune response in chronic HBV infection. In addition, further

assessment of type III IFN response in HBV infection would allow a more complete characterisation of ISG response in liver organoids. In addition, the donor selection process in this study created a gender bias with males predominating. Further experiment to assess differences between males and females could uncover differences in sex related innate responses.

In addition, the infection rates in differentiated human organoids are not high, possibility due to incomplete differentiation, as indicated by persistence of ductal cell markers (e.g., SOX9) following differentiation. The consequence of this is that only some cells are susceptible to HBV infection within the differentiated organoids. Further improvement of human liver organoids differentiation through assessment of different culture conditions and co-culturing liver organoids with other non-parenchymal cells (e.g., Kupffer cells, stellate cells, liver fibroblasts etc) may be warranted.

One limitation of this study is the sexual bias in our tissue donor selection. As we were only looking for healthy tissue from liver resection, most of the cases were from elderly men undergoing liver resection due to metastatic colon cancer and all the infection experiments were performed using organoids from male patients. There is increasing understanding of the presence of sexual differences in immune response to viral infections [385]. Using SARS-CoV-2 as an example, female patients have a higher level of T cell response and IFN-α response whereas male patients have a higher level of IL-8 and IL-18 response, and these differences have an implication on diseases severity and clinical outcome [385-387]. The sexual differences in innate immune response for HBV is currently unknown and could be explored further using our organoid model. In addition, it is recently recognised that Hepatitis B infection affects men more than women, with men having more rapidly progressive liver

disease and HCC than women [388, 389]. The contributing factors to these differences are not clear and could be potentially explored in the liver organoid model.

Collectively, our preliminary findings suggest that HBV is a poor activator of the innate response and subsequent induction of ISGs. This is consistent with other studies using PHH in which HBV did not induce ISG expression [89, 390]. It further emphasises the importance of using a physiologic model system when assessing the innate immune response. In addition, any interactions of individual components of HBV proteins with ISGs must also be confirmed with the global effect of HBV infection. Future organoid studies should explore if these individual HBV proteins are capable of activating the innate immune system and whether additional mechanisms shut down this process.

6 Conclusion and Future Directions

Chronic Hepatitis B (CHB) has been described as a global silent epidemic by the WHO and continues to grow as a major public health issue in the developing world, despite having an effective preventative vaccine for decades. It accounts for a significant number of patients with liver cirrhosis and/or hepatocellular carcinoma and is a major indication for liver transplantation worldwide. To date, there is no effective curative therapy available for CHB. Current treatment with nucleoside/nucleotide analogues are required for long-term suppression of HBV and do not totally ameliorate the risk of HCC [391]. This treatment strategy continues to impose significant health care costs and pill burden to patients. Another therapeutic strategy is short-term use of pegylated IFN-α-2a to induce a "cytokine storm" in the hope of controlling the virus temporarily. The exact mechanism of how IFN therapy achieve viral suppression is not known, but most likely through augmentation of cell mediated immunity to interfere with various aspects of the HBV lifecycle, including RNA transcription [392]. Furthermore, the use of IFN therapy could only benefit a very small proportion of patients for a number of reasons: (1) only some HBV genotypes are responsive to IFN therapy, (2) HBeAg positive patients are most likely to benefit from IFN therapy than HBeAg negative patients, (3) high pre-treatment IFN levels is associated with treatment failure, and (4) risk of liver decompensation in cirrhotic patients and (5) poor toxicity profiles including exacerbation of mental illness. Clearly, a novel approach to achieving HBV cure is required to eradicate CHB globally. There has been a significant push to develop curative therapies, however in many cases there is a lack of a good model system to assess their efficacies. Despite having a myriad of *in vitro* model systems for HBV infection, very few of these systems, are primary in nature and do not account for patient's host genetic and gender variability and thus have limited application in clinical use. As an example, our understanding of the HBV lifecycle, pathogenesis and drug treatment, has relied on cancer

derived cell lines and animal models. The main limitation is the lack of applicability in predicting drug response, viral rebound in the setting of multiple drug resistant mutations, antiviral withdrawal or the use of immunosuppressants. Understanding of the lifecycle of HBV is also rather limited and compounded by conflicting results from various non-physiological model systems.

As new immunotherapies are slowly emerging for HBV, coupled with recent advances in our understanding of liver regeneration, stem cell-derived liver model systems have gained more research and clinical interests. Patient derived stem cells (iPSC, ESC, AdSC), pluripotent or multipotent, have shown great promise in personalised medicine as they retain the genetic signatures of the hosts. A prime example of this is the response of tumour derived organoids to certain chemotherapeutic agents [393]. This opens the door for assessment of individual immune response to viral infections, a concept that is relatively unexplored. Development of tissue engineering techniques and 3D cell culture system further enhance the differentiation of stem cells into hepatocyte-like cells (HLCs) that resemble PHH. Each stem cell model systems have its own unique advantages and limitations. iPSC-derived HLCs are the most developed stem cell model system to date as it is not hampered by the ethical issues of ESCs. iPSC-HLCs have been shown to sustain HBV and HCV infections and retain an intact JAK-STAT signalling pathway. However, high mutation rates introduced during stem cell reprogramming and culture limit its advancement in regenerative medicine. Adult liver stem cells (LGR5+) derived HLCs/organoids represent a more recent advancement in stem cell biology with genetic stability. Assessment of this novel model system in sustaining HBV infection is limited. In this thesis, we described and characterise the differentiation process of adult stem cell derived HLCs in the organoids model system, and important features that

sustain HBV infection. In addition, we demonstrate the utility of organoids culture in assessing the innate immune response to viral infection and antiviral response.

6.1 Summary of Findings and Future Direction

This thesis encompasses a series of experiments that focused on the development and differentiation of human liver organoids and has identified a number of advantages and limitations of this model system. These experiments highlighted the AdSC ability to differentiate into HLCs, its susceptibility to HBV infection and its robust innate immune response (Figure 42). Understanding of these novel characteristics of the liver organoid model system allows us to further explore the liver biology, pathogenesis of HBV infection and associated diseases and applicability of this model system in translational medicine.

This thesis has demonstrated, for the first time the relationship between functional NTCP expression and susceptibility to HBV infection in a primary stem cell model. In addition, this thesis also explored the innate immune response of AdSC-derived organoids to various stimulations (IFN, PolyI:C) and HBV infection, which have not been previously described. One limitation of the organoid model system has also been identified, in which the cellular differentiation into hepatocyte is incomplete and can potentially affect the susceptibility of the organoids to HBV infection. Further improvement of organoids differentiation process using different culture conditions (e.g., physiologic oxygen tension, coculture with other non-parenchymal cells and additional growth factors) should therefore be explored.

The novel biological characteristics of the organoids culture system described here have allowed us to identify several major areas of research that could stem from this thesis (Figure 43). Examples are (1) modelling for clinical HBV infection (2) transcriptomic characterisation of host responses to HBV infection (e.g., RNA Seq), (3) evaluation of novel

HBV therapeutics, (4) CRISPR Cas9 editing to knock-out/screen for essential HBV host factors, (5) HBV tumourigenesis using organoid system, (6) hepatocyte differentiation and HBV infection in co-culture system with liver non-parenchymal and immune cells, (7) effects of host-variation (e.g., gender, age) in HBV infection and innate immune responses (8) infection and/or co-infection with other hepatotropic viral infections (e.g., HCV, HAV, HDV, HEV) and (9) NTCP biology.

To improve the clinical applicability of human liver organoids, future experiments would include transplantation of human liver organoids in SCID mice to evaluate if the human liver organoids are able to engraft and develop its full metabolic potentials in the liver microenvironment. Transcriptomic analysis of engrafted liver organoids in comparison with liver organoids cultured *in vitro* may identify important cellular factors required for hepatocyte maturation. Further characterisation of the immune response of liver organoids especially type III IFN response and basal expression of ISGs would help complete the picture of the innate immune response of human liver organoids. This can be achieved by assessing the transcriptomics of human liver organoids using RNA Seq in the setting of viral infection and/or IFN stimulation. Assessment of other hepatotropic viral infections (HCV, HAV, HDV) and co-infection in liver organoids can be done by first assessing the viral receptor expression for each virus. Subsequent viral dynamic study either in mono- or co-infection setting would allow further assessment of viral-viral interactions using qRT-PCR.

In conclusion, we have demonstrated the metabolic characteristics and ability of the human liver organoids to support the full life cycle of HBV infection. In addition, the presence of donor variations and an intact innate immune response would allow us to further develop this model system to inform personalised drug response, toxicity and viral reactivation. The

human liver organoids are likely to play an important role in the future of drug testing for novel antivirals.

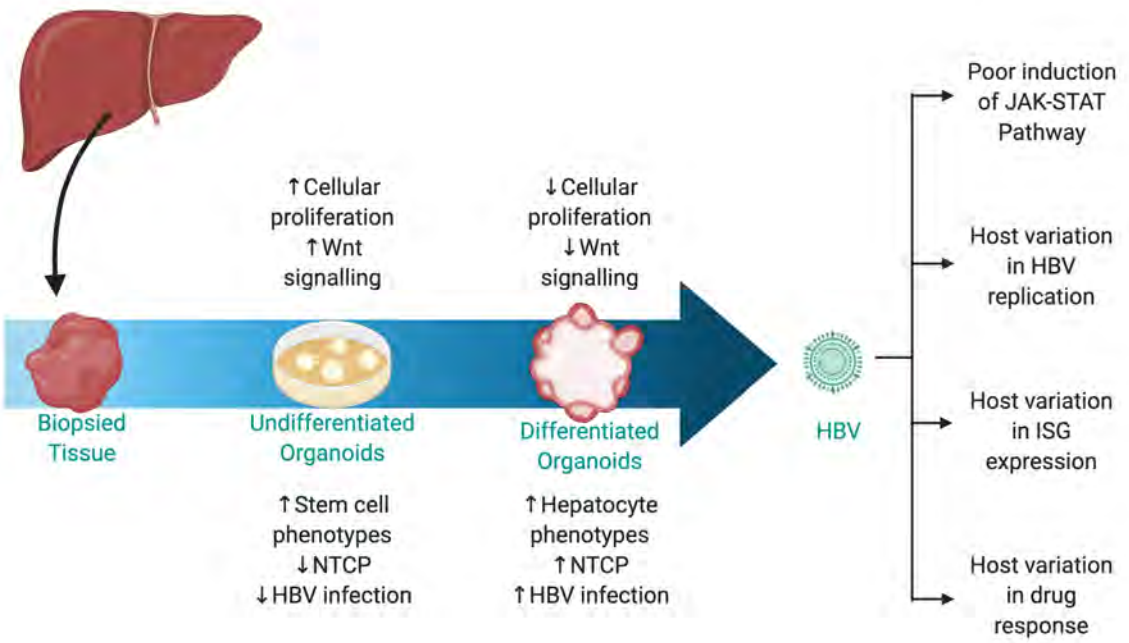

Figure 42: Proposed Organoids HBV Model System

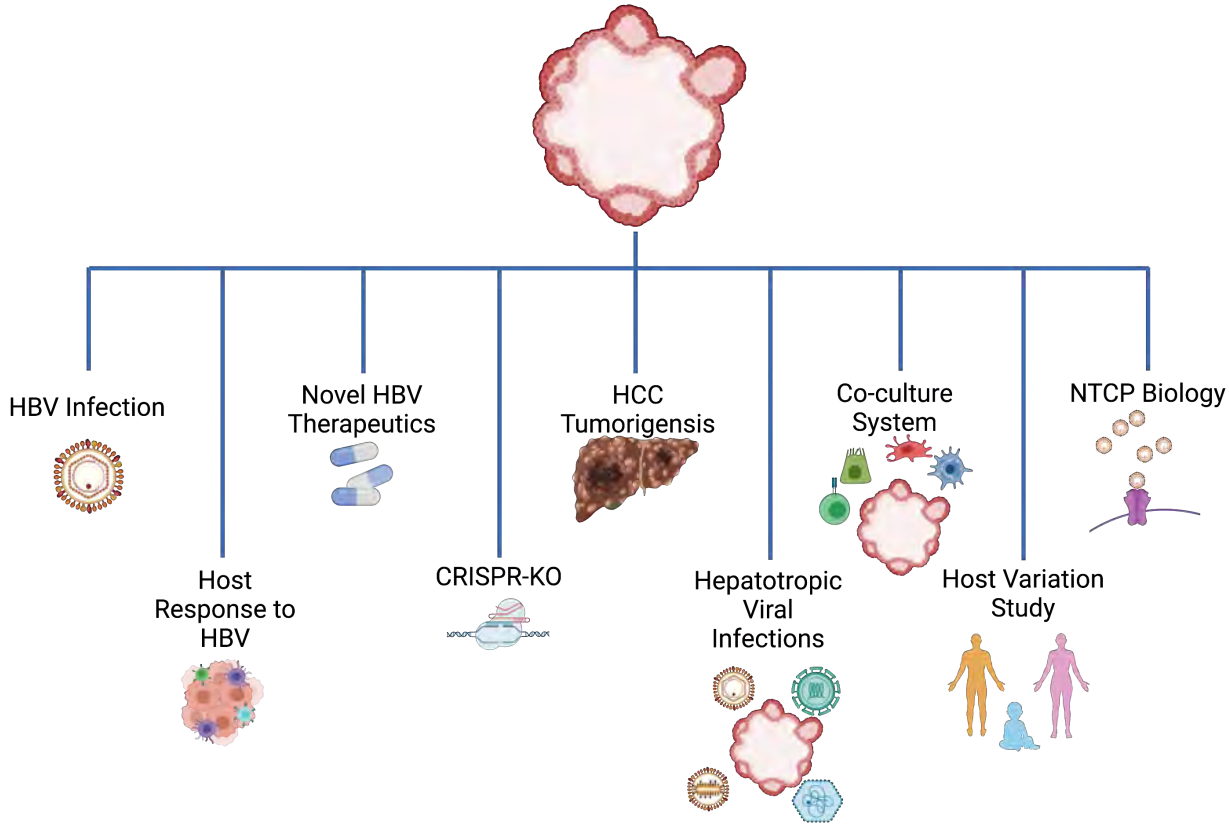

Figure 43: Applications of Human Liver Organoid Model System

7 Appendices

7.1 Mouse Liver Organoids Culture Reagents

Mouse Liver Digestion Medium

Components	Stock Concentration (mg/mL)	Working Concentration (mg/mL)
Collagenase D	Neat (lyophilised)	0.125 mg/mL
Dispase II	10	0.125 mg/mL
DNaseI	10	0.1 mg/mL
DMEM	Neat	Neat

Mouse Liver Organoids Isolation Medium

Components	Stock Concentration	Working Concentration
Mouse Liver Expansion Medium	Neat	Neat
Noggin-conditioned medium	Neat	5% (v/v)
Wnt3a-conditioned medium	Neat	30% (v/v)
Rho kinase (ROCK) inhibitor (Y-27632)	10mM	10uM

Mouse Liver Organoids Expansion Medium

Components	Stock Concentration	Working Concentration
Basal Medium	Neat	Neat
B27 (with/without vitamin A)	50x	1x
N-acetylcysteine	1M	1mM
Rspo1 conditioned medium	Neat	5% (v/v)
Nicotinamide	1M	10mM
Recombinant human [Leu15]-gastrin	10uM	10nM
Recombinant mouse EGF	1µg/mL	50ng/mL
Recombinant human FGF10	100µg/mL	100ng/mL
Recombinant human HGF	25µg/mL	50ng/mL

7.2 Mouse Liver Organoids Differentiation Reagents

Mouse Liver Organoids Differentiation Medium (Day 0-12)

Components	Stock Concentration	Working Concentration
Basal Medium	Neat	Neat
B27 supplement (with/without vitamin A)	50X	1x
N2 supplement	100X	1x

N-acetylcysteine	1M	1mM
Recombinant human [Leu15]-gastrin I	10μM	10nM
mEGF	1	50ng/mL
Recombinant human FGF-10	100	100ng/mL
A83-01	50mM	50nM
DAPT	10mM	10μM

Mouse Liver Organoids Differentiation Medium (Day 13-15)

Components	Stock Concentration	Working Concentration
Basal Medium	Neat	Neat
B27 supplement (with/without vitamin A)	50X	1x
N2 supplement	100X	1x
N-acetylcysteine	1M	1mM
Recombinant human [Leu15]-gastrin I	10μM	10nM
mEGF	1μg/mL	50ng/mL
Recombinant human FGF-10	100μg/mL	100ng/mL
A83-01	50mM	50nM
DAPT	10mM	10μM
Dexamethasone (day 13-15)	3mM	3μM

7.3 Human Liver Organoids Culture Reagents

Human Liver Digestion Solution

Components	Stock Concentration (mg/mL)	Working Concentration (mg/mL)
Collagenase D (mg)	Neat	2.5
EBSS	Neat	Neat
DNaseI (dissolve in water)	10	0.1

Human Liver Isolation Medium

Components	Stock Concentration	Working Concentration
Human Liver Expansion Medium	Neat	Neat
Noggin-conditioned medium	Neat	5% (v/v)
Wnt3a-conditioned medium	Neat	30% (v/v)
Rho kinase (ROCK) inhibitor (Y-27632)	10mM	10uM

Human Liver Expansion Medium

Components	Stock Concentration	Working Concentration
Basal Medium	Neat	Neat
N2 supplement	100X	1x

B27 (without vitamin A)	50x	1x
N-acetylcysteine	1M	1mM
Rspo1 conditioned medium (uL)	Neat	10%
Nicotinamide	1M	10mM
Recombinant human[Leu15]-gastrin	10µM	10nM
Recombinant human EGF	1µg/mL	50ng/mL
Recombinant human FGF10	100µg/mL	100ng/mL
Recombinant human HGF	25µg/mL	25ng/mL
Forskolin	10mM	10µM
A83-01	50µM	5µM

7.4 Human Liver Organoids Differentiation Reagents

Components	Stock Concentration	Working Concentration
Basal Medium	Neat	NA
B27 supplement (with vitamin A)	50X	1x
N2 supplement	100X	1x
N-acetylcysteine	1M	1mM
Recombinant human [Leu15]-gastrin I	10µM	10nM
hEGF	1µg/mL	50ng/mL
Recombinant human HGF	25µg/mL	25ng/mL
Recombinant human FGF-10	100µg/mL	100ng/mL
A83-01	50uM	0.5µM
DAPT	10mM	10µM
Dexamethasone**	30mM	30µM
BMP7	25µg/mL	25ng/mL
Recombinant human FGF19	100µg/mL	100ng/mL

7.5 Human Hepatocyte Organoids Reagents

Components	Stock Concentration (µg/mL)	Working Concentration
Basal Medium	Neat	Neat
B27 (without vitamin A)	50x	1x
N-acetylcysteine	1M	1.25mM
Rspo1 conditioned medium (µL)	Neat	15%
Nicotinamide	1M	10mM
Recombinant human[Leu15]-gastrin	10µM	10nM
Recombinant human EGF	1µg/mL	50ng/mL
Recombinant human FGF10	100µg/mL	100ng/mL

Recombinant human HGF	25µg/mL	50ng/mL
FGF7	100µg/mL	100ng/mL
CHIR99021	3mM	3µM
Rho Inhibitor	10mM	10µM
TGFa	20µg/mL	20ng/mL
A83-01	50µM	5µM

7.6 Primer Sequences

Name	Sequence 5' – 3'	Reference
HBV DNA Forward	GTG TCT GCG GCG TTT TAT CA	[394]
HBV DNA Reverse	GAC AAA CGG GCA ACA TAC CTT	
HBV pgRNA Forward	TGTGGAGTTACTCTCGTTTTTGC	[395]
HBV pgRNA Reverse	AAGGCTTCCCGATACAGAGC	[395]
HBV Total RNA Forward	GCACTTCGCTTCACCTCTGC	[81]
HBV Total RNA Reverse	CTCAAGGTCGGTCGTTGACA	[81]
HBV cccDNA Forward	CCAAGTGTTTGCTGACGCAAC	In house
HBV cccDNA Reverse	GGAGTTCCGCAGTATGGATCG	In house
NTCP Forward	CATCTTGGTCTGTGGCTGCT	In house
NTCP Reverse	GGTGGTCATCACAATGCTGAG	In house
Albumin Forward	CTGCCTGCCTGTTGCCAAAGC	[159]
Albumin Reverse	GGCAAGGTCCGCCCTGTCATC	[159]
CYP2D6 Forward	CTTCAGCTTCTCGGTGCCCA	In house
CYP2D6 Reverse	GCACAAAGCTCATAGGGGGATGG	In house
CYP3A4 Forward	TGTGCCTGAGAACACCAGAG	[159]
CYP3A4 Reverse	GTGGTGGAAATAGTCCCGTG	[159]
HNF4a Forward	GTACTCCTGCAGATTTAGCC	[159]
HNF4a Reverse	CTGTCCTCATAGCTTGACCT	[159]
LGR5 Forward	GACTTTAACTGGAGCACAGA	[159]
LGR5 Reverse	AGCTTTATTAGGGATGGCAA	[159]
SOX9 Forward	GGAAGTCGGTGAAGAACGGG	[159]
SOX9 Reverse	TGTTGGAGATGACGTCGCTG	[159]
KRT19 Forward	CGCGGCGTATCCGTGTCCTC	[159]
KRT19 Reverse	AGCCTGTTCCGTCTCAAACTTGGT	[159]
HPRT Forward	AAGAGCTATTGTAATGACCAGT	[159]
HPRT Reverse	CAAAGTCTGCATTGTTTTGC	[159]
GAPDH Forward	GCATCTTCTTTTGCGTCG	[159]
GAPDH Reverse	TGTAAACCATGTAGTTGAGGT	[159]

Viperin Forward	AATTGAATTCATGTGGGTGCTTACACCTGCTG	In house [231]
Viperin Reverse	AATAGGATCCCTACCAATCCAGCTTCAGATCA	In house [231]
IFITM1 Forward	CGCCAAGTGCCTGAACATCT	In house [231]
IFITM1 Reverse	CCCGTTTTTCCTGTATTATCTGTA	In house [231]
ISG15 Forward	TGGCGGGCAACGAATT	In house [231]
ISG15 Reverse	GGGTGATCTGCGCCTTCA	In house [231]
CXCL10 Forward	GTGGCATTCAAGGAGTACCTC	In house [231]
CXCL10 Reverse	TGATGGCCTTCGATTCTGGATT	In house [231]
RIG-I Forward	ACAACACCCGTACAATATGATCATG	In house [231]
RIG-I Reverse	ACACCAACCGAGGCAGTCA	In house [231]
MDA5 Forward	GAGCAACTTCTTTCAACCACAG	In house [231]
MDA5 Reverse	CACTTCCTTCTGCCAAACTTG	In house
IFN-β Forward	TGTCAACATGACCAACAAGTGTCT	In house [231]
IFN-β Reverse	GCAAGTTGTAGCTCATGGAAAGAG	In house [231]

7.7 Antibodies

Antibodies	Identifier	Application	Concentration
Anti-Human Albumin	(Bethyl Cat# A80-129, RRID:AB_67016)	IF	1:100-200
Anti-Human E-Cadherin	Santa Cruz Biotechnology Cat# sc-7870, RRID:AB_2076666	IF	1:100-200
Anti-Human HBsAg	Agilent Cat# M3506, RRID:AB_2114741	IF	1:100-200
Anti-Human HBcAg	Abcam Cat# ab8637, RRID:AB_306684	IF	1:100-200
Anti-Human HBcAg	Agilent Cat# B0586, RRID:AB_2335704	IF	1:100-200
Anti-Human NTCP	Sigma-Aldrich Cat# HPA042727, RRID:AB_10960691	IF	1:100-200
Anti-Human NTCP	(Thermo Fisher Scientific Cat# PA5-80001, RRID:AB_2747116	IF WB	1:100-200 1:1000
Anti-Human ZO-1	Thermo Fisher Scientific Cat# 40-2200, RRID:AB_2533456	IF	1:1000
Anti-Human ZO-1	BD Biosciences Cat# 610966, RRID:AB_398279	IF	1:100-200
Anti-Human HNF4a	Abcam Cat# ab41898, RRID:AB_732976	IF	1µg/µL
Anti-Human SOX9	Millipore Cat# AB5535, RRID:AB_2239761	IF	1:100-200
Anti-Flavivirus Group Envelope (E) Protein [D1-4G2-4-15]	ATCC® VR-1852™, RRID:AB_827205	IF	Neat
Goat Anti-Mouse Alexa Fluor 488	Thermo Fisher Scientific Cat# A32723, RRID:AB_2633275	IF	1:200
Goat Anti-Rabbit Alexa Fluor 488	Thermo Fisher Scientific Cat# A32731, RRID:AB_2633280	IF	1:200
Goat Anti-Mouse Alexa Fluor 555	Thermo Fisher Scientific Cat# A32727, RRID:AB_2633276	IF	1:200
Goat Anti-Rabbit Alexa Fluor 555	Thermo Fisher Scientific Cat# A32732, RRID:AB_2633281	IF	1:200
Goat Anti-Mouse Alexa Fluor 647	Thermo Fisher Scientific Cat# A32728, RRID:AB_2633277	IF	1:200

7.8 Drugs

	Catalogue Number	Company	Concentration
Baricitinib	HY-15315A	Focus Bioscience	1μM
Mycludex B	N/A	Auspep	100nM
Pegylated interferon-α2b	SRP4595	Sigma Aldrich	Variable

7.9 Supplementary Figures

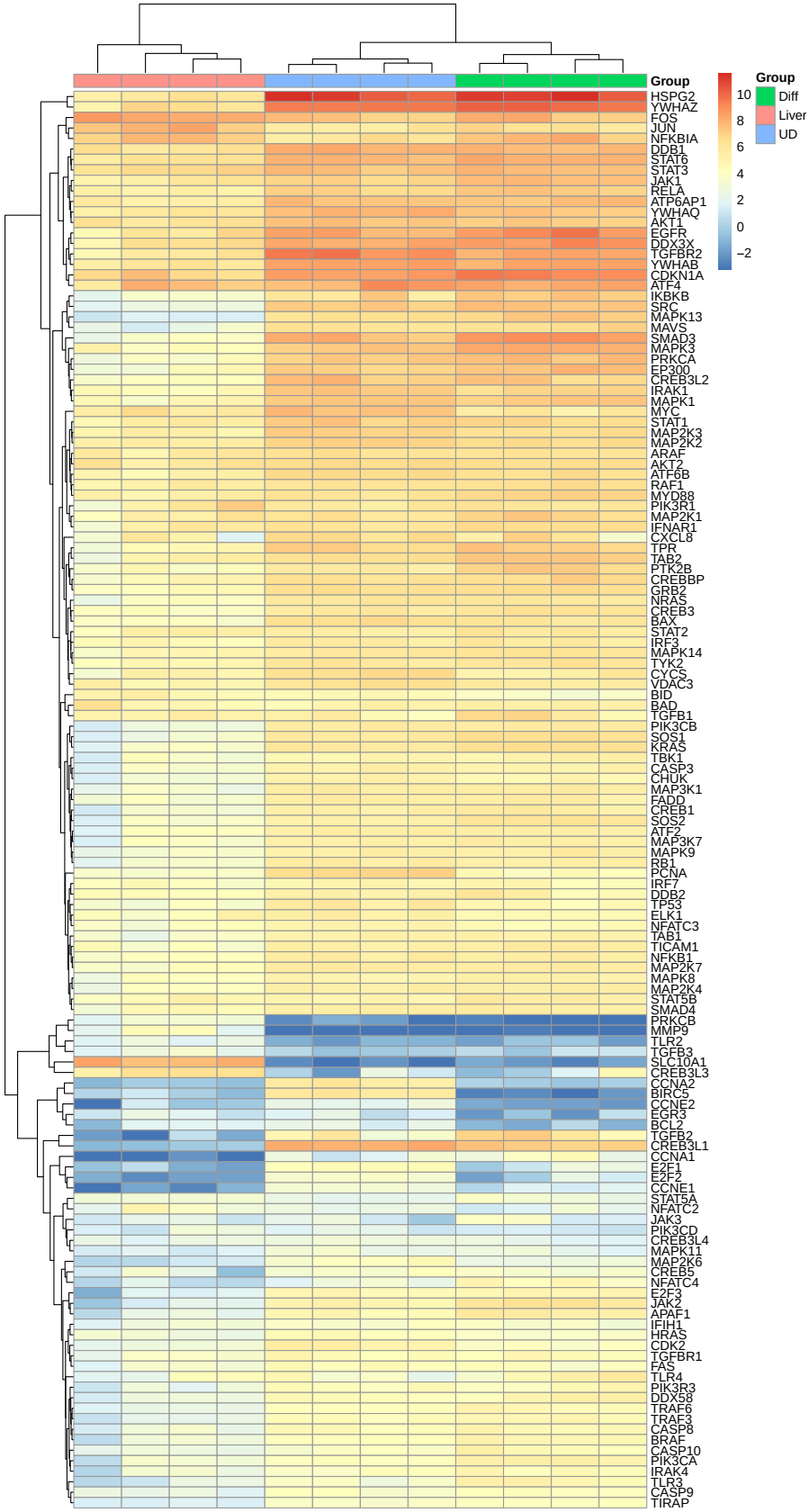

S1: RNA Sequencing Analysis of Host-Factors Involved in HBV Pathway

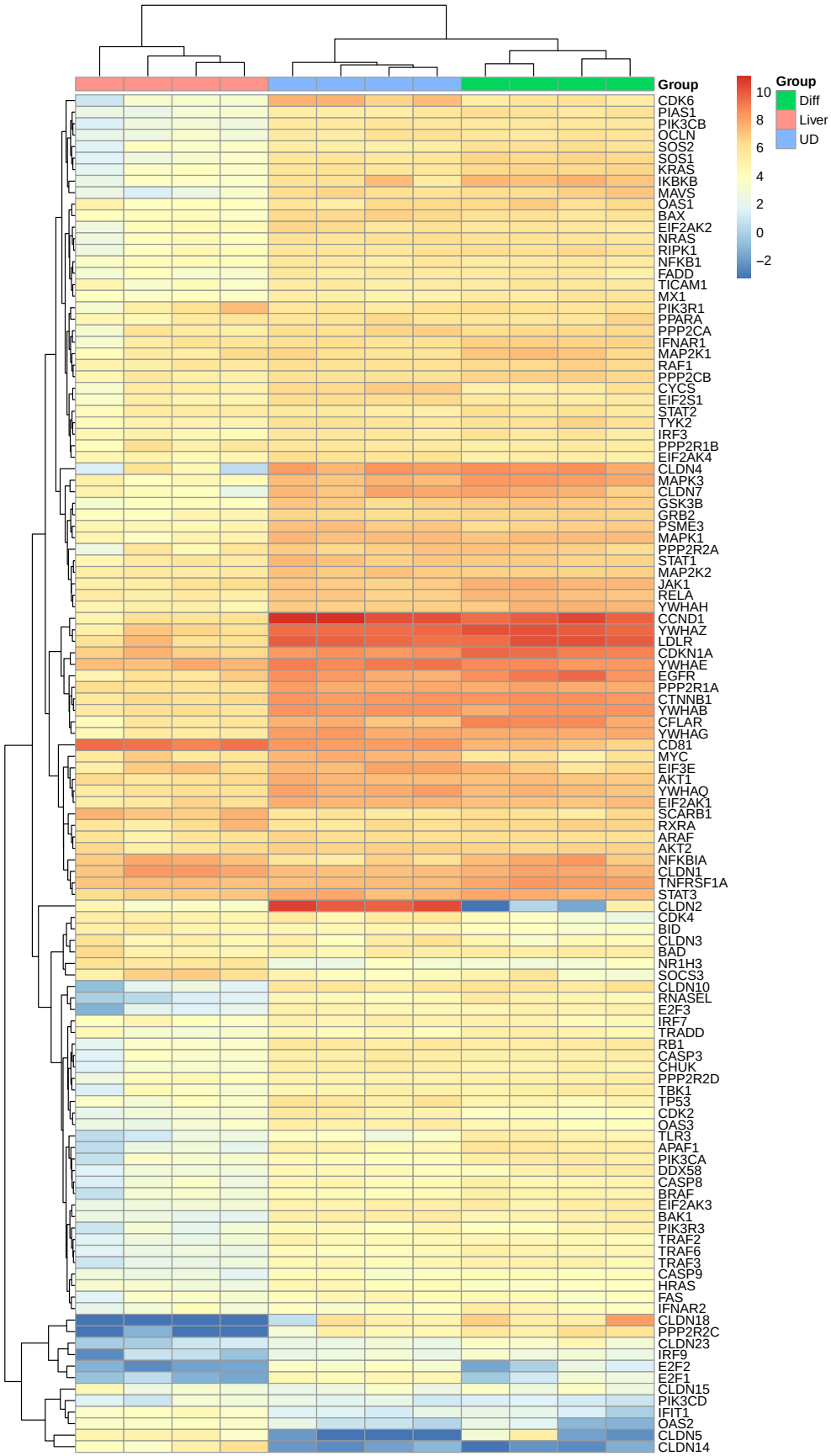

S2: RNA Sequencing Analysis of Host-Factors Involved in HCV Pathway

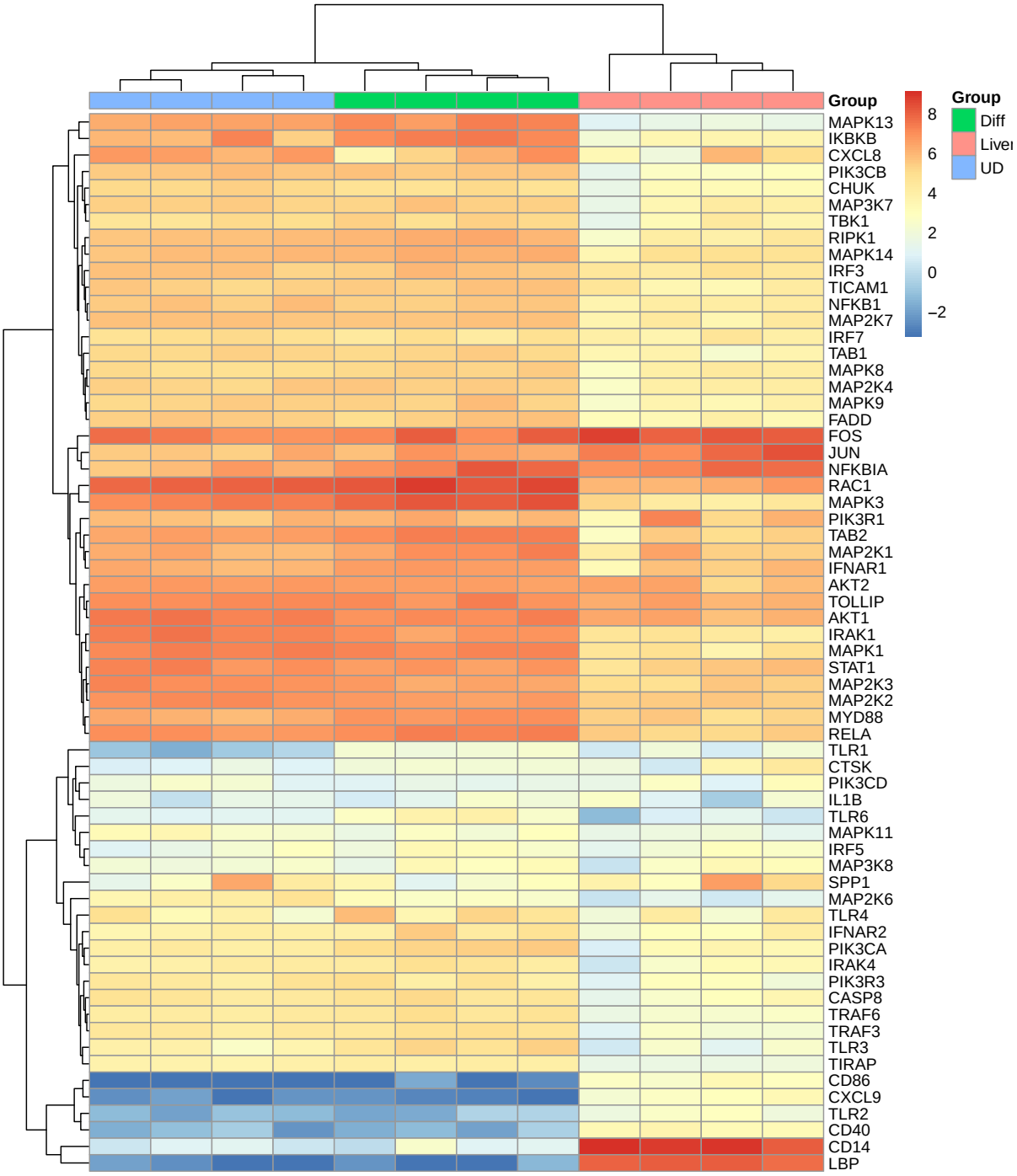

S3: RNA Sequencing Analysis of Host-Factors Involved in Toll-like Pathway

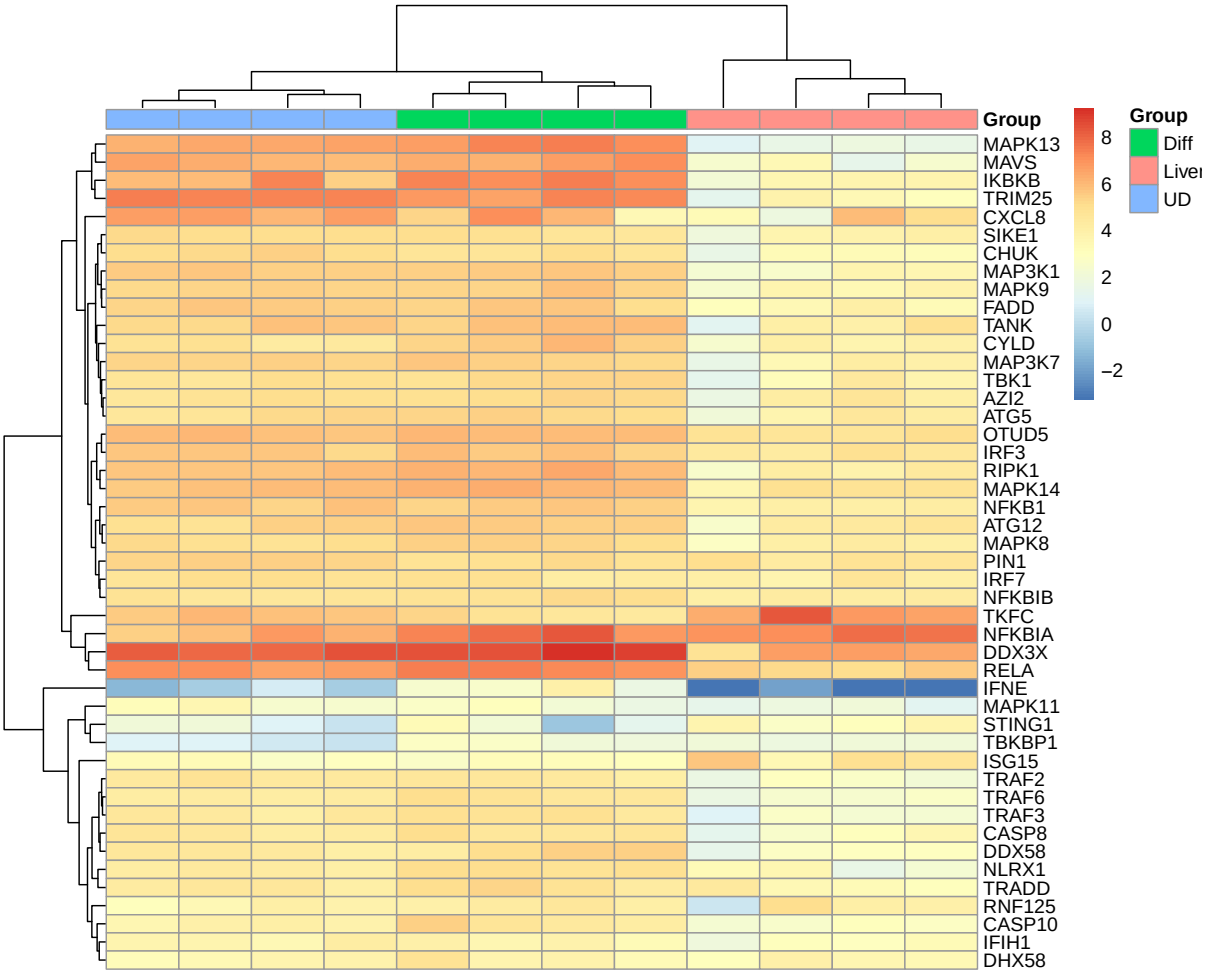

S4: RNA Sequencing Analysis of Host-Factors Involved in RIG-I Pathway

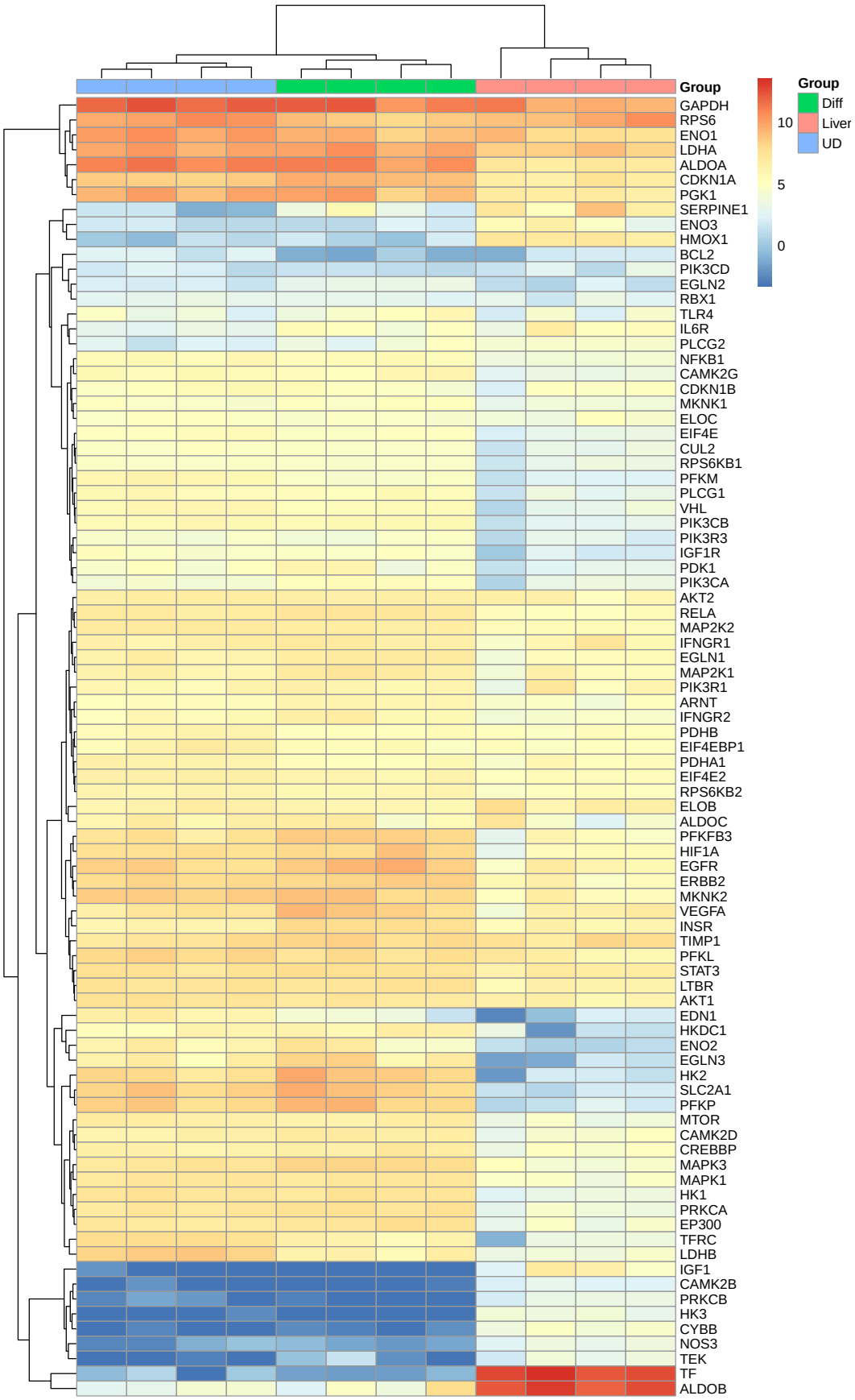

S5: RNA Sequencing Analysis of Host-Factors Involved in HIF-1 Pathway

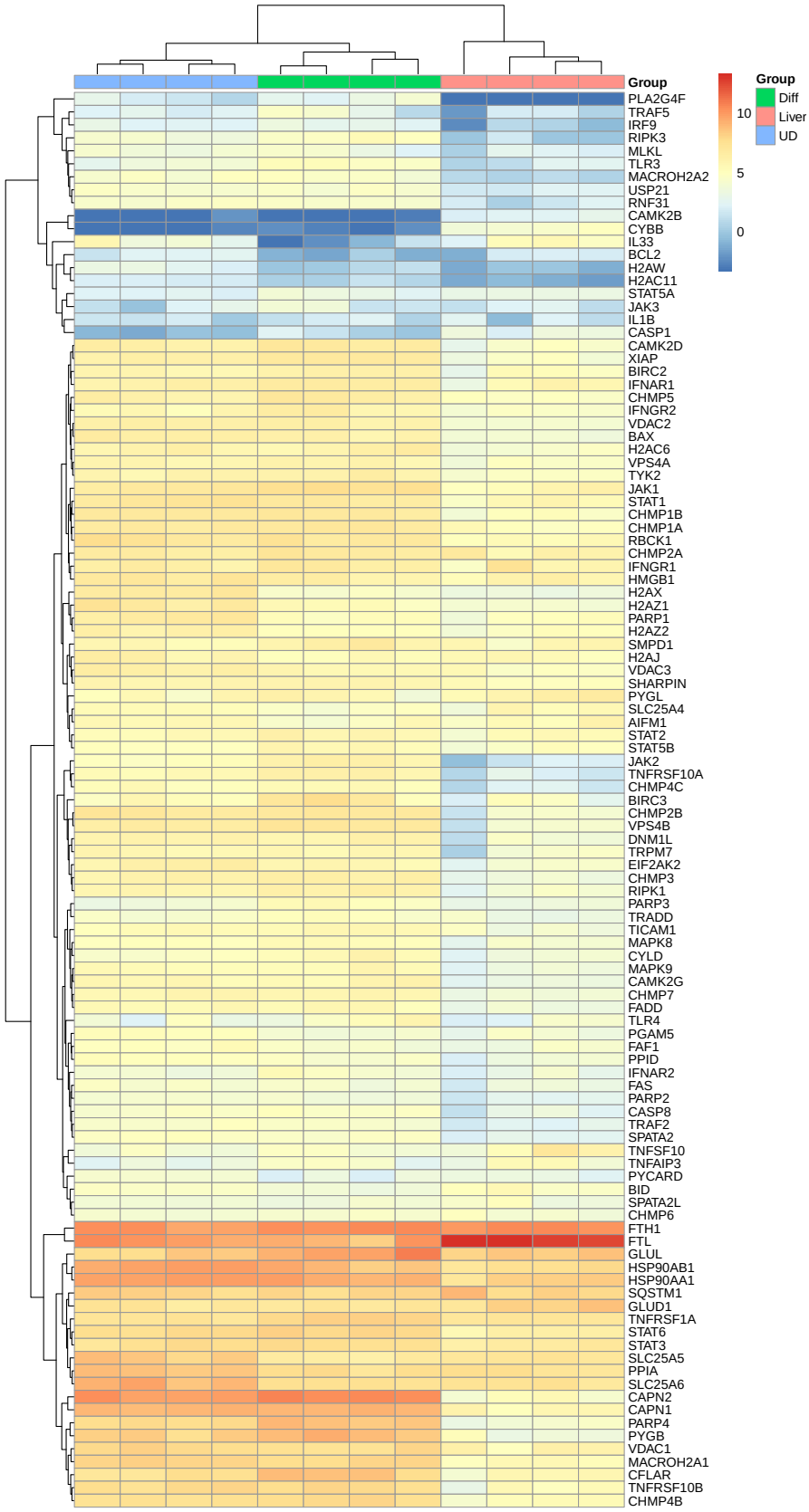

S6: RNA Sequencing Analysis of Host-Factors Involved in Necroptosis Pathway

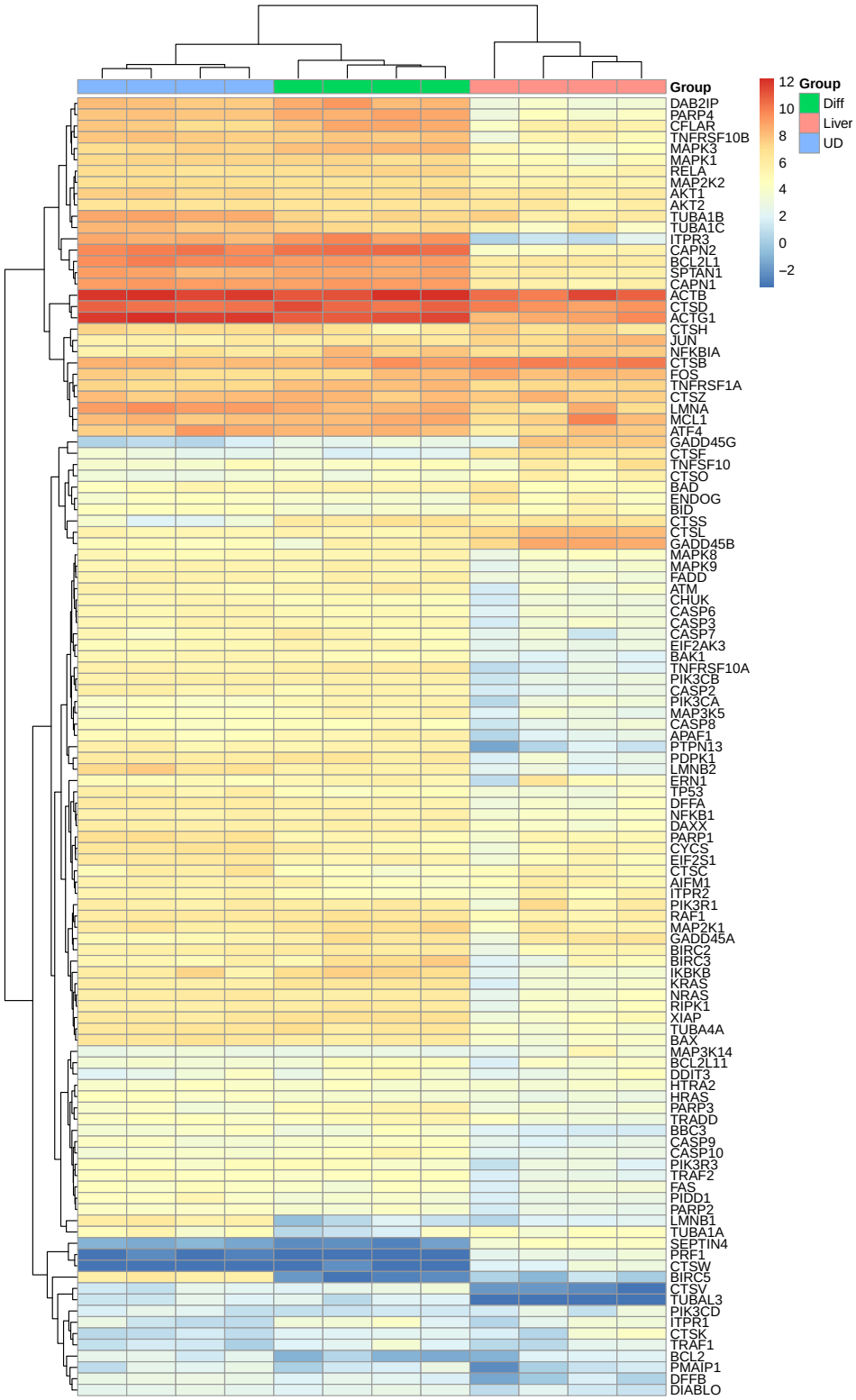

S7: RNA Sequencing Analysis of Host-Factors Involved in Apoptosis Pathway

8 Reference

1. *Global surveillance and control of hepatitis C. Report of a WHO Consultation organized in collaboration with the Viral Hepatitis Prevention Board, Antwerp, Belgium.* J Viral Hepat, 1999. **6**(1): p. 35-47.
2. Stanaway, J.D., et al., *The global burden of viral hepatitis from 1990 to 2013: findings from the Global Burden of Disease Study 2013.* Lancet, 2016. **388**(10049): p. 1081-1088.
3. Liaw, Y.F., et al., *Clinical and virological course of chronic hepatitis B virus infection with hepatitis C and D virus markers.* Am J Gastroenterol, 1998. **93**(3): p. 354-9.
4. Singh, K.P., et al., *HIV-hepatitis B virus coinfection: epidemiology, pathogenesis, and treatment.* AIDS, 2017. **31**(15): p. 2035-2052.
5. Dharel, N. and R.K. Sterling, *Hepatitis B Virus-HIV Coinfection: Forgotten but Not Gone.* Gastroenterol Hepatol (N Y), 2014. **10**(12): p. 780-8.
6. Li, T., et al., *Hepatitis B virus surface antigen-negative and hepatitis C virus antibody-negative hepatocellular carcinoma: clinical characteristics, outcome, and risk factors for early and late intrahepatic recurrence after resection.* Cancer, 2013. **119**(1): p. 126-35.
7. Cho, W.H., et al., *Development of tenofovir disoproxil fumarate resistance after complete viral suppression in a patient with treatment-naive chronic hepatitis B: A case report and review of the literature.* World J Gastroenterol, 2018. **24**(17): p. 1919-1924.
8. Pallier, C., et al., *Dynamics of hepatitis B virus resistance to lamivudine.* J Virol, 2006. **80**(2): p. 643-53.
9. Chang, M.L. and Y.F. Liaw, *Hepatitis B flares in chronic hepatitis B: pathogenesis, natural course, and management.* J Hepatol, 2014. **61**(6): p. 1407-17.
10. Revill, P., et al., *Global strategies are required to cure and eliminate HBV infection.* Nat Rev Gastroenterol Hepatol, 2016. **13**(4): p. 239-48.
11. Schadler, S. and E. Hildt, *HBV life cycle: entry and morphogenesis.* Viruses, 2009. **1**(2): p. 185-209.
12. Liang, T.J., *Hepatitis B: the virus and disease.* Hepatology, 2009. **49**(5 Suppl): p. S13-21.
13. Zeisel, M.B., et al., *Towards an HBV cure: state-of-the-art and unresolved questions--report of the ANRS workshop on HBV cure.* Gut, 2015. **64**(8): p. 1314-26.
14. Ni, Y., et al., *Hepatitis B and D viruses exploit sodium taurocholate co-transporting polypeptide for species-specific entry into hepatocytes.* Gastroenterology, 2014. **146**(4): p. 1070-83.
15. Yan, H., et al., *Viral entry of hepatitis B and D viruses and bile salts transportation share common molecular determinants on sodium taurocholate cotransporting polypeptide.* J Virol, 2014. **88**(6): p. 3273-84.
16. Urban, S., et al., *Strategies to inhibit entry of HBV and HDV into hepatocytes.* Gastroenterology, 2014. **147**(1): p. 48-64.
17. Glebe, D. and S. Urban, *Viral and cellular determinants involved in hepadnaviral entry.* World J Gastroenterol, 2007. **13**(1): p. 22-38.
18. Schmitz, A., et al., *Nucleoporin 153 arrests the nuclear import of hepatitis B virus capsids in the nuclear basket.* PLoS Pathog, 2010. **6**(1): p. e1000741.

19. Xia, Y. and H. Guo, *Hepatitis B virus cccDNA: Formation, regulation and therapeutic potential.* Antiviral Res, 2020. **180**: p. 104824.
20. Hai, H., A. Tamori, and N. Kawada, *Role of hepatitis B virus DNA integration in human hepatocarcinogenesis.* World J Gastroenterol, 2014. **20**(20): p. 6236-43.
21. Duriez, M., et al., *Alternative splicing of hepatitis B virus: A novel virus/host interaction altering liver immunity.* J Hepatol, 2017. **67**(4): p. 687-699.
22. Urban, S., et al., *The replication cycle of hepatitis B virus.* J Hepatol, 2010. **52**(2): p. 282-4.
23. Watanabe, T., et al., *Involvement of host cellular multivesicular body functions in hepatitis B virus budding.* Proc Natl Acad Sci U S A, 2007. **104**(24): p. 10205-10.
24. Jones, S.A., et al., *Comparative analysis of hepatitis B virus polymerase sequences required for viral RNA binding, RNA packaging, and protein priming.* J Virol, 2014. **88**(3): p. 1564-72.
25. Le Pogam, S., et al., *Exposure of RNA templates and encapsidation of spliced viral RNA are influenced by the arginine-rich domain of human hepatitis B virus core antigen (HBcAg 165-173).* J Virol, 2005. **79**(3): p. 1871-87.
26. Koziel, M., Thio, CL, *Mandell, Douglas, and Bennett's Principles and Practice of Infectious Diseases*. 7th ed, ed. G. Mandell, Bennett, J, Dolin, R. Vol. Volume 1. Churchill Livingstone Elsevier.
27. Kuipery, A., A.J. Gehring, and M. Isogawa, *Mechanisms of HBV immune evasion.* Antiviral Res, 2020. **179**: p. 104816.
28. Milich, D. and T.J. Liang, *Exploring the biological basis of hepatitis B e antigen in hepatitis B virus infection.* Hepatology, 2003. **38**(5): p. 1075-86.
29. Mitra, B., et al., *Hepatitis B Virus Precore Protein p22 Inhibits Alpha Interferon Signaling by Blocking STAT Nuclear Translocation.* J Virol, 2019. **93**(13).
30. Heijtink, R.A., et al., *Interferon-alpha therapy for chronic hepatitis B: early response related to pre-treatment changes in viral replication.* J Med Virol, 2001. **63**(3): p. 217-9.
31. Eble, B.E., V.R. Lingappa, and D. Ganem, *The N-terminal (pre-S2) domain of a hepatitis B virus surface glycoprotein is translocated across membranes by downstream signal sequences.* J Virol, 1990. **64**(3): p. 1414-9.
32. Seeger, C. and J.A. Sohn, *Targeting Hepatitis B Virus With CRISPR/Cas9.* Mol Ther Nucleic Acids, 2014. **3**: p. e216.
33. Clippinger, A.J., T.L. Gearhart, and M.J. Bouchard, *Hepatitis B virus X protein modulates apoptosis in primary rat hepatocytes by regulating both NF-kappaB and the mitochondrial permeability transition pore.* J Virol, 2009. **83**(10): p. 4718-31.
34. Tanaka, Y., et al., *The hepatitis B virus X protein enhances AP-1 activation through interaction with Jab1.* Oncogene, 2006. **25**(4): p. 633-42.
35. Lucito, R. and R.J. Schneider, *Hepatitis B virus X protein activates transcription factor NF-kappa B without a requirement for protein kinase C.* J Virol, 1992. **66**(2): p. 983-91.
36. Um, H.R., et al., *Raf-1 and protein kinase B regulate cell survival through the activation of NF-kappaB in hepatitis B virus X-expressing cells.* Virus Res, 2007. **125**(1): p. 1-8.
37. Yun, C., et al., *NF-kappaB activation by hepatitis B virus X (HBx) protein shifts the cellular fate toward survival.* Cancer Lett, 2002. **184**(1): p. 97-104.

38. Hsieh, A., et al., *Hepatitis B viral X protein interacts with tumor suppressor adenomatous polyposis coli to activate Wnt/beta-catenin signaling.* Cancer Lett, 2011. **300**(2): p. 162-72.
39. Iyer, S. and J.D. Groopman, *Interaction of mutant hepatitis B X protein with p53 tumor suppressor protein affects both transcription and cell survival.* Mol Carcinog, 2011. **50**(12): p. 972-80.
40. Chung, T.W., Y.C. Lee, and C.H. Kim, *Hepatitis B viral HBx induces matrix metalloproteinase-9 gene expression through activation of ERK and PI-3K/AKT pathways: involvement of invasive potential.* FASEB J, 2004. **18**(10): p. 1123-5.
41. Lamontagne, R.J., S. Bagga, and M.J. Bouchard, *Hepatitis B virus molecular biology and pathogenesis.* Hepatoma Res, 2016. **2**: p. 163-186.
42. Liu, C.J., et al., *Role of hepatitis B viral load and basal core promoter mutation in hepatocellular carcinoma in hepatitis B carriers.* J Infect Dis, 2006. **193**(9): p. 1258-65.
43. Schaefer, S., *Hepatitis B virus taxonomy and hepatitis B virus genotypes.* World J Gastroenterol, 2007. **13**(1): p. 14-21.
44. Fletcher, G.J., C.E. Eapen, and P. Abraham, *Hepatitis B genotyping: The utility for the clinicians.* Indian J Gastroenterol, 2019.
45. Velkov, S., et al., *The Global Hepatitis B Virus Genotype Distribution Approximated from Available Genotyping Data.* Genes (Basel), 2018. **9**(10).
46. Yu, M.W., et al., *Hepatitis B virus genotype and DNA level and hepatocellular carcinoma: a prospective study in men.* J Natl Cancer Inst, 2005. **97**(4): p. 265-72.
47. Toan, N.L., et al., *Impact of the hepatitis B virus genotype and genotype mixtures on the course of liver disease in Vietnam.* Hepatology, 2006. **43**(6): p. 1375-84.
48. Chu, C.J., M. Hussain, and A.S. Lok, *Hepatitis B virus genotype B is associated with earlier HBeAg seroconversion compared with hepatitis B virus genotype C.* Gastroenterology, 2002. **122**(7): p. 1756-62.
49. Kumar, A., et al., *Hepatitis B virus genotype A is more often associated with severe liver disease in northern India than is genotype D.* Indian J Gastroenterol, 2005. **24**(1): p. 19-22.
50. Sanchez-Tapias, J.M., et al., *Influence of hepatitis B virus genotype on the long-term outcome of chronic hepatitis B in western patients.* Gastroenterology, 2002. **123**(6): p. 1848-56.
51. Kao, J.H., et al., *Hepatitis B genotypes and the response to interferon therapy.* J Hepatol, 2000. **33**(6): p. 998-1002.
52. Chu, R.H., et al., *Influence of HLA-DRB1 alleles and HBV genotypes on interferon-alpha therapy for chronic hepatitis B.* World J Gastroenterol, 2005. **11**(30): p. 4753-7.
53. Erhardt, A., et al., *Response to interferon alfa is hepatitis B virus genotype dependent: genotype A is more sensitive to interferon than genotype D.* Gut, 2005. **54**(7): p. 1009-13.
54. Koedijk, F.D., et al., *[Hepatitis B virus transmission patterns in the Netherlands, 2004].* Ned Tijdschr Geneeskd, 2008. **152**(49): p. 2673-80.
55. Alavian, S.M., et al., *Preliminary report of hepatitis B virus genotype prevalence in Iran.* World J Gastroenterol, 2006. **12**(32): p. 5211-3.
56. Hou, J., Z. Liu, and F. Gu, *Epidemiology and Prevention of Hepatitis B Virus Infection.* Int J Med Sci, 2005. **2**(1): p. 50-57.

57. Komatsu, H., et al., *Cellular immunity in children with successful immunoprophylactic treatment for mother-to-child transmission of hepatitis B virus.* BMC Infect Dis, 2010. **10**: p. 103.
58. Koumbi, L., et al., *Hepatitis B-specific T helper cell responses in uninfected infants born to HBsAg+/HBeAg- mothers.* Cell Mol Immunol, 2010. **7**(6): p. 454-8.
59. Wang, W.T., et al., *Immune response pattern varies with the natural history of chronic hepatitis B.* World J Gastroenterol, 2019. **25**(16): p. 1950-1963.
60. Maini, M.K., et al., *The role of virus-specific CD8(+) cells in liver damage and viral control during persistent hepatitis B virus infection.* J Exp Med, 2000. **191**(8): p. 1269-80.
61. Vanwolleghem, T., et al., *Re-evaluation of hepatitis B virus clinical phases by systems biology identifies unappreciated roles for the innate immune response and B cells.* Hepatology, 2015. **62**(1): p. 87-100.
62. Chang, M.H., et al., *Prospective study of asymptomatic HBsAg carrier children infected in the perinatal period: clinical and liver histologic studies.* Hepatology, 1988. **8**(2): p. 374-7.
63. Lee, H.W., et al., *Comparison between chronic hepatitis B patients with untreated immune-tolerant phase vs. those with virological response by antivirals.* Sci Rep, 2019. **9**(1): p. 2508.
64. Saxena, R., et al., *Association of interleukin-10 with hepatitis B virus (HBV) mediated disease progression in Indian population.* Indian J Med Res, 2014. **139**(5): p. 737-45.
65. Wu, J.F., et al., *Serum levels of interleukin-10 and interleukin-12 predict early, spontaneous hepatitis B virus e antigen seroconversion.* Gastroenterology, 2010. **138**(1): p. 165-72 e1-3.
66. Wu, J.F., et al., *The effects of cytokines on spontaneous hepatitis B surface antigen seroconversion in chronic hepatitis B virus infection.* J Immunol, 2015. **194**(2): p. 690-6.
67. Chou, H.H., et al., *Age-related immune clearance of hepatitis B virus infection requires the establishment of gut microbiota.* Proc Natl Acad Sci U S A, 2015. **112**(7): p. 2175-80.
68. Wu, J.F., et al., *Suppression of furin by interferon-gamma and the impact on hepatitis B virus antigen biosynthesis in human hepatocytes.* Am J Pathol, 2012. **181**(1): p. 19-25.
69. Muhlbauer, M., et al., *PD-L1 is induced in hepatocytes by viral infection and by interferon-alpha and -gamma and mediates T cell apoptosis.* J Hepatol, 2006. **45**(4): p. 520-8.
70. Wu, J.F., et al., *Predictive effect of serial serum alanine aminotransferase levels on spontaneous HBeAg seroconversion in chronic genotype B and C HBV-infected children.* J Pediatr Gastroenterol Nutr, 2012. **54**(1): p. 97-100.
71. Wu, J.F., et al., *Effect of puberty onset on spontaneous hepatitis B virus e antigen seroconversion in men.* Gastroenterology, 2010. **138**(3): p. 942-8 e1.
72. Hazeldine, J., W. Arlt, and J.M. Lord, *Dehydroepiandrosterone as a regulator of immune cell function.* J Steroid Biochem Mol Biol, 2010. **120**(2-3): p. 127-36.
73. Fattovich, G., et al., *Long-term outcome of chronic hepatitis B in Caucasian patients: mortality after 25 years.* Gut, 2008. **57**(1): p. 84-90.
74. Liaw, Y.F., M.R. Brunetto, and S. Hadziyannis, *The natural history of chronic HBV infection and geographical differences.* Antivir Ther, 2010. **15 Suppl 3**: p. 25-33.

75. Chen, C.H., et al., *Clinical significance of hepatitis B virus (HBV) genotypes and precore and core promoter mutations affecting HBV e antigen expression in Taiwan.* J Clin Microbiol, 2005. **43**(12): p. 6000-6.
76. Fang, Z.L., et al., *HBV A1762T, G1764A mutations are a valuable biomarker for identifying a subset of male HBsAg carriers at extremely high risk of hepatocellular carcinoma: a prospective study.* Am J Gastroenterol, 2008. **103**(9): p. 2254-62.
77. Hsu, Y.S., et al., *Long-term outcome after spontaneous HBeAg seroconversion in patients with chronic hepatitis B.* Hepatology, 2002. **35**(6): p. 1522-7.
78. Yang, H.C., Y.F. Shih, and C.J. Liu, *Viral Factors Affecting the Clinical Outcomes of Chronic Hepatitis B.* J Infect Dis, 2017. **216**(suppl_8): p. S757-S764.
79. Kikkert, M., *Innate Immune Evasion by Human Respiratory RNA Viruses.* J Innate Immun, 2020. **12**(1): p. 4-20.
80. Li, M., et al., *Kupffer Cells Support Hepatitis B Virus-Mediated CD8+ T Cell Exhaustion via Hepatitis B Core Antigen-TLR2 Interactions in Mice.* J Immunol, 2015. **195**(7): p. 3100-9.
81. Sato, S., et al., *The RNA sensor RIG-I dually functions as an innate sensor and direct antiviral factor for hepatitis B virus.* Immunity, 2015. **42**(1): p. 123-32.
82. Cui, X., et al., *Viral DNA-Dependent Induction of Innate Immune Response to Hepatitis B Virus in Immortalized Mouse Hepatocytes.* J Virol, 2016. **90**(1): p. 486-96.
83. Guidotti, L.G., et al., *Viral clearance without destruction of infected cells during acute HBV infection.* Science, 1999. **284**(5415): p. 825-9.
84. Webster, G.J., et al., *Incubation phase of acute hepatitis B in man: dynamic of cellular immune mechanisms.* Hepatology, 2000. **32**(5): p. 1117-24.
85. Thimme, R., et al., *CD8(+) T cells mediate viral clearance and disease pathogenesis during acute hepatitis B virus infection.* J Virol, 2003. **77**(1): p. 68-76.
86. Ferrari, C., et al., *Cellular immune response to hepatitis B virus-encoded antigens in acute and chronic hepatitis B virus infection.* J Immunol, 1990. **145**(10): p. 3442-9.
87. Dunn, C., et al., *Temporal analysis of early immune responses in patients with acute hepatitis B virus infection.* Gastroenterology, 2009. **137**(4): p. 1289-300.
88. Peppa, D., et al., *Up-regulation of a death receptor renders antiviral T cells susceptible to NK cell-mediated deletion.* J Exp Med, 2013. **210**(1): p. 99-114.
89. Mutz, P., et al., *HBV Bypasses the Innate Immune Response and Does Not Protect HCV From Antiviral Activity of Interferon.* Gastroenterology, 2018. **154**(6): p. 1791-1804 e22.
90. Khan, M., et al., *Hepatitis B Virus-Induced Parkin-Dependent Recruitment of Linear Ubiquitin Assembly Complex (LUBAC) to Mitochondria and Attenuation of Innate Immunity.* PLoS Pathog, 2016. **12**(6): p. e1005693.
91. Wang, S., et al., *Hepatitis B virus surface antigen selectively inhibits TLR2 ligand-induced IL-12 production in monocytes/macrophages by interfering with JNK activation.* J Immunol, 2013. **190**(10): p. 5142-51.
92. Chen, J., et al., *Hepatitis B virus polymerase impairs interferon-alpha-induced STA T activation through inhibition of importin-alpha5 and protein kinase C-delta.* Hepatology, 2013. **57**(2): p. 470-82.
93. Liu, S., et al., *Human hepatitis B virus surface and e antigens inhibit major vault protein signaling in interferon induction pathways.* J Hepatol, 2015. **62**(5): p. 1015-23.

94. Miyakawa, K., et al., *Molecular dissection of HBV evasion from restriction factor tetherin: A new perspective for antiviral cell therapy.* Oncotarget, 2015. **6**(26): p. 21840-52.
95. Wang, H. and W.S. Ryu, *Hepatitis B virus polymerase blocks pattern recognition receptor signaling via interaction with DDX3: implications for immune evasion.* PLoS Pathog, 2010. **6**(7): p. e1000986.
96. Liu, D., et al., *Hepatitis B virus polymerase suppresses NF-kappaB signaling by inhibiting the activity of IKKs via interaction with Hsp90beta.* PLoS One, 2014. **9**(3): p. e91658.
97. Wan, Y., et al., *Inducible Rubicon facilitates viral replication by antagonizing interferon production.* Cell Mol Immunol, 2017. **14**(7): p. 607-620.
98. Zhang, Q. and G. Cao, *Genotypes, mutations, and viral load of hepatitis B virus and the risk of hepatocellular carcinoma: HBV properties and hepatocarcinogenesis.* Hepat Mon, 2011. **11**(2): p. 86-91.
99. Zhou, Y., et al., *Hepatitis B virus protein X-induced expression of the CXC chemokine IP-10 is mediated through activation of NF-kappaB and increases migration of leukocytes.* J Biol Chem, 2010. **285**(16): p. 12159-68.
100. Zheng, F., et al., *[Study on tumor formation of hepatocyte transformed by hepatitis B virus X gene in nude mice.].* Zhonghua Gan Zang Bing Za Zhi, 2009. **17**(2): p. 117-9.
101. Yoo, Y.D., et al., *Regulation of transforming growth factor-beta 1 expression by the hepatitis B virus (HBV) X transactivator. Role in HBV pathogenesis.* J Clin Invest, 1996. **97**(2): p. 388-95.
102. Xie, H., et al., *Potent cell growth inhibitory effects in hepatitis B virus X protein positive hepatocellular carcinoma cells by the selective cyclooxygenase-2 inhibitor celecoxib.* Mol Carcinog, 2009. **48**(1): p. 56-65.
103. Wu, S., et al., *Cooperative effects of hepatitis B virus and TNF may play important roles in the activation of metabolic pathways through the activation of NF-kappaB.* Int J Mol Med, 2016. **38**(2): p. 475-81.
104. Wang, Y.J., et al., *[The studies of hepatitis B virus X gene induces oval cell malignant transformation].* Zhonghua Wai Ke Za Zhi, 2009. **47**(18): p. 1410-4.
105. Urban, S., et al., *Isolation and molecular characterization of hepatitis B virus X-protein from a baculovirus expression system.* Hepatology, 1997. **26**(4): p. 1045-53.
106. Shin, E.C., et al., *Expression of fas ligand in human hepatoma cell lines: role of hepatitis-B virus X (HBX) in induction of Fas ligand.* Int J Cancer, 1999. **82**(4): p. 587-91.
107. Shi, T., et al., *Downregulation of miR-200a-3p induced by hepatitis B Virus X (HBx) Protein promotes cell proliferation and invasion in HBV-infection-associated hepatocarcinoma.* Pathol Res Pract, 2017. **213**(12): p. 1464-1469.
108. Feitelson, M.A., *Parallel epigenetic and genetic changes in the pathogenesis of hepatitis virus-associated hepatocellular carcinoma.* Cancer Lett, 2006. **239**(1): p. 10-20.
109. Kremsdorf, D., et al., *Hepatitis B virus-related hepatocellular carcinoma: paradigms for viral-related human carcinogenesis.* Oncogene, 2006. **25**(27): p. 3823-33.
110. Zhang, X., H. Zhang, and L. Ye, *Effects of hepatitis B virus X protein on the development of liver cancer.* J Lab Clin Med, 2006. **147**(2): p. 58-66.

111. Shih, W.L., et al., *Hepatitis B virus X protein inhibits transforming growth factor-beta -induced apoptosis through the activation of phosphatidylinositol 3-kinase pathway.* J Biol Chem, 2000. **275**(33): p. 25858-64.
112. Cha, M.Y., et al., *Hepatitis B virus X protein is essential for the activation of Wnt/beta-catenin signaling in hepatoma cells.* Hepatology, 2004. **39**(6): p. 1683-93.
113. Merle, P., et al., *Oncogenic role of the frizzled-7/beta-catenin pathway in hepatocellular carcinoma.* J Hepatol, 2005. **43**(5): p. 854-62.
114. Benn, J. and R.J. Schneider, *Hepatitis B virus HBx protein deregulates cell cycle checkpoint controls.* Proc Natl Acad Sci U S A, 1995. **92**(24): p. 11215-9.
115. Ma, J., et al., *The role of hepatitis B virus X protein is related to its differential intracellular localization.* Acta Biochim Biophys Sin (Shanghai), 2011. **43**(8): p. 583-8.
116. Cong, Y.S., et al., *The hepatitis B virus X-associated protein, XAP3, is a protein kinase C-binding protein.* J Biol Chem, 1997. **272**(26): p. 16482-9.
117. Tian, Y., et al., *HBx promotes cell proliferation by disturbing the cross-talk between miR-181a and PTEN.* Sci Rep, 2017. **7**: p. 40089.
118. Elmore, L.W., et al., *Hepatitis B virus X protein and p53 tumor suppressor interactions in the modulation of apoptosis.* Proc Natl Acad Sci U S A, 1997. **94**(26): p. 14707-12.
119. Matsubara, K. and T. Tokino, *Integration of hepatitis B virus DNA and its implications for hepatocarcinogenesis.* Mol Biol Med, 1990. **7**(3): p. 243-60.
120. Bonilla Guerrero, R. and L.R. Roberts, *The role of hepatitis B virus integrations in the pathogenesis of human hepatocellular carcinoma.* J Hepatol, 2005. **42**(5): p. 760-77.
121. Yamashita, T., et al., *Activation of hepatic stem cell marker EpCAM by Wnt-beta-catenin signaling in hepatocellular carcinoma.* Cancer Res, 2007. **67**(22): p. 10831-9.
122. Yamashita, T., et al., *EpCAM-positive hepatocellular carcinoma cells are tumor-initiating cells with stem/progenitor cell features.* Gastroenterology, 2009. **136**(3): p. 1012-24.
123. Clippinger, A.J. and M.J. Bouchard, *Hepatitis B virus HBx protein localizes to mitochondria in primary rat hepatocytes and modulates mitochondrial membrane potential.* J Virol, 2008. **82**(14): p. 6798-811.
124. Zhang, M.Y., et al., *Systematic review with network meta-analysis: Comparative efficacy of oral nucleos(t)ide analogues for the prevention of chemotherapy-induced hepatitis B virus reactivation.* Oncotarget, 2016. **7**(21): p. 30642-58.
125. Girones, R. and R.H. Miller, *Mutation rate of the hepadnavirus genome.* Virology, 1989. **170**(2): p. 595-7.
126. Zoulim, F., *Antiviral therapy of chronic hepatitis B: can we clear the virus and prevent drug resistance?* Antivir Chem Chemother, 2004. **15**(6): p. 299-305.
127. Menendez-Arias, L., M. Alvarez, and B. Pacheco, *Nucleoside/nucleotide analog inhibitors of hepatitis B virus polymerase: mechanism of action and resistance.* Curr Opin Virol, 2014. **8**: p. 1-9.
128. Menendez-Arias, L., *Molecular basis of human immunodeficiency virus type 1 drug resistance: overview and recent developments.* Antiviral Res, 2013. **98**(1): p. 93-120.
129. Wang, X., et al., *Nucleos(t)ide Analogues for Reducing Hepatocellular Carcinoma in Chronic Hepatitis B Patients: A Systematic Review and Meta-Analysis.* Gut Liver, 2020. **14**(2): p. 232-247.
130. Vittal, A., et al., *Systematic review with meta-analysis: the impact of functional cure on clinical outcomes in patients with chronic hepatitis B.* Aliment Pharmacol Ther, 2022. **55**(1): p. 8-25.

131. Buster, E.H., et al., *Factors that predict response of patients with hepatitis B e antigen-positive chronic hepatitis B to peginterferon-alfa.* Gastroenterology, 2009. **137**(6): p. 2002-9.
132. Lok, A.S., et al., *A controlled trial of interferon with or without prednisone priming for chronic hepatitis B.* Gastroenterology, 1992. **102**(6): p. 2091-7.
133. Belloni, L., et al., *IFN-alpha inhibits HBV transcription and replication in cell culture and in humanized mice by targeting the epigenetic regulation of the nuclear cccDNA minichromosome.* J Clin Invest, 2012. **122**(2): p. 529-37.
134. Papatheodoridis, G.V., et al., *Risk of hepatocellular carcinoma in chronic hepatitis B: assessment and modification with current antiviral therapy.* J Hepatol, 2015. **62**(4): p. 956-67.
135. Blank, A., et al., *The NTCP-inhibitor Myrcludex B: Effects on Bile Acid Disposition and Tenofovir Pharmacokinetics.* Clin Pharmacol Ther, 2018. **103**(2): p. 341-348.
136. Yuen, M.F., et al., *RNA Interference Therapy with ARC-520 Results in Prolonged HBsAg Response in Patients with Chronic Hepatitis B Infection.* Hepatology, 2019.
137. Thi, E.P., et al., *ARB-1740, a RNA Interference Therapeutic for Chronic Hepatitis B Infection.* ACS Infect Dis, 2019. **5**(5): p. 725-737.
138. Ye, X., et al., *Hepatitis B Virus Therapeutic Agent ARB-1740 Has Inhibitory Effect on Hepatitis Delta Virus in a New Dually-Infected Humanized Mouse Model.* ACS Infect Dis, 2019. **5**(5): p. 738-749.
139. Rat, V., et al., *BAY 41-4109-mediated aggregation of assembled and misassembled HBV capsids in cells revealed by electron microscopy.* Antiviral Res, 2019. **169**: p. 104557.
140. Zhao, N., et al., *A First-in-Human Trial of GLS4, a Novel Inhibitor of Hepatitis B Virus Capsid Assembly, following Single- and Multiple-Ascending-Oral-Dose Studies with or without Ritonavir in Healthy Adult Volunteers.* Antimicrob Agents Chemother, 2019. **64**(1).
141. Korolowicz, K.E., et al., *Antiviral Efficacy and Host Innate Immunity Associated with SB 9200 Treatment in the Woodchuck Model of Chronic Hepatitis B.* PLoS One, 2016. **11**(8): p. e0161313.
142. Khan, A., et al., *NOD2/RIG-I Activating Inarigivir Adjuvant Enhances the Efficacy of BCG Vaccine Against Tuberculosis in Mice.* Front Immunol, 2020. **11**: p. 592333.
143. Jones, M., et al., *SB 9200, a novel agonist of innate immunity, shows potent antiviral activity against resistant HCV variants.* J Med Virol, 2017. **89**(9): p. 1620-1628.
144. Gane, E., et al., *Anti-PD-1 blockade with nivolumab with and without therapeutic vaccination for virally suppressed chronic hepatitis B: A pilot study.* J Hepatol, 2019. **71**(5): p. 900-907.
145. Phillips, S., et al., *Peg-Interferon Lambda Treatment Induces Robust Innate and Adaptive Immunity in Chronic Hepatitis B Patients.* Front Immunol, 2017. **8**: p. 621.
146. Martin, P., et al., *TG1050, an immunotherapeutic to treat chronic hepatitis B, induces robust T cells and exerts an antiviral effect in HBV-persistent mice.* Gut, 2015. **64**(12): p. 1961-71.
147. Yan, H. and W. Li, *Sodium taurocholate cotransporting polypeptide acts as a receptor for hepatitis B and D virus.* Dig Dis, 2015. **33**(3): p. 388-96.
148. Hantz, O., et al., *Persistence of the hepatitis B virus covalently closed circular DNA in HepaRG human hepatocyte-like cells.* J Gen Virol, 2009. **90**(Pt 1): p. 127-35.

149. Yang, D., et al., *Complete replication of hepatitis B virus and hepatitis C virus in a newly developed hepatoma cell line.* Proc Natl Acad Sci U S A, 2014. **111**(13): p. E1264-73.
150. Huang, H.C., et al., *Entry of hepatitis B virus into immortalized human primary hepatocytes by clathrin-dependent endocytosis.* J Virol, 2012. **86**(17): p. 9443-53.
151. Yu, S., et al., *Hepatitis B virus polymerase inhibits RIG-I- and Toll-like receptor 3-mediated beta interferon induction in human hepatocytes through interference with interferon regulatory factor 3 activation and dampening of the interaction between TBK1/IKKepsilon and DDX3.* J Gen Virol, 2010. **91**(Pt 8): p. 2080-90.
152. Galle, P.R., et al., *In vitro experimental infection of primary human hepatocytes with hepatitis B virus.* Gastroenterology, 1994. **106**(3): p. 664-73.
153. Xu, S., et al., *Development of a 3D spheroid system of primary human hepatocytes that supports efficient HBV infection.* Journal of Viral Hepatitis, 2018. **25**: p. 191-191.
154. Thomas, H., *Viral hepatitis: A new model for HBV infection of primary human hepatocytes.* Nat Rev Gastroenterol Hepatol, 2018. **15**(4): p. 190.
155. Ortega-Prieto, A.M., et al., *"Liver-on-a-Chip" Cultures of Primary Hepatocytes and Kupffer Cells for Hepatitis B Virus Infection.* J Vis Exp, 2019(144).
156. Ortega-Prieto, A.M., et al., *3D microfluidic liver cultures as a physiological preclinical tool for hepatitis B virus infection.* Nat Commun, 2018. **9**(1): p. 682.
157. Kang, Y.B., et al., *Human Liver Sinusoid on a Chip for Hepatitis B Virus Replication Study.* Micromachines, 2017. **8**(1).
158. Xiang, C.G., et al., *Long-term functional maintenance of primary human hepatocytes in vitro.* Science, 2019. **364**(6438): p. 399-+.
159. Huch, M., et al., *Long-term culture of genome-stable bipotent stem cells from adult human liver.* Cell, 2015. **160**(1-2): p. 299-312.
160. Shlomai, A., et al., *Modeling host interactions with hepatitis B virus using primary and induced pluripotent stem cell-derived hepatocellular systems.* Proc Natl Acad Sci U S A, 2014. **111**(33): p. 12193-8.
161. Takebe, T., et al., *Generation of a vascularized and functional human liver from an iPSC-derived organ bud transplant.* Nat Protoc, 2014. **9**(2): p. 396-409.
162. Sakurai, F., et al., *Human induced-pluripotent stem cell-derived hepatocyte-like cells as an in vitro model of human hepatitis B virus infection.* Sci Rep, 2017. **7**: p. 45698.
163. Kaneko, S., et al., *Human induced pluripotent stem cell-derived hepatic cell lines as a new model for host interaction with hepatitis B virus.* Sci Rep, 2016. **6**: p. 29358.
164. Xia, Y., et al., *Human stem cell-derived hepatocytes as a model for hepatitis B virus infection, spreading and virus-host interactions.* J Hepatol, 2017. **66**(3): p. 494-503.
165. Nie, Y.Z., et al., *Recapitulation of hepatitis B virus-host interactions in liver organoids from human induced pluripotent stem cells.* Ebiomedicine, 2018. **35**: p. 114-123.
166. Fu, G.B., et al., *Expansion and differentiation of human hepatocyte-derived liver progenitor-like cells and their use for the study of hepatotropic pathogens.* Cell Research, 2019. **29**(1): p. 8-22.
167. Tascher, G., et al., *In-Depth Proteome Analysis Highlights HepaRG Cells as a Versatile Cell System Surrogate for Primary Human Hepatocytes.* Cells, 2019. **8**(2).
168. Mayati, A., et al., *Functional polarization of human hepatoma HepaRG cells in response to forskolin.* Sci Rep, 2018. **8**(1): p. 16115.

169. Mebarki, S., et al., *De novo HAPLN1 expression hallmarks Wnt-induced stem cell and fibrogenic networks leading to aggressive human hepatocellular carcinomas.* Oncotarget, 2016. **7**(26): p. 39026-39043.
170. Gerbal-Chaloin, S., et al., *The WNT/beta-catenin pathway is a transcriptional regulator of CYP2E1, CYP1A2, and aryl hydrocarbon receptor gene expression in primary human hepatocytes.* Mol Pharmacol, 2014. **86**(6): p. 624-34.
171. Cerec, V., et al., *Transdifferentiation of hepatocyte-like cells from the human hepatoma HepaRG cell line through bipotent progenitor.* Hepatology, 2007. **45**(4): p. 957-67.
172. Meier, A., et al., *Myristoylated PreS1-domain of the hepatitis B virus L-protein mediates specific binding to differentiated hepatocytes.* Hepatology, 2013. **58**(1): p. 31-42.
173. Yuan, L., et al., *Optimized HepaRG is a suitable cell source to generate the human liver chimeric mouse model for the chronic hepatitis B virus infection.* Emerg Microbes Infect, 2018. **7**(1): p. 144.
174. Ramaiahgari, S.C., et al., *From the Cover: Three-Dimensional (3D) HepaRG Spheroid Model With Physiologically Relevant Xenobiotic Metabolism Competence and Hepatocyte Functionality for Liver Toxicity Screening.* Toxicol Sci, 2017. **159**(1): p. 124-136.
175. Wisskirchen, K., et al., *Isolation and functional characterization of hepatitis B virus-specific T-cell receptors as new tools for experimental and clinical use.* PLoS One, 2017. **12**(8): p. e0182936.
176. Aly, H.H., et al., *Serum-derived hepatitis C virus infectivity in interferon regulatory factor-7-suppressed human primary hepatocytes.* J Hepatol, 2007. **46**(1): p. 26-36.
177. Huang, H.C., et al., *(-)-Epigallocatechin-3-gallate inhibits entry of hepatitis B virus into hepatocytes.* Antiviral Res, 2014. **111**: p. 100-11.
178. Noguchi, M. and S. Hirohashi, *Cell lines from non-neoplastic liver and hepatocellular carcinoma tissue from a single patient.* In Vitro Cell Dev Biol Anim, 1996. **32**(3): p. 135-7.
179. Hara, K., et al., *Lactoferrin inhibits hepatitis B virus infection in cultured human hepatocytes.* Hepatol Res, 2002. **24**(3): p. 228.
180. Meier-Stephenson, V., et al., *Identification and characterization of a G-quadruplex structure in the pre-core promoter region of hepatitis B virus covalently closed circular DNA.* J Biol Chem, 2021. **296**: p. 100589.
181. Michailidis, E., et al., *A robust cell culture system supporting the complete life cycle of hepatitis B virus.* Sci Rep, 2017. **7**(1): p. 16616.
182. Qiao, L., J. Sui, and G. Luo, *Robust Human and Murine Hepatocyte Culture Models of Hepatitis B Virus Infection and Replication.* J Virol, 2018. **92**(23).
183. Lempp, F.A., et al., *Hepatitis B Virus Infection of a Mouse Hepatic Cell Line Reconstituted with Human Sodium Taurocholate Cotransporting Polypeptide.* J Virol, 2016. **90**(9): p. 4827-4831.
184. Zhou, M., et al., *Productive HBV infection of well-differentiated, hNTCP-expressing human hepatoma-derived (Huh7) cells.* Virol Sin, 2017. **32**(6): p. 465-475.
185. Durantel, D. and F. Zoulim, *Going towards more relevant cell culture models to study the in vitro replication of serum-derived hepatitis C virus and virus/host cell interactions?* J Hepatol, 2007. **46**(1): p. 1-5.

186. Witt-Kehati, D., M. Bitton Alaluf, and A. Shlomai, *Advances and Challenges in Studying Hepatitis B Virus In Vitro.* Viruses, 2016. **8**(1).
187. Hu, H., et al., *Long-Term Expansion of Functional Mouse and Human Hepatocytes as 3D Organoids.* Cell, 2018. **175**(6): p. 1591-1606 e19.
188. de Wert, G. and C. Mummery, *Human embryonic stem cells: research, ethics and policy.* Hum Reprod, 2003. **18**(4): p. 672-82.
189. Bhattacharya, B., et al., *Comparison of the gene expression profile of undifferentiated human embryonic stem cell lines and differentiating embryoid bodies.* BMC Dev Biol, 2005. **5**: p. 22.
190. Hay, D.C., et al., *Efficient differentiation of hepatocytes from human embryonic stem cells exhibiting markers recapitulating liver development in vivo.* Stem Cells, 2008. **26**(4): p. 894-902.
191. Medine, C.N., et al., *Robust generation of hepatocyte-like cells from human embryonic stem cell populations.* J Vis Exp, 2011(56): p. e2969.
192. Payne, C.M., et al., *Persistence of functional hepatocyte-like cells in immune-compromised mice.* Liver Int, 2011. **31**(2): p. 254-62.
193. Sohn, Y.D., J.W. Han, and Y.S. Yoon, *Generation of induced pluripotent stem cells from somatic cells.* Prog Mol Biol Transl Sci, 2012. **111**: p. 1-26.
194. Ang, L.T., et al., *A Roadmap for Human Liver Differentiation from Pluripotent Stem Cells.* Cell Rep, 2018. **22**(8): p. 2190-2205.
195. Khetani, S.R. and S.N. Bhatia, *Microscale culture of human liver cells for drug development.* Nat Biotechnol, 2008. **26**(1): p. 120-6.
196. Schwartz, R.E., et al., *Modeling hepatitis C virus infection using human induced pluripotent stem cells.* Proc Natl Acad Sci U S A, 2012. **109**(7): p. 2544-8.
197. Hussein, S.M., et al., *Copy number variation and selection during reprogramming to pluripotency.* Nature, 2011. **471**(7336): p. 58-62.
198. Laurent, L.C., et al., *Dynamic changes in the copy number of pluripotency and cell proliferation genes in human ESCs and iPSCs during reprogramming and time in culture.* Cell Stem Cell, 2011. **8**(1): p. 106-18.
199. Meissner, A., et al., *Genome-scale DNA methylation maps of pluripotent and differentiated cells.* Nature, 2008. **454**(7205): p. 766-70.
200. Mikkelsen, T.S., et al., *Dissecting direct reprogramming through integrative genomic analysis.* Nature, 2008. **454**(7200): p. 49-55.
201. Ohnuki, M. and K. Takahashi, *Present and future challenges of induced pluripotent stem cells.* Philos Trans R Soc Lond B Biol Sci, 2015. **370**(1680): p. 20140367.
202. Prior, N., et al., *Lgr5(+) stem and progenitor cells reside at the apex of a heterogeneous embryonic hepatoblast pool.* Development, 2019. **146**(12).
203. Khan, Z., et al., *Immunohistochemical Analysis of the Stem Cell Marker LGR5 in Pediatric Liver Disease.* Pediatr Dev Pathol, 2017. **20**(1): p. 16-27.
204. Aloia, L., et al., *Epigenetic remodelling licences adult cholangiocytes for organoid formation and liver regeneration.* Nat Cell Biol, 2019. **21**(11): p. 1321-1333.
205. Russell, J.O. and S.P. Monga, *Wnt/beta-Catenin Signaling in Liver Development, Homeostasis, and Pathobiology.* Annu Rev Pathol, 2018. **13**: p. 351-378.
206. Takeishi, T., et al., *The role of Kupffer cells in liver regeneration.* Arch Histol Cytol, 1999. **62**(5): p. 413-22.
207. Xu, C.S., et al., *The role of Kupffer cells in rat liver regeneration revealed by cell-specific microarray analysis.* J Cell Biochem, 2012. **113**(1): p. 229-37.

208. Carmon, K.S., et al., *R-spondins function as ligands of the orphan receptors LGR4 and LGR5 to regulate Wnt/beta-catenin signaling.* Proc Natl Acad Sci U S A, 2011. **108**(28): p. 11452-7.
209. *GraphPad QuickCalcs*. 2018, GraphPad Software.
210. Fischer, A.H., et al., *Hematoxylin and eosin staining of tissue and cell sections.* CSH Protoc, 2008. **2008**: p. pdb prot4986.
211. Iwamoto, M., et al., *Evaluation and identification of hepatitis B virus entry inhibitors using HepG2 cells overexpressing a membrane transporter NTCP.* Biochem Biophys Res Commun, 2014. **443**(3): p. 808-13.
212. Blight, K.J., J.A. McKeating, and C.M. Rice, *Highly permissive cell lines for subgenomic and genomic hepatitis C virus RNA replication.* J Virol, 2002. **76**(24): p. 13001-14.
213. Li, J., et al., *Unusual Features of Sodium Taurocholate Cotransporting Polypeptide as a Hepatitis B Virus Receptor.* J Virol, 2016. **90**(18): p. 8302-13.
214. Sayers, E.W., et al., *Database resources of the National Center for Biotechnology Information.* Nucleic Acids Res, 2020. **48**(D1): p. D9-D16.
215. Hayer, J., et al., *HBVdb: a knowledge database for Hepatitis B Virus.* Nucleic Acids Res, 2013. **41**(Database issue): p. D566-70.
216. [cited 2020 10.01.2020]; Available from: http://www.endmemo.com/algebra/log2.php.
217. Singh, M., et al., *Quantitation of hepatitis B virus (HBV) covalently closed circular DNA (cccDNA) in the liver of HBV-infected patients by LightCycler real-time PCR.* J Virol Methods, 2004. **118**(2): p. 159-67.
218. S, A. *FastQC: A quality control tool for high throughput sequence data*. 2010; Available from: http://www.bioinformatics.babraham.ac.uk?/projects/fastqc/. Accessed 2019 Dec 9.
219. Ward, C., To, H, Pederson, SM, *ngsReports: An R Package for managing FastQC reports and other NGS related log files*. 2018, Unversity of Adelaide: bioRxiv.
220. Dobin, A., et al., *STAR: ultrafast universal RNA-seq aligner.* Bioinformatics, 2013. **29**(1): p. 15-21.
221. Ritchie, M.E., et al., *limma powers differential expression analyses for RNA-sequencing and microarray studies.* Nucleic Acids Res, 2015. **43**(7): p. e47.
222. Robinson, M.D., D.J. McCarthy, and G.K. Smyth, *edgeR: a Bioconductor package for differential expression analysis of digital gene expression data.* Bioinformatics, 2010. **26**(1): p. 139-40.
223. Law, C.W., et al., *voom: Precision weights unlock linear model analysis tools for RNA-seq read counts.* Genome Biol, 2014. **15**(2): p. R29.
224. DeLaForest, A., et al., *HNF4A Regulates the Formation of Hepatic Progenitor Cells from Human iPSC-Derived Endoderm by Facilitating Efficient Recruitment of RNA Pol II.* Genes (Basel), 2018. **10**(1).
225. Walesky, C. and U. Apte, *Role of hepatocyte nuclear factor 4alpha (HNF4alpha) in cell proliferation and cancer.* Gene Expr, 2015. **16**(3): p. 101-8.
226. Kawai, Y., et al., *Increased growth ability and pathogenicity of American- and Pacific-subtype Zika virus (ZIKV) strains compared with a Southeast Asian-subtype ZIKV strain.* PLoS Negl Trop Dis, 2019. **13**(6): p. e0007387.
227. Eyre, N.S., et al., *Identification of Estrogen Receptor Modulators as Inhibitors of Flavivirus Infection.* Antimicrob Agents Chemother, 2020. **64**(8).

228. Wu, X., et al., *Intrinsic Immunity Shapes Viral Resistance of Stem Cells.* Cell, 2018. **172**(3): p. 423-438 e25.
229. Zhu, C., et al., *Hepatitis B virus enhances interleukin-27 expression both in vivo and in vitro.* Clin Immunol, 2009. **131**(1): p. 92-7.
230. Burke, D.C., C.F. Graham, and J.M. Lehman, *Appearance of interferon inducibility and sensitivity during differentiation of murine teratocarcinoma cells in vitro.* Cell, 1978. **13**(2): p. 243-8.
231. Van der Hoek, K.H., et al., *Viperin is an important host restriction factor in control of Zika virus infection.* Sci Rep, 2017. **7**(1): p. 4475.
232. Helbig, K.J., et al., *Viperin is induced following dengue virus type-2 (DENV-2) infection and has anti-viral actions requiring the C-terminal end of viperin.* PLoS Negl Trop Dis, 2013. **7**(4): p. e2178.
233. Monson, E.A., et al., *Lipid droplet density alters the early innate immune response to viral infection.* PLoS One, 2018. **13**(1): p. e0190597.
234. Severgnini, M., et al., *A rapid two-step method for isolation of functional primary mouse hepatocytes: cell characterization and asialoglycoprotein receptor based assay development.* Cytotechnology, 2012. **64**(2): p. 187-95.
235. Klinger, W., T. Devereux, and J.R. Fouts, *Functional and structural zonal hepatocyte heterogeneity--dynamics and ontogenic development.* Exp Pathol, 1988. **35**(2): p. 69-91.
236. Fanning, A.S., C.M. Van Itallie, and J.M. Anderson, *Zonula occludens-1 and -2 regulate apical cell structure and the zonula adherens cytoskeleton in polarized epithelia.* Mol Biol Cell, 2012. **23**(4): p. 577-90.
237. Treyer, A. and A. Musch, *Hepatocyte polarity.* Compr Physiol, 2013. **3**(1): p. 243-87.
238. Dao Thi, V.L., et al., *Stem cell-derived polarized hepatocytes.* Nat Commun, 2020. **11**(1): p. 1677.
239. Subramanian, K., et al., *Spheroid culture for enhanced differentiation of human embryonic stem cells to hepatocyte-like cells.* Stem Cells Dev, 2014. **23**(2): p. 124-31.
240. Zhang, R.R., et al., *Efficient hepatic differentiation of human induced pluripotent stem cells in a three-dimensional microscale culture.* Methods Mol Biol, 2014. **1210**: p. 131-41.
241. Jia, Z., et al., *3D Culture System for Liver Tissue Mimicking Hepatic Plates for Improvement of Human Hepatocyte (C3A) Function and Polarity.* Biomed Res Int, 2020. **2020**: p. 6354183.
242. Irudayaswamy, A., et al., *Long-Term Fate of Human Fetal Liver Progenitor Cells Transplanted in Injured Mouse Livers.* Stem Cells, 2018. **36**(1): p. 103-113.
243. Kania, G., et al., *Generation of glycogen- and albumin-producing hepatocyte-like cells from embryonic stem cells.* Biol Chem, 2004. **385**(10): p. 943-53.
244. Yu, Y., et al., *Hepatocyte-like cells differentiated from human induced pluripotent stem cells: relevance to cellular therapies.* Stem Cell Res, 2012. **9**(3): p. 196-207.
245. Oesterheld, J.R., *A review of developmental aspects of cytochrome P450.* J Child Adolesc Psychopharmacol, 1998. **8**(3): p. 161-74.
246. Peter Guengerich, F. and N.G. Avadhani, *Roles of Cytochrome P450 in Metabolism of Ethanol and Carcinogens.* Adv Exp Med Biol, 2018. **1032**: p. 15-35.
247. Williams, J.A., et al., *Drug-drug interactions for UDP-glucuronosyltransferase substrates: a pharmacokinetic explanation for typically observed low exposure (AUCi/AUC) ratios.* Drug Metab Dispos, 2004. **32**(11): p. 1201-8.

248. Huch, M. and L. Dolle, *The plastic cellular states of liver cells: Are EpCAM and Lgr5 fit for purpose?* Hepatology, 2016. **64**(2): p. 652-62.
249. Vestentoft, P.S., *Development and molecular composition of the hepatic progenitor cell niche.* Dan Med J, 2013. **60**(5): p. B4640.
250. Ang, C.H., et al., *Lgr5(+) pericentral hepatocytes are self-maintained in normal liver regeneration and susceptible to hepatocarcinogenesis.* Proc Natl Acad Sci U S A, 2019. **116**(39): p. 19530-19540.
251. Huch, M., S.F. Boj, and H. Clevers, *Lgr5(+) liver stem cells, hepatic organoids and regenerative medicine.* Regen Med, 2013. **8**(4): p. 385-7.
252. Behari, J., *The Wnt/beta-catenin signaling pathway in liver biology and disease.* Expert Rev Gastroenterol Hepatol, 2010. **4**(6): p. 745-56.
253. Kim, K.A., et al., *R-Spondin family members regulate the Wnt pathway by a common mechanism.* Mol Biol Cell, 2008. **19**(6): p. 2588-96.
254. Binnerts, M.E., et al., *R-Spondin1 regulates Wnt signaling by inhibiting internalization of LRP6.* Proc Natl Acad Sci U S A, 2007. **104**(37): p. 14700-5.
255. Dubey, R., et al., *R-spondins engage heparan sulfate proteoglycans to potentiate WNT signaling.* Elife, 2020. **9**.
256. Lebensohn, A.M. and R. Rohatgi, *R-spondins can potentiate WNT signaling without LGRs.* Elife, 2018. **7**.
257. Zabulica, M., et al., *Guide to the Assessment of Mature Liver Gene Expression in Stem Cell-Derived Hepatocytes.* Stem Cells Dev, 2019. **28**(14): p. 907-919.
258. Yanger, K., et al., *Adult hepatocytes are generated by self-duplication rather than stem cell differentiation.* Cell Stem Cell, 2014. **15**(3): p. 340-349.
259. Rodrigo-Torres, D., et al., *The biliary epithelium gives rise to liver progenitor cells.* Hepatology, 2014. **60**(4): p. 1367-77.
260. Tschesche, H., et al., *Latent collagenase and gelatinase from human neutrophils and their activation.* Matrix Suppl, 1992. **1**: p. 245-55.
261. Chen, J., et al., *Matrix Metalloproteinase 9 Facilitates Hepatitis B Virus Replication through Binding with Type I Interferon (IFN) Receptor 1 To Repress IFN/JAK/STAT Signaling.* J Virol, 2017. **91**(8).
262. Calabro, S.R., et al., *Hepatocyte produced matrix metalloproteinases are regulated by CD147 in liver fibrogenesis.* PLoS One, 2014. **9**(7): p. e90571.
263. Fabregat, I., et al., *TGF-beta signalling and liver disease.* FEBS J, 2016. **283**(12): p. 2219-32.
264. Fabregat, I. and D. Caballero-Diaz, *Transforming Growth Factor-beta-Induced Cell Plasticity in Liver Fibrosis and Hepatocarcinogenesis.* Front Oncol, 2018. **8**: p. 357.
265. Urbaczek, A.C., et al., *Recombinant hepatitis C virus-envelope protein 2 interactions with low-density lipoprotein/CD81 receptors.* Mem Inst Oswaldo Cruz, 2015. **110**(4): p. 534-42.
266. Westhaus, S., et al., *Scavenger receptor class B member 1 (SCARB1) variants modulate hepatitis C virus replication cycle and viral load.* J Hepatol, 2017. **67**(2): p. 237-245.
267. Fan, H., et al., *Attachment and Postattachment Receptors Important for Hepatitis C Virus Infection and Cell-to-Cell Transmission.* J Virol, 2017. **91**(13).
268. Yamamoto, S., et al., *Lipoprotein Receptors Redundantly Participate in Entry of Hepatitis C Virus.* PLoS Pathog, 2016. **12**(5): p. e1005610.

269. Feneant, L., et al., *New Insights into the Understanding of Hepatitis C Virus Entry and Cell-to-Cell Transmission by Using the Ionophore Monensin A.* J Virol, 2015. **89**(16): p. 8346-64.
270. Douam, F., D. Lavillette, and F.L. Cosset, *The mechanism of HCV entry into host cells.* Prog Mol Biol Transl Sci, 2015. **129**: p. 63-107.
271. Guegan, J.P., C. Fremin, and G. Baffet, *The MAPK MEK1/2-ERK1/2 Pathway and Its Implication in Hepatocyte Cell Cycle Control.* Int J Hepatol, 2012. **2012**: p. 328372.
272. Park, S.J., et al., *Taxol induces caspase-10-dependent apoptosis.* J Biol Chem, 2004. **279**(49): p. 51057-67.
273. Dutton, A., L.S. Young, and P.G. Murray, *The role of cellular FLICE inhibitory protein (c-FLIP) in the pathogenesis and treatment of cancer.* Expert Opin Ther Targets, 2006. **10**(1): p. 27-35.
274. Ebert, G., et al., *Eliminating hepatitis B by antagonizing cellular inhibitors of apoptosis.* Proc Natl Acad Sci U S A, 2015. **112**(18): p. 5803-8.
275. Lian, J., et al., *Hepatitis B virus upregulates cellular inhibitor of apoptosis protein 2 expression via the PI3K/AKT/NF-kappaB signaling pathway in liver cancer.* Oncol Lett, 2020. **19**(3): p. 2043-2052.
276. Cocquerel, L., C. Voisset, and J. Dubuisson, *Hepatitis C virus entry: potential receptors and their biological functions.* J Gen Virol, 2006. **87**(Pt 5): p. 1075-84.
277. Belouzard, S., L. Cocquerel, and J. Dubuisson, *Hepatitis C virus entry into the hepatocyte.* Cent Eur J Biol, 2011. **6**(6): p. 933-945.
278. Taddei, M.L., et al., *Anoikis: an emerging hallmark in health and diseases.* J Pathol, 2012. **226**(2): p. 380-93.
279. Smets, F.N., et al., *Loss of cell anchorage triggers apoptosis (anoikis) in primary mouse hepatocytes.* Mol Genet Metab, 2002. **75**(4): p. 344-52.
280. Wang, X., et al., *Inhibition of caspase-mediated anoikis is critical for basic fibroblast growth factor-sustained culture of human pluripotent stem cells.* J Biol Chem, 2009. **284**(49): p. 34054-64.
281. Olson, M.F., *Applications for ROCK kinase inhibition.* Curr Opin Cell Biol, 2008. **20**(2): p. 242-8.
282. Koyanagi, M., et al., *Inhibition of the Rho/ROCK pathway reduces apoptosis during transplantation of embryonic stem cell-derived neural precursors.* J Neurosci Res, 2008. **86**(2): p. 270-80.
283. Godoy, P., et al., *Recent advances in 2D and 3D in vitro systems using primary hepatocytes, alternative hepatocyte sources and non-parenchymal liver cells and their use in investigating mechanisms of hepatotoxicity, cell signaling and ADME.* Arch Toxicol, 2013. **87**(8): p. 1315-530.
284. Friedman, S.L., *Hepatic stellate cells: protean, multifunctional, and enigmatic cells of the liver.* Physiol Rev, 2008. **88**(1): p. 125-72.
285. Gregory, S.H., et al., *IL-6 produced by Kupffer cells induces STAT protein activation in hepatocytes early during the course of systemic listerial infections.* J Immunol, 1998. **160**(12): p. 6056-61.
286. Roberts, R.A., et al., *Role of the Kupffer cell in mediating hepatic toxicity and carcinogenesis.* Toxicol Sci, 2007. **96**(1): p. 2-15.
287. Henkel, J., et al., *Oncostatin M produced in Kupffer cells in response to PGE2: possible contributor to hepatic insulin resistance and steatosis.* Lab Invest, 2011. **91**(7): p. 1107-17.

288. De Bleser, P.J., et al., *Transforming growth factor-beta gene expression in normal and fibrotic rat liver.* J Hepatol, 1997. **26**(4): p. 886-93.
289. Boulter, L., et al., *Macrophage-derived Wnt opposes Notch signaling to specify hepatic progenitor cell fate in chronic liver disease.* Nat Med, 2012. **18**(4): p. 572-9.
290. Bussolino, F., et al., *Hepatocyte growth factor is a potent angiogenic factor which stimulates endothelial cell motility and growth.* J Cell Biol, 1992. **119**(3): p. 629-41.
291. Chen, C., et al., *Biotechnology Challenges to In Vitro Maturation of Hepatic Stem Cells.* Gastroenterology, 2018. **154**(5): p. 1258-1272.
292. Levy, G., et al., *Long-term culture and expansion of primary human hepatocytes.* Nat Biotechnol, 2015. **33**(12): p. 1264-1271.
293. Hoehme, S., et al., *Prediction and validation of cell alignment along microvessels as order principle to restore tissue architecture in liver regeneration.* Proc Natl Acad Sci U S A, 2010. **107**(23): p. 10371-6.
294. Gallin, W.J., G.M. Edelman, and B.A. Cunningham, *Characterization of L-CAM, a major cell adhesion molecule from embryonic liver cells.* Proc Natl Acad Sci U S A, 1983. **80**(4): p. 1038-42.
295. Yeaman, C., K.K. Grindstaff, and W.J. Nelson, *New perspectives on mechanisms involved in generating epithelial cell polarity.* Physiol Rev, 1999. **79**(1): p. 73-98.
296. Hua, M., et al., *Molecular mechanisms regulating the establishment of hepatocyte polarity during human hepatic progenitor cell differentiation into a functional hepatocyte-like phenotype.* J Cell Sci, 2012. **125**(Pt 23): p. 5800-10.
297. Nelson, W.J., *Adaptation of core mechanisms to generate cell polarity.* Nature, 2003. **422**(6933): p. 766-74.
298. Wang, L. and J.L. Boyer, *The maintenance and generation of membrane polarity in hepatocytes.* Hepatology, 2004. **39**(4): p. 892-9.
299. Tilles, A.W., et al., *Effects of oxygenation and flow on the viability and function of rat hepatocytes cocultured in a microchannel flat-plate bioreactor.* Biotechnol Bioeng, 2001. **73**(5): p. 379-89.
300. Seeger, C. and W.S. Mason, *Molecular biology of hepatitis B virus infection.* Virology, 2015. **479-480**: p. 672-86.
301. Schulze, A., P. Gripon, and S. Urban, *Hepatitis B virus infection initiates with a large surface protein-dependent binding to heparan sulfate proteoglycans.* Hepatology, 2007. **46**(6): p. 1759-68.
302. Verrier, E.R., et al., *A targeted functional RNA interference screen uncovers glypican 5 as an entry factor for hepatitis B and D viruses.* Hepatology, 2016. **63**(1): p. 35-48.
303. Le Seyec, J., et al., *Infection process of the hepatitis B virus depends on the presence of a defined sequence in the pre-S1 domain.* J Virol, 1999. **73**(3): p. 2052-7.
304. Blanchet, M. and C. Sureau, *Infectivity determinants of the hepatitis B virus pre-S domain are confined to the N-terminal 75 amino acid residues.* J Virol, 2007. **81**(11): p. 5841-9.
305. Bruss, V., et al., *Myristylation of the large surface protein is required for hepatitis B virus in vitro infectivity.* Virology, 1996. **218**(2): p. 396-9.
306. Gripon, P., et al., *Myristylation of the hepatitis B virus large surface protein is essential for viral infectivity.* Virology, 1995. **213**(2): p. 292-9.
307. Bae, S.H., et al., *L-ascorbic acid 2-phosphate and fibroblast growth factor-2 treatment maintains differentiation potential in bone marrow-derived mesenchymal*

stem cells through expression of hepatocyte growth factor. Growth Factors, 2015. **33**(2): p. 71-8.
308. Fujisawa, K., et al., *Evaluation of the effects of ascorbic acid on metabolism of human mesenchymal stem cells.* Stem Cell Res Ther, 2018. **9**(1): p. 93.
309. Magner, N.L., et al., *Insulin and IGFs enhance hepatocyte differentiation from human embryonic stem cells via the PI3K/AKT pathway.* Stem Cells, 2013. **31**(10): p. 2095-103.
310. Varghese, D.S., T.T. Alawathugoda, and S.A. Ansari, *Fine Tuning of Hepatocyte Differentiation from Human Embryonic Stem Cells: Growth Factor vs. Small Molecule-Based Approaches.* Stem Cells Int, 2019. **2019**: p. 5968236.
311. Ayatollahi, M., et al., *Hepatogenic differentiation of mesenchymal stem cells induced by insulin like growth factor-I.* World J Stem Cells, 2011. **3**(12): p. 113-21.
312. Co, J.Y., et al., *Controlling Epithelial Polarity: A Human Enteroid Model for Host-Pathogen Interactions.* Cell Rep, 2019. **26**(9): p. 2509-2520 e4.
313. Appelman, M.D., et al., *N-Glycosylation of the Na+-Taurocholate Cotransporting Polypeptide (NTCP) Determines Its Trafficking and Stability and Is Required for Hepatitis B Virus Infection.* PLoS One, 2017. **12**(1): p. e0170419.
314. Miyakawa, K., et al., *Development of a cell-based assay to identify hepatitis B virus entry inhibitors targeting the sodium taurocholate cotransporting polypeptide.* Oncotarget, 2018. **9**(34): p. 23681-23694.
315. Yan, H., et al., *Molecular determinants of hepatitis B and D virus entry restriction in mouse sodium taurocholate cotransporting polypeptide.* J Virol, 2013. **87**(14): p. 7977-91.
316. Passioura, T., et al., *De Novo Macrocyclic Peptide Inhibitors of Hepatitis B Virus Cellular Entry.* Cell Chem Biol, 2018. **25**(7): p. 906-915 e5.
317. Gripon, P., C. Diot, and C. Guguen-Guillouzo, *Reproducible high level infection of cultured adult human hepatocytes by hepatitis B virus: effect of polyethylene glycol on adsorption and penetration.* Virology, 1993. **192**(2): p. 534-40.
318. Konig, A., et al., *Efficient long-term amplification of hepatitis B virus isolates after infection of slow proliferating HepG2-NTCP cells.* J Hepatol, 2019. **71**(2): p. 289-300.
319. Yan, R., et al., *Spinoculation Enhances HBV Infection in NTCP-Reconstituted Hepatocytes.* PLoS One, 2015. **10**(6): p. e0129889.
320. Gripon, P., et al., *Hepatitis B virus infection of adult human hepatocytes cultured in the presence of dimethyl sulfoxide.* J Virol, 1988. **62**(11): p. 4136-43.
321. Paran, N., B. Geiger, and Y. Shaul, *HBV infection of cell culture: evidence for multivalent and cooperative attachment.* EMBO J, 2001. **20**(16): p. 4443-53.
322. Ko, C., et al., *The FDA-approved drug irbesartan inhibits HBV-infection in HepG2 cells stably expressing sodium taurocholate co-transporting polypeptide.* Antivir Ther, 2015. **20**(8): p. 835-42.
323. Evripioti, A.A., et al., *Phosphodiesterase-induced cAMP degradation restricts hepatitis B virus infection.* Philos Trans R Soc Lond B Biol Sci, 2019. **374**(1773): p. 20180292.
324. Cangelosi, Q., S.A. Means, and H. Ho, *A multi-scale spatial model of hepatitis-B viral dynamics.* PLoS One, 2017. **12**(12): p. e0188209.
325. Chu, C.M., et al., *Subcellular localization of hepatitis B core antigen in relation to hepatocyte regeneration in chronic hepatitis B.* Gastroenterology, 1995. **109**(6): p. 1926-32.

326. Sari, A., et al., *Relation of hepatitis B core antigen expression with histological activity, serum HBeAg, and HBV DNA levels.* Indian J Pathol Microbiol, 2011. **54**(2): p. 355-8.
327. Funk, A., et al., *Spread of hepatitis B viruses in vitro requires extracellular progeny and may be codetermined by polarized egress.* J Virol, 2004. **78**(8): p. 3977-83.
328. Hamel, R., et al., *Biology of Zika Virus Infection in Human Skin Cells.* J Virol, 2015. **89**(17): p. 8880-96.
329. Sherman, K.E., et al., *Zika virus replication and cytopathic effects in liver cells.* PLoS One, 2019. **14**(3): p. e0214016.
330. Van Rompay, K.K.A., et al., *A combination of two human monoclonal antibodies limits fetal damage by Zika virus in macaques.* Proc Natl Acad Sci U S A, 2020. **117**(14): p. 7981-7989.
331. Tricot, T., et al., *Human stem cell-derived hepatocyte-like cells support Zika virus replication and provide a relevant model to assess the efficacy of potential antivirals.* PLoS One, 2018. **13**(12): p. e0209097.
332. Willems, W.R., et al., *Semliki forest virus: cause of a fatal case of human encephalitis.* Science, 1979. **203**(4385): p. 1127-9.
333. Lu, Y.E. and M. Kielian, *Semliki forest virus budding: assay, mechanisms, and cholesterol requirement.* J Virol, 2000. **74**(17): p. 7708-19.
334. Vihinen, H. and J. Saarinen, *Phosphorylation site analysis of Semliki forest virus nonstructural protein 3.* J Biol Chem, 2000. **275**(36): p. 27775-83.
335. Takkinen, K., et al., *The Semliki-Forest-virus-specific nonstructural protein nsP4 is an autoproteinase.* Eur J Biochem, 1990. **189**(1): p. 33-8.
336. Takkinen, K., *Complete nucleotide sequence of the nonstructural protein genes of Semliki Forest virus.* Nucleic Acids Res, 1986. **14**(14): p. 5667-82.
337. Saul, S., et al., *Differences in Processing Determinants of Nonstructural Polyprotein and in the Sequence of Nonstructural Protein 3 Affect Neurovirulence of Semliki Forest Virus.* J Virol, 2015. **89**(21): p. 11030-45.
338. Dong, C., et al., *Clinical and histopathologic features of sodium taurocholate cotransporting polypeptide deficiency in pediatric patients.* Medicine (Baltimore), 2019. **98**(39): p. e17305.
339. Qiu, J.W., et al., *Sodium taurocholate cotransporting polypeptide (NTCP) deficiency: Identification of a novel SLC10A1 mutation in two unrelated infants presenting with neonatal indirect hyperbilirubinemia and remarkable hypercholanemia.* Oncotarget, 2017. **8**(63): p. 106598-106607.
340. Qiu, G., et al., *Functional proteins of mesenchymal stem cell-derived extracellular vesicles.* Stem Cell Res Ther, 2019. **10**(1): p. 359.
341. Sticova, E., M. Jirsa, and J. Pawlowska, *New Insights in Genetic Cholestasis: From Molecular Mechanisms to Clinical Implications.* Can J Gastroenterol Hepatol, 2018. **2018**: p. 2313675.
342. Sargiacomo, C., et al., *Age-dependent glycosylation of the sodium taurocholate cotransporter polypeptide: From fetal to adult human livers.* Hepatol Commun, 2018. **2**(6): p. 693-702.
343. Hu, Q., et al., *E-cadherin Plays a Role in Hepatitis B Virus Entry Through Affecting Glycosylated Sodium-Taurocholate Cotransporting Polypeptide Distribution.* Front Cell Infect Microbiol, 2020. **10**: p. 74.

344. Lee, J., et al., *N-Linked Glycosylation Is Not Essential for Sodium Taurocholate Cotransporting Polypeptide To Mediate Hepatitis B Virus Infection In Vitro.* J Virol, 2018. **92**(15).
345. Nishitsuji, H., et al., *Investigating the hepatitis B virus life cycle using engineered reporter hepatitis B viruses.* Cancer Sci, 2018. **109**(1): p. 241-249.
346. Nishitsuji, H., et al., *Development of a Hepatitis B Virus Reporter System to Monitor the Early Stages of the Replication Cycle.* J Vis Exp, 2017(120).
347. Nishitsuji, H., et al., *Novel reporter system to monitor early stages of the hepatitis B virus life cycle.* Cancer Sci, 2015. **106**(11): p. 1616-24.
348. Gripon, P., et al., *Infection of a human hepatoma cell line by hepatitis B virus.* Proc Natl Acad Sci U S A, 2002. **99**(24): p. 15655-60.
349. Mabit, H., et al., *In vitro infection of human hepatoma cells (HepG2) with hepatitis B virus (HBV): spontaneous selection of a stable HBV surface antigen-producing HepG2 cell line containing integrated HBV DNA sequences.* J Gen Virol, 1994. **75 (Pt 10)**: p. 2681-9.
350. Luckenbaugh, L., et al., *Genome-free hepatitis B virion levels in patient sera as a potential marker to monitor response to antiviral therapy.* J Viral Hepat, 2015. **22**(6): p. 561-70.
351. Ning, X., et al., *Secretion of genome-free hepatitis B virus--single strand blocking model for virion morphogenesis of para-retrovirus.* PLoS Pathog, 2011. **7**(9): p. e1002255.
352. Hu, J. and K. Liu, *Complete and Incomplete Hepatitis B Virus Particles: Formation, Function, and Application.* Viruses, 2017. **9**(3).
353. Gagey, D., et al., *Antiviral activity of 5'-O-carbonate-2',3'-dideoxy-3'-thiacytidine prodrugs against hepatitis B virus in HepG2 2.2.15 cells.* Int J Antimicrob Agents, 2010. **36**(6): p. 566-9.
354. Zhao, R., et al., *Hepatoma cell line HepG2.2.15 demonstrates distinct biological features compared with parental HepG2.* World J Gastroenterol, 2011. **17**(9): p. 1152-9.
355. Cai, D., et al., *Establishment of an inducible HBV stable cell line that expresses cccDNA-dependent epitope-tagged HBeAg for screening of cccDNA modulators.* Antiviral Res, 2016. **132**: p. 26-37.
356. Guo, H., et al., *Characterization of the intracellular deproteinized relaxed circular DNA of hepatitis B virus: an intermediate of covalently closed circular DNA formation.* J Virol, 2007. **81**(22): p. 12472-84.
357. Priyambada, S.A., et al., *Cell surface N-glycan alteration in HepAD38 cell lines expressing Hepatitis B virus.* Virus Res, 2017. **238**: p. 101-109.
358. Ladner, S.K., et al., *Inducible expression of human hepatitis B virus (HBV) in stably transfected hepatoblastoma cells: a novel system for screening potential inhibitors of HBV replication.* Antimicrob Agents Chemother, 1997. **41**(8): p. 1715-20.
359. Sanyal, D., G. Kudesia, and G. Corbitt, *Comparison of ultracentrifugation and polyethylene glycol precipitation for concentration of hepatitis B virus (HBV) DNA for molecular hybridisation tests and the relationship of HBV-DNA to HBe antigen and anti-HBe status.* J Med Microbiol, 1991. **35**(5): p. 291-3.
360. Choijilsuren, G., et al., *Heparin at physiological concentration can enhance PEG-free in vitro infection with human hepatitis B virus.* Sci Rep, 2017. **7**(1): p. 14461.

361. Cui, X., et al., *Maturation-associated destabilization of hepatitis B virus nucleocapsid.* J Virol, 2013. **87**(21): p. 11494-503.
362. Reuschel, E., et al., *Comparative purification and characterization of hepatitis B virus-like particles produced by recombinant vaccinia viruses in human hepatoma cells and human primary hepatocytes.* PLoS One, 2019. **14**(2): p. e0212800.
363. Chai, N., et al., *Properties of subviral particles of hepatitis B virus.* J Virol, 2008. **82**(16): p. 7812-7.
364. Huang, H.L., et al., *Identification and characterization of a structural protein of hepatitis B virus: a polymerase and surface fusion protein encoded by a spliced RNA.* Virology, 2000. **275**(2): p. 398-410.
365. Wilson, R., et al., *The hepatitis B e antigen suppresses IL-1beta-mediated NF-kappaB activation in hepatocytes.* J Viral Hepat, 2011. **18**(10): p. e499-507.
366. Chang, W.W., et al., *The role of inducible nitric oxide synthase in a murine acute hepatitis B virus (HBV) infection model induced by hydrodynamics-based in vivo transfection of HBV-DNA.* J Hepatol, 2003. **39**(5): p. 834-42.
367. Li, J., et al., *Inhibition of hepatitis B virus replication by MyD88 involves accelerated degradation of pregenomic RNA and nuclear retention of pre-S/S RNAs.* J Virol, 2010. **84**(13): p. 6387-99.
368. Metz, P., et al., *Identification of type I and type II interferon-induced effectors controlling hepatitis C virus replication.* Hepatology, 2012. **56**(6): p. 2082-93.
369. Yang, J., et al., *Inhibition of Hepatitis B virus replication by phospholipid scramblase 1 in vitro and in vivo.* Antiviral Res, 2012. **94**(1): p. 9-17.
370. Guidotti, L.G., et al., *Interferon-regulated pathways that control hepatitis B virus replication in transgenic mice.* J Virol, 2002. **76**(6): p. 2617-21.
371. Zhang, X.N., et al., *Hyper-activated IRF-1 and STAT1 contribute to enhanced interferon stimulated gene (ISG) expression by interferon alpha and gamma co-treatment in human hepatoma cells.* Biochim Biophys Acta, 2006. **1759**(8-9): p. 417-25.
372. Helbig, K.J., et al., *Analysis of ISG expression in chronic hepatitis C identifies viperin as a potential antiviral effector.* Hepatology, 2005. **42**(3): p. 702-10.
373. He, X.S., et al., *Global transcriptional response to interferon is a determinant of HCV treatment outcome and is modified by race.* Hepatology, 2006. **44**(2): p. 352-9.
374. Ji, X., et al., *Interferon alfa regulated gene expression in patients initiating interferon treatment for chronic hepatitis C.* Hepatology, 2003. **37**(3): p. 610-21.
375. Radaeva, S., et al., *Interferon-alpha activates multiple STAT signals and down-regulates c-Met in primary human hepatocytes.* Gastroenterology, 2002. **122**(4): p. 1020-34.
376. Dansako, H., et al., *The cyclic GMP-AMP synthetase-STING signaling pathway is required for both the innate immune response against HBV and the suppression of HBV assembly.* FEBS J, 2016. **283**(1): p. 144-56.
377. Smith, S.E., et al., *Interferon-Induced Transmembrane Protein 1 Restricts Replication of Viruses That Enter Cells via the Plasma Membrane.* J Virol, 2019. **93**(6).
378. Wilkins, C., et al., *IFITM1 is a tight junction protein that inhibits hepatitis C virus entry.* Hepatology, 2013. **57**(2): p. 461-9.
379. Li, T., et al., *Human Hepatitis B Virus Core Protein Inhibits IFNalpha-Induced IFITM1 Expression by Interacting with BAF200.* Viruses, 2019. **11**(5).

380. Eggenberger, J., et al., *Type I interferon response impairs differentiation potential of pluripotent stem cells.* Proc Natl Acad Sci U S A, 2019. **116**(4): p. 1384-1393.
381. Strick-Marchand, H. and D. Durantel, *Who Defends the Stem Cell's Citadel?* Cell Stem Cell, 2018. **22**(3): p. 287-289.
382. Honda, K., et al., *IRF-7 is the master regulator of type-I interferon-dependent immune responses.* Nature, 2005. **434**(7034): p. 772-7.
383. Li, Y., et al., *Interferon-Stimulated Gene 15 Conjugation Stimulates Hepatitis B Virus Production Independent of Type I Interferon Signaling Pathway In Vitro.* Mediators Inflamm, 2016. **2016**: p. 7417648.
384. Qiu, X., et al., *ISG15 as a novel prognostic biomarker for hepatitis B virus-related hepatocellular carcinoma.* Int J Clin Exp Med, 2015. **8**(10): p. 17140-50.
385. Takahashi, T. and A. Iwasaki, *Sex differences in immune responses.* Science, 2021. **371**(6527): p. 347-348.
386. Takahashi, T., et al., *Sex differences in immune responses to SARS-CoV-2 that underlie disease outcomes.* medRxiv, 2020.
387. Takahashi, T., et al., *Sex differences in immune responses that underlie COVID-19 disease outcomes.* Nature, 2020. **588**(7837): p. 315-320.
388. Ruggieri, A., M.C. Gagliardi, and S. Anticoli, *Sex-Dependent Outcome of Hepatitis B and C Viruses Infections: Synergy of Sex Hormones and Immune Responses?* Front Immunol, 2018. **9**: p. 2302.
389. Bashir Hamidu, R., D.M. Chalikonda, and H.W. Hann, *Gender Disparity in Host Responses to Hepatitis B-Related Hepatocellular Carcinoma: A Case Series.* Vaccines (Basel), 2021. **9**(8).
390. Niu, C., et al., *The Smc5/6 Complex Restricts HBV when Localized to ND10 without Inducing an Innate Immune Response and Is Counteracted by the HBV X Protein Shortly after Infection.* PLoS One, 2017. **12**(1): p. e0169648.
391. Lee, S.W., et al., *Comparison of tenofovir and entecavir on the risk of hepatocellular carcinoma and mortality in treatment-naive patients with chronic hepatitis B in Korea: a large-scale, propensity score analysis.* Gut, 2020. **69**(7): p. 1301-1308.
392. Woo, A.S.J., R. Kwok, and T. Ahmed, *Alpha-interferon treatment in hepatitis B.* Ann Transl Med, 2017. **5**(7): p. 159.
393. Narasimhan, V., et al., *Medium-throughput Drug Screening of Patient-derived Organoids from Colorectal Peritoneal Metastases to Direct Personalized Therapy.* Clin Cancer Res, 2020. **26**(14): p. 3662-3670.
394. Mendy, M.E., et al., *Hepatitis B viral load and risk for liver cirrhosis and hepatocellular carcinoma in The Gambia, West Africa.* J Viral Hepat, 2010. **17**(2): p. 115-22.
395. Halgand, B., et al., *Hepatitis B Virus Pregenomic RNA in Hepatocellular Carcinoma: A Nosological and Prognostic Determinant.* Hepatology, 2018. **67**(1): p. 86-96.